DOCTOR OF PHILOSOPHY

Investigating the Effects of Glycaemic Variability on Hypoxic and Ischaemic Preconditioning

Ross, Claire

Award date:
2022

University of Dundee

Investigating the Effects of Glycaemic Variability on Hypoxic and Ischaemic Preconditioning

Claire Elizabeth Ross

Thesis submitted for the degree of Doctor of Philosophy

University of Dundee

October 2022

Contents

List of Figures

List of Tables

Abbreviations

2-BME	β-mercaptoethanol
ACCORD	Action to Control Cardiovascular Risk in Diabetes
ACh	Acetylcholine
ADP	Adenosine Diphosphate
ADVANCE	Action in Diabetes and Vascular Disease: Preterax and Diamicron MR Controlled Evaluation Trial
AGE	Advanced Glycation End Products
AMP	Adenosine Monophosphate
AMPK	Adenosine Monophosphate Activated Kinase
AOP	Arterial Occlusion Pressure
APS	Ammonium Persulfate
ATP	Adenosine Triphosphate
BSA	Bovine Serum Albumin
CABG	Coronary Artery Bypass Graft
$CoCl_2$	Cobalt Chloride
cTnI	Cardiac Troponin-I
CV	Cardiovascular
CVC	Cutaneous Vascular Conductance
CVD	Cardiovascular Disease
CVS	Cardiovascular System
DAP	Diastolic Arterial Pressure
DAPI	4’,6-diamidino-2-phenylindole
DCCT	Diabetes Control and Complications Trial
dH_2O	Distilled Water
DMEM	Dulbecco’s Modified Eagle Medium
DNA	Deoxyribonucleic Acid
DTT	Dithiothreitol
EBA	Evan’s Blue-Labelled Albumin
ECG	Electrocardiogram
EDIC	Epidemiology of Diabetes Interventions and Complications
EDTA	Ethylenediaminetetracetic Acid
EGM	Endothelial Growth Media
EGTA	Ethylene Glycol-bis(β-aminoethyl ether)-N,N,N’,N’-tetraacetic Acid
eNOS	Endothelial Nitric Oxide Synthase

ET-1	Endothelin
FIELD	Fenofibrate Intervention and Event Lowering in Diabetes
FIH	Factor Inhibiting HIF
FLPI	Full Field Laser Perfusion Imaging
FMD	Flow Mediated Dilatation
GLO1	Glyoxalase I
H_2O_2	Hydrogen Peroxide
HbA1c	Glycated Haemoglobin
HBSS	Hanks' Balanced Salt Solution
HCl	Hydrochloric
HCMVEC	Cardiac Human Microvascular Endothelial Cells
hERG	human Ether-à-go-go-Related Gene
HI FBS	Heat Inactivated Foetal Bovine Serum
HIF1α	Hypoxia Inducible Factor α
HIF1β	Hypoxia Inducible Factor β
HPC	Hypoxic Preconditioning
HRE	Hypoxia Response Element
HRP	Horseradish Peroxidase
HUVEC	Human Umbilical Vein Endothelial Cells
IAH	Impaired Awareness to Hypoglycaemia
ICAM-1	Intercellular Adhesion Molecule-1
IL-	Interleukin
iNOS	Inducible Nitric Oxide Synthase
IPC	Ischaemic Preconditioning
KC/GRO	Keratinocyte Chemoattractant/Human Growth-Regulated Oncogene
LAD	Left Anterior Descending
LDF	Laser Doppler Flowmetry
LDI	Laser Doppler Imaging
LDS	Loading Dye Solution
LVDP	Left Ventricular Developed Pressure
MAC	Minimum Alveolar Concentration
MAP	Mean Arterial Pressure
MAPK	Mitogen-Activated Protein Kinase
MCAO	Middle Cerebral Artery Occlusion

mPTP	Mitochondrial Permeability Transition Pore
mRNA	Messenger Ribonucleic Acid
MSRU	Medical School Research Unit
MTS	(3-(4,5-dimethylthiazol-2-yl)-5-(3carboxymethoxyphenyl)-2-(4-sulfophenyl)-2H-tetrazolium)
NaPp	Sodium Pyrophosphate Tetrabasic Decahydrate
NF-κB	Nuclear Factor κ-Light-Chain-Enhancer of Activated B Cells
nNOS	Neuronal Nitric Oxide Synthase
NO	Nitric Oxide
NOS	Nitric Oxide Synthase
NPPO	Negative Pressure Pulmonary Oedema
O-GlcNAc	O-linked GlcNAc
OGD	Oxygen Glucose Deprivation
P2-P5	Passage 2-5
p38 MAPK	p38 Mitogen Activated Protein Kinase
PAI-1	Plasminogen Activator Inhibitor-1
p-Akt	phospho-Akt
p-AMPK	phospho-AMPK
PBS	Phosphate Buffered Saline
PBS-T	Phosphate Buffered Saline Tween
PE	Phenylephrine
Pen/Strep	Penicillin/Streptomycin
p-eNOS	phospho-eNOS
PET	Positron Emission Tomography
PHD	Prolyl Hydroxylase
PI3-K	Phosphoinositide 3-kinase
PKC	Protein Kinase C
PMSF	Phenylmethylsulfonyl Fluoride
p-p38 MAPK	phospho-p38 MAPK
PTT	Partial Thromboplastin Time
pVHL	Von Hippel-Lindau Tumor Suppressor
R-IPC	Remote Ischaemic Preconditioning
ROI	Region of Interest
ROS	Reactive Oxygen Species
RT	Room Temperature

SAP	Systolic Arterial Pressure
SD	Standard Deviation
SDS	Sodium Dodecyl Sulphate
T1D	Type 1 Diabetes
T2D	Type 2 Diabetes
TAT	Thrombin Antithrombin
TBS	Tris Buffered Saline
TBS-T	Tris Buffered Saline - Tween
TCRT	Total Cosine R to T
TEER	Transendothelial Electrical Resistance
TEMED	Tetramethylethylenediamine
TNFα	Tumour Necrosis Factor α
tPa	Tissue Plasminogen Activator
TUNEL	Terminal Deoxynucleotidyl transferase dUTP Nick End Labeling
UDP-GlcNAc	Uridine diphosphate N-acetylglucosamine
UKPDS	UK Prospective Diabetes Study
VCAM	Vascular Cell Adhesion Molecule
VEGF	Vascular Endothelial Growth Factor
vWF	von Willebrand Factor
WT	Wild-type

Acknowledgements

Firstly, I would like to acknowledge my supervisors Professor Rory McCrimmon, Professor Faisel Khan and Dr Alison McNeilly for giving me the opportunity to complete my PhD under their valuable guidance. Without your expertise I would never have learnt so much or developed such an interest in research.

I would like to thank past and present members of the McCrimmon/McNeilly lab for all their help and support over the past 3 and a half years. I am particularly grateful to Dr Calum Forteath for your work in the animal unit, and Jennifer Gallagher for keeping the lab running during such unprecedented times. Additionally, I send a huge thank you to fellow PhD student and lab mate Heather for keeping me motivated and for coming with me on my weekly visit to the liquid nitrogen room. I would also like to express my gratitude to Dr Celine Pourreyron, for all your little gems of advice on the bench, as well as to Jess, Julian and Catriona. Finally, I am extremely thankful to all the other research groups who allowed me to borrow equipment without which my work would have been impossible.

I wish to thank my friends, both old and new. Thank you to Agathe, Ola, Laura, and Anna, who provided unwavering support throughout my PhD. Thank you for the amazing road trips which helped me to get through the late nights in the lab – I am already looking forward to our next adventure! I also wish to acknowledge Natasha, Liv, Charlie, Ragini, and Juliet, to whom I am forever indebted to for your advice and friendship over the last 9+ years.

Thank you to Dad for your unconditional love and for regularly visiting me in my new home. I would like to thank my Mum for always being there for me no matter what. I also am grateful to my stepdad Step-hen and stepbrothers José and Nick. Finally, I must give a shout out to Rosie who kept me company during the write up period.

Declarations

Student Declaration

I hereby declare that I am the author of this thesis and, unless otherwise stated, all work recorded was carried out by me. Where the work of other individuals has contributed to this thesis, this has been indicated and acknowledged accordingly. None of the material within has previously been submitted for a higher degree. Finally, unless stated otherwise, I have consulted all references cited within this thesis.

Claire Elizabeth Ross 29th April 2022

Supervisor Declaration

I certify that Claire Elizabeth Ross has fulfilled the conditions of Ordinance 39 and is eligible to submit this thesis in application for the degree of Doctor of Philosophy.

Professor Rory McCrimmon 29th April 2022

Summary

Cardiovascular diseases (CVDs) are the principal cause of death in people with diabetes. Initially, this was attributed to chronic hyperglycaemia and reduced insulin sensitivity. However, clinical trials have revealed that aggressive glycaemic control does not necessarily improve macrovascular outcomes in these individuals. One possible explanation for this is an increased occurrence of hypoglycaemia associated with intensive glucose lowering therapy. Hypoxic (HPC), ischaemic (IPC) and remote ischaemic preconditioning (R-IPC) are phenomena in which a degree of protection against a severe hypoxic or ischaemic insult is conferred by prior exposure to hypoxia or ischaemia. Evidence regarding the efficacy of IPC and R-IPC treatment in those with diabetes is somewhat contradictory although it seems that glycaemic events before preconditioning can be of influence. A project was designed to investigate how glycaemic variability can affect HPC, IPC and R-IPC. The primary objectives of this project were to develop *in vitro* and *in vivo* models of preconditioning after which acute hypoglycaemic and hyperglycaemic events were to be introduced within the timelines of any established models. The proposed *in vivo* R-IPC model consisted of repeated cycles of 5 minutes ischaemia/5 minutes reperfusion, induced using a blood pressure cuff around a murine hindlimb, for a total of 9 cycles over 3 days. Using laser doppler imaging (LDI) combined with phenylephrine (PE) and acetylcholine (ACh) iontophoresis, *in vivo* studies appeared to show that endothelial function paradoxically decreased following R-IPC treatment. In contrast, it appears that when the injectable anaesthesia agents midazolam and Alfaxan were used in lieu of isoflurane, R-IPC led to an improvement in endothelial function. Taken together, these data provided evidence that isoflurane anaesthesia independently influences vascular function *in vivo* and thus, should not be used in models of preconditioning with assessment of peripheral vascular function. Validation of an *in vitro* IPC model in human umbilical vein endothelial cells (HUVECs) using cobalt chloride ($CoCl_2$) was unsuccessful, as was development of both IPC and HPC models in HUVECs using a hypoxic incubator. However, a model of HPC was validated through the treatment of HUVECs for 24 hours with 200µM $CoCl_2$. A screening study determined that single 3-hour episodes of hypoglycaemia and hyperglycaemia can potentially abolish HPC induced protection against a severe hypoxic insult. However, this disruption appears to depend upon when the glycaemic event

occurs in relation to the HPC treatment. In conclusion, the studies reported in this thesis suggest that the potential benefits of HPC are ameliorated in diabetes as a consequence of significant changes in glycaemia prior to the ischaemic insult.

Chapter 1

Introduction

1.1 Diabetes

Diabetes is a term relating to a group of metabolic disorders largely characterised by hyperglycaemia. In 2013, 382 million people were known to be living with the disease (Forouhi and Wareham, 2014), a figure which had already increased to 415 million by 2017 (Chatterjee *et al*., 2017). Case numbers are expected to rise further with it being predicted that 592 million people will have the condition by 2035 (Forouhi and Wareham, 2014). In reality, this figure is likely to be a significant underestimate with approximately 193 million people being undiagnosed (Chatterjee *et al*., 2017). Unsurprisingly, these figures result in diabetes being a significant financial burden for health services around the globe with it costing the United Kingdom £23.7 billion in just one financial year alone (Hex *et al*., 2012).

There are 2 main types of diabetes, type 1 diabetes (T1D) and type 2 diabetes (T2D), which also account for the bulk of the research into the disorder. T1D is an autoimmune disease in which the insulin producing β-cells of the pancreas are destroyed following infiltration by macrophages, CD8+ and CD4+ T cells (Gillespie, 2006). T2D, however, is characterised by insulin resistance and defects in the production of insulin by pancreatic β-cells (Chatterjee *et al*., 2017). T1D is normally detected before adulthood whereas T2D is more commonly diagnosed after the age of 45. As both diseases have environmental and genetic factors contributing to their development, this difference in age of onset suggests that the T1D susceptibility genes are activated at a younger age, and exposure to the environmental factors affecting disease development occurs much earlier in life. T1D and T2D account for approximately 10% (Gillespie, 2006) and 90% (Chatterjee *et al*., 2017) of those diagnosed with diabetes respectively. However, these percentage values vary significantly based upon the location of a population. For example, it has been reported that children in Finland are approximately 400 times more likely to be diagnosed with T1D than those in Venezuela (Gillespie, 2006).

There are several complications attributed to diabetes which explain why Rao Kondapally Seshasai *et al*. (2011) found the hazard ratio for premature death, from any cause, for those with diabetes, compared to those without, is higher. The risk of developing an array of fatal cancers, particularly liver cancer which

has the most elevated hazard ratio of 2.16, increases in individuals with diabetes. It was also realised that the rise in hazard ratio for death in diabetes is linked to several other renal, gastrointestinal, respiratory, liver, mental health, and nervous system disorders (Rao Kondapally Seshasai *et al*., 2011). The most significant complications, however, are those related to cardiovascular (CV) deterioration.

1.1.1 CV Complications of Diabetes

Individuals with diabetes are at a significantly increased risk of developing both microvascular and macrovascular complications. Microvascular complications generally refer to those involving the smaller blood vessels such as: retinopathy, nephropathy, and neuropathy. Macrovascular complications, however, tend to relate to those regarding larger blood vessels including: myocardial infarction, stroke, peripheral arterial disease, and atherosclerosis. CVDs are the leading cause of death for those with diabetes. Indeed, CVDs account for a substantial 45-52% of fatalities associated with diabetes (Howangyin and Silvestre, 2014) and they are 4 times more prevalent in these individuals than those without diabetes (Snell Bergeon and Wadwa, 2012). Reasons as to why these diseases are so prevalent in this population of individuals has been the focus of much research over the years, with high, low, and oscillating blood glucose levels all playing their own roles in the pathogenesis of the CVDs.

1.2 Hyperglycaemia and CV Dysfunction

Hyperglycaemia is the condition of abnormally high blood glucose. Normally, in response to hyperglycaemia, insulin secretion would act to lower blood glucose to a euglycaemic range. However, in diabetes, due to defects in insulin production and sensitivity, chronic hyperglycaemia is prevalent. Hyperglycaemia contributes to CV dysfunction in numerous ways including induction of oxidative stress, impairing the response to hypoxia, increasing advanced glycation end products (AGEs) and invoking protein kinase C (PKC) pathway activity.

1.2.1 Impaired Response to Hypoxia

Hypoxia can be defined as a state in which the useable oxygen levels are below what is normal. This would typically occur due to an inability to inhale enough

oxygen, such as is the case with respiratory disorders and sleep apnoea. A characteristic of ischaemia is also oxygen deprivation. However, there is also a decrease in the availability of glucose, as well as other essential nutrients present in the circulation, due to occlusion of blood flow to a tissue, as is seen during a myocardial infarction. The consequences of hypoxia and ischaemia are similar with prolonged deprivation of oxygen and glucose leading to cell and tissue death which can be fatal.

The cellular response to hypoxia is largely mediated by the transcription factor hypoxia inducible factor α (HIF1α) (Fig. 1.1). HIF1α mediates a pathway with the aim of reoxygenating the hypoxic or ischaemic tissue before irreversible tissue death. The HIF1α protein is constitutively present in the cytoplasm but is degraded exceptionally quickly, usually within 5 minutes, to prevent it from continuously translocating to the nucleus and initiating transcription when not stimulated in a hypoxic environment (Masoud and Li, 2015). Under normoxic conditions, oxygen and Fe^{3+} ions activate prolyl hydroxylase (PHD) enzymes which hydroxylate the HIF1α protein at proline residues 402 and 564. The Von Hippel-Lindau tumor suppressor (pVHL) component of the E3 ubiquitin ligase complex recognises and associates with the hydroxylated HIF1α protein. The ubiquitin ligase activity of the complex allows the polyubiquitination of the HIF1α protein. The ubiquitin labelled HIF1α protein is then degraded by the 26S proteosome. Additionally, with the aid of these same cofactors, factor inhibiting HIF (FIH) enzymes are activated which hydroxylate the HIF1α to inhibit it from binding to CBP/p300 in the nucleus should any unintentionally dimerise with hypoxia inducible factor β (HIF1β) and translocate.

When no oxygen is present, PHD and FIH enzymes are unable to activate. Therefore, the HIF1α protein is not hydroxylated for recognition by the pVHL or for the inhibition of its binding to CBP/p300. Therefore, the HIF1α protein can dimerise with HIF1β and translocate into the nucleus. Here, the dimer binds to its transcriptional coactivator CBP/p300. Together, this complex associates with the hypoxia response element (HRE) of the relevant promoter region to initiate transcription of genes related to angiogenesis, erythropoiesis, metabolism, cell survival, and proliferation. In individuals with diabetes, there is an impaired response to hypoxia which is largely believed to be mediated by the chronic

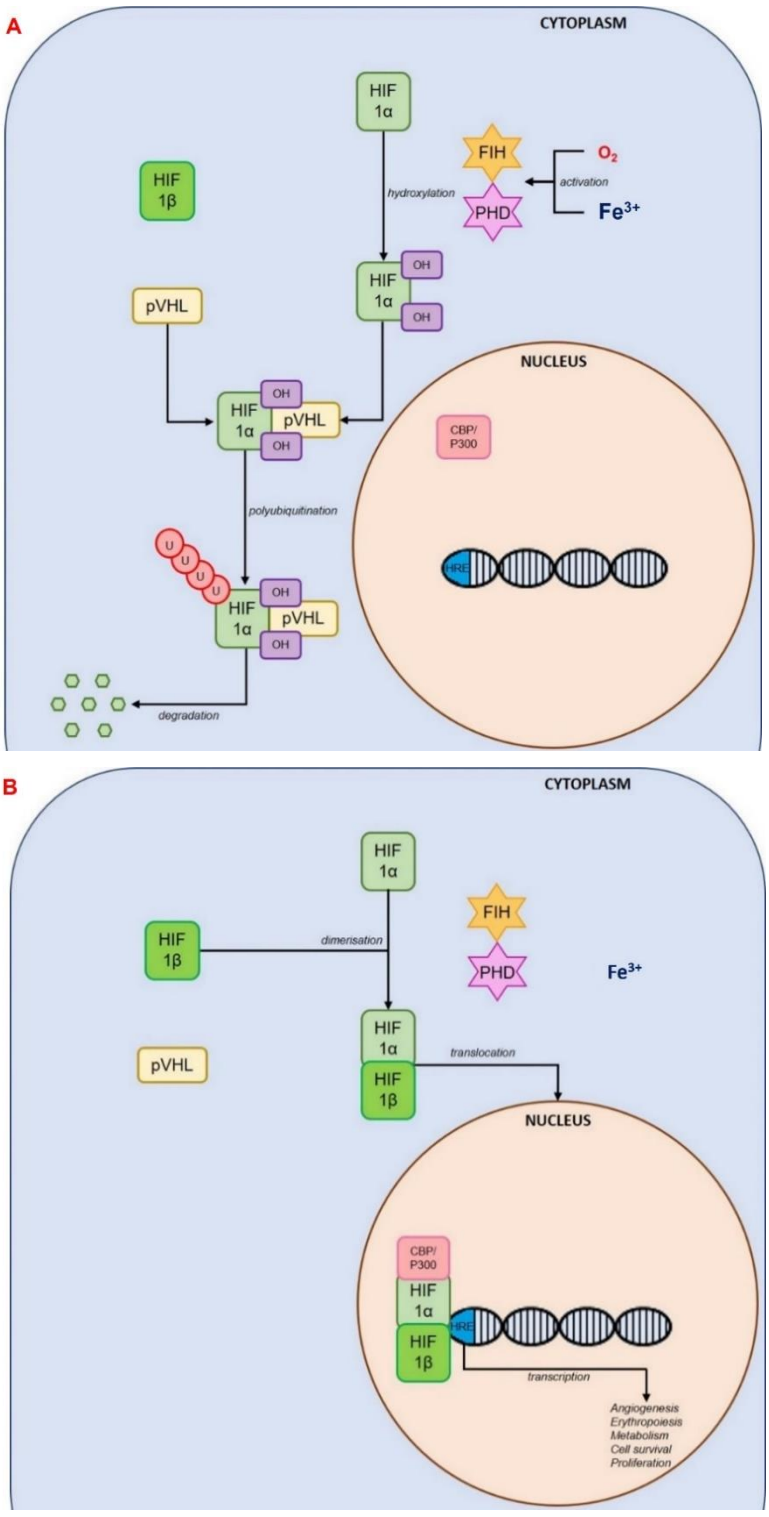

Fig. 1.1 HIF1α in normoxia and hypoxia. Under normoxic conditions (A), in the presence of oxygen and Fe^{3+}, PHDs are activated. HIFα is hydroxylated (OH) and detected by the pVHL. This enables to HIF1α to be polyubiquitinated by the E3 ubiquitin ligase activity of the pVHL complex. This labels the HIF1α for degradation by 26S proteosome. Under hypoxic conditions (B), PHDs are not activated meaning HIF1α dimerises with HIF1β and together they translocate into the nucleus. Here the dimer associates with co-transcription factor CBP/P300 and bind to the HRE of the promoter region for genes inducing transcription of angiogenesis, erythropoiesis, metabolism, cell survival and proliferation. (*Adapted* from Masoud and Li, 2015)

hyperglycaemia experienced by these persons. There appear to be 4 mechanisms of this hyperglycaemia induced dysfunction in the normal response to hypoxia, all of which interfere with the HIF1α pathway.

The increased expression of methylglyoxal, which is observed with chronic hyperglycaemia, mediates 3 of these mechanisms. Methylglyoxal is a cytotoxic compound synthesised from the glycolysis intermediates dihydroxyacetone phosphate and glyceraldehyde 3-phosphate. Whilst it can be detoxified by glutathione, the decrease in NADPH available, due to increased activity of the polyol pathway during hyperglycaemia as discussed in section 1.2.2.2, results in a reduced rate of the neutralisation of methylglyoxal. Under hyperglycaemic conditions, glycolytic activity increases therefore producing even more methylglyoxal. This combination leads to a significant accumulation of methylglyoxal within the cells. In separate studies, methylglyoxal has been shown to directly modify the HIF1α protein and its transcriptional cofactor CBP/p300. Ceradini *et al*. (2008) cultured murine dermal fibroblasts and infected approximately one third with glyoxalase I (GLO1), an enzyme key in the catabolism of methylglyoxal. Cells were exposed to normoglycaemia or hyperglycaemia following which they were treated with hypoxia. Immunoblot analysis revealed that HIF1α expression was not altered, but that of HIF1β was significantly decreased in hyperglycaemic cells. Also, methylglyoxal expression increased under the same conditions. These effects were reversed in cells overexpressing GLO1 suggesting that methylglyoxal has a direct effect on the HIF1β protein resulting in a decrease in its expression (Ceradini *et al*., 2008). The dimerization of HIF1α and HIF1β is necessary for the translocation of the HIF1α protein to the nucleus. Therefore, as there is less of the HIF1β protein available, the rate at which this process can occur is reduced under hyperglycaemic conditions. Thangarajan *et al*. (2009) investigated the effect of hyperglycaemia and methylglyoxal on the association of HIF1α to CBP/p300. Human aortic endothelial cells were first transfected with the HIF1α-CAD and p300-CHI domains. Approximately one third were infected with GLO1. For a period of 5 days, all cells were cultured in either normoglycaemia or hyperglycaemia at, 5mmM and 30mM glucose respectively. Cells were then exposed to a period of hypoxia for 18 hours. The resulting 2 hybrid system luciferase assay revealed that there was reduced binding between HIF1α and p300 during hyperglycaemia.

This effect was abolished with the presence of GLO1. In non-transfected human aortic endothelial cells, the same experiment was performed with methylglyoxal expression being measured by western blot. An inverse correlation was observed between the association of HIF1α with p300 and the levels of methylglyoxal indicating the latter interferes with the former (Thangarajan *et al*., 2009). This means that any dimerised HIF1α/HIF1β which has managed to translocate into the nucleus is unable to bind to the HRE due to being inhibited from associating with CBP/p300. The ultimate outcome of both these mechanisms is a reduction in the initiation of the transcription of HIF1α target genes.

The third way in which methylglyoxal exerts its effects on the HIF1α pathway is by affecting its degradation. Bento *et al*. (2010) exposed ARPE-19 cells to hypoxia for 6 hours. This was followed by treatment for 30 minutes or 3 hours with 1 or 3mM methylglyoxal. There was no visible HIF1α protein band at the 3-hour timepoint in the 3mM treated cells but there was in those exposed to 1mM. This indicated that methylglyoxal increases the rate of degradation of the HIF1α protein. To deduce the underlying mechanism, ARPE-19 cells were transfected with mutant HIF1α where the proline 402 and 564 hydroxylation sites were replaced with alanine, therefore preventing PDH from hydroxylating the protein and the pVHL complex initiating is polyubiquitination. However, the increased degradation of HIF1α in the presence of 3mM methylglyoxal was still observed. To investigate further, CHIP, a chaperone bound ligase, was silenced in Cos-7 cells by infection with short hairpin RNA. Cells treated with both hypoxia and hypoxia plus methylglyoxal exhibited similar HIF1α protein expression indicating that the silencing of CHIP abolished the effect of methylglyoxal on the degradation of HIFα. Therefore, the increased degradation of the HIF1α protein is independent of the pVHL complex and is instead linked to CHIP (Bento *et al*., 2010).

There is additional evidence that hyperglycaemia affects the HIF1α pathway in a pVHL dependent manner. Human SKRC-7 cells, with a non-functional form of pVHL resulting from a point mutation, were exposed to either hyperglycaemia or normoglycaemia at 30mM and 5.5mM glucose respectively. The expression of HIF1α had not been affected in the hyperglycaemia treated cells meaning the investigators concluded that elevated glucose disrupted its pathway in a manner

dependent on pVHL (Botusan *et al*., 2008) The underlying mechanism behind this is still not certain, therefore more research into this is required to gain further understanding. It should be noted that in the previously discussed Ceradini *et al*. (2008) study, HIF1α expression did not change with hyperglycaemia, and that in the Bento *et al*. (2010) study, the observed increase in the degradation rate of the HIF1α protein did not appear instantaneously. It is unclear from the literature how soon after hypoxia treatment the cells were analysed in the Botusan *et al.* (2008) and Ceradini *et al.* (2008) studies. Therefore, depending on the actual design of these experiments, the inability to respond normally to hypoxia, induced by hyperglycaemia, may not be mediated by the pVHL as Botusan *et al*. (2008) claim.

1.2.2 Oxidative Stress

1.2.2.1 Mitochondrial Dysfunction

Mitochondrial dysfunction is one cause for the oxidative stress associated with hyperglycaemia. Joshi *et al*. (2015) cultured human cardiac microvascular endothelial cells (HCMVECs) in either 5.5mM or 25mM glucose and determined mitochondrial oxygen consumption rate. In HCMVECs exposed to hyperglycaemia for 24 hours, analysis of the data revealed there was a significant decrease in adenosine triphosphate (ATP)-linked mitochondrial respiration, spare respiratory capacity, and maximal respiration implying. This reduced respiratory rate implies that hyperglycaemia induces mitochondrial dysfunction (Joshi *et al*., 2015).

Mitochondria are well recognised for their role in producing ATP but are also important for regulating calcium influx, free radical generation, and pro-apoptotic factor release. When mitochondrial dysfunction occurs, there is an increase in intracellular calcium, production of free radicals leading to oxidative stress and stimulation of apoptosis via the release of cytochrome c (Rehni *et al*., 2015). Mitochondrial reactive oxygen species (ROS) production is also linked to activation of the polyol, hexosamine and PKC pathways, and generation of AGEs (Rolo and Palmeira, 2006).

1.2.2.2 Polyol Pathway

The polyol pathway is a simple 2 step pathway by which excess, glucose, unable to be used in saturated glycolysis pathways, is converted into sorbitol, and then into fructose by reduction and oxidation respectively (Fig. 1.2). When episodes of hyperglycaemia are not of a pathological frequency, this does not have a significantly detrimental effect. However, with chronic hyperglycaemia, this can contribute to destructive amounts of oxidative stress, particularly within the microvasculature of the eye. As the time spent in hyperglycaemia increases, the polyol pathway becomes more active, meaning greater reduction of glucose takes place in this manner. This results in less NADPH being available for any other processes (Lee and Chung, 1999). NADPH is essential for cellular metabolism as well as glutathione reduction. Glutathione is an antioxidant necessary for the reduction of ROS. A decrease in the reduction of glutathione results in glutathione deficiency meaning less ROS can be neutralised (Brownlee, 2004). Therefore, increased polyol pathway activity contributes to vascular deterioration via oxidative stress.

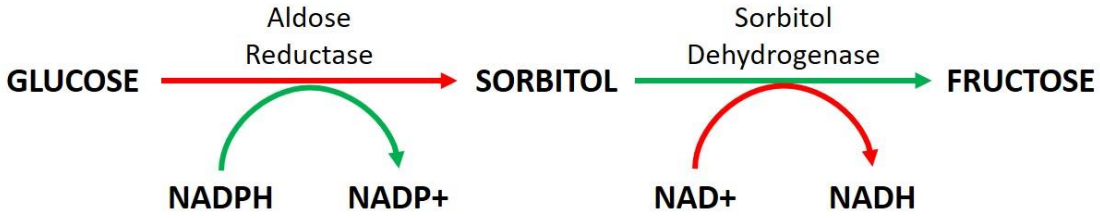

Fig. 1.2 Polyol pathway. The 2-step pathway is activated as glucose levels increase to produce sorbitol and fructose in a series of redox reactions. Green arrows indicate when a compound undergoes oxidation whereas red arrows represent reduction.

1.2.3 PKC Pathway Activation

PKC refers to a multi-purpose family of enzymes consisting of 13 members. Amongst many other processes, they are involved in the regulation of cell growth, apoptosis, differentiation, and tumorigenesis. They have been implicated in the pathogenesis of CVDs although in a review article by Singh *et al*. (2017), it is suggested that this may be subtype dependent (Singh *et al*., 2017). There is a substantial collection of published data which implies that hyperglycaemia induces endothelial dysfunction via the PKC pathway.

Human brain microvascular endothelial cells were cultured in a euglycaemic or

hyperglycaemia media, consisting of 5.5mM and 25mM glucose respectively, for 72 hours. A selection of the hyperglycaemic cells were incubated with PKCα inhibitor Ro-32-0432, PKCβ inhibitor LY333531 or PKCβ_{II} inhibitor CGP53353. In comparison to cells cultured at euglycaemia, those treated with hyperglycaemia exhibited significantly elevated superoxide anion levels which were normalised by the PKC inhibitors. Additionally, hyperglycaemia significantly increased the rate of apoptosis, caspase 3/7 activity and expression of pro-apoptotic protein Bax. Again, this effect was inhibited by co-treatment with any of the PKC inhibitors hence implying that hyperglycaemia induced cellular damage is associated with activation of the PKC pathway (Shao and Bayraktutan, 2014).

In a study by Quagliaro et al. (2005), HUVECs were divided into 3 groups dependent on treatment conditions: i) euglycaemia 5.5mM glucose, ii) hyperglycaemia 20mM glucose, iii) euglycaemia and hyperglycaemia. PKC activity and intercellular adhesion molecule-1 (ICAM-1), vascular cell adhesion molecule (VCAM) and e-selectin expression were measured after 14 days of being cultured. After completion of the culture period, activity of the β_I, β_{II}, and δ isoforms of PKC, and ICAM-1, VCAM and e-selectin expression were all significantly increased in the cells cultured at hyperglycaemia compared to those incubated at euglycaemia. Furthermore, those subjected to glycaemic variability showed an even greater increase in these variables (Quagliaro *et al*., 2005).

Beckman *et al*. (2002), aimed to determine the effect of inhibiting PKC on endothelial function during hyperglycaemia in healthy humans. Subjects were also treated with PKC inhibitor LY333531 or a placebo for 8 days. Endothelial dependent vasodilation was determined by administration of increasing doses of methacholine chloride, at 0.3, 1, 3 and 10μg/min, and observing the flow of blood within the forearm. These measurements were made following the final LY33331 or placebo treatment and also after a 6-hour hyperglycaemic clamp, during which 50% dextrose was infused for a blood glucose target of 300mg/dL. At euglycaemia, there was decreased blood flow in both the LY333531 and placebo treated subjects in comparison to at hyperglycaemia. However, in the placebo group, at all methacholine chloride concentrations, there was a significant reduction in the change in blood flow during hyperglycaemia indicating an impairment in endothelial function and the ability to respond to a vasodilatory

stimulus. However, in subjects pre-treated with the PKC inhibitor, the change in blood flow in response to methacholine chloride was similar between euglycaemia and hyperglycaemia (Beckman *et al*., 2002). This therefore indicates that hyperglycaemia induces endothelial dysfunction, at least in part, via the PKC pathway.

Human brain microvascular endothelial cells and human astrocytes were cultured to develop an *in vitro* model of the blood brain barrier. Cells were incubated in either normoglycaemia or hyperglycaemia, for 72 hours, at glucose concentration of 5.5mmol/L and 25mmol/L respectively. Also, some of the hyperglycaemic cells were treated with the PKC inhibitor Ro-32-0432. Transendothelial electrical resistance (TEER), an indicator of integrity of the endothelial barrier, and Evans blue-labelled albumin (EBA) flux, a marker of permeability, were measured after the 72-hour incubation period with lower TEER and higher EBA flux implying defective blood brain barrier structure. Additionally, PKC activity was analysed to correlate changes in blood brain barrier integrity with the protein's expression. TEER was significantly reduced, and both EBA flux and PKC activity significantly increased, in hyperglycaemic cells compared to the normoglycaemic cells. However, when hyperglycaemic cells were additionally treated with Ro-32-0432, TEER, EBA flux and PKC activity were not significantly different from normoglycaemic cells (Srivastava and Bayraktutan, 2017). This suggests that hyperglycaemia induces endothelial and blood brain barrier dysfunction in a PKC dependent manner.

1.2.4 Hexosamine Pathway

Oxidative stress is associated with inhibition of glyceraldehyde-3-phosphate dehydrogenase, an enzyme involved in glycolysis (Van der Reest *et al*., 2018). Cells attempt to utilise the excess glucose during hyperglycaemia by elevating activity of the hexosamine pathway (Fig. 1.3). In this, fructose-6-phosphate, which has already been converted from glucose, undergoes a series of enzymatic reactions transforming it into glucosamine-6-phosphate, GlcNAc-6-phosphate, GLcNAc-1-phosphate, and finally, uridine diphosphate N-acetylglucosamine (UDP-GlcNAc). The enzymes involved in each stage are GFAT, FNA1/GNPNAT1, PGM3/AGM1 and UAP/AGX1 (Akella *et al*., 2019).

UDP-GlcNAc is a substrate for the enzyme O-linked GlcNAc (O-GlcNAc) transferase which catalyses the reaction to modify proteins by attaching O-GlcNAc. Therefore, increased hexosamine pathway activity results in elevated O-GlcNAc transferase activity and more O-GlcNAc protein modification events. In a detailed review by Chatham *et al*. (2021), consequences of raised O-GlcNAc presence on CV function are discussed. By inducing a selection of changes to protein function and transcriptional activity, O-GlcNAc ultimately leads to significant cellular dysfunction (Chatham *et al*., 2021). Therefore, it can be concluded that hyperglycaemia invokes CV dysfunction through an increase in hexosamine pathway activity.

Fig. 1.3 Hexosamine pathway. Fructose-6-phosphate (F-6-P) is converted, in a series of enzyme dependent reactions, into glucosamine-6-phosphate (G-6-P), GlcNAc-6-phosphate (GlcNAc-6-P), GLcNAc-1-phosphate (GlcNAc-1-P), and finally, UDP-GlcNAc. Enzymes involved in catalysing each reaction, GFAT, FNA1/GNPNAT1, PGM3/AGM1 and UAP/AGX1, are indicated.where appropriate (*Adapted* from Akella *et al*., 2019).

1.2.5 Advanced Glycation End Products

AGEs are lipids, proteins and nucleic acids which have undergone glycation and oxidation via the Maillard reaction (Fig. 1.4) causing them to potentially experience alterations in their function. In high glucose environments, the lipids, proteins, or nucleic acids are glycosylated to form a Schiff base in an enzyme free process which takes a few hours. Over the succeeding days, in the presence of water, the Schiff base can be transformed into Amadori product in another non-enzymatic reaction. Finally, enzyme independent oxidation of the Amadori product produces AGEs over a period of months. The processes of transforming the lipid, protein, or nucleic acid into the Schiff base and then into the Amadori product are all reversible. However, the final step, the formation of the AGE, is irreversible leading to their build up over time (Hegab *et al*., 2012). An increase in the abundance of AGEs is associated with the development of microvascular diseases linked to diabetes.

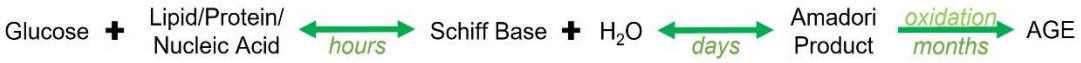

Fig. 1.4 Maillard reaction to generate AGEs. AGEs are formed through non enzymatic glycation and oxidation of lipids, proteins, and nucleic acids in high glucose environments. Reversible and irreversible processes are indicated by double and single headed arrows respectively **(***Adapted* from Hegab *et al.,* 2012)

AGEs have been implicated in the development of retinopathy and it has been discovered that there is accumulation of Amadori products and AGEs within the retinal vessels of individuals with diabetes (Stitt, 2003). One *in vitro* study indicated that AGEs cause cellular destruction within the retina. Bovine retinal pericytes, endothelial cells, and bovine aortic endothelial cells were treated with 8 different concentrations of AGE-bovine serum albumin (BSA), 0, 7.9, 31.3, 62.5, 125, 250 and 500µg/mL, for 4 days after which cell viability was determined using a Trypan blue assay. AGE-BSA concentrations above 15.7 and 31.3µg/mL caused a significant reduction in the cell viability of pericytes and aortic endothelial cells. Interestingly, up to 250µg/mL AGE-BSA, there was an increase in the viability of the endothelial cells. There is a particularly substantial effect of AGE on the pericytes as, at 250µg/mL AGE-BSA, their viability had dropped to 55-65% whilst it only decreased to 75-85% in the aortic endothelial cell population (Chibber *et al*., 1997). These findings are supported by Yamagishi *et al*. (2002) who treated pericytes for 10 days with 100µg/mL of 1 of 3 AGEs or, BSA alone. They found that pericytes which had been exposed to any of the AGEs exhibited a significant decrease in cell number and increase in apoptosis detected using a deoxyribonucleic acid (DNA) fragmentation assay. Pericytes express AGE receptors whose activation influences vascular endothelial growth factor (VEGF) expression. Therefore, in the attempt to identify potential mechanisms, the abundance of VEGF messenger ribonucleic acid (mRNA) within the AGE treated pericytes was determined. It was observed that in the presence of AGE, there was an increase in VEGF mRNA within the cells (Yamagishi *et al*., 2002). In the retina from non-diabetic rats, immunohistochemical analysis revealed that VEGF expression was weak and mainly located within the nerve fibres and ganglions. However, in rats with diabetes, there was a significant increase in VEGF in all areas of the retina, but particularly within the area surrounding the blood vessels. Increased permeability was confirmed in the vessels within the retinas from the

rats with diabetes by monitoring the extravasation of albumin (Murata *et al*., 1995). Loss of pericytes and increased permeability of retinal blood vessels are early indicators of retinopathy (Ahmed, 2005; Yamagishi *et al*., 2002). Therefore, increased AGE generation in diabetes can be linked to the development of retinopathy which is at least partially due to VEGF induced vascular permeability and pericyte destruction.

AGEs may contribute to the development of neuropathy through direct action upon the neurons, such as increasing the demyelination resulting in reduced conductivity, or by destructing the neuronal microvasculature leading to deprivation of oxygen and glucose required for cellular survival and function. Glycation of laminin and collagen can cause basement membranes, within which these proteins are located, to thicken and affect the permeability of the vasculature (Wada and Yagihashi, 2005). Also, alterations in nitric oxide synthase (NOS) activity have been identified as a potential a cause for microvascular dysfunction, such as that seen in the pathogenesis of neuropathy as well as other CVDs. Murine endothelioma cells exposed to 12 hours of 17 and 35mg/mL glycated albumin expressed a significant elevation in NOS activity. Furthermore, with additional incubations using 1.7, 3.4 and 6.8mg/mL glycated albumin, there appeared to be a positive correlation between dosage and NOS activity. Finally, in cells treated with 17 or 35 mg/mL glycated albumin, there was a significant increase in mRNA expression of inducible nitric oxide synthase (iNOS). However, in cells only exposed to normal albumin, there was no detectable expression of iNOS mRNA (Amore *et al*., 1997). iNOS is a form of NOS whose expression is typically associated with non-physiological conditions. Upon its activation, it can generate pathological quantities of nitric oxide (NO) therefore further exacerbating oxidative stress caused by mitochondrial dysfunction and the polyol pathway.

AGEs have also been implicated in nephropathy development. In a study conducted by Forbes *et al*. (2003), Sprague Dawley rats, with and without 50mg/kg streptozotocin induced diabetes, were administered with the AGE cross-link breaker ALT-711 or received no treatment. Expression of AGEs and their receptors was significantly increased in the kidneys of rats with diabetes compared to the controls. Conversely, diabetic animals, treated with ALT-711,

had reduced AGE and AGE receptor expression in comparison to those with diabetes who did not receive the AGE cross-link breaker. Also, in rats with diabetes, the glomerulosclerotic index, a marker of damage to the vasculature of the glomeruli, was significantly elevated compared to controls. However, with early treatment with the AGE cross-link breaker, this value was significantly reduced to a similar level seen in the controls (Forbes *et al*., 2003).

From the data discussed, it is evident that hyperglycaemia induced AGE generation is responsible for the development of CVDs in patients with diabetes partly due to increased permeability and oxidative stress. However, as the formation of AGEs can take months, these may not necessarily cause significant amounts of CV damage during the early stages of the disease.

1.3 Glycaemic Variability and CV Dysfunction

As evidenced in the literature, hyperglycaemia contributes to the poor CV outcomes in those with diabetes. A series of clinical trials has taken place to investigate the effects of maintaining tight glycaemic control on these CV outcomes with interesting results.

1.3.1 UK Prospective Diabetes Study (UKPDS)

The UKPDS was one of the earliest major clinical trials investigating the effect of tight glycaemic control on macrovascular and microvascular complications in persons newly diagnosed with T2D (Turner, 1998). The study consisted of an intervention period until 1997 which was succeeded by a 10 year-follow up. All individuals, aged between 25-65 years old initially received therapy in the form of diet management. They were then divided into 1 of 4 groups: i) diet therapy only, ii) sulfonylurea therapy with up to 500mg chlorpropamide or 20mg glyburide daily supplemented with metformin and insulin if fasting plasma glucose remained above 15mmol/L, iii) insulin therapy by a single daily injection of ultralente insulin with the dose dependent on the current fasting plasma glucose eventually switching to multiple daily injections or treatment with isophane insulin iv) metformin therapy given to obese subjects who received up to a maximum of 2,550mg per day. Groups ii, iii and iv were labelled as intense glucose control

groups and had a fasting plasma glucose target of 6mmol/L except for those receiving multiple insulin injections who had a target of 4-7mmol/L.

Group i exhibited gradual rising fasting plasma glucose levels throughout the study which never fell below the hyperglycaemic range. In groups ii and iii, the fasting plasma glucose was decreased but only to a mean of 6.5-7mmol/L which was higher than the target for most individuals. Additionally, the fasting plasma glucose began to continuously rise to 7.5-8mmol/L between 1 and 6 years since the commencement of the study (Turner 1998). This could potentially be due to a degree of tolerance developed against the pharmacological agents or even an aspect of medical non-compliance which can occur in individuals with chronic conditions such as diabetes (Kleinsinger, 2018). The dysfunction of pancreatic β cells, and therefore decrease of endogenous insulin production, is more likely to be the significant factor influencing the rise in fasting plasma glucose. Indeed, an inverse correlation between the percentage of functional pancreatic β cells and the fasting plasma glucose levels was found. At the beginning of the study, those in group i had 51% normal β cell function which had decreased to just 28% after 6 years. In group ii, the percentage of normal β cell function did initially increase from 46% to 78% after 1 year, although this decreased to 52% within the 6 years of the study (Turner, 1998).

Following completion of the study's interventional period, it was found that there was a significant 25% reduction in the risk of developing microvascular diseases in participants belonging to the intense glycaemic control groups ii and iii. However, there was no significant decrease in the risk of a myocardial infarction. During the 10-year follow-up period, the risk of microvascular disease remained reduced in these individuals and results emerged indicating that the risk of myocardial infarction also decreased. This indicates that whilst intense glycaemic control in these participants is beneficial to microvascular outcomes relatively rapidly, any benefits to macrovascular outcomes take substantially longer to arise (Holman *et al*., 2008).

Obese subjects receiving metformin, in group iv, similarly exhibited a decreased risk of developing microvascular diseases during the study's interventional period. However, unlike in groups ii and iii, the risk of myocardial infarct, for

participants in group iv, was also reduced during the intervention period. This indicates that in this particular cohort, intense glycaemic control has immediately improved microvascular and macrovascular outcomes (Holman *et al*., 2008).

1.3.2 Diabetes Control and Complications Trial (DCCT) and Epidemiology of Diabetes Interventions and Complications (EDIC) Study

The DCCT and EDIC study trials confirmed that maintaining glycaemic stability reduces the risk of developing CV dysfunction. These trials were run successively with the 10-year DCCT followed by the 18-year EDIC observation-based study. They were both conducted to investigate the effect of tight glycaemic control on CV events in those with T1D, with particular focus on retinopathy and nephropathy. Subjects were enrolled into the interventional study, the DCCT, and divided into 1 of 2 groups: i) intense glucose control with either an insulin pump or by administration of 3 or more daily insulin injections, and ii) conventional treatment group with 1 or 2 insulin injections given every day. The daily glycated haemoglobin (HbA1c) target for group i was 6.05% whilst there was no specific goal for group ii other than to maintain glucose levels within the normoglycaemic range. The primary outcome for the study was the time taken to experience one of the following CV events: CV related death, angina, the necessity for a revascularisation procedure, subclinical myocardial infarction, non-fatal myocardial infarction, or stroke.

Following completion of the DCCT, HbA1c levels were lower in the intensive glucose control group, at 7.4%, in comparison to the conventional treatment group, at 9.1%. The intensive glucose control treatment was associated with a 42% reduction in risk of a first-time CV event and a 57% decrease of non-fatal myocardial infarction, stroke, or CV related death (DCCT/EDIC Study Research Group, 2005). A more in-depth analysis of the data revealed that whilst the HbA1c value itself can be used as a predictor of the risk of experiencing a CV event, greater variability within the HbA1c over time, which represents greater glycaemic variability, increases the risk substantially. Indeed, using different analytical models, the investigators confirmed that just a 1% increase in the standard deviation of HbA1c resulted in 80% and 100% increases in the risk value for the development of nephropathy and retinopathy respectively. Therefore, it was

concluded that the degree of fluctuations in the HbA1c would be better as a predictor for the risk of an individual developing a CVD rather than the mean value alone (Kilkpatrick, Rigby and Atkin, 2008).

Similarly to the UKPDS, following the interventional period of the DCCT, it was decided that a follow-up should be conducted as part of the EDIC trial during which subjects resumed their normal diabetes treatments. After 1 year of the EDIC study, the difference in HbA1c observed during the DCCT reduced greatly with group i and ii having levels of 7.7% and 8.1% respectively. The differences in HbA1c between the groups remained negligible for the duration of the EDIC study. Initially, it could be assumed that the lack of difference in the HbA1c levels between the 2 groups would also result in there no longer being a reduction in the risk of a CV event. However, after the first 4 years of the EDIC trial, the percentage of individuals requiring photocoagulation therapy or experiencing proliferative retinopathy, severe non-proliferative retinopathy or macular oedema remained significantly lower in group i compared to group ii. Additionally, the risk of renal dysfunction remained reduced in group i for at least 3-4 years following the commencement of the EDIC study as first-time microalbuminuria, a marker of endothelial dysfunction and permeability, was detected in just 5% of these individuals in comparison to 11% of those in group ii (DCCT/EDIC Study Research Group, 2000). It is clear therefore that despite the abolishment of a difference in the HbA1c levels between the groups, there is still a sustained benefit of the intense glucose control treatment received during the DCCT. It was hypothesised that this was due to the relatively novel phenomenon termed metabolic memory.

1.3.3 Action in Diabetes and Vascular Disease: Preterax and Diamicron MR Controlled Evaluation Trial (ADVANCE)

The ADVANCE trial built upon the findings from the UKPDS trial by aiming to establish whether more intense glucose control improved CV outcomes in people with T2D, aged over 55 years old who had established CVD or were at high risk of CVD. Subjects were divided into 2 groups: i) intense glucose control treatment with a HbA1c target below 6.5% controlled primarily using gliclazide MR, as well as any additional therapy needed to reach this goal, and ii) standard glucose

control treatment managed with any therapy recommended in clinical guidelines other than gliclazide. The HbA1c target in the intense treatment group was achieved with it being significantly lower, at 6.5%, than that in the standard treatment group, at 7.3%.

The percentage of subjects in the intense glycaemic control group experiencing either a microvascular or macrovascular event, 18.1%, was slightly lower in comparison to the percentage of these individuals in the standard glycaemic control group, 20%. In addition, whilst non-significant, a promising 12% reduction in cardiac mortality was found in the intense control group. No significant differences were found in the number of macrovascular events between the treatment groups but there was a substantial improvement in the prevalence of diabetic nephropathy in the intense glycaemic control group.

Interestingly, the number of hospitalisations increased in the intense treatment group, although it is not clear from the article what the reason for this finding was. A probable cause, however, for this is the occurrence of severe hypoglycaemic events arising due to greater pressure to maintain a lower HbA1c target and prevent hyperglycaemia. Indeed, the percentage of subjects experiencing at least 1 severe hypoglycaemia event was higher in the intense glucose control group, at 2.7%, compared to the standard glucose control group, at 1.5%.

The main finding from this trial was that by aggressively lowering HbA1c to 6.5%, there would be a reduction in microvascular complications, especially nephropathy, however, there is no significant benefit on other macrovascular outcomes. (Heller, 2009)

1.3.4 Fenofibrate Intervention and Event Lowering in Diabetes Study (FIELD)

The FIELD study further confirmed the findings from the ADVANCE trial indicating that managing glycaemic variability is an important technique in reducing the prevalence of CVDs in those with T2D. Whilst the principle aim of this study was to determine whether long term fenofibrate treatment, over at least 5 years, improves CV health, glycaemic variability was also monitored allowing

this factor to be incorporated into the analysis of outcomes for the subjects. All subjects were initially given a 4-week period of lifestyle intervention followed by treatment of 6 weeks with a placebo drug then a further 6 weeks of fenofibrate. Participants were then randomly assigned to 1 of 2 groups for the remaining 5 years of the study: i) daily fenofibrate drug, or ii) daily placebo drug. Glycaemic variability was calculated using 4 different values: i) coefficient of variation of HbA1c, ii) HbA1c standard deviation, iii) coefficient of variation of fasting plasma glucose, and iv) fasting plasma glucose standard deviation. The relationship between each of these factors and occurrence of microvascular and macrovascular events or disorders was determined following completion of the study.

As the coefficient of variation of HbA1c increased, there was a significant rise in the occurrence of: retinopathy, total mortality, CV mortality, non-CV mortality, and macrovascular events. The remaining 3 values also showed a positive correlation with these outcomes as well as with the number of amputations due to microvascular damage. Hence this study clearly demonstrates that by reducing glycaemic variability it is possible to significantly improve CV outcomes for T2D patients (Scott *et al*., 2020).

1.3.5 Action to Control Cardiovascular Risk in Diabetes (ACCORD)

One of the main aims of the ACCORD clinical trial was to determine whether the rate of CV events, in high-risk individuals with T2D, could be reduced with an even more intense glucose controlling treatment than that given in the ADVANCE trial. As with that previous trial, subjects were divided into 2 groups: i) intense treatment with a HbA1c of less than 6% and ii) normal treatment with a HbA1c target of 7-7.9%. Standard pharmacological agents, including metformin, sulfonylureas, insulin and thiazolidinediones, alongside changes in lifestyle were used in an attempt to achieve the desired HbA1c targets in both groups (ACCORD Study Group, 2007).

Whilst the study was intended to last for 5 years, the total mortality rate and number of deaths related to CVD were so high in the intense treatment group that the remaining individuals were moved onto the normal treatment regime after 3.5

years. This resulted in the intense group having an average HbA1c of 7.2% by the end of the study whilst still maintaining elevated total and CVD mortality rates. Conversely, the number of subjects experiencing a non-fatal myocardial infacrtion and retinopathy was found to be significantly lower in the intense treatment group. However, despite these positive findings, due to the substantial effect on mortality, it was concluded that using such an intense therapeutic approach to keeping HbA1c below 6% was not recommended in patients with T2D (Genuth and Ismail-Beigi, 2012).

Some of the clinical trials discussed here showed the benefits of glycaemic control and limiting hyperglycaemia on CV outcomes. However, the UKPDS and ADVANCE trials have highlighted that glycaemic control can improve microvascular outcomes but does not provide the same immediate benefit for macrovascular outcomes. Additionally, the ACCORD study indicated that if management of glycaemic variability is done too aggressively, this can exacerbate already poor CV outcomes in individuals with diabetes. The likely cause of this was identified as recurrent episodes of hypoglycaemia which primarily arise due to attempts to limit hyperglycaemia. Hypoglycaemia itself is associated with CV dysfunction which may explain why macrovascular outcomes are not significantly improved with aggressive glycaemic control.

1.4 Hypoglycaemia and CV Dysfunction

Hypoglycaemia refers to blood glucose levels below the euglycaemic range. One of the principal reasons that hypoglycaemia has a deteriorative effect on the cardiovascular system (CVS), is due to the induction of a counterregulatory response in an attempt to restore euglycaemic conditions by inhibiting skeletal muscle glucose uptake, supressing insulin secretion and mobilising hepatic glycogen stores. Detection of low plasma levels results in the activation of 3 physiological defence mechanisms: i) decreased insulin secretion by pancreatic β cells, ii) increased glucagon secretion by pancreatic α cells, iii) increased adrenomedullary adrenaline secretion (Sprague and Arbelaez, 2011). The secreted adrenaline activates several mechanisms, discussed here, to enhance the development of CVDs.

1.4.1 Haemodynamic Changes

1.4.1.1 Changes in the Electrocardiogram (ECG)

The adrenaline released as a result of hypoglycaemia stimulates several haemodynamic changes via activation of adrenoceptors. The effects were confirmed in a study by Kerr *et al*., in which heart rate and blood pressure were recorded in healthy subjects throughout a 2.5mmol/L glucose clamp protocol. Individuals were divided into 4 groups who had taken either: a placebo, β1 adrenoceptor antagonist metoprolol or atenolol or the non-selective β adrenoceptor antagonist propranolol for seven days. It was found that hypoglycaemia significantly increased the heart rate for those taking the placebo and metoprolol. Therefore, conclusions can be made that due to hypoglycaemia, heart rate will increase following activation of the β1 adrenoceptor, and the lack of heart rate suppression by metoprolol was attributed to insufficient adrenoceptor blockade being present in comparison to atenolol and propranolol (Kerr *et al*., 1990). In an earlier study, by Fisher *et al*. (1987), a single injection of 0.15U/kg insulin was administered to healthy persons and again, haemodynamic parameters were measured. The heart rate was significantly increased once severe hypoglycaemia was achieved and decreased back to the basal rate as blood glucose began to increase back to mild hypoglycaemic levels. Fluctuations in blood pressure were also observed but occurred following the rise in heart rate. Whilst the mean arterial pressure (MAP) remained consistent, diastolic arterial pressure (DAP) and systolic arterial pressure (SAP) significantly decreased and increased, respectively, for a period between 15 and 30 minutes. The overall cardiac output also significantly increased, to approximately 225% of the baseline level, when blood glucose had reached its minimum level (Fisher *et al*., 1987). More recently, findings from these earlier trials were replicated in persons with T1D. In a study by Koivikko *et al*. (2005), healthy individuals, and those with T1D underwent both a euglycaemic and hypoglycaemic clamp seven days apart whilst CV measurements were recorded. In both groups, the heart rate increased, and MAP decreased as blood glucose levels dropped from 5.5 to 2.0mmol/L. In the T1D group, the heart rate was significantly higher compared to the healthy group, at all blood glucose levels, indicating potential differences in CV physiology between the groups dependent on T1D status (Koivikko *et al*., 2005).

The effect of hypoglycaemia on the ECG trace of patients with type 1 diabetes was investigated by inducing hypoglycaemia by administration of an Actrapid® insulin saline solution to drop plasma glucose by 1.0mmol/L every 15 minutes (Larsen *et al*., 2013). This continued until glucose levels dropped below 1.7mmol/L or the subject exhibited symptoms of hypoglycaemia. ECG traces were monitored throughout the procedure (Fig. 1.5), and it was observed that the overall wavelength of each cardiac cycle is extended likely due to a lengthened and flattened T wave, a property which represents the repolarisation of cardiac muscle and relaxation of the ventricles. This ultimately leads to a prolonged QT interval which was detected in 6 of the 9 subjects which is a cause of ventricular arrhythmia and ventricular fibrillation development. It should be noted that unfortunately, almost half of the subjects from this study had to be excluded due to inappropriate positioning of ECG electrodes meaning the final sample size was only 9. Furthermore, 6 of these individuals exhibited signs of some degree of hypoglycaemic unawareness although it is not clear whether these were the same who exhibited the changes in QT interval (Larsen *et al*., 2013).

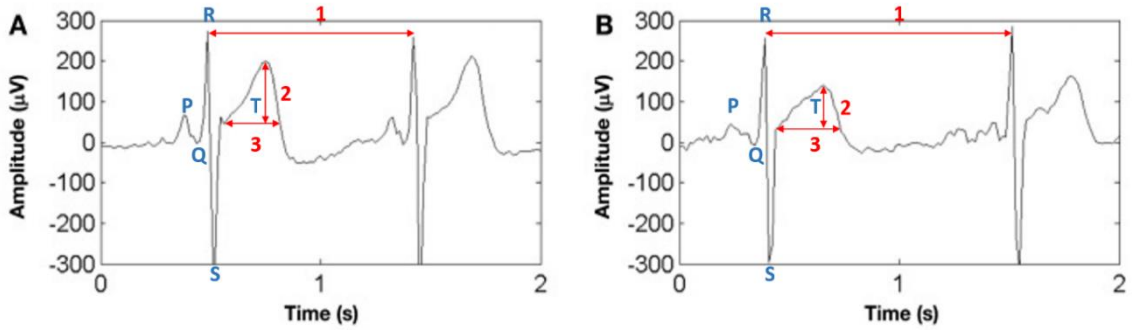

Fig. 1.5 ECG trace in type 1 diabetes at euglycaemia versus hypoglycaemia. Representative examples of 3-point electrode ECG traces from a patient with type 1 diabetes during euglycaemia (A) and hypoglycaemia (B). Typical ECG markers are placed with T and P denoting the T wave and P wave respectively. Cardiac cycle length (1), T wave amplitude (2) and T wave length (3) are also labelled to allow comparison (Larsen *et al*., 2013).

The total cosine R to T (TCRT) measurement has been found to be a potential prognostic parameter for ventricular arrhythmia and is derived from the ECG trace. TCRT values of 0.4 to 0.8 are considered to be normal whereas smaller values are usually found in those suffering from CVDs. Sixteen people with T1D and 8 healthy subjects had 12-lead ECG recordings whilst undergoing a

euglycaemic clamp, at 4.5-5.5mmol/L plasma glucose, and a hypoglycaemic clamp, with an initial target of 3.0-3.5mmol/L plasma glucose and a second of 2.0-2.5mmol/L. In T1D subjects, there was a significant reduction in the TRCT values from 0.41 to 0.17 as blood glucose levels decreased from 4.5-5.5mmol/L to 2.0-2.5mmol/L. A similar, non-significant, trend was also observed within the healthy subjects although TRCT values remained within the physiological range throughout. An additional observation made was that there was no change in the morphology of the QRS complex whilst the magnitude of the T wave was significantly decreased in all individuals during hypoglycaemia. Hence the conclusion was made that hypoglycaemia mainly affected repolarisation of the myocardium without having a major effect on depolarisation (Koivikko *et al*., 2008).

1.4.1.2 Hypoglycaemia, Hypokalaemia and human Ether-à-go-go Related Gene (hERG) Channels

Hypokalaemia refers to the low level of potassium in the circulation and, due to the important role of potassium in regulation of the cardiac contraction cycle, contributes to the development of changes in ECG traces. Hypokalaemia results at least partially from malfunction of hERG potassium channels which are responsible for the diffusion of potassium out of cardiac muscle cells to ensure repolarisation occurs at the correct time thereby allowing safe coordination of myocardial contraction and relaxation. Zhang *et al*. (2003) exposed human embryonic kidney 293 cells to normoglycaemic, at 5mM glucose, and hypoglycaemic conditions, at 2.5mM, 1mM and 0mM glucose for 30 minutes. Patch clamp recordings were conducted on the cells to monitor modulations of the activity of hERG potassium channels. Under hypoglycaemic conditions, the function of the hERG potassium channels was found to be impaired with the degree of impairment increasing and the glucose levels decreased. To further investigate whether glucose metabolism is related to this phenomenon, the investigators performed a similar experiment under hypoglycaemic, 0mM glucose, and normoglycaemic, 5mM glucose, conditions in conjunction with 5mM of the non-hydrolysable analogue 2DG, used to inhibit glucose metabolism. Regardless of the glucose concentration, it was found that in the presence of 2DG, the current density of hERG potassium channels was reduced thereby

mimicking what was observed under hypoglycaemic conditions without 2DG. This indicated that normal hERG potassium channel function is at least partly dependent on maintaining normal glucose metabolism (Zhang *et al*., 2003).

1.4.2 Coagulation and Thrombosis

1.4.2.1 Platelet Activation

Atherosclerosis is a principal risk factor for the development of cerebral ischaemia. Platelets play a key role in the development of atherothrombosis and their activation has been reported as being affected by hypoglycaemia. In a report by Joy *et al*. (2015), elevated P-selectin, a marker indicative of platelet activation, was observed in healthy individuals who had undergone 1-3 hyperinsulinaemic hypoglycaemic clamps, at 2.9mmol/L glucose, suggesting that platelet activation occurs when any number of severe hypoglycaemic episodes are experienced. There does appear to be a slight, but non-significant, trend in that the more episodes of hypoglycaemia a healthy person receives, the less P-selectin is expressed. However, as this particular study only performed a maximum of three clamps in total, more clamps may be required to determine whether the effect of recurrent hypoglycaemia on P-selectin levels would normalise with habituation to repeated hypoglycaemia (Joy *et al*., 2015).

Results of a later glucose clamp trial of healthy subjects supported some of the results observed in the Joy *et al*. (2015) study with subjects undergoing a 2.9mmol/L plasma glucose hyperinsulinaemic hypoglycaemic clamp exhibiting a significant increase in P-selectin expression. Conversely, a decrease in plasma P-selectin was observed in subjects who underwent a 11.1 mmol/L hyperglycaemic clamp or a 5.0mmol/L euglycaemic clamp (Joy *et al*., 2016).

Similar results are seen when both healthy subjects and those with T1D experienced a 120-minute hypoglycaemic clamp, causing P-selectin levels to become significantly elevated when compared to when subjects underwent euglycaemic clamps (Joy *et al*., 2010).

Thrombin plays an important role in the aggregation of platelets through activation of protease-activated receptors on the platelet (Fig. 1.6). It also causes von

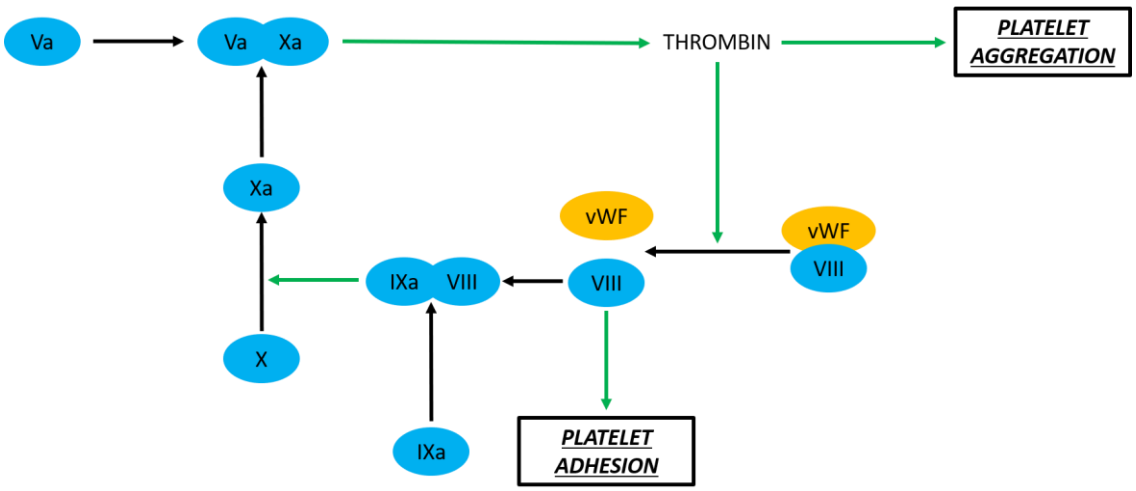

Fig. 1.6 Thrombin and platelet activation. Platelet aggregation and adhesion are promoted by thrombin and coagulation factor VIII. Thrombin regulates itself through a positive feedback loop involving activation and interaction of several coagulation factors (blue). Catalytic processes (green) are also identified within the pathway.

Willebrand Factor (vWF) to release FVIII to which it is bound. FVIII interacts with its cofactor, FIXa, to activate FXa. FXa then associates with its cofactor, FVa to activate more thrombin therefore creating a positive feedback loop. Whilst the principal role of vWF is to bind to, and hence inactivate, FVIII, it is also able to aid the adhesion of platelets to the lining of blood vessels by binding to glycoprotein Ib located on the platelets. This binding process occurs with greater efficiency under conditions of shear stress which persons with hypoglycaemia may be more likely to experience due to previously discussed alterations in haemodynamics, such as cardiac output and myocardial contractility. Therefore, increases in both FVIII and vWF are associated with increased platelet activation, aggregation, and adhesion.

In a study by Fisher *et al*. (1991), 6 healthy males and 6 with poorly controlled insulin dependent diabetes, likely T1D although this is not specified, were given a single episode of severe hypoglycaemia, and the blood concentration of vWF was determined immediately prior to insulin administration, once the hypoglycaemia target had been reached, and both 15- and 60-minutes post insulin administration. Baseline levels of vWF between both groups were not significantly different and each experienced an increase in expression following hypoglycaemia. However, in the persons with diabetes, this rise occurred more quickly, and the maximal increase was significantly greater compared to that in the healthy subjects suggesting there is perhaps a defect in the feedback

mechanisms regulating vWF production (Fisher *et al*., 1991).

A study by Aberer *et al*. (2019), presented similar conclusions to Fisher *et al*. (1991) in persons with T2D. Subjects received a hyperinsulinaemic hypoglycaemic clamp, at 2.5mmol/L blood glucose, and markers of platelet activation were measured throughout the clamp as well as one and seven days after. A significant increase in vWF activity, measured using an activity assay, was detected 1 day after the clamp although this reverted back towards baseline by the day 7 timepoint. Similarly, FVIII levels were significantly elevated both one day following the clamp and, also after seven days post-clamp. Interestingly, the increases in FVIII and vWF were not detectable during the hypoglycaemic clamp suggesting it is not a short-term rapid response. This is likely due to the elevation requiring protein synthesis and, as mRNA was not measured, any earlier detection would not have been possible. It should be noted that in this study, the potential effects of hyperinsulinaemia were controlled for using a hyperinsulinaemic euglycaemic clamp conducted 1-3 weeks prior to the hypoglycaemic clamp (Aberer *et al*., 2019). Activation of these platelets is a component of the initiation phase of the coagulation cascade ultimately resulting in the development of a fibrin clot.

1.4.2.2 Inhibition of Fibrinolysis

Normal fibrinolytic balance (Fig. 1.7) is required to ensure a delicate equilibrium between formation and breakdown of fibrin clots. Under normal physiological conditions, a clot develops due to the conversion of fibrinogen into fibrin by the enzyme thrombin. Thrombin also aids to stabilise the clot by activation of thrombin activatable fibrinolysis inhibitor which works to inhibit breakdown of fibrin. This clot may then be degraded by the enzyme plasmin which is activated by tissue plasminogen activator (tPa) from its inactive form plasminogen.

In patients with T2D, significantly elevated levels of fibrinogen were detected glucose during a 2.5mmol/L hyperinsulinaemic hypoglycaemic clamp (Aberer *et al*., 2019). During the clamp, blood samples were analysed once patients had stabilised at both 3.5mmol/L and 2.5 mmol/L blood glucose for 30 minutes. The rise in fibrinogen was not significant until subjects had become severely

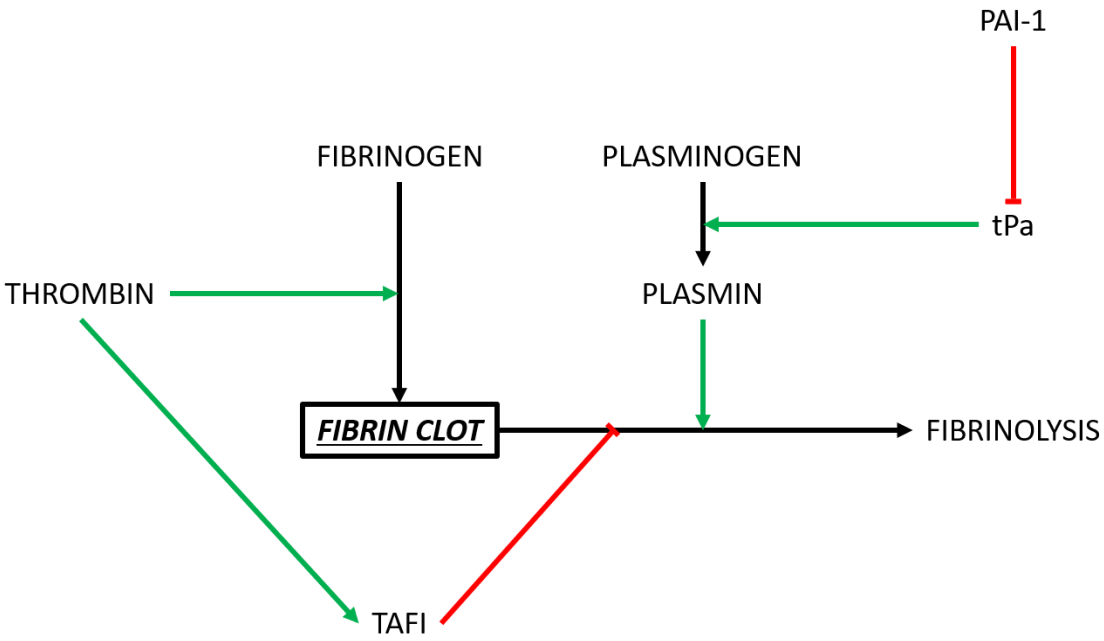

Fig. 1.7 Maintaining fibrinolytic balance. Fibrinolytic balance is maintained by tightly regulating the conversion of fibrinogen into a fibrin clot which undergoes fibrinolysis to produce fibrin degradation products. Inhibition (red) and catalysis (green) processes within the pathway are also identified. *Adapted* from Antovic and Blomback (2013)

hypoglycaemic, however, suggesting that mild or moderate hypoglycaemia may not be sufficient to influence this aspect of the coagulation cascade (Aberer *et al*., 2019).

Levels of thrombin-antithrombin (TAT) are a good indicator of the levels of thrombin within the blood. A study by Joy *et al*. (2015) reported that in healthy individuals, hypoglycaemia significantly increases TAT levels compared to at euglycaemia. Additionally, this increase in TAT was significantly greater in a subject who had received 3 hyperinsulinaemic hypoglycaemic clamps over 2 days compared to those who had received two clamps over one day (Joy *et al*., 2015). This data indicates that a single hypoglycaemia episode is sufficient to cause an elevation in thrombin levels with each additional episode capable of inducing a further increase. The partial thromboplastin time (PTT) is a test performed on blood samples which may determine the rate at which blood will clot and may also be indicative of vWF or thrombin expression with a shorter time suggesting the blood within the patient is able to clot faster. The effects of insulin induced hypoglycaemia on PTT have been determined on people with T1D and age matched healthy subjects (Dalsgaard Nielsen *et al*., 1982). Haemostatic data was analysed immediately, 60 minutes and 120 minutes following receival of

insulin. It was found that whilst the activated PTT decreased in both groups, it was significantly decreased in the individuals with T1D compared to the healthy subjects, 120 minutes after infusion of insulin had stopped (Dalsgaard Nielsen *et al*., 1982).

In addition to this, the degradation of fibrin is also affected after a period of hypoglycaemia. Following a 4-hour period of euglycaemic plasma glucose being maintained, healthy individuals were infused with insulin at 9pmol/kg/min and plasma glucose kept at 2.9mmol/L for 2 hours. Analysis of arterial blood, acquired at both the beginning of the euglycaemic period and the end of the clamp, revealed an increase in plasminogen activator inhibitor-1 (PAI-1), which inhibits the activation of plasmin by tPa. This is in contrast to those undergoing a hyperinsulinaemic hyperglycaemic or hyperinsulinaemic euglycaemic clamp who exhibited a significant decrease in PAI-1 levels (Joy *et al*., 2016). This report complements the findings of an earlier study, involving healthy subjects, in which a 2.9mmol/L glucose hyperinsulinaemic hypoglycaemic clamp performed the day after a euglycaemic clamp resulted in significantly increased PAI-1 levels (Joy *et al*., 2015). In this same study, however, the potential benefits of recurrent hypoglycaemic episodes were also observed. By subjecting participants to a hypoglycaemic clamp one day following two additional hypoglycaemic clamps, the levels of PAI-1 decreased, though non-significantly, compared to what they were after the Day 1 procedure. Nevertheless, even in this group of patients, the circulating levels of PAI-1 were still significantly higher compared to those who had not been exposed to hypoglycaemic during the trial (Joy *et al*., 2015). When comparing the baseline PAI-1 values of persons with T1D to those of healthy individuals, it was discovered that those with diabetes express higher PAI-1 levels under euglycaemic conditions suggesting that those with diabetes are frequently in a pro-thrombotic state. However, when these patients underwent a hypoglycaemic clamp, again at 2.9mmolL blood glucose, the PAI-1 levels dropped significantly to what is expected in a person without the condition thereby supporting the hypothesis that hypoglycaemia possesses the potential to be at least partially beneficial (Joy *et al*., 2010).

Finally, an early clinical study, between healthy subjects and insulin dependent persons with poorly controlled diabetes, which is likely to be T1D although this is

not specified, revealed that those in the diabetic group had significantly reduced baseline levels of tPa reasserting the idea that those with diabetes are in a state of fibrinolytic imbalance (Fisher *et al*., 1991). The result of these pathway alterations is that there is an increase in clot formation with a decrease in its degradation.

Under physiological conditions, leukocytes assist in maintaining normal coagulation and blood flow by producing cytokines which modulate vascular endothelial cell adhesion molecule expression. Leukocytes also release enzymes which interact with coagulation cascade components to inhibit anticoagulant activity and activate fibrinolytic factors. However, during a pro-inflammatory stimulus, leukocytes undergo a significant change in their phenotype. They become a primary source of pro-coagulation factors with monocytes being the biggest source of tissue factor which itself is responsible for the initiation of the coagulation cascade. Additionally, leukocytes provide a surface for aggregation of coagulation factors and assembly of complexes required for the coagulation cascade to proceed (Swystun and Liaw, 2016). Therefore, the pro-thrombotic state may be induced largely due to the induction of a pro-inflammatory state.

1.4.3 Induction of an Inflammatory State

Several studies have gone on to confirm that hypoglycaemia is associated with changes in levels of various cytokines due to the increase in the population of circulating immune cells. In one clinical trial, healthy subjects as well as T1D patients both with and without impaired awareness to hypoglycaemia (IAH) were recruited. They underwent a hyperinsulinaemic euglycaemic, 5.0mmol/L plasma glucose, and severe hypoglycaemic, 2.6 mmol/L plasma glucose, clamp. Hypoglycaemia was maintained for 60 minutes, and blood samples taken throughout to perform inflammatory analysis. When stimulated with a toll-like receptor 4 agonist, isolated PBMCs produced greater levels of the cytokines Interleukin (IL)-6, IL-1β and tumour necrosis factor α (TNFα) when taken from both healthy subjects and T1D patients without IAH following 1 hour of hypoglycaemia. This effect however was not observed in those with IAH which correlated with the suppressed adrenaline response to hypoglycaemia in this group (Ratter et al., 2017). This reaffirmed findings from an earlier study in which

healthy persons and those with T1D were subjected to a 2.9 mmol/L glucose hypoglycaemic clamp (Joy *et al*., 2010). In this study, IL-6 was significantly increased in both groups during hypoglycaemia in comparison to euglycaemia. In the subjects with T1D, TNFα also significantly increased whilst hypoglycaemic. Additionally, levels of the adhesion molecules VCAM and ICAM-1 significantly increased during hypoglycaemia in both groups and significantly decreased during euglycaemia (Joy *et al*., 2010).

Cytokines and histones have significant effects on the coagulation cascade. Cytokines and oxidants generated by neutrophils impair the cleavage of vWF which would go some way to explain why prior studies have seen the increase in vWF levels following hypoglycaemia (Swystun and Liaw, 2016). Cytokines can also stimulate exocytosis of Weibel Palade bodies which induces the release of vWF as well as P-selectin (Swystun and Liaw, 2016).

A principal mediator of inflammatory pathways is the CD40 antigen. Binding of CD154 on T cells to CD40 triggers activation of B cells and increases the expression of CD40 and TNF receptors on the surface of macrophages increasing their chance of being activated to release reactive oxygen species. Healthy subjects and those with T1D were exposed to euglycaemia at 4.5 mmol/L and hypoglycaemia at 2.5 mmol/L blood glucose. In both groups, expression of CD40 increased to a maximum 24 hours after hypoglycaemia with a slightly greater rise observed in the T1D group. This not only indicates that hypoglycaemia promotes inflammation but that the effect is not necessarily rapid acting (Wright *et al*., 2010).

Using flow cytometry, it was confirmed that adrenaline was a key mediator of the pro-inflammatory response due to hypoglycaemia. It was found that an increase in adrenaline correlates with an increase in the mobilisation of potential cytotoxic cells, namely: $CD8^+$ T cells, γ/δ T cells, natural killer T-like cells, cytotoxic natural killer cells and proinflammatory monocytes, through activation of β2 adrenoceptors. Interestingly however, there was no increase in the mobilisation of cells which did not possess cytotoxic potential (Dimitrov *et al*., 2010).

1.4.4 Endothelial Dysfunction and Cardiovascular Tissue Damage

Hypoglycaemia appears to affect the degree of permanent tissue damage following a significant ischaemic episode. In a study by Paelestik *et al*. (2017), Zucker fatty diabetic rats, used as a model of T2D, and lean controls, were exposed to either hypoglycaemia or normoglycaemia targeted at blood glucose of 3mmol/L or 11mmol/L respectively. Rats were anaesthetised and a tracheotomy and cannulation of the heart were performed. Hearts were perfused for a period of 40 minutes after which they were subjected to a 40-minute period of ischaemia followed by 2 hours of reperfusion. Hearts were removed and assembled upon Langendorff perfusion apparatus. An in-line flow probe was used to measure coronary flow and haemodynamic data was obtained. Once this was complete, hearts were frozen and sliced for staining with 2,3,5-triphenyltetrazolium chloride to measure infarct size. In both the diabetic and healthy groups, infarct size was significantly larger in those who had been hypoglycaemic. Conversely, rate pressure product, used as an indicator of the energy used by the heart and the stress placed upon the cardiac muscle, was lower after hypoglycaemia was given to the diabetic rats which suggests that oxygen may be being used in a more efficient manner (Paelestik *et al*., 2017). In a similar study by Dave *et al*. (2011), Wistar rats were injected with 60mg/kg streptozotocin to induce T1D by destruction of pancreatic β cells. Rats in the recurrent hypoglycaemia group underwent 2 hyperinsulinaemic hypoglycaemic clamps, targeted at blood glucose of approximately 3.0-3.6mmol/L, per day for 5 consecutive days. Those in the control group experienced a similar protocol although a 10% dextrose solution was simultaneously infused to maintain euglycaemia at 5.5-6.5mmol/L plasma glucose. In 2 separate groups of T1D rats, either a single 30-minute hypoglycaemic episode was induced via an 8U/kg insulin injection or a 40-minute period of euglycaemia was maintained by 4 separate 2U/kg insulin injections alongside 1mL of a 10% dextrose solution. One day following the final hypoglycaemic episode, all rats were anaesthetised and received 8 minutes of cerebral ischaemia. Rats were allowed to recover and 7 days later, their hippocampi analysed. It was concluded that insulin treatment decreased the amount of ischaemic damage by 64% compared to untreated rats with T1D who showed 70% more damage than the control group. However, those who experienced recurrent hypoglycaemia alongside insulin treatment exhibited 44% more damage than those treated with insulin without recurrent

hypoglycaemia. Additionally, the insulin treated recurrently hypoglycaemic T1D rats also generated larger quantities of free radicals from their mitochondria (Dave *et al*., 2011)

Healthy piglets have been used to demonstrate a link between hypoglycaemia and ROS generation due to mitochondrial dysfunction. Piglets were given 25U/kg lispro insulin and hypoglycaemia was maintained, with additional 5U/kg insulin boluses and 5% dextrose infusion, for a 2-hour time period once blood glucose levels had reached 2mmol/L. The control group was given a 5% dextrose infusion to maintain euglycaemia at 4-6mmol/L. Following euthanasia, the cerebral cortexes of the piglets were dissected, and mitochondria isolated. ROS generation by the mitochondria was determined using chemiluminescence and found that both superoxide and peroxide levels were significantly elevated in piglets who had undergone hypoglycaemia (McGowan *et al*., 2006). The precise mechanisms underlying the cause of mitochondrial dysfunction are still under investigation although existing studies have highlighted the potential importance of intracellular calcium levels. Calcium plays a pivotal role in the pathogenesis of several CVDs and cardiac remodelling (Berridge *et al*., 2003). Cells are extremely sensitive to changes in calcium levels and excess calcium within the cytosol leads to mitochondrial dysfunction. Increased intramitochondrial calcium has been associated with the production of ROS as well as deterioration of cellular function as nuclear signalling and organelle dynamics are dysregulated (Pivovarova and Andrews, 2010). During hypoglycaemia, an increase in intracellular calcium release has been observed although much of this research has been largely conducted within the brain and neuronal cells (Rehni *et al*., 2015)

Elevations in mitochondrial superoxide levels are associated with hypoglycaemia hence reducing the bioavailability of NO. In a previously discussed study by Joy et al. (2016), NO mediated vasodilation was determined through the use of flow mediated dilatation (FMD) ultrasound of the main brachial artery during nitroglycerin administration and reactive hyperaemia. This procedure was performed immediately before the commencement of a glucose clamp and during the final 30 minutes of the clamp period. The result of this experiment revealed a significant decrease in endogenous NO stimulated vasodilation following a hyperinsulinaemic hypoglycaemic clamp which is not observed in subjects who

had undergone either the hyperinsulinaemic euglycaemic or hyperglycaemic clamps (Joy *et al*., 2016).

Endothelins are a family of vasoconstrictors which play a major role in regulating CV function. They are also implicated in the pathogenesis of diabetes associated vascular dysfunction and are proposed to be important in developing microangiopathy (Wright *et al*., 2007). Using radioimmunoassay techniques, it has been observed that individuals with both T1D and T2D had significantly elevated plasma endothelin levels (Takahashi *et al*., 1990). They are produced by vascular endothelial cells following stimulation by adrenaline as well as ischaemia and hypoxia. Endothelin-1 is the main isoform found in humans and induces proliferation of smooth muscle and a prolonged period of vasoconstriction. Wright *et al*. (2007) gave T1D patients, without evidence of microangiopathy, a 2.0mU/kg/min insulin infusion until autonomic symptoms of hypoglycaemia, such as increased heart rate, systolic blood pressure and sweating, were evident. Plasma endothelin (ET-1) levels were determined prior to insulin infusion commencement, at the onset of hypoglycaemia as well as 15 and 60 minutes after this hypoglycaemia onset. Levels steadily rose once infusion had begun and were significantly higher by 60 minutes following onset of hypoglycaemia. The trend in endothelin followed that of adrenaline thereby supporting previous studies suggesting adrenaline stimulates ET-1 production (Wright *et al*., 2007).

In an additional study by Gimenez *et al*. (2010), patients with T1D with or without recurrent hypoglycaemia were held at euglycaemia and approximately 2.8mmol/L plasma glucose hypoglycaemia for 30 minutes whilst completing evaluations for hypoglycaemic awareness. These individuals, plus healthy controls, received ultrasound imaging of brachial, carotid, and femoral arteries in order to determine endothelium dependent vasodilation following reactive hyperaemia as well as the thickness of the intima and media layers of the arteries. Both T1D groups exhibited reduced FMD following ischemia in comparison to the healthy controls, and those with a history of recurrent hypoglycaemia exhibited a further reduced response in comparison to their non-diabetic counterparts. The intima media thickness of carotid and femoral arteries was higher in the recurrent hypoglycaemia group compared to those without recurrent hypoglycaemia and

the healthy individuals. Additionally, there was no difference in the thickness of the intima media between the healthy subjects and those without recurrent hypoglycaemia (Gimenez *et al*., 2010). This data therefore suggests that diabetes alone does not necessarily cause endothelial dysfunction, yet recurrent hypoglycaemia has a major impact on the functionality of the arteries.

1.5 Hypoxic and Ischaemic Preconditioning

In hypoxic and ischaemic preconditioning, prior exposure to a mild hypoxic or ischaemic stimulus results in protection being conferred against a more severe hypoxic or ischaemic insult. In a review article by Bolli (2000), it is stated that protection is conferred in a biphasic manner. The early phase lasts 2-3 hours and develops rapidly following exposure to ischaemia. The delayed phase begins between 12 and 24 hours post ischaemia and can last for 72-96 hours (Bolli, 2000).

1.5.1 Ischaemic Preconditioning

Murry *et al*. (1986) were the first people to publish data relating to the proof of principal of IPC induced cardioprotection. Dogs received IPC of the circumflex coronary artery by performing 4 cycles of 5 minutes occlusion/5 minutes reperfusion. Subjects then underwent a severe ischaemic insult by occluding the same artery for an additional 40 minutes and allowing reperfusion for 4 days. Control animals were not given IPC but did undergo the ischaemic insult. After the 4-day reperfusion period, infarct size was significantly reduced in the IPC group of dogs compared to the controls therefore indicating there is a cardioprotective effect of the treatment (Murry et al., 1986)

1.5.2 Remote Ischaemic Preconditioning

R-IPC is a phenomenon in which a peripheral tissue, such as an arm or leg, undergoes the IPC treatment which allows protection to be conferred to another area of the body, including the heart, brain, and liver. This can arise due to the circulating mediators which are released at the IPC site and are able to travel to other tissues within the body. The advantage of this technique, over standard IPC, is that the technique is non-invasive and therefore can easily be translated into the clinic.

The theory of R-IPC was initially posited by Przyklenk *et al*. (1993) who exhibited that inducing IPC via one artery can confer protection against ischaemic damage to the heart caused by the prolonged occlusion of a second supplying blood to the same organ. Dogs underwent 4 cycles of 5 minutes occlusion/5 minutes reperfusion of the circumflex coronary artery. This was followed by 1 hour occlusion of the left anterior descending (LAD) coronary artery and 4.5 hours of reperfusion. There was also a control group which did not receive the R-IPC treatment but was subjected to the ischaemic insult. The investigators found that the infarct size was significantly reduced in the hearts given R-IPC in comparison to the controls (Przyklenk *et al*., 1993).

Oxman *et al*. (1997) went a stage further and determined that by preconditioning a limb with ischaemia, the myocardium is protected. R-IPC was induced in Sprague-Dawley rats by tightening a tourniquet around the lower hindlimb to occlude blood flow for 10 minutes. This was then removed for a 10-minute reperfusion period. Hearts were excised and a prolonged ischaemic insult invoked by ligation of the left descending coronary artery for 30 minutes, succeeded by 15 minutes reperfusion. A control group of rat hearts, taken from subjects that had not undergone R-IPC, received the ischaemic insult only. Analysis revealed that the prevalence of reperfusion arrhythmia, a type of irregularity in heart rate which develops immediately following the restoration of blood flow after ischaemia, was significantly decreased in the hearts removed from the rats treated with R-IPC compared to those belonging to the controls. This therefore suggested that preconditioning one tissue confers protection to another against a more severe form of that stimulus (Oxman *et al*., 1997).

The first documented clinical application of R-IPC was in children due to undergo cardiopulmonary bypass surgery. To induce R-IPC, 4 cycles of 5 minutes ischaemia/5 minutes reperfusion were performed on the lower limb of children using a blood pressure cuff. The remaining patients received a control treatment by wearing a deflated blood pressure cuff around the leg. Cardiopulmonary bypass surgery was conducted between 5- and 10-minutes following R-IPC or control intervention. Postoperative cardiac troponin-I (cTnI) levels were significantly higher in children given control treatment compared to those who received R-IPC. Elevated cTnI levels are indicative of greater myocardial injury

meaning this data suggests that the R-IPC protocol employed provides a degree of cardioprotection to an individual (Cheung *et al*., 2006).

There are several murine models of R-IPC recorded in the literature (Table 1.1) which were taken into consideration when designing an *in vivo* R-IPC model as in chapters 3 and 4. However, other species and *in vitro* models have also been employed to elucidate mechanisms and to investigate the effects of various pathologies, including diabetes, on the efficacy of R-IPC.

1.5.3 Hypoxic Preconditioning

HPC was first demonstrated by Shizukuda *et al*. (1992) by perfusing mongrel dogs with deoxygenated blood. IPC and HPC treatment were given by performing a cycle of 5 minutes occlusion/10 minutes reperfusion of the LAD artery, or 5 minutes hypoxic blood perfusion/10 minutes reoxygenation respectively. A control group did not receive any preconditioning. Severe ischaemia was induced in all groups by occluding the LAD artery for 60 minutes followed by a 5-hour period of reperfusion. In hearts pre-treated with HPC or IPC, infarct size was reduced to 7.2% and 4.6%, respectively, compared to 22.4% in those in the control cohort (Shizukuda *et al*., 1992). It was therefore concluded that HPC and IPC offer similar degrees of cardioprotection in the event of a severe ischaemic insult. It should be noted that, in a clinical setting, deoxygenated blood would not be used to administer HPC but instead the patient would inhale deoxygenated gas using suitable apparatus.

1.5.4 Impact of Diabetes on IPC and R-IPC

The efficacy of R-IPC in persons with diabetes is a controversial subject with several studies providing contradictory data. It appears the bulk of the literature would imply that the treatment cannot invoke CV protection in these individuals. Kersten *et al*. (2000), concluded that IPC was unable to offer protection in dogs with diabetes. Dogs, with and without diabetes, were exposed to 40 minutes IPC, consisting of 4 cycles of 5 minutes occlusion/5 minutes reperfusion, followed by 60 minutes occlusion and 3 hours reperfusion of the LAD artery. Infarct size was measured and those without diabetes had a significantly smaller area of risk (Kersten *et al*., 2000). Therefore, it could be deduced that diabetes abolishes the

Mouse Strain	Method of Inducing R-IPC	Method Used to Confirm Successful Induction of R-IPC	Anaesthetic Agent Used	Reference
Bmal1 -/- and WT C57BL/6 mice	2 cycles of 10 minutes ischaemia/10 minutes reperfusion by using an elastic band around the left hindlimb	Reduced infarct size following a period of cerebral ischaemia	Isoflurane	Brager *et al*., 2016
C57BL/6 mice	3 cycles of 5 minutes ischaemia/5 minutes reperfusion by clamping of the femoral vascular bundle	Reduced acute tubular injury following induction of renal ischaemia-reperfusion injury	Xylazine and Zoletil	Cho *et al*., 2017
IL-10 -/- and WT C57BL/6 mice	3 cycles of 5 minutes ischaemia/5 minutes reperfusion using a micro vessel clip on the left femoral artery	Reduced infarct size following a myocardial infarction and subsequent reperfusion period	Pentobarbital	Cai *et al*., 2012
HIF1α +/- and WT mice	3 cycles of 5 minutes ischaemia/5 minutes reperfusion by clamping the femoral artery	Reduced infarct size following a myocardial infarction and subsequent reperfusion period	Pentobarbital	Cai *et al*., 2013
C57BL/6 mice	3 cycles of 5 minutes ischaemia/5 minutes reperfusion using a vascular occluder placed around the hind limb	Reduced infarct size following a myocardial infarct and subsequent reperfusion period	Pentobarbitone	Yellon *et al*., 2018

STZ induced T1D C57BL/6 mice	3 cycles of 10 minutes ischaemia/10 minutes reperfusion using gauze ropes placed around the hind limbs	Reduced infarct size and oedema following a period of cerebral ischaemia	Isoflurane	Liu C *et al*., 2019
T2D db/db mice	3 cycles of 10 minutes ischaemia/10 minutes reperfusion using gauze ropes placed around the hind limbs	Reduced infarct size and oedema following a period of cerebral ischaemia	Isoflurane	Liu *et al*., 2020
WT C57BL/6 mice	4 cycles of 5 minutes ischaemia/5 minutes reperfusion by femoral vascular bundle clamping	Reduced necrosis of the liver and alanine amino-transferase following hepatic ischaemia-reperfusion injury	Isoflurane	Oberkofler *et al*., 2014
C57BL/6 mice	4 cycles of 5 minutes ischaemia/5 minutes reperfusion using a blood pressure placed around the hindlimb	Changes in the microcirculatory blood flow in both the preconditioned and non-preconditioned hind limbs	Unspecified	Abdul Ghani *et al*., 2014
Mb -/- mice	4 cycles of 5 minutes ischaemia/5 minutes reperfusion using a cuff placed around the hindlimb	Reduced infarct size following a myocardial infarct and subsequent period of reperfusion	Unspecified	Rassaf *et al*., 2014

miR-21 -/- and WT C57BL/6 mice	4 cycles of 5 minutes ischaemia/5 minutes reperfusion by clamping the femoral arteries with microvascular clips	Improved survival rate and reduced damage resulting from cecal ligation and puncture	Sodium pentobarbital	Pan *et al*., 2019
WT C57BL/6 mice	4 cycles of 5 minutes ischaemia/5 minutes reperfusion using a blood pressure cuff around the hindlimb	Reduced infarct size and creatine kinase release following a myocardial infarct and subsequent reperfusion	Tribromoethanol	Abdul Ghani *et al*., 2017
WT C57BL/6 mice	6 cycles of 4 minutes ischaemia/4 minutes reperfusion by applying pressure over the femoral vessels	No specific validation method was employed although changes in myocardial genes were observed	Ketamine and xylazine	Konstantinov *et al*., 2005
eNOS -/- WT C57BL/6 mice	6 cycles of 4 minutes ischaemia/5 minutes reperfusion by using a tourniquet around the hindlimb	Preservation of hepatic micro-vascular blood flow following induction of hepatic ischaemic-reperfusion injury	Isoflurane	Abu Amara *et al*., 2011
C57BL/6 mice	6 cycles of 4 minutes ischaemia/4 minutes reperfusion by clamping of the femoral vascular bundle	Reduced apoptosis, injury score and alanine aminotransferase following hepatic ischaemia	Isoflurane	Li *et al*., 2016

HIF +/- and WT hybrid 129/Sv X Swiss mice	4 cycles of 5 minutes ischaemia/5 minutes reperfusion by clamping the right femoral artery	Reduced infarct size following a myocardial infarct and subsequent period of reperfusion	Sodium pentobarbital	Kalakech *et al*, 2013

Table 1.1. Mouse models of R-IPC. A summary of the most prevalent mouse models of R-IPC indicating the strain of animal, method of R-IPC induction and confirmation, and anaesthetic agents used.

cardioprotection normally exerted by R-IPC. There are a few reasons as to why this may be but the effect of hyperglycaemia, a glycaemic state associated with diabetes, could be the main cause for this.

IPC has been shown to exacerbate the hyperglycaemia mediated increase in ischaemia reperfusion injury *in vitro*. Glomerular endothelial cells were cultured in either normoglycaemia, 5.5mmol/L glucose, or hyperglycaemia, 25.5mmol/L glucose, for 7 days. IPC treatment was given to half of the cells by inducing oxygen glucose deprivation (OGD) for 1 hour followed by 24 hours of reoxygenation and glucose replenishment. Cells were then subjected to prolonged ischaemia-reperfusion through 8 hours of OGD succeeded by a 12-hour recovery period. TEER was measured at various points through the protocol. After 7 days of hyperglycaemic culture, TEER was lower in comparison to those incubated in normoglycaemia indicating high glucose alone disrupts integrity of the endothelial barrier. The same trend was also seen in hyperglycaemia-cultured cells exposed to both prolonged ischaemia-reperfusion only, and IPC with prolonged ischaemia reperfusion. This implies that hyperglycaemia exacerbates ischaemic-reperfusion injury even when IPC treatment is given. Interestingly, in normoglycaemia-cultured cells, there was an increased trend in TEER between the baseline, post IPC and post prolonged ischaemia-reperfusion whereas a decrease was observed in the hyperglycaemia treated cells (Schenning *et al*., 2015).

Further evidence of this was provided in dogs divided into 5 groups: i) control, ii) IPC, iii) 300mg/dl glucose hyperglycaemia with IPC, iv) 300mg/dl hyperglycaemia. In groups iii and iv, dogs were administered with dextrose for 70 minutes to glucose concentrations of 300mg/dl. Subjects in groups ii and iv received IPC treatment using 4 cycles of 5 minutes ischaemia/5 minutes reperfusion of the LAD artery. All animals were subjected to 60 minutes of ischaemia, by ligation of the LAD artery, followed by 3 hours of reperfusion. Average infarct sizes in the hearts from the control group were 24% whereas IPC conferred protection to the hearts by reducing infarct size to 8%. The presence of hyperglycaemia alone did not significantly increase the infarct size, compared to controls, although it was elevated to 34%. However, when given preceding

IPC, the cardioprotective effects were abolished as infarct size increased to 30% (Kersten *et al*., 1998).

In a separate study by Yang Z *et al.* (2013), using C57BL6 mice, subjects were injected with 20% dextrose, to induce hyperglycaemia, or saline. One of the hyperglycaemic groups was infused 0.1unit/mL insulin for 10 minutes 20 minutes after dextrose injection. After this time, animals underwent IPC by receiving 2 cycles of 5 minutes ischaemia/5 minutes reperfusion. Severe ischaemia was induced by ligation of the LAD artery for 40 minutes followed by 60 minutes reperfusion. Animals preconditioned and injected exhibited an infarct size of 25.8%. However, in those who had been exposed to hyperglycaemia, the infarct size was increased to 58%. When hyperglycaemia was corrected with administration of insulin, the preconditioning effect was partially restored and the infarct size reduced to 33% (Yang Z *et al*., 2013).

As previously discussed, in section 1.2.1, hyperglycaemia negatively affects the HIF1α pathway which itself it necessary for eliciting IPC. Additionally, another pathway involved in mediating the response to IPC is the PKC pathway (Weinbrenner *et al*., 2002) which, as mentioned in section 1.2.3, is also influenced by hyperglycaemia. Therefore, it could be hypothesised that this may be why hyperglycaemia leads to the abolishment of IPC induced cardioprotection.

Paelestik *et al*. (2017), have investigated how IPC may provide protection to the myocardium in rats with T2D. Zucker fatty diabetic rats, and lean controls, were exposed to hypoglycaemia, 3mmol/L glucose, or normoglycaemia, 11mmol/L glucose. Whilst anaesthetised, they underwent a tracheotomy and hearts were isolated for cannulation. Hearts were perfused for 20 minutes, and IPC was induced in half of the subjects by completing two cycles of 5 minutes ischaemia/5 minutes reperfusion whilst the remaining half continued with a further 20 minutes of stabilisation. All hearts were subjected to a 40-minute period of ischaemia followed by 2 hours of reperfusion after which they were removed and transferred onto Langendorff apparatus. In the diabetic rats, infarct size was significantly reduced in those who had received IPC treatment in both the normoglycaemic and hypoglycaemic groups. However, this effect was only seen in the normoglycaemic group for the lean controls. Therefore, in this study, it was

concluded that hearts from the T2D rodents, yet not healthy rodents, could be offered some degree of cardioprotection during hypoglycaemia due to IPC treatment. Additionally, O-GlcNAc expression, an indicator of glucose uptake, was monitored and correlated with these findings. All hearts in the IPC groups, except those in the healthy hypoglycaemic group, exhibited significantly elevated O-GlcNAc levels. Hence, it confirmed prior conclusions that glucose uptake plays a significant role in the mechanism of IPC (Paelestik *et al*., 2017).

It was indicated by Russel *et al*. (2019) that successful induction of IPC depends upon the type of diabetes affecting the subject. For the purpose of their studies, T1D and T2D were induced in wild-type (WT) C57BL/6 mice by injecting them with 50mg/kg streptozotocin or, administering 75mg/kg streptozotocin and feeding them a high fat diet for 12 weeks, respectively. Control mice were also used who did not have any form of diabetes. Hearts were excised and perfused using Langendorff apparatus. IPC was given using 3 cycles of 5 minutes ischaemia/5 minutes reperfusion. Hearts were subjected to a severe ischaemic insult period of 25 minutes followed by 45 minutes of reperfusion. Out of the results obtained, expression of pro-apoptotic protein Bax and the recovery of left ventricular developed pressure (LVDP) are of particular interest. Bax expression was significantly decreased in control hearts treated with IPC. However, in hearts taken from mice with T2D, IPC was associated with a significant increase in Bax expression. Interestingly, there is no change in the expression of Bax when given IPC. This implies that IPC given to those with T2D only exacerbates apoptotic activity associated with ischaemic insult. Additionally, LVDP recovery was significantly elevated in the control and T1D IPC treated hearts, compared to those which were not given IPC. However, no such change was observed in those with T2D. This suggests that IPC may be of benefit to those with T1D but is possibly ineffective in patients with T2D (Russell *et al*., 2019). However, this is not confirmed by additional studies in individuals with diabetes.

In a study by Liu *et al.* (1993), diabetes was induced in Wistar rats by injection with 90mg/kg streptozotocin whilst controls received citrate buffer only. At 11 months of age, myocardial infarction was induced by ligating the left coronary artery for 45 minutes and reperfusion was allowed for 120 minutes. Immediately prior to this, a selection of the diabetic rats underwent IPC consisting of 3 cycles

of 5 minutes ischaemia/5 minutes reperfusion. Infarct size was significantly reduced in the preconditioned rats with diabetes indicated successful induction of cardioprotection by IPC (Liu *et al*., 1993).

In a study by Tatsumi *et al*. (1998), diabetes was induced in Sprague-Dawley rats using a single injection of 70mg/kg streptozotocin. These, plus non-diabetic controls, were allocated into 1 of 4 groups: i) normal control, ii) diabetic control, iii) normal preconditioned, iv) diabetic preconditioned. In groups ii and iv, hearts were preconditioned using 2 cycles of 5 minutes ischaemia/5 minutes reperfusion. All rats were subjected to a severe ischaemic insult by clamping the aorta for 30 minutes followed by a 30-minute reperfusion period. In the non-preconditioned hearts, the LVDP was reduced substantially throughout the prolonged ischaemia and never really recovered during the subsequent reperfusion period. However, in both preconditioning groups, there was a significant increase in the recovery of the LVDP, during the reperfusion period, although it remained below the pre-ischaemic value. Additionally, myocardial lactate was significantly reduced in both preconditioned cohorts after prolonged ischaemia (Tatsumi *et al*., 1998). These results indicate a degree of protection is conferred to the hearts by IPC taken from both healthy and diabetic rats although only very short-term effects of the preconditioning were assessed.

Tsang *et al*. (2005) determined that IPC may successfully invoke protection in persons with diabetes but depends on a stimulus threshold being achieved. Langendorff prepared hearts excised from Goto-Kakizaki and non-diabetic Wistar rats were treated with 1, 2 or 3 cycles of IPC, with each cycle consisting of 5 minutes ischaemia/10 minutes reperfusion. Control hearts from each rat species did not receive any IPC treatment. All hearts were subjected to a prolonged period of ischaemia. Wistar rat hearts treated with any number of IPC cycles exhibited a significant reduction in infarct size in comparison to controls. However, only Goto Kazikazi hearts receiving 3 cycles of IPC showed a significant decrease in infarct size. This implies that to invoke IPC mediated protection, a threshold must be reached which requires greater stimulation in those with diabetes. Therefore, this indicates that IPC could be induced in those with diabetes by increasing the number of cycles given (Tsang *et al*., 2005).

A preliminary clinical trial, reported by Maxwell *et al*. (2019), on individuals with T2D indicated that a 7-day R-IPC model could potentially improve the function of the peripheral vasculature. Daily R-IPC was induced by inflating and deflating a blood pressure cuff around the arm for 4 cycles of 5 minutes ischaemia/5 minutes reperfusion. Immediately before, as well as 1 and 8 days post the R-IPC regimen, endothelial function of the brachial artery was assessed. FMD measurements were taken twice per assessment day separated by an episode of 20 minutes ischaemia/20 minutes reperfusion of the arm. In R-IPC treated individuals, there was a 1.3% improvement in FMD in comparison to the control (Maxwell *et al*., 2019). This study contradicts data collected from the Russel *et al*. (2019) study but supports the preliminary conclusions made by Tsang *et al*. (2005) which suggests that greater preconditioning stimuli can exert a protective effect in those with T2D.

Therefore, after analysis of the literature, it is concluded that these preconditioning therapies could be of benefit to individuals with diabetes so long as certain criteria are met. It is worth noting, however, that R-IPC may be abolished in individuals displaying neuropathy due to the importance of neural mechanisms in eliciting the protection invoked. Firstly, glucose management, at least in the period immediately before preconditioning treatment, is essential to prevent hyperglycaemia which may render the therapy ineffective. Secondly, to achieve the threshold necessary to elicit the preconditioning response, more R-IPC cycles and/or treatment sessions should be given to those with diabetes.

1.5.5 Mechanisms of Protection

Preconditioning leads to increased cellular proliferation and glucose uptake as well as decreased apoptosis. The mechanisms underlying hypoxic and ischaemic preconditioning, resulting in these changes, are very complicated involving multiple neuronal and humoral mediators. However, it was decided that the focus on this thesis would be the humoral mediators due to impracticalities associated with using neuronal markers particularly regarding the *in vitro* experiments conducted using HUVECs, as discussed in chapter 5.

One protein which nicely explains the observed similarities between the

mechanisms of IPC and HPC is HIF1α. The effect of HPC on HIF1α has been demonstrated *in vitro* by Lu *et al.* (2018). Human SH-SY5Y neuroblastoma cells were either treated with HPC, using a single cycle of 9 hours 5% oxygen hypoxia/12 hours normoxia, or, maintained at normoxia throughout. Cells were exposed to severe hypoxia at 1% oxygen for 10 hours followed by a reoxygenation period of 12 hours. A cell viability assay confirmed protection conferred by HPX as the number of viable cells in the HPC with hypoxic insult group was significantly higher than those exposed to the hypoxic insult without HPC. Expression of HIF1α was significantly higher in cells treated with HPC plus hypoxic insult, in comparison to controls and those receiving only the severe hypoxia. As HIF1α promotes cell proliferation, this would suggest that increased HIF1α expression is involved in the induction of HPC mediated protection (Lu *et al*., 2018). To identify the role of HIF1α in WT and HIF1α heterogenous mice in IPC/R-IPC, subjects were treated with R-IPC using 3 cycles of 5 minutes occlusion/5 minutes reperfusion of the femoral artery. Control mice of each genotype were not given R-IPC treatment. A selection of mice was subjected to a myocardial infarction by ligation of the left coronary artery for 30 minutes followed by a 120 minute reperfusion period. Hearts were excised, and it was revealed that the infarct area was significantly reduced in the WT R-IPC mice in comparison to those in the WT control cohort. However, there was no difference in the infarct size between the R-IPC and control treated HIF1α heterogenous individuals. For mice who did not receive this ischaemic insult, 24 hours after the R-IPC period, immunoblots were performed on the heart tissue and revealed that there was a significant increase in phospho-Akt (p-Akt) in those taken from WT mice that had been given R-IPC (Cai *et al*., 2013). Therefore, it was concluded that HIF1α is necessary for successful induction of R-IPC and HPC. Due to the significant role of HIF1α in mediating the effects of both treatments, it is no real surprise that HPC is able to offer protection against ischaemia as previously discussed, in section 1.5.3.

There are many pathways involved in mediating the IPC and HPC response. However, for the purpose of this thesis, it was decided that, due to its ability to upregulate HIF1α translation (Masoud and Li, 2015), analysis of the phosphoinositide 3-kinase (PI3-K) pathway, via analysis of its downstream

targets, should be the primary focus (Fig. 1.8). The PI3-K pathway, also known as the PI3-K/Akt/mTOR pathway, is an important regulator of the cell cycle and its activation is required to elicit IPC, as confirmed by Rossello *et al.* (2018) Hearts were excised from C57BL/6 mice and divided into 4 experimental groups. In 3 of these groups, IPC was induced using 4 cycles of 5 minutes ischaemia/5 minutes reperfusion, whilst in a control cohort, no IPC was given. All 4 groups were subjected to a 35-minute severe ischaemic insult followed by a 120-minute reperfusion period. 100nM Akt inhibitor wortmannin was administered to 2 of the IPC groups at different timepoints during the protocol. In 1 of these cohorts, wortmannin was given 20 minutes prior to and throughout the IPC procedure. In the second group, wortmannin was administered during the first 30 minutes following the 35-minute period of severe ischaemia. Infarct size in the IPC group was significantly reduced to 21%, in comparison to the control subjects with an infarct size of 59%. However, treatment with wortmannin did not allow IPC to be invoked as infarct sizes were 46% when the drug was given before or after the preconditioning (Rossello *et al*., 2018). This indicates that the PI3-K pathway is critical in mediating IPC and when inhibited, protection cannot be conferred.

The anti-inflammatory cytokine IL-10 activates the PI3-K pathway (Sharma *et al*., 2011), and mediates IPC. An early study implicated changes in IL-10 expression dependent upon whether IPC treatment was given. Lean Zucker rats were allocated into 3 groups: i) control, ii) ischaemic insult only, iii) IPC plus ischaemic insult. In group iii, animals were treated with a single cycle of IPC consisting of 5 minutes occlusion/10 minutes reperfusion. The livers of rats in groups ii and iii were given an ischaemic insult. When compared to livers obtained from control and ischaemic insult only individuals, there was a significant elevation in the IL-10 expression in livers from subjects treated with IPC prior to being given a severe ischaemic insult (Serafin *et al*., 2004). To confirm the role of IL-10 in R-IPC, preconditioning treatment was given by performing 4 cycles of 5 minutes ligation/5 minutes reperfusion of the femoral vascular bundle. 1 hour following the R-IPC treatment group, expression of IL-10 was consistently elevated in the intestine, lung, kidney, heart, and liver in comparison to the controls who did not receive R-IPC (Oberkofler *et al*., 2014).

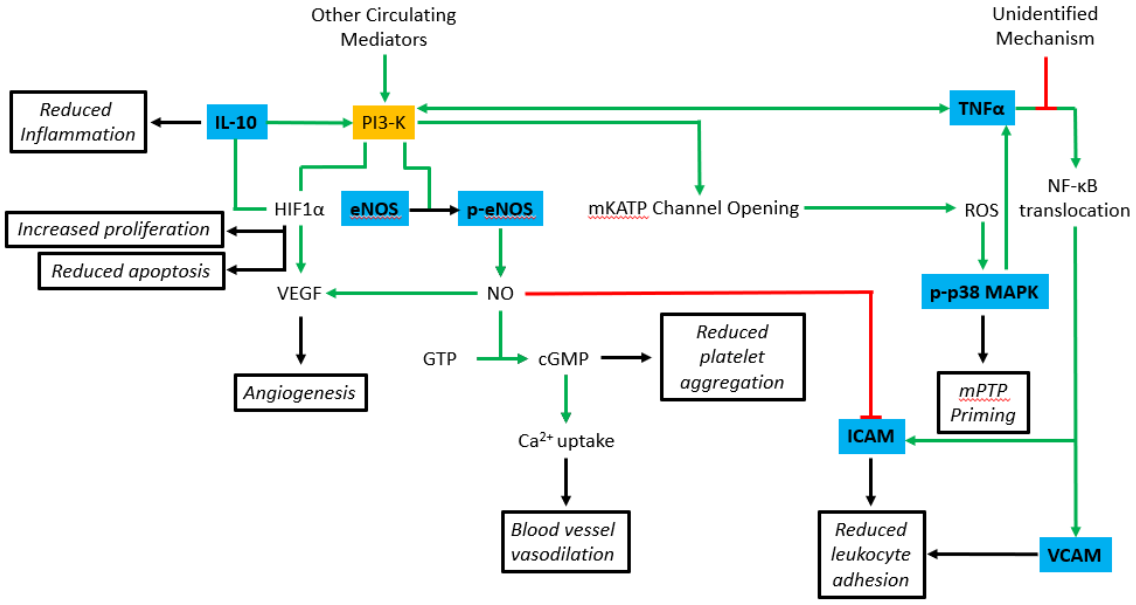

Fig. 1.8 Molecular mechanism of R-IPC via the PI3-K pathway at the vascular endothelium. A principal mediator in the R-IPC induced improvements in endothelial function is the PI3-K (orange) pathway. The PI3-K pathway is activated by circulating mediators, including the cytokines IL-10 and TNFα, which are released in response to the shear stress following a cycle of ischaemic-reperfusion. Activation of the PI3-K pathway results in: blood vessel vasodilation, increased cellular proliferation, reduced platelet aggregation, reduced apoptosis, angiogenesis, reduced leukocyte adhesion and priming of the mitochondrial permeability transition pore (mPTP). The precise mechanisms are extremely complex but the role of the blue highlighted molecules are discussed further in section 1.5.5 and were the focus of this thesis. Green and red lines indicate activation and inhibition of a process respectively.

There are changes in the expression of biomarkers, downstream of PI3-K, associated with preconditioning. The PI3-K pathway regulates expression of other inflammatory cytokines including TNFα. Qiu *et al*. found that osteoblasts treated with 1nM calyculin A for 2 hours exhibit a significant increase in TNFα mRNA expression. However, when also incubated with 10μM of PI3-K inhibitor LY294002, expression of TNFα was decreased to levels seen in untreated cells therefore implying that the PI3-K pathway modulates TNFα expression (Qiu *et al*., 2008).

TNFα is another cytokine which when secreted regulates expression of VCAM and ICAM-1 in the body (Qureshi *et al*., 2003). TNFα typically increases the transcription of VCAM and ICAM-1 via initiating the translocation of the transcription factor nuclear factor κ-light-chain-enhancer of activated B cells (NF-κB) to the nucleus. Following IPC, it appears that this process is inhibited resulting

in reduced leukocyte adhesion. However, the precise cause of this disruption is not yet clear (Ji *et al*., 2015). Ji *et al*. (2015) have suggested a role for these proteins in mediating IPC in the intestine. Rats were allocated into 3 groups: i) sham, ii) ischaemic insult only, iii) IPC plus ischaemic insult. Rats received IPC treatment by performing 3 cycles of 5 minutes ischaemia/5 minutes reperfusion of the superior mesenteric artery. An ischaemic insult was induced in groups ii and iii via occlusion of the superior mesenteric artery for 40 minutes followed by a 4-hour reperfusion period. Haemotoxylin and eosin staining revealed that the degree of intestinal injury in the ischaemic insult only group was significantly elevated in comparison to the sham group. There was also an increase in the intestinal injury scores in the IPC plus ischaemic insult group, but this was non-significant. They were, however, significantly decreased in comparison to those obtained from the ischaemic insult only cohort. Intestinal TNFα levels were increased in both cohorts receiving the ischaemic insult, although this was only significant in group ii. Additionally, those pre-treated with IPC exhibited significantly less TNFα expression compared to those in the ischaemic insult only group. Expression profiles of both VCAM and ICAM-1 followed the same trend. In each of the ischaemic insult cohorts, VCAM and ICAM-1 expression was increased with significance only being found in group ii. Also, intestinal tissue taken from rats pre-treated with IPC exhibited significantly decreased expressions of VCAM and ICAM-1 compared to the ischaemic insult only group (Ji *et al*., 2015). This data therefore implies that TNFα, VCAM and ICAM-1 are involved in mediating IPC conferred protection.

TNFα also regulates p38 mitogen activated protein kinase (p38 MAPK) activity. Interestingly, p38 MAPK is then able to regulate TNFα expression (Sabio and Davis, 2014). p38 MAPKs are 1 of the 3 classes of mitogen activated kinase which are activated in response to stress stimuli and influence cell differentiation and apoptosis. p38 MAPKs have also been associated with priming of the mitochondrial permeability transition pore (mPTP). Activation of PI3-K and TNFα lead to the opening of the mitochondrial KATP (mKATP) channels which in turn increases the production of ROS. p38 MAPK is activated in response to ROS and causes the mPTP to open. Under periods of prolonged ischaemia, this would be destructive to the mitochondria. However, the period of ischaemia associated with IPC is brief, and the mPTP closes again during the reperfusion period. This

process has been associated with an increase in myocardial survival (Abete *et al*., 2011). In a study by Mocanu *et al*. (2000), the effect of p38 MAPK inhibitor SB203580 on IPC was determined. Rat hearts were isolated and perfused using the Langendorff setup. Some were given IPC using 2 cycles of 5 minutes occlusion/10 minutes reperfusion whereas controls did not receive this treatment. Hearts were then subjected to prolonged ischaemia for 35 minutes and reperfusion allowed for an additional 120 minutes. subjected to p38 MAPK activity is involved in mediating IPC. 10μM SB203580 was perfused into the hearts either during the IPC treatment or immediately prior to the ischaemic insult. IPC alone significantly reduced infarct size to 13.4% compared to 38.9% in those that did not receive IPC. When the p38 MAPK inhibitor was given during the IPC protocol, protection was still conferred, leading to infarct size of 14.6%. However, when perfused before the ischaemic insult, IPC was not effective in mediating cardioprotection as infarct size was 36.2% (Mocanu *et al*., 2000). This therefore implies that p38 MAPK activity is required to invoke IPC induced protection against ischaemia.

eNOS is a member of the NOS family involved in regulating vasodilation by catalysing synthesis of NO. NO also inhibits IL-1β mediated ICAM-1 transcription thereby decreasing leukocyte adhesion (Berendji Grun *et al*., 2001). Additionally, via its activation of cyclic guanosine monophosphate, NO reduces platelet aggregation (Nong *et al*., 1997). When eNOS knockout mice were exposed to R-IPC, protection was not conferred against a severe ischaemic insult. To confirm the protocol had potential for success, both male and female WT and eNOS knockout mice were treated with either IPC, consisting of 3 cycles of 5 minutes ischaemia/5 minutes reperfusion, or a control treatment. They were then subjected to a severe ischaemic insult in which the LAD coronary artery was occluded for 30 or 60 minutes. Infarct size was significantly reduced in WT mice pre-treated with IPC in comparison to those who only received the ischaemic insult, regardless of gender and whether the 30- or 60-minute occlusion period was used. However, in the eNOS knockouts, infarct sizes between the IPC and insult only groups were non-significant when 30 minutes of prolonged ischaemia was used, in both genders, and in females exposed to 60 minutes severe ischaemia. In male eNOS knockouts, the 60 minutes of severe ischaemia proved to be fatal in the IPC treated and insult only groups indicating the females may

maintain innate protection likely due to hormonal differences. (Talukder *et al*., 2010). A further study was conducted linking eNOS in IPC to PI3-K pathway activity by Yang C *et al*. (2013) Hearts were excised from Sprague Dawley rats and perfused using Langendorff apparatus. In 2 groups, hearts were given IPC treatment by performing 3 cycles of 5 minutes ischaemia/5 minutes reperfusion. After this, both IPC groups, plus an insult only cohort, were subjected to 30 minutes of prolonged global ischaemia followed by 120 minutes of reperfusion. Also, one of the IPC groups received an infusion of PI3-K inhibitor LY294002. An additional group was also used as a control that did not receive IPC or the severe ischaemic insult. Confirmation of protection was achieved by measuring infarct size which was significantly reduced in those who received IPC compared to those who were only subjected to prolonged ischaemia. It was found that expression of phospho-eNOS (p-eNOS), the activated form of eNOS, was significantly elevated in hearts pre-treated with IPC in comparison to the controls. In the insult only group, however, p-eNOS expression was significantly decreased reiterating the importance of p-eNOS activity in eliciting IPC. Also, when LY294002 was also administered, p-eNOS levels were not significantly elevated compared to controls (Yang C *et al*., 2013). Therefore, using the data collected here, it was concluded that IPC is mediated by PI3-K induced eNOS activity.

1.6 Aims and Objectives

It is evident that there is a great need for the introduction of new strategies in tackling the development of diabetes linked CVDs. CV outcomes are worse in people with diabetes, and hyperglycaemia, hypoglycaemia and increased glycaemic variability have been shown to contribute to these poorer outcomes. IPC and HPC have been shown to improve CV outcomes in people without diabetes, and as such offer novel therapeutic approaches. However, the data regarding the efficacy of these preconditioning treatments in those with diabetes is somewhat contradictory. Additionally, hyperglycaemia, and hypoglycaemia in healthy subjects, have been shown to interfere with IPC and R-IPC treatments. Therefore, it was hypothesised that glycaemic variability, and acute glycaemic events, will disrupt HPC, IPC and R-IPC. To investigate this hypothesis, a series of aims and objectives were constructed:

i) **Develop *in vitro* models of HPC and IPC** – induce HPC and IPC in HUVECs, which can subsequently be employed to perform aim iv), using $CoCl_2$ and a hypoxic incubator, and validate these models by assessing changes in cell viability and apoptosis in response to a severe hypoxic or ischaemic stimulus

ii) **Develop an *in vitro* model of R-IPC** – induce R-IPC in cardiomyocytes, which can subsequently be employed to perform aim iv) as below, using preconditioned media obtained from HUVECs, and validate the model by assessing changes in cell viability and apoptosis in response to a severe ischaemic stimulus

iii) **Develop an *in vivo* model of R-IPC** – induce R-IPC in WT mice, which can subsequently be employed to perform aim iv), and validate the model by assessing changes in endothelial function

iv) **Investigate the effects of glycaemic variability on HPC, IPC and R-IPC** – introduce hypoglycaemic and hyperglycaemic events to the validated HPC, IPC and R-IPC models and determine if the preconditioning treatments are disrupted by assessment of cell viability, apoptosis, and endothelial function

Chapter 2

Materials and Methods

2.1 Standard Laboratory Chemicals

Unless otherwise specified, all laboratory chemicals and reagents were provided by Sigma Aldrich. Tris base and glycine were purchased from Melford. 100X HALT protease inhibitor and hydrochloric (HCl) acid were bought from Thermo Fisher Scientific. Methanol and ethanol were acquired from VWR. Acrylamide came from National Diagnostics. The following solutions were made in their stock concentrations prior to commencement of the project by another member of the laboratory group: 0.1M dithiothreitol (DTT), 0.1M phenylmethylsulfonyl fluoride (PMSF), 0.75M Sodium Fluoride, 0.5M sodium pyrophosphate tetrabasic decahydrate (NaPp), 1M Tris pH 6.8, 1M Tris pH 7.0, 1M Tris pH 7.4, 0.5M Ethylenediaminetetracetic Acid (EDTA), 0.2M Ethylene Glycol-bis(β-aminoethyl ether)-N,N,N',N'-tetraacetic Acid (EGTA). Room temperature (RT) was defined as being 20^{o}C.

2.2 Animal Use

All procedures were conducted in accordance with the Animals (Scientific Procedures) Act 1986 by licensed and trained persons. Procedures conducted as in chapters 3 and 4 were done so under project licences PE82C1898 and PP2258914 respectively. WT Male C57BL/6J mice were housed in cages of 2-5 individuals, where possible, under standard environmental conditions in the Medical School Resource Unit (MSRU) located in Ninewells Hospital and Medical School, Dundee. All mice were obtained from Charles River except for 8 of the 18 used in the preliminary study, discussed in section 3.2, which were bred in house. Upon arrival at the MSRU, they were allowed a 1-week acclimatisation period prior to being handled and a further week of handling training to reduce handling induced stress artefacts during experiments. Mice used for procedures conducted as in chapter 3 were aged 12-15 weeks. To allow time for the hindlimbs to grow large enough to administer injectable anaesthesia and position the blood pressure cuff, mice used for procedures conducted as in chapter 4 were aged 25-30 weeks. Unless stated otherwise, mice were provided with an *ad libitum* supply of standard RM1 chow [Special Diets Services, 801002] and water for the duration of the study.

2.3 Anaesthesia

All *in vivo* procedures, except for that inducing hypoglycaemia, required the mice to be immobilised using general anaesthesia. As part of the optimisation process, both inhalational and injectable anaesthetic agents, namely isoflurane and Alfaxan in combination with the sedative midazolam respectively, were utilised. Animals were routinely monitored throughout their recovery from anaesthesia. In all cases, anaesthesia was confirmed through the loss of the righting reflex and the toe and tail pinch reflexes. Mice were deemed to have recovered following the return of consciousness and the ability to walk around and feed as normal.

2.3.1 Isoflurane

Liquid isoflurane was vaporised and administered to an individual using medical oxygen as a carrier gas at a flow rate of 1L/min via an anaesthetic rig [Vet Tech Solutions, AN001]. A scavenger machine [Vet Tech Solutions, AN005] was also used to remove any anaesthetic gas which may escape through the induction box or nose cone into the procedure room. Mice were placed into the induction box and were anaesthetised through inhalation of 4% isoflurane. Once anaesthesia was confirmed, to maintain a steady core body temperature, subjects were placed onto a heat mat set to 37^{o}C with gauze adhered to buffer the temperature directly in contact with the mouse. Anaesthesia was maintained by inhaling 1-2% isoflurane through a nose cone throughout the procedure aiming for a respiratory rate of 60-70 respirations per minute. Recovery from anaesthesia was induced by turning the isoflurane concentration dial on the vaporiser to 0% and moving the mouse away from the nose cone.

2.3.2 Injectables

Anaesthesia was also induced used injectable agents' midazolam and Alfaxan. Midazolam is a sedative, belonging to the benzodiazepine class of drugs, utilised to relax the animals, reduce pain associated with the administration of the Alfaxan, and inhibit memory formation during the procedure. Midazolam was given via intraperitoneal injection at a dose of 5mg/kg in saline vehicle. The animals were housed individually in a quiet environment on a heat pad left until they appeared lethargic, and their gait became wobbly, which took approximately

15-30 minutes. Alfaxan was given at a dose of 10mg/kg via intramuscular injection in the quadricep from neat 10mg/mL stock. Alternate legs were injected on consecutive days to avoid tissue damage and additional discomfort to the animals. Anaesthesia was confirmed within 5 minutes by loss of consciousness and lack of response to paw pinch and whisker touch. Animals were allowed to recover naturally on a heat pad with softened chow, without pharmacological intervention, as the effects of the midazolam and Alfaxan wore off. Animals were deemed to have recovered once fully alert, eating, and behaving normally by foraging and grooming.

2.4 Assessing Vascular Function *In Vivo*

2.4.1 Laser Doppler Imaging

LDI is a technique which utilises the Doppler phenomenon to generate heat maps representing areas of increased or decreased blood flow velocity within the skin.

The Doppler effect is a phenomenon which is commonly associated with sound waves but also applies to lasers. Briefly, it describes the shift in the frequency and wavelength of reflected sound or light waves relative to those emitted by a source due to asynchronous motion of the source and the object off which the waves are reflected. When a laser is shone onto a stationary object, the light is reflected with the same frequency and wavelength. However, if the laser is in contact with a moving object, such as a red blood cell, the reflected light experiences a change in frequency and wavelength corresponding to the rate and direction of movement. This shift in frequency and wavelength is known as the Doppler effect (Murray *et al*., 2004).

For the purposes of this project, LDI was performed by directing a class 3R helium-neon laser towards the subject from 36cm away. Instead of the light being reflected directly, it is scattered due to the movement of red blood cells in the cutaneous microvasculature. This backscatter is captured, and photodiodes convert the light into an electrical current. This is processed further, and a heat map is produced in which pixels are assigned a flux value allowing one to visualise the degree of blood flow in detail. Higher flux values would indicate a greater blood flow rate and, therefore, increased vasodilation.

To perform LDI experiments, an LDI laser [Moor Instruments, moorLDI2-IR] and moorLDI Measurement V6.1 software were used for imaging whilst the images themselves were analysed using moorLDI Review v6.1 software. The properties of the LDI scans are displayed below in section 2.4.1.1. It should be considered that whilst this technique provides excellent spatial resolution, each scan takes several seconds meaning the images generated are not real-time and rapid transient changes in blood flow may be missed. This can be used as a technique alone although it is frequently used in conjunction with iontophoresis of PE and ACh iontophoresis or application of localised heating.

2.4.1.1 LDI Scan Properties

Scan resolution: x=50, y=50

Scan image: x0=90, y0=90, dx=90, dy=90

Scan area: 3.6cm x 3.6cm

Scan speed: 4ms/pixel

Scan time: 29 seconds per image

Time between scans: 1 second

Total scan time: 30 seconds per repeat scan

2.4.2 PE and ACh Iontophoresis

Iontophoresis is a non-invasive method, commonly used in conjunction with LDI to assess endothelial function, in which transdermal administration of vasoactive drugs takes place using a voltage gradient. Whilst other compounds can be utilised, for the purposes of this project, only the vasoconstrictor PE and vasodilator ACh were used. Solutions of PE and ACh were applied topically inside an iontophoresis chamber adhered to the flank, and a reference electrode was positioned under the subject on the opposing flank (Fig. 2.1). Both PE and ACh are composed of positively charged ions which would be repelled by a positive charge and attracted to a negative charge. Both the iontophoresis chamber and reference electrode were connected to an iontophoresis controller. Programming of the controller results in the application of current which leads to the iontophoresis chamber and reference electrode becoming positively and negatively charged respectively. This causes the positive ions within the PE and ACh solutions to be pushed away from the positively charged iontophoresis ring

and pulled towards the negatively charged reference electrode through the skin thereby allowing the vasoactive compounds to interact with the cutaneous microvasculature.

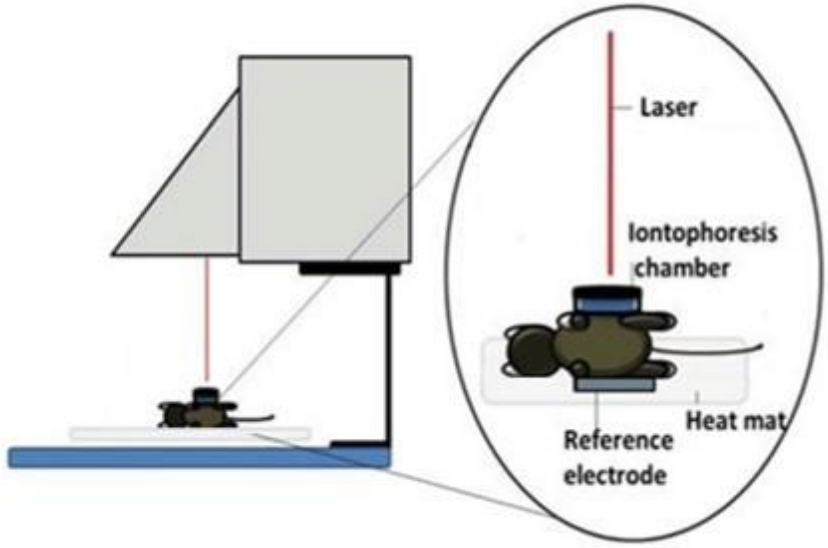

Fig. 2.1 LDI and iontophoresis mouse setup. The anaesthetised mouse was placed on its shaved flank over a reference electrode on a heat mat. The iontophoresis chamber, to which vasoactive substances could be added, was then adhered to the hairless flank within the scanning region of the LDI laser. (*Adapted* from Akbar, 2014)

On the day of the procedure, 1% and 2% solutions of PE and ACh were made in dH_2O, respectively. To allow successful ion flow, the flank in contact with the reference electrode was shaved. Additionally, to enable direct scanning of the cutaneous microcirculation, and to ensure the iontophoresis chamber could be securely adhered to the skin, hair was also removed from the flank to be scanned by shaving and depilatory cream was used to completely remove residual hair. Depilatory cream was thoroughly washed off with dH_2O and wiped clean with wet cotton wool until no further hair was visible on the wool.

Mice were positioned on their shaved flank, over a reference electrode, and the iontophoresis chamber was attached to the entirely hairless flank using specially fitting adhesive rings. To establish steady-state blood flow, 3 LDI scans were taken of the flank with dH_2O within the ring. The dH_2O was removed, and PE added to the ring. The current was set at 100mA for 10 further LDI scans allowing administration of PE via iontophoresis. The current was turned off, to halt iontophoresis, and the PE was removed from the chamber. dH_2O was used to rinse any residual PE out of the chamber which was then filled with the ACh solution. The current was reset to 100mA, and another 10 LDI scans were

performed with ACh now being administered by iontophoresis. The anaesthetic was turned off and whilst the mouse regained consciousness, the iontophoresis chamber was removed, the skin gently cleaned with dH_2O, and a moisturising ointment was applied to prevent skin irritation.

From each of the 23 scans, a flux image and associated median flux value were generated based upon the rate of blood flow. Vasoconstriction, such as that induced by iontophoresis of PE, causes reduced blood flow and flux values. Conversely, vasodilation, such as that induced by iontophoresis of ACh, leads to increased flow therefore, producing higher average flux values (Fig. 2.2). Using this data, 4 separate parameters were calculated for each scanning session: i) delta flux, ii) steady state flux, iii) minimum flux due to PE induced vasoconstriction, iv) maximum flux due to ACh induced vasodilation. The delta flux was calculated by subtracting variable iii from iv. The steady state flux was determined by calculating the mean flux from the 3 LDI scans performed prior to turning on the current to initiate iontophoresis. A decrease in variable i was indicative of decreased endothelial function.

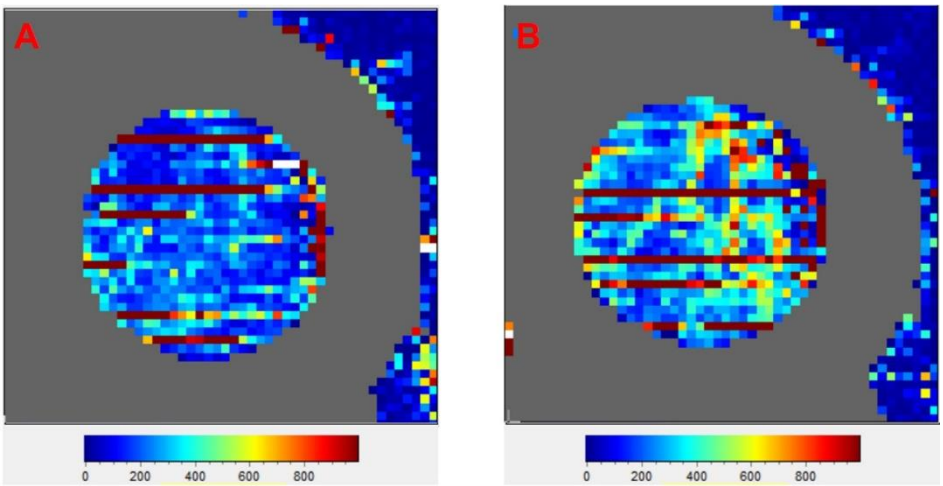

Fig. 2.2 Effect of PE and ACh administration of the rate of blood flow. Flux images obtained by LDI with PE/ACh iontophoresis with flux values indicated by the colour scale. Upon administration of PE (A), the resulting vasoconstriction leads to a decreased rate of blood flow rate and therefore a lower average flux. Administration of the vasodilator ACh has the opposite effect causing an increased rate of blood flow resulting in a higher average flux.

2.4.3 Full-Field Laser Perfusion Imaging

FLPI is an additional technique which can be used to assess microvascular function *in vivo*. The function of both FLPI and LDI rely upon similar phenomena

regarding movement of an object and scattered light although the precise principles used to approach this effect are slightly different.

A low power class 1 laser is directed onto the skin. Scattered light returns to a camera and a speckle pattern is generated due to the movement of red blood cells within the cutaneous microvasculature as described in section 2.4.1. Due to this continuous motion, the speckle pattern will continuously fluctuate. When the camera exposure time is greater than the rate of speckle pattern fluctuation, the speckle pattern intensities at each given pixel are integrated. The integrated speckle at each pixel can be processed and ultimately assigned a flux value which positively correlates with the rate of flow of red blood cells (Dunn, 2012).

To perform experiments using FLPI, a distinct FLPI laser [Moor Instruments, moorFLPI] and MoorFLPI Measurement V4.0 software were utilised for imaging whilst the images themselves were analysed using MoorFLPI Review V4.0. This laser has reduced penetrative power but can produce up to 25 images per second thereby generating real-time videos to represent the movement of red blood cells within the cutaneous microvasculature.

2.4.4 Reactive Hyperaemia

Reactive hyperaemia refers to the short-term increase in blood flow to a tissue or organ following a period of ischaemia before returning to a steady state similar to the pre-ischaemic rate. A reduced reactive hyperaemic response is indicative of endothelial dysfunction.

The FLPI laser, a sphygmomanometer [P.M.S (Instruments) Ltd., ERK291203037290] and custom made 1X9cm blood pressure cuff [P.M.S (Instruments) Ltd., HOK1X9CustC] were used to assess reactive hyperaemia in mice (Fig. 2.3). Subjects were positioned on their front with their hindlimbs pointed towards the FLPI laser which scanned the soles of both rear feet throughout the protocol. The blood pressure cuff was placed around one of the rear limbs and the flux of both feet was measured for 1-2 minutes. The cuff was then inflated to 250mmHg for 5 minutes to induce ischaemia. After this, it was deflated for a further 5 minutes of reperfusion.

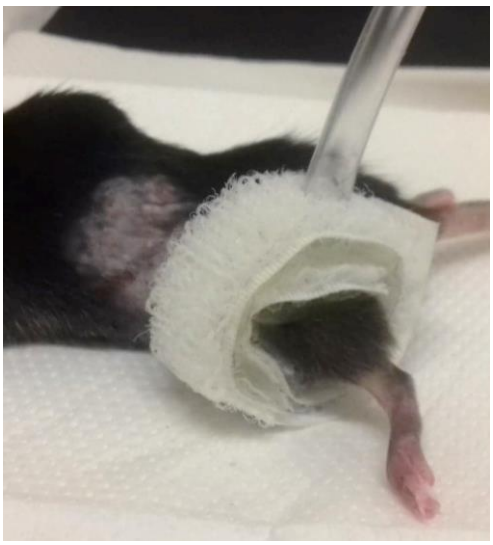

Fig. 2.3 Positioning of the blood pressure cuff on the hindlimb. The custom-made blood pressure cuff is wrapped around a hindlimb of the anaesthetised mouse whilst positioned on its front.

From the resulting mean flux trace generated for each foot, the following parameters were calculated (Fig. 2.4): pre-ischaemic steady state of both feet, post-ischaemic steady state of both feet, magnitude of reactive hyperaemic response in the test foot, total of excess flow in the test foot, duration of reactive hyperaemia in the test foot, peak flux reached during reactive hyperaemia in the test foot.

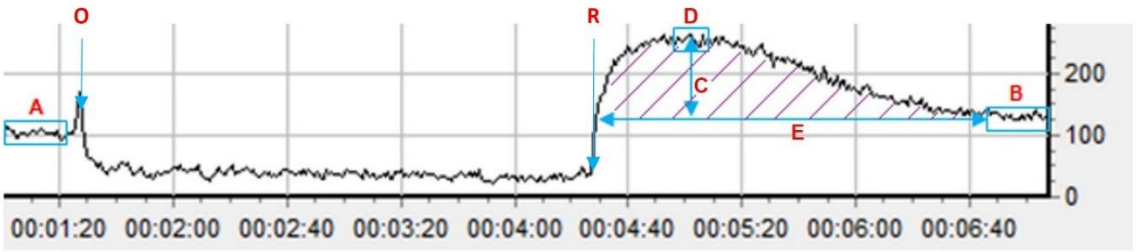

Fig. 2.4 Parameters calculated from a reactive hyperaemia flux trace. A representative image of the reactive hyperaemic response from which 6 parameters were calculated. The x axis represents time in minutes whilst the y axis displays the mean flux value. The points at which induction of blood vessel occlusion (O) and reperfusion (R) occur are indicated. Pre-ischaemic steady state (A) and post ischaemic steady state (B) refer to the stabilised flux values observed before ischaemia and after reactive hyperaemia had concluded respectively. Magnitude of reactive hyperaemia (C) is the difference in flux between the peak reached once reperfusion commenced (D) and the post ischaemic steady state. Total excess flow was calculated as the area under the flux curve (purple shaded region) during the period of the reactive hyperaemic response (E).

2.5 *In Vivo* R-IPC

2.5.1 In Vivo R-IPC Model

Induction of R-IPC was attempted by performing repeated cycles of ischaemia/reperfusion on one of the hindlimbs of the mice using the sphygmomanometer and blood pressure cuff. Additionally, the FLPI laser was utilised to confirm occlusion, by the perfusion image turning blue indicating absence of blood flow, and reperfusion. Mice were laid on their ventral side, again on a heat mat, and the soles of their hindlimbs were positioned to be within the scanning region of the FLPI laser. The blood pressure cuff was placed around one of these limbs and inflated to 250mmHg for 5 minutes to induce ischaemia. It was then deflated for another 5 minutes for a period of reperfusion. This ischaemia/reperfusion cycle was repeated, on the same hindlimb, for a total of 3-4 times depending on the study being conducted. In control animals, the deflated cuff was worn around one of their hindlimbs for the entire 30–40-minute time period.

2.5.2 Inducing Hypoglycaemia In Vivo

A single episode of hypoglycaemia was induced in the mice to investigate its effects on the R-IPC model and endothelial function. Mice were placed into fresh cages and fasted for 5 hours. Insulin - Actrapid, Novo Nordisk - was prepared in sterile saline to a stock concentration of 0.2U. Animals were dosed depending on their weight using the formula below to achieve a dose of 1.0U:

$$\text{volume}(\mu L) = \frac{\text{weight}(g) \times 1.0U}{0.2U}$$

Basal tail vein blood glucose levels were recorded by pricking the tail with a needle and using a glucose meter [Contour, 85726688] with test strips [Contour, 84669997]. Mice were injected subcutaneously with either 1.0U insulin or volume matched saline. Tail vein blood glucose was measured again after 30 minutes for those in the insulin group to ensure blood glucose was dropping appropriately. At 45 minutes, final tail vein blood glucose levels were taken from all mice and food was returned upon reaching the 60-minute timepoint. If mice began to exhibit early symptoms of severe hypoglycaemia, such as immobility and poor gait rendering them unable to eat unaided, 100µL 40% glucose solution was injected

intraperitoneally, and the mouse was closely monitored on a heat mat until it had recovered.

2.6 Tissue and Plasma Analysis

2.6.1 Tissue Harvest

On the final day of study, mice were euthanised - under anaesthesia - via cervical dislocation, and death was confirmed by either cardiac puncture and exsanguination or severing of the femoral artery. The aortas were harvested and immediately placed into liquid nitrogen. Additionally, blood was collected in EDTA coated tubes and centrifuged at 13,200rpm at 4^{o}C for 15 minutes. The plasma layer was transferred to a standard cryotube [Thermo Fisher Scientific, 363401] and the remaining contents of the EDTA tube discarded. All tissue and plasma samples were transferred to a -80^{o}C freezer for long term storage.

2.6.2 TNFα ELISA

An ELISA [R&D Systems, DY410-05] was used according to manufacturer's instructions to determine the levels of TNFα in the collected murine plasma samples. All reagents were brought to RT prior to use and reconstituted antibodies were gently agitated and allowed 15 minutes to sit before further dilution. The volumes required to reconstitute the solutes were determined using the appropriate certificate of analysis dependent on the lot number of the kit utilised. Additionally, 1L 0.05% phosphate buffered saline tween (PBS-T) wash buffer and 1L filtered 1% BSA phosphate buffered saline (PBS) reagent diluent were made up before conducting the ELISA. All filters used had pore sizes of 0.22µM.

The capture antibody was reconstituted with 500µL PBS providing a stock concentration of 100µg/mL. This was required to be diluted to a working concentration of 800ng/mL by adding 90µL stock to 11,160µL PBS. A clear flat bottomed 96 well microplate was coated with 100µL diluted capture antibody per well. The plate was sealed and left to incubate overnight at RT whilst the remaining capture antibody stock was aliquoted and stored at -20^{o}C.

The following day, the capture antibody was aspirated, and the wells washed 3

times with 200µL of wash buffer. Wells were blocked with 200µL reagent diluent, and the plate was incubated for 1 hour at RT. During this time, the standards were prepared, and plasma samples were retrieved from the -80ºC and thawed on ice. A working concentration of standard was prepared by reconstituting the solute with 500µL reagent diluent to make a 200ng/mL stock. This was further diluted to a 2000pg/mL by adding 10µL stock to 990µL reagent diluent. 500µL reagent diluent was added to each of 6 Eppendorf tubes and serial dilutions were performed as indicated (Fig. 2.5).

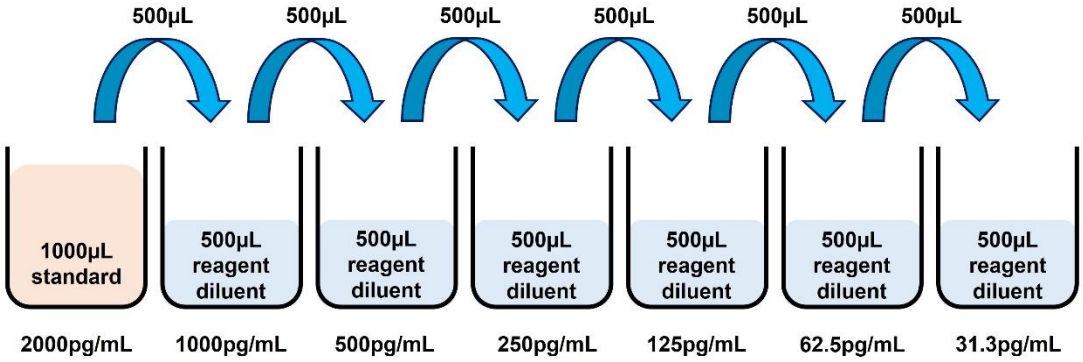

Fig. 2.5 TNFα ELISA standards preparation. 6 Eppendorf tubes contained 500µL reagent diluent and a series of 1 in 2 dilutions were conducted to make 6 concentrations of standard from a 2000pg/mL solution.

The reagent diluent was removed from the wells which were then washed 3 times with 200µL wash buffer. 100µL of samples and standards were added to the wells in duplicate and the plate was sealed before a 2-hour incubation period at RT. The well contents were discarded and a further 3 200µL washes were performed with the wash buffer.

The detection antibody was reconstituted with 1mL reagent diluent to make a stock concentration of 2.25µg/mL. This was diluted further to a working concentration of 37.5ng/mL by adding 83.3µL stock to 4916.7µL reagent diluent. 100µL diluted detection antibody was added to each well and the plate was sealed and incubated at RT for 2 hours. Remaining antibody stock was stored at -20ºC. The detection antibody was aspirated, and the wells were washed 3 times with 200µL wash buffer.

Streptavidin-horseradish peroxidase (HRP) was prepared by diluting the provided 2mL stock solution 40-fold with reagent diluent. 100µL working Streptavidin-HRP

was added to each well and the plate was sealed and kept in the dark at RT for 20 minutes. The Straptavidin-HRP was removed and a final 3 200µL washes were conducted with the wash buffer.

For each well, 100µL substrate solution was made by adding together 50µL hydrogen peroxide (H_2O_2) and 50µL tetramethylbenzidine [R&D Systems, D&999]. This substrate solution was added to the wells and the plates were incubated at RT in the dark for 20 minutes. 50µL stop solution [R&D Systems, DY994] was added to each well and the plate was gently tapped to ensure it was sufficiently mixed. Optical density was immediately determined using a microplate reader set to 450nm and 540nm. The readings taken at the 540nm wavelength were subtracted from those at 450nm to account for any optical imperfections caused by the plate.

Standard curves were generated for TNFα by plotting the signal against the concentration of the standards. The concentration of TNFα in each sample was then determined via interpolation of their signals with the standard curve.

2.6.3 Cytokine Array

Plasma cytokine expression was determined using a multiplex cytokine array [MSD, K15048D] as according to manufacturer's instructions. This sandwich immunoassay allowed the quantification of 10 cytokines: interferon γ, IL-1β, IL-2, IL-4, IL-5, IL-6, IL-10, IL-12p70, keratinocyte chemoattractant/human growth-regulated oncogene (KC/GRO) and TNFα. The surface of each well of the provided 96-well plate acts as a working electrode onto which capture antibodies for the 10 cytokines are precisely positioned. Solutions containing samples and detection antibodies conjugated with an electrochemiluminescent label are added to the wells. The analytes within the samples bind to the capture antibodies and the detection antibodies are recruited to interact with the bound analyte thereby forming the sandwich. Using an appropriate plate reader and software, a voltage is applied causing the bound conjugated detection antibodies to emit light. The amount of light is measured and the concentration of the cytokines within the sample is calculated.

Prior to commencing the array, samples and solutions had to be prepared. A wash buffer of 0.05% PBS-T was made. Additionally, a 2X working solution of read buffer was prepared by combining 10mL 4X read buffer T to 10mL dH_2O Plasma samples were thawed and diluted with diluent 41 using a 2-fold dilution. The antibody detection solution was made by adding 60µL of each of the 10 individual 50X antibody stocks, one for each cytokine, to 2400µL diluent 45 to make 1X working concentrations. To prepare the standards, the lyophilised calibrator provided was reconstituted with 1mL diluent 41. This was mixed vigorously using a vortex and allowed to sit for 5 minutes prior to use. 300µL diluent 41 was added to 7 Eppendorf tubes. A series of 4-fold dilutions were made as indicated to generate 8 different concentrations of standards (Fig. 2.6). The concentration of each cytokine within the standards was dependent on the lot number of the kit used and were determined using the appropriate certificate analysis.

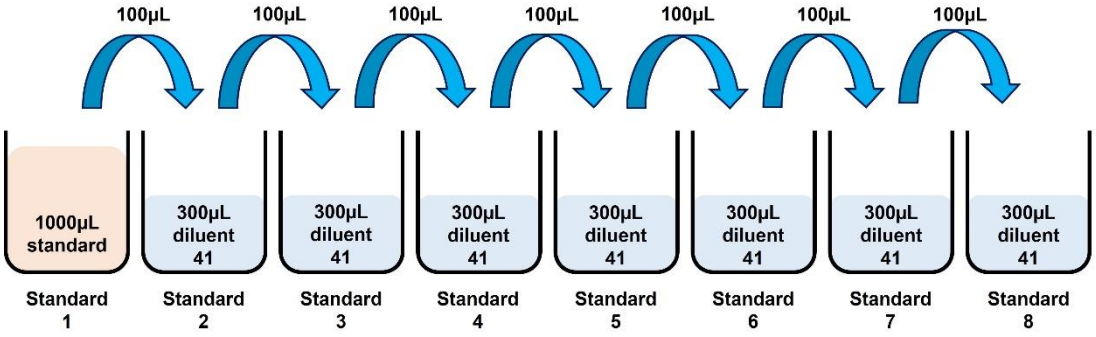

Fig. 2.6 Cytokine array standards preparation. 7 Eppendorf tubes contained 300µL diluent 41 and a series of 1 in 4 dilutions were conducted to make 7 concentrations of standard from a reconstituted stock.

50µL of sample or standard was added to the wells of the 96 well plate provided. Standards were prepared in duplicate whereas the samples were only added to a single well due to reduced plasma availability. The plate was sealed using adhesive microfilm and incubated on a plate shaker for 2 hours at RT.

The plate was washed 3 times with 150µL wash buffer per well. 25µL antibody detection solution was added to each well. The plate was resealed and once again incubated on a plate shaker for 2 hours at RT.

Each well was washed with 150µL wash buffer 3 times. 150µL 2X read buffer

was added to each well. The plate was read using an MESO QuickPlex SQ 120 plate reader [MSD, AI0AA-0] using MSD discovery work bench 4.0 software. By measuring the light emitted, and using the concentrations of the cytokines within the standards as stipulated by the certificate of analysis, concentrations of the cytokines within each sample were calculated and a spreadsheet displaying these was automatically generated

2.6.4 Aorta Preparation

Prior to being lysed, the aortas needed to be cleaned of any adipose and cardiac tissue, as well as any other debris. The aortas were collected from the -80ºC freezer and placed directly into liquid nitrogen. Individual aortas were then removed and positioned on a petri dish kept cool on ice. Then, using a microscope and needles, the unwanted tissue could be separated from the aorta and discarded. The aortas were placed back into the liquid nitrogen until all had been dissected. They were all then lysed immediately, as in section 2.10.1.1.

2.7 Tissue Culture

All tissue culture was conducted in a class II biological safety cabinet. Cells were incubated in a 37ºC/5% CO_2 incubator. HUVECs and cardiomyocytes were utilised and incubated in different cabinets and incubators. Unless stated otherwise, all reagents were stored at 4ºC, and warmed to 37ºC in a water bath prior to being in contact with the cells. All recipes for media and buffers, to which cells were exposed, are located in the appendix of this thesis (Table 8.1-8.6, 8.21-8.22). Unless otherwise specified, all plates, petri dishes and flasks were produced by Nunc. Where indicated, cells were starved prior to experiments using basal media (Table 8.3). Filtering of relevant solutions was conducted using a filter with a pore size of 0.22µM.

2.7.1 Gelatin Coating Plates/Flasks

All plates, petri dishes and flasks to be used for plating HUVECs and cardiomyocytes must be pre-coated with 1% gelatin to ensure adherence of the cells to their surfaces. A 2% gelatin solution [Sigma Aldrich, G1393-100ML] was diluted to 1% with sterile dH_2O. This was added to the plates, petri dishes and flasks, ensuring complete coverage of the adherent surface. These were then

incubated for at least 30 minutes at 37ºC to ensure the gelatin was completely dissolved in its solution and had successfully coated the plates, petri dishes and flasks as desired. The gelatin was removed and returned to a conical tube to be stored at 4ºC for reuse at a later date.

2.7.2 HUVEC Maintenance

HUVECs were chosen to verify *in vitro* models of HPC and IPC. HUVECs are human endothelial cells collected from the umbilical vein (Jaffe *et al*., 1973). Following birth, the umbilical vein becomes a waste product. As many births occur each day, there is great availability of tissue from which HUVECs can be isolated. Hence, it is possible to obtain large quantities of these cells within a short period of time. This may explain why there is a vast quantity of published research using HUVECs. Despite being commercially available, they are still primary cells. Therefore, they can only be used up to 5 passages as there are significant changes in the structure and function of the cells as they divide further. Additionally, they are more susceptible to damage caused by suboptimal culture conditions. However, primary human cells are beneficial over cell lines as they more accurately represent *in vivo* and clinical findings. Vials of passage (P) 2 HUVECs [Caltag Medsystems, ZHC-2102], each containing cells collected from multiple donors, were obtained and stored in liquid nitrogen until ready to commence cell culture.

2.7.2.1 Thawing HUVECs

Following retrieval from liquid nitrogen storage, each purchased vial of HUVECs was found to be sufficient to plate 1 T75 flask. Cells were rapidly thawed in a water bath at 37ºC. 1mL endothelial growth media (EGM) (Table 8.1) was immediately added to the vial and the contents gently agitated. This was then transferred to a 15mL conical tube where an additional 3mL EGM was added dropwise. The tube was centrifuged for 3 minutes at 1100rpm to pellet the cells. The supernatant was aspirated, and the pellet resuspended in 1mL EGM. This cellular suspension and 14mL EGM were added to a gelatin coated T75 and carefully mixed. The flask was then placed in an incubator and were passaged to P3 once they reached over 80% confluency.

2.7.2.2 Passaging HUVECs

EGM was removed from the flask which was then gently rinsed with PBS. 5mL trypsin was added to the flask and the cells were incubated for 3-5 minutes. The flask was tapped lightly to encourage complete detachment of the cells. 5mL EGM was added to inactivate the trypsin. The contents of the flask were transferred to a 15mL conical tube. This was centrifuged at 1100rpm for 5 minutes. The supernatant was aspirated, and the pellet resuspended in 4mL EGM. Cells were counted using a haemocytometer [Hawksley, AS1000], and the volume of suspended cells required to ensure 1.25 million cells per flask was determined. 14mL media was added to each gelatin coated T75 flask to be plated. The calculated volume of the cellular suspension was added to each flask for a maximum of 4 new T75 flasks. These flasks were placed in the incubator until 80% confluency was achieved.

2.7.2.3 Freezing HUVECs

30mL 10% Dimethyl sulfoxide heat inactivated foetal bovine serum (HI FBS) freezing media was made, filtered, and kept cool on ice. Media was aspirated, and cells were washed with warm PBS, trypsinised and counted with a haemocytometer as done when passaging HUVECs in section 2.7.2.2. Resuspended cells were centrifuged again at 1100rpm for 3 minutes. The supernatant was aspirated, and the cell pellet resuspended in freezing media ensuring 1-1.5 million cells per mL. 1mL of this suspension was aliquoted into cryotubes which were placed into the BioCision CoolCell® cell freezing device. This was then transferred into the -80^{o}C freezer for at least 24 hours allowing the cells to be frozen down gradually at a rate of 1^{o}C/min thereby preventing damage which can occur via snap freezing. Cryotubes could then be moved into a liquid nitrogen dewar for long term storage.

2.7.2.4 Plating HUVECs for Experimentation

When P4 HUVECs reached 80% confluency, they were passaged and counted with a haemocytometer. P5 HUVECs were plated at a density of 12,500/cm^2 72 hours prior to commencing an experiment. Cells to be used for protein expression analysis were plated in 60mm petri dishes. Those due to be analysed by immunocytochemistry were plated on coverslips positioned in the

wells of 6 well plates. All other P5 HUVECs were plated into 96 well plates.

2.7.3 Optimising HUVEC Growth Conditions

Determining the optimal media for cell growth and survival was done so by performing a cell proliferation, adhesion, and viability assay. P4 HUVECs were thawed and expanded in either Dulbecco's Modified Eagle Medium (DMEM) or EGM. These were passaged and P5 HUVECs were seeded into 12 or 24 well plates, at the same density, in either DMEM or EGM. The cell adhesion assay was performed 24 hours later whilst both the proliferation and cell viability assays were conducted 72 hours after plating.

2.7.3.1 Cell Adhesion Assay

Cell media was removed and set aside whilst the remaining cells were trypsinised as conducted when passaging HUVECs in section 2.7.2.2. All samples were centrifuged at 1100rpm for 3 minutes after which the supernatant was aspirated, and cells were resuspended with fresh EGM. Cells were counted using a haemocytometer. The number of floating and adherent cells, those which were present in the set aside cell media and trypsinised respectively, was calculated. Added together, this represented the total number of cells and so the percentage of adherent cells was determined.

2.7.3.2 Cell Proliferation Assay

P5 HUVECs were counted using a haemocytometer, as described in section 2.7.4, prior to and 72 hours following seeding. The percentage change in cell number between these timepoints was calculated.

2.7.3.3 Cell Viability Assay

Media was aspirated, and cells were washed, trypsinised and centrifuged as conducted when passaging HUVECs in section 2.7.2.2. The supernatant was removed, and fresh EGM was used to resuspend the pellet. 50µL Trypan blue reagent [Thermo Fisher Scientific, 15250061] was added to 50µL cell suspension. Samples were incubated for 5 minutes. The number of non-viable cells, stained blue, and viable cells, which remained unstained, were determined

by counting with a haemocytometer. Again, the sum of these values equalled the total number of cells, and the percentage of viable cells was calculated.

2.7.4 Counting Cells with a Haemocytometer

Cells were counted manually using a haemocytometer. Prior to use, the haemocytometer was cleaned with ethanol and a coverslip positioned on top. Under the coverslip, 10µL undiluted cell suspension was pipetted. The haemocytometer is made up of 4 large quadrants, each consisting of 16 smaller squares. Cells were counted, under a microscope, in 2 quadrants diagonally opposite each other. The volume of cell suspension required to plate the number of desired cells was calculated using the formula below:

$$\text{volume(mL)} = \frac{\text{desired number of cells (million)} \times \text{suspension volume (mL)}}{\text{Total number of cells in suspension (million)}}$$

2.7.5 Isolation of Neonatal Rat Cardiomyocytes

The isolation protocol for neonatal rat cardiomyocytes was adapted from one utilised for the isolation of murine neonatal cardiomyocytes by Dr Erika Gutierrez-Lara, formerly of the University of Dundee. Relevant media was prepared in advance of the cardiomyocyte isolation procedure (Tables 8.21 and 8.22). Firstly, 50mL HI FBS [Thermo Fisher Scientific, 10500064] was thawed and filtered and 100mL M1 and M2 media were prepared. Then, 2 conical tubes containing 10mL Hanks' Balanced Salt Solution (HBSS) [Thermo Fisher Scientific, 14175095] were chilled on ice per preparation of cardiomyocytes, which each consisted of 4 hearts. For each preparation, 2 wells of a 6 well plate were coated with 1% gelatin as previously described in section 2.7.1. Finally, 50mL collagenase buffer was prepared by adding 22.5mg collagenase II powder [Thermo Fisher Scientific, 17101015] to sterile HBSS and filtering it.

For each preparation, 4 neonatal rat pups aged between 1-4 days old were euthanised via cervical dislocation with death being confirmed by decapitation. Hearts were removed and immediately placed in 10mL ice cold HBSS. The contents of this tube were then poured into a 100mm petri dish. The hearts were gently squeezed with a pair of blunt forceps to ensure no blood was left within.

Any non-cardiac detritus was dissected away, and the hearts were transferred to another petri dish containing the ice cold HBSS from the second conical tube. Here, they were each chopped into 5 small 2mm pieces. These were placed into a 50mL conical tube containing 5mL collagenase buffer. The tube was incubated as 37^{o}C for 5 minutes to allow the removal of pericardial collagen. After this, the buffer was discarded, being careful not to take any of the heart tissue and replaced with 5mL collagenase buffer. This was then placed in the incubator at 37^{o}C for 10 minutes. The contents were triturated using a 10mL stripette and the buffer transferred to a 15mL conical tube containing 0.5mL HI FBS. This smaller tube was centrifuged at 300xg for 5 minutes. The resulting supernatant was removed, and the cell pellet resuspended in 2.5mL of HI FBS and kept in the incubator. Another 5mL of collagenase buffer was added to the hearts and the process from buffer addition to resuspension in 2.5mL HI FBS was repeated until 4 conical tubes had been collected per preparation. The contents of the 4 tubes were collated into 1 which was centrifuged at 300xg for 5 minutes after which the supernatant was discarded.

Cells were resuspended in 10mL M1 media and transferred into a 100mm petri dish. This was then placed into an incubator for 90 minutes. After this time, a large proportion of endothelial cells and fibroblasts had adhered to the plate surface whilst the cardiomyocytes remained floating in the media. The media was transferred into a 50mL conical tube. 5mL M1 media was used to rinse any loosely bound cardiomyocytes off the surface of the plate and was then also added to the conical tube. The tube was centrifuged at 300xg for 5 minutes. The supernatant was removed, and the pellet resuspended in 6mL M1 media. 3mL of this suspension was added to 1 9.6cm^{2} well of the gelatin coated 6 well plate which was subsequently placed in an incubator.

The following morning, the M1 media was replaced with M2 media which was changed every 48 hours thereafter. The cardiomyocytes began beating within 7 days.

2.8 *In Vitro* Hypoxic and Ischaemic Preconditioning

2.8.1 Nitrogen Gas Induced Hypoxic and Ischaemic Preconditioning

To induce hypoxia and ischaemia using gas mediated methods, a Galaxy® 48R incubator, with the capacity to regulate oxygen levels, was employed. To generate a hypoxic environment, the incubator was connected to a nitrogen gas cylinder. The oxygen concentration within the incubator decreased, to a set target of 1%, due to displacement by the nitrogen gas. Hypoxic basal media and ischaemic buffer were deoxygenated by incubating the solutions in 1% oxygen for a minimum of 24 hours. To induce hypoxia and ischaemia, HUVECs were incubated at 1% oxygen in deoxygenated basal media or ischaemic buffer, respectively, for the timescales stated in section 5.3.1.

2.8.2 $CoCl_2$ Induced Hypoxic and Ischaemic Preconditioning

$CoCl_2$ was used as a chemical mediated method of inducing hypoxia and ischaemia. A 1M stock of $CoCl_2$ solution was made by dissolving 2.38g $CoCl_2$ hexahydrate powder in 10mL sterile dH_2O. To minimise the errors which can arise from pipetting small volumes, this stock was further diluted to 10mM by adding 100µL to 9900µL sterile dH_2O. It was from this 10mM solution that experimental concentrations were made. To induce HPC and the hypoxic insult, the 10mM $CoCl_2$ solution was diluted in basal media, whereas it was added to ischaemic buffer when invoking IPC or the ischaemic insult. To induce HPC and the hypoxic insult, HUVECs were treated with the selected $CoCl_2$ concentrations for 24 hours. To invoke IPC and the ischaemic insult, HUVECs were exposed to $CoCl_2$ for 3 hours. Only 1 HPC cycle was used for its induction whereas between 1 and 4 were conducted when trying to invoke IPC. It should be noted that between every media and buffer change, a PBS rinse was performed. Additionally, after the conclusion of the preconditioning treatment, a 24-hour recovery period was allowed in EGM prior to the hypoxic or ischaemic insult being given.

2.8.3 Glycaemic Variability in HUVECs

To determine effects of glycaemic variability on HPC and IPC in HUVECs, they were exposed to acute hypoglycaemia, euglycaemia or hyperglycaemia as well as chronic hyperglycaemia. Acute exposures, as discussed in section 5.6, lasted for 3 hours using either a glucose free, 5.5mM glucose, or 30mM glucose, saline

solution. To make the 5.5mM and 30mM saline solutions, the necessary volume of 0.5M glucose stock solution was added to saline. The 0.5M glucose stock solution was prepared by dissolving glucose powder in sterile dH_2O and filtering prior to storing at 4^oC. For chronic hyperglycaemia exposure of P5 HUVECs, as in section 5.7, cells were incubated with 30mM glucose EGM or basal media. EGM and basal media were supplemented with glucose powder to final concentrations of 30mM and filtered.

2.9 Functional Analysis *In Vitro*

2.9.1 MTS Assay

The MTS assay is a popular test used to determine the effect of a treatment on cell viability and proliferation. This rapid assay allows simultaneous analysis of several experimental groups making it ideal for the preliminary identification of treatments which would warrant further in-depth investigation within a short time frame. HUVECs were plated in a 96 well plate and experiments conducted in triplicate after which the MTS cell proliferation assay was performed. 20µL MTS reagent [abcam, ab197010] was added to 200µL EGM in each HUVEC containing well, plus at least 2 empty wells to act as a blank to later be subtracted to account for background absorbance. The plate was incubated for 2 hours. It was then gently agitated and read at 490nm using a microplate reader. Blank values were averaged and subtracted from each sample replicate. The mean was then calculated from the triplicates of each sample and statistical analysis performed.

2.9.2 IncuCyte® Caspase 3/7 Apoptosis Assay

An IncuCyte® caspase 3/7 apoptosis assay was conducted to determine the proportion of cells exhibiting caspase 3/7 activity following a hypoxic or hypoxic control stimulus. A 1:1000 dilution of caspase 3/7 green reagent [Sartorius, 4440] was made in EGM. 100µL of this was added to each well containing cells in a 96 well plate which was placed into the IncuCyte® S3 Live-Cell Analysis Instrument. This in turn was kept inside a tissue culture incubator under a 37^oC/5% CO_2 as is standard. Every hour, for 18 hours, 5 images were taken per well using a magnification of 10X. Analysis of the images was completed using the IncuCyte® computer software. The caspase 3/7 reagent includes the caspase 3/7

recognition motif and DNA dye. As the reagent enters the cells, any activated caspase 3/7 cleaves the substrate to release the fluorescent dye which stains the DNA of the cell and appears green on the resulting images. The ratio of caspase 3/7 positive cells to the total cell number for each well at each timepoint was calculated indicating the proportion of cells which had commenced the apoptotic process.

2.9.3 HUVEC Immunostaining

2.9.3.1 Fixation and Permeabilisation

To fix HUVECs for immunostaining, media was aspirated from the cells and 2 PBS washes were performed. A 10% formalin solution was prepared by adding 10mL formalin stock [Genta Medical, BNFC50] to 40mL sterile dH_2O. 2mL 10% formalin was added to each well and the plate was allowed to sit at RT for 15 minutes. The formalin was removed, and an additional 3 PBS washes were conducted. 2mL PBS was added to each well and the fixed cells stored at 4^oC until ready to continue the staining process for up to 4 weeks.

HUVECs were permeabilised, as described by Al Mamun *et al*. (2020) prior to staining to allow detection of intracellular markers of interest (Al Mamum *et al*., 2020). It was achieved, concurrently with the blocking process, by incubating the coverslips with a 0.3M glycine 1% BSA 0.1% PBS-T solution for 1 hour at RT.

2.9.3.2 TUNEL Apoptosis Assay

A TUNEL apoptosis assay was conducted using manufacturer's guidelines [Thermo Fisher Scientific, C10617]. Several working solutions were prepared prior to commencing the assay. 1X TUNEL reaction buffer was made by adding the 500µL stock to 4.5mL dH_2O. To make the 1X TUNEL supermix, 2630µL 1X TUNEL reaction buffer, 67µL copper protectant and 3.7µL Alexa Fluor™ 488 picolyl azide were combined. Finally, the 100X TUNEL reaction buffer additive was made by adding 2mL of dH_2O to the 400mg powder provided. Premade solutions were aliquoted and the 1X TUNEL reaction buffer was stored at 4^oC whilst both the 1X TUNEL supermix and 100X TUNEL reaction buffer additive were kept at -20^oC.

HUVECs were fixed and permeabilised as in section 2.9.3.1. 100µL TdT reaction buffer was added to each of the coverslips which were incubated for 10 minutes at 37^{o}C. During this time, 50µL TdT reaction mixture was prepared per coverslip using: 47µL TdT reaction buffer, 1µL EdUTP, 2µL TdT enzyme. 50µL of the TdT reaction mixture was added to each coverslip and these were incubated for 1 hour at 37^{o}C. Coverslips were washed with 3% BSA PBS for 5 minutes twice.

For each coverslip, 10µL 10X TUNEL reaction buffer additive was made by diluting 1µL of the premade 100X TUNEL reaction buffer additive in 10µL sterile dH_2O. Using this, 50µL TUNEL reaction cocktail was prepared using: 45µL 1X TUNEL supermix, 5µL 10X TUNEL reaction buffer additive. 50µL TUNEL reaction cocktail was applied to each coverslip, and these were incubated for 30 minutes at 37^{o}C in the dark. They were then washed with 3% BSA PBS for 5 minutes.

Coverslips were stained with 4',6-diamidino-2-phenylindole (DAPI) and mounted onto slides as in section 2.9.3.3. As high resolution was not as important for this assay, a fluorescence microscope was used to image the slides. ImageJ software was utilised to visualise the images obtained and to count the number of DAPI positive cells per image whilst the number of TUNEL positive cells were counted manually. The percentage of TUNEL positive cells was calculated by dividing the number of these cells by the number of DAPI positive cells, per image, and multiplying by 100. For each slide, the mean of the percentage of TUNEL positive cells was determined and statistical analysis performed.

2.9.3.3 DAPI Staining and Coverslip Mounting

To prepare the DAPI antibody, 2.1µL 14.3mM stock [Thermo Fisher Scientific, D-13066] was diluted with 100µL PBS making a 300µM intermediate solution which could be stored at -20^{o}C. The nuclei of the cells were stained by diluting the intermediate solution 1:500 in PBS, to a working concentration of 600nM, and incubating coverslips with 50µL for 10 minutes at RT. Coverslips were briefly rinsed 3 times with PBS. To mount the sides, 30µL mounting medium [Thermo Fisher Scientific, P36930] was pipetted onto to the cell surface of the coverslips. Polysine coated slides were pressed onto the coverslips ensuring no bubbles were present. Clear nail polish was carefully applied along the edges of

the coverslips to ensure they were sealed to the slides.

2.10 Protein Analysis

2.10.1 Protein Quantification

2.10.1.1 Standard Cell and Tissue Lysis for Western Blot

This protocol was suitable for the lysis, using standard lysis buffer (Table 8.8), of HUVECs and aortas due to undergo protein analysis for all proteins of interest except for when determining HIF1α protein expression which requires a specialised procedure, as in section 2.10.1.2. For HUVECs, media was aspirated, and petri dishes were placed on ice. They were rinsed once with cold PBS and 100µL standard lysis buffer was added. Cells were harvested into the lysis buffer using a cell scraper which was subsequently transferred into an Eppendorf tube using a pipette. Tubes were allowed to sit on ice for 15 minutes.

For the aortas, prepared as in section 2.6.4, 300µL standard lysis buffer was added to each Eppendorf tube and samples were immediately lysed.

To encourage lysis or the aorta and HUVECs, the tube contents underwent sonication. Briefly, the sonicator was set to an amplitude of 40%. Each tube was sonicated for a total of 20 seconds in 4 second pulses separated by 2 second pauses. Tubes were immediately placed back onto ice following sonication. The sonicator probe was washed using ethanol and dH_2O in between each tube being sonicated as well as both before the commencement and after the completion of the procedure. For aortas, the sonication process for each sample was repeated to ensure complete lysis. Tubes were centrifuged at 13,000rpm for 20 minutes at 4^{o}C. The supernatants were transferred into fresh Eppendorf tubes and stored at -20^{o}C until such a time that the Bradford protein concentration assay was due to be completed.

2.10.1.2 Specialised Cell Lysis for HIF1α Western Blot

Due to the rapid degradation of HIF1α, Dr James Cantley, of the University of Dundee, recommended a specialised lysis buffer (Table 8.9) should be used to lyse cells quickly thereby enabling the protein to be detected via western blot. The presence of sodium dodecyl sulphate (SDS) and urea in the specialised lysis

buffer causes the denaturation of proteins and increases their solubility helping to stabilise the HIF1α protein. Cell dishes were placed on ice, media aspirated and immediately washed twice in ice cold PBS. Using a cell scraper, cells were scraped into the PBS and transferred into an Eppendorf tube. Samples were centrifuged for 5 minutes at 2500rpm at 4^{o}C before discarding the PBS supernatant and resuspending the pellet in 100µL SDS-urea lysis buffer. Lysates were sonicated, as described in section 2.10.1.1, however the sonicator probe was rinsed using 0.1% SDS, diluted in dH_2O in between sonicating the sample and washing with 70% ethanol. Samples were left on ice for 10 minutes and transferred for storage at -20^{o}C until ready to quantify the protein concentration within.

2.10.1.3 Bradford Protein Quantification Assay

A Bradford assay is conducted to determine the protein concentration in a given cell or tissue lysate (Bradford, 1976). The BSA standards were prepared as indicated from a pre-prepared 2mg/mL stock (Table 2.1). 5µL BSA standards and lysates were added to wells of a standard clear 96 well plate in triplicate. 150µL Bradford reagent was added to each well and the plate incubated at RT for 10 minutes in the dark. The absorbance was measured using a microplate reader set to a wavelength of 590nm. A standard curve was generated from the resulting absorbance values and if the coefficient of determination, also termed R^2, was above 0.95, concentration calculations were performed on the samples.

Final Concentration (mg/mL)	**Volume of 2mg/mL BSA Stock (µL)**	**Volume of dH_2O (µL)**
0	0	100
0.25	12.5	87.5
0.50	25	75
0.75	37.5	62.5
1.0	50	50
1.5	75	25

Table 2.1 BSA Standards for the Bradford protein quantification assay. To generate a standard curve for the Bradford protein quantification assay, 6 concentrations of BSA are made up using a 2mg/mL stock and dH_2O.

2.10.2 Western Blot

2.10.2.1 Sample Preparation

100µL western blot samples were prepared using the proportions of lysate and dH_2O calculated by the Bradford protein quantification assay. Each 100µL western blot sample consisted of a minimum of 0.5µg/µL protein and, depending on the protein concentration within the sample, included either 50µL complete loading dye (Table 8.11) or 25µL loading dye solution (LDS) sample buffer (Table 8.12). The resulting sample cocktail was heated at 95^{o}C for 5 minutes to denature the protein content.

2.10.2.2 SDS-PAGE

The 10% lower gel (Table 8.13) was poured into the casting apparatus [Bio-Rad, 1658013], ensuring enough space was left at the top for the comb. This gap was topped up with dH_2O to make sure the gel set straight. Once the gel had set, the dH_2O was removed and replaced with the 4% upper gel (Table 8.14). The comb was inserted into this to create loading wells. After the upper gel had set, the gels were transferred into the electrophoresis tank [Bio-Rad, 1658004]. This was filled with 1X tris-glycine running buffer made by diluting the 10X tris-glycine running buffer (Table 8.17) 1:10 in dH_2O. The comb was removed, and the wells washed with the buffer within the tank. Samples were carefully pipetted into wells ensuring 10-20µg of protein was added per well. 5µL protein ladder [Thermo Fisher Scientific, LC5925] was added to at least one well of each gel. The lid was positioned onto the tank, connecting the electrodes, and electrophoresis was run at 150V. The power was removed when the pink, 22kDa band of the ladder reached the bottom of the gel.

2.10.2.3 Wet Transfer

To prepare for the wet transfer, 1X transfer buffer was made, by combining 100mL 10X transfer buffer (Table 8.18), 200mL methanol and 700mL dH_2O. For each gel to be transferred, the following were soaked in the 1X transfer buffer: 2 sponges, 4 squares of filter paper and 1 square of nitrocellulose membrane. The transfer tank was set up by inserting the transfer electrodes and an ice block, then placing the tank in a box with ice. Once gel electrophoresis was complete, gels were soaked in the 1X transfer buffer for at least 5 minutes. Transfer

cassettes were set up (Fig. 2.7) and 2 were inserted into each tank. For most proteins, the transfer was run for 2 hours at 70V whilst for proteins of larger than 110kDa, the transfer was performed overnight for 999 minutes at 25mA and 12V.

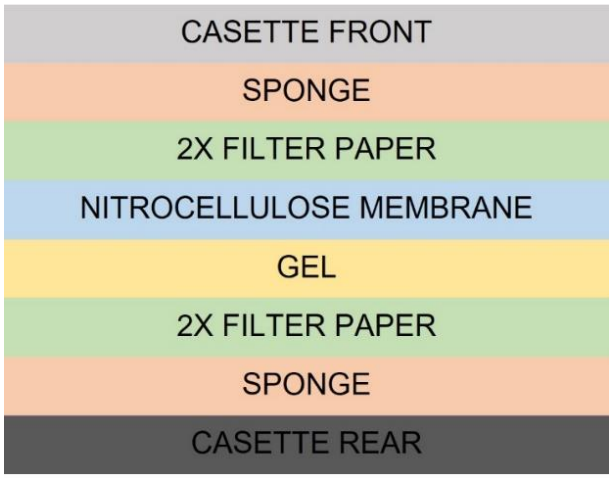

Fig. 2.7: Wet transfer cassette set up. For each gel to be transferred, the wet transfer cassette was assembled by forming a sandwich consisting of, from the rear to the front of the setup, 1 sponge, 2 squares of filter paper, the gel containing the separated proteins, a square of nitrocellulose membrane, 2 squares of filter paper and 1 sponge all of which had been soaked in 1X transfer buffer.

2.10.2.4 Ponceau Stain

A ponceau stain was used to confirm proteins had been successfully transferred onto the membrane. Membranes were incubated with 10mL ponceau [Sigma Aldrich, P7170] for 2 minutes. The ponceau was removed and replaced into its conical tube for reuse. Membranes were briefly rinsed with dH_2O to visualise bands. Membranes were cut if multiple proteins of different sizes were to be detected on one enabling several targets to be probed for simultaneously. Membranes were washed twice with 1X tris buffered saline-tween (TBS-T) (Table 8.20) for 5 minutes.

2.10.2.5 Total Protein Stain

Quantification of total protein using a Revert™ 700 Total Protein Stain Kit [Li-Cor, 926-11014] was occasionally performed following wet transfer in place of a ponceau stain and probing for a single housekeeping protein. The nitrocellulose membrane was allowed to dry out on a piece of filter paper for 60 minutes. It was rehydrated by incubating with PBS for 5 minutes after which it was rinsed with ultrapure dH_2O. The membrane was stained with 5mL Revert™ 700 Total Protein

Stain for 5 minutes. The Stain solution was discarded and 2 30 second washes were performed using the Revert™ 700 Wash Solution. This was discarded and the membrane rinsed with ultrapure dH_2O. Bands were imaged on the Li-Cor Odyssey CLx. The membrane was again rinsed with ultrapure dH_2O. The stain was removed by incubating the membrane for 10 minutes with 5mL Revert™ Destaining Solution. Antibody incubation proceeded as described in section 2.10.2.6. Total protein stain was quantified using Imperia Studio software.

2.10.2.6 Antibody Incubation

Membranes were blocked by incubating them in 5% BSA TBS-T for 1 hour. Primary antibodies were diluted in 5% BSA TBS-T (Table 8.23). Each membrane, or membrane segment, was incubated on a rocker overnight at 4^{o}C in 10mL primary antibody.

2.10.2.7 Antibody Detection

Primary antibodies were removed from the membranes and replaced into their respective conical tubes for reuse. Membranes were then washed three times in TBS-T for 5 minutes. As the washes may remove some of the blocking conducted in section 2.10.2.6, to limit the background caused by the secondary antibody, the membranes were again blocked with 5% BSA TBS-T for just 20 minutes. Membranes were rinsed 3 times with TBS-T. Secondary antibodies were diluted in 5% BSA TBS-T (Table 8.24). Membranes were incubated in the appropriate secondary antibodies for 1 hour at RT on a rocker. They were washed 3 times for 5 minutes with TBS-T to remove unbound antibody before imaging. Proteins were visualised using a Licor Odyssey® CLx which read membranes at wavelengths of 700nm, red, and 800nm, green. Images were analysed as in section 2.10.2.8 and membranes were stored in TBS-T at 4^{o}C.

2.10.2.8 Quantification

Densitometry was performed on the images using Image Studio Lite software version 5.2.5, except for the total protein stain where Imperia Studio software was used, to quantify the proteins. Proteins were normalised to either actin, loading control, or total protein expression. For proteins where a phosphorylated and non-phosphorylated form were detected, the normalised value of the former was

divided by that of the latter to determine the proportion of the protein that was activated.

2.11 Statistical Analysis

All graphs were generated, and statistical analysis performed using GraphPad Prism version 9.3.1. Grubbs' tests were used to detect anomalous values within the data, and any subjects with at least one anomalous data point were removed from all graphs and statistical analyses. To identify outliers, a Grubbs' test with maximum significance threshold of 0.05 was used. A Shapiro-Wilk normality test was used to determine whether data was normally distributed. Parametric tests were conducted on complete data sets which passed the normality test, or which did not have sufficient sample sizes to provide statistical power. Other data sets were analysed using non-parametric tests. The statistical tests used are indicated in each results section of chapter 3-5 whilst the reasoning for their selection is highlighted below.

Results obtained from *in vitro* and *in vivo* studies which comprised of 2 independent variables, usually treatment type and time, were analysed using Bonferroni's repeated measures multiple comparisons 2-way ANOVA. Complete data sets could be measured using this method but due to faults with the FLPI laser resulting in missing data points, a proportion of the reactive hyperaemia data had to be analysed using Bonferroni's multiple comparisons mixed effects model instead.

Within each experiment during the *in vitro* studies, all treatments were given to each biological replicate meaning data obtained here were matched across both timepoint and treatment type. Dose-response curves were analysed using Dunnett's repeated measures multiple comparisons 2-way ANOVA.

Data with only 1 independent variable, but more than 2 treatment types were analysed using Tukey's repeated measures one-way ANOVA. Data with 1 independent variable and just 2 treatment types were analysed by performing the unpaired t test with Welch's correction except for when data was matched in

which case a paired t test was conducted. A Wilcoxon matched pairs signed rank test was used as a non-parametric substitute for the paired t test.

In situations where only a selection of comparisons was made, Bonferroni's correction was utilized. Whilst correcting for multiple comparisons using the Sidak method would afford greater power, this can only be used if the variables to be compared are independent which was not the case for experiments performed within this project. The post hoc Tukey test was conducted when all combinations of comparisons were being made. Finally, Dunnett's test was employed when comparing values from treatment groups to those obtained
from a control cohort.

Chapter 3

Optimisation of an *in vivo* Model of R-IPC

3.1 Introduction

The aim of this initial results chapter was to validate an *in vivo* model of R-IPC which could later be used to investigate if it is affected by glycaemic variability. To validate the R-IPC model, it was hypothesised that there would be an improvement in endothelial function when LDI was performed, alongside PE/ACh iontophoresis, following receipt of the preconditioning treatment.

A literature search revealed that there are 2 methods of occluding and reperfusing blood vessels to induce R-IPC in mice: internal and external. The internal method typically involves directly ligating the femoral vascular bundle and performing cycles of ischaemia/reperfusion by repeatedly loosening and tightening the ligature (Oberkofler *et al*., 2014). A principal advantage of using the internal ligation technique is that it is possible to be sure exactly which vessels are being occluded. However, method was deemed unsuitable for the following studies for numerous reasons. Firstly, given there are non-surgical alternatives, it seemed somewhat invasive and there was a concern that the chances of death, injury, and poor post-surgery recovery would have been increased. It also would have required the animal to be anaesthetised for longer due to the time taken to open and close the surgical site. Finally, the external method of inducing vessel occlusion/reperfusion is more equivalent to the R-IPC treatment given in humans. Hence, for the purposes of this project, the decision was made to use the external method to induce occlusion/reperfusion of the blood vessels.

The most common way to induce R-IPC using the external technique is to wrap a blood pressure cuff around the hindlimb of the mouse (Table 1.1), although other forms of tourniquet have also been employed. Ischaemia is induced by inflating the cuff to a pressure between 200mmHg and 250mmHg. To ensure cessation of blood flow, the pressure exerted must be higher than that of the arterial occlusion pressure (AOP) which can be calculated using the formula below (Tuncali *et al*., 2006):

$$\text{AOP (mmHg)} = \frac{\text{DAP (mmHg)} + 10}{\text{Tissue Padding Coefficient}}$$

Rather than measure the blood pressure for each animal, 120mmHg is used as the SAP as this is the calculated daily average for C57BL/6J mice (Mattson, 2001). The tissue padding coefficient is related to the circumference of the limb around which the cuff is to be placed in the form of an inverse correlation. As a coefficient, the maximal number possible for this variable is 1. Tuncali *et al*. found a circumference of 20cm related to a tissue padding coefficient of 0.91 (Tuncali *et al*., 2006). Therefore, as the hindlimb of a mouse is significantly smaller than this, the coefficient will be somewhere between 0.91 and 1. This resulted in an AOP of 130-143mmHg being calculated. As this value was drastically lower than those utilised in the literature, it was decided that a pressure of 200-250mmHg should be used to mimic these previously published R-IPC models. As the degree of vessel occlusion can be maximised by using greater pressure, 250mmHg was selected as the target pressure to be applied to the hindlimb. There was a concern from veterinary personnel within the MSRU that a pressure higher than 250mmHg would damage the hindlimb resulting in the mouse being unable to walk correctly. Hence, it was decided that this should be the maximum pressure used. Reperfusion is then invoked by simply releasing the cuff or tourniquet allowing blood to flow to the foot once more. To confirm complete occlusion, some studies wait until there is an absence of a femoral artery pulse in the leg, below the tourniquet site, (Oberkofler *et al*., 2014) or, for a change in the colour of the foot. These techniques were deemed inappropriate due to the lack of pulse not necessarily indicating complete occlusion, and the presence suggesting reperfusion, and alterations in foot colour potentially being too subtle and subject to personal interpretation. A more superior method used to determine the induction of ischaemia is to directly monitor the blood flow through the foot. FLPI can provide live imaging, meaning sudden changes in blood flow could be observed which may be missed with LDI.

As exhibited in section 1.5.2 (Table 1.1), R-IPC has been induced in mice in multiple ways. However, the most prevalent appeared to be by performing 4 cycles of 5 minutes ischaemia/5 minutes reperfusion on the hindlimb. Hence, this protocol was selected when designing a preliminary study.

3.2 Preliminary Study to Validate an *in vivo* R-IPC Model

A preliminary *in vivo* study was designed with the aim of validating a R-IPC model (Fig. 3.1). Isoflurane anaesthetised animals underwent a baseline LDI scan with PE/ACh iontophoresis. They subsequently received either R-IPC treatment, consisting of 4 cycles of 5 minutes ischaemia/5 minutes reperfusion or, a control treatment, in which a deflated cuff was worn for 40 minutes. Mice immediately underwent a second acute LDI scan with PE/ACh iontophoresis. 72 hours later, a final delayed LDI scan with PE/ACh iontophoresis was performed after which the animals were immediately euthanised and tissue harvested. Additionally, plasma was collected following completion of the baseline, acute and delayed LDI with PE/ACh iontophoresis scans. A cytokine array was conducted on the plasma obtained from a small cohort of the study animals. The multiplex was chosen, over single marker ELISAs, due to the wide range of cytokines which R-IPC affects, as well as the need to conserve the limited quantity of plasma collected per mouse.

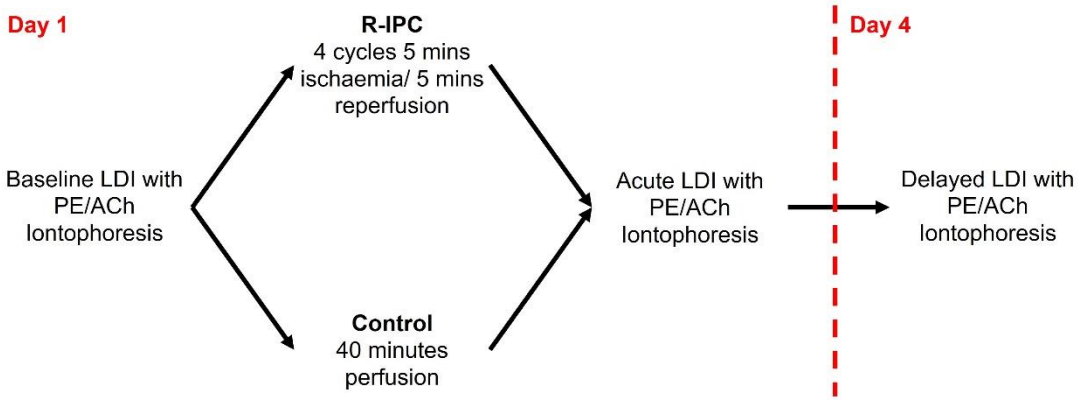

Fig. 3.1 Preliminary in vivo study protocol timeline. Schematic indicating the procedures C57BL/6J mice underwent in the preliminary *in vivo* study. Animals were anaesthetised with isoflurane for all procedures and randomly allocated into 1 of 2 groups depending on whether they received R-IPC or control treatment. All animals were euthanised and tissue harvested following completion of day 4.

3.2.1 Pressure of 250mmHg Induced Occlusion of Blood Flow to the Foot

Vessel occlusion of the foot was confirmed by inflating the blood pressure cuff around a hindlimb and monitoring blood flow to it using FLPI. Inflating the cuff to a pressure of 250mmHg led to the absence of flux within the images produced indicating blood flow through the foot had been blocked. Deflating the cuff

allowed the return of flow exhibited by the presence of flux values (Fig. 3.2).

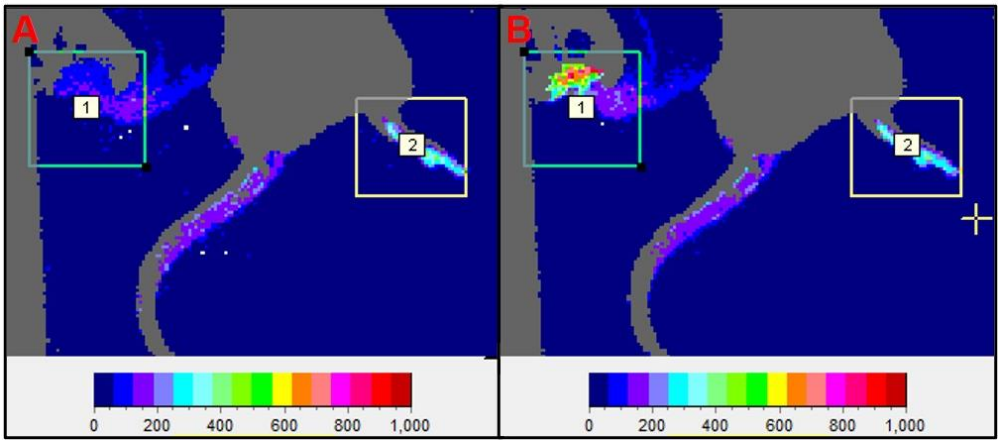

Fig. 3.2 Pressure of 250mmHg occludes blood flow. Flux images generated using FLPI demonstrate the presence or absence of blood flow to an individual's hindlimb (region of interest (ROI) 1). Inflating a blood pressure cuff to 250mHg caused inhibition of blood flow to the foot signified by the absence of flux (A). Blood flow to the foot resumed upon deflation of the cuff and was observed through the return of flux (B).

3.2.2 Both R-IPC and Control Treatment Significantly Increased the Endothelial Response to ACh in the Preliminary Model

To determine if acute and delayed effects of the R-IPC protocol were present, LDI data was analysed to identify the impact of treatment type on any of the 3 scanning timepoints using Bonferroni's repeated measures multiple comparisons 2-way ANOVA (Fig. 3.3). There was a significant increase in the delta flux in both groups at the acute scan (control mean=190.2, p=0.0490 and R-IPC mean=167.3, p=0.0257) compared to their respective baselines (control mean=80.40 and R-IPC mean=77.75). It was only in the control group though where this elevated delta flux response remained significant at the delayed scan 72 hours post R-IPC (mean=147.6, p=0.0149). There was no significance between the acute and delayed scans in either group for any of the 4 parameters calculated. Additionally, when comparing the acute and delayed scans to their baselines, no significant differences were detected in the steady-state flux, or the minimum flux reached due to PE mediated vasoconstriction. In both treatment groups however, there was a significant increase in the maximum flux caused by ACh induced vasodilation between the acute scan (control mean=354.4, p=0.0091 and R-IPC mean=340.0, p=0.0193) and their respective baselines (control mean=257.8 and R-IPC mean=189.3). There were no significant differences between groups at the same time point.

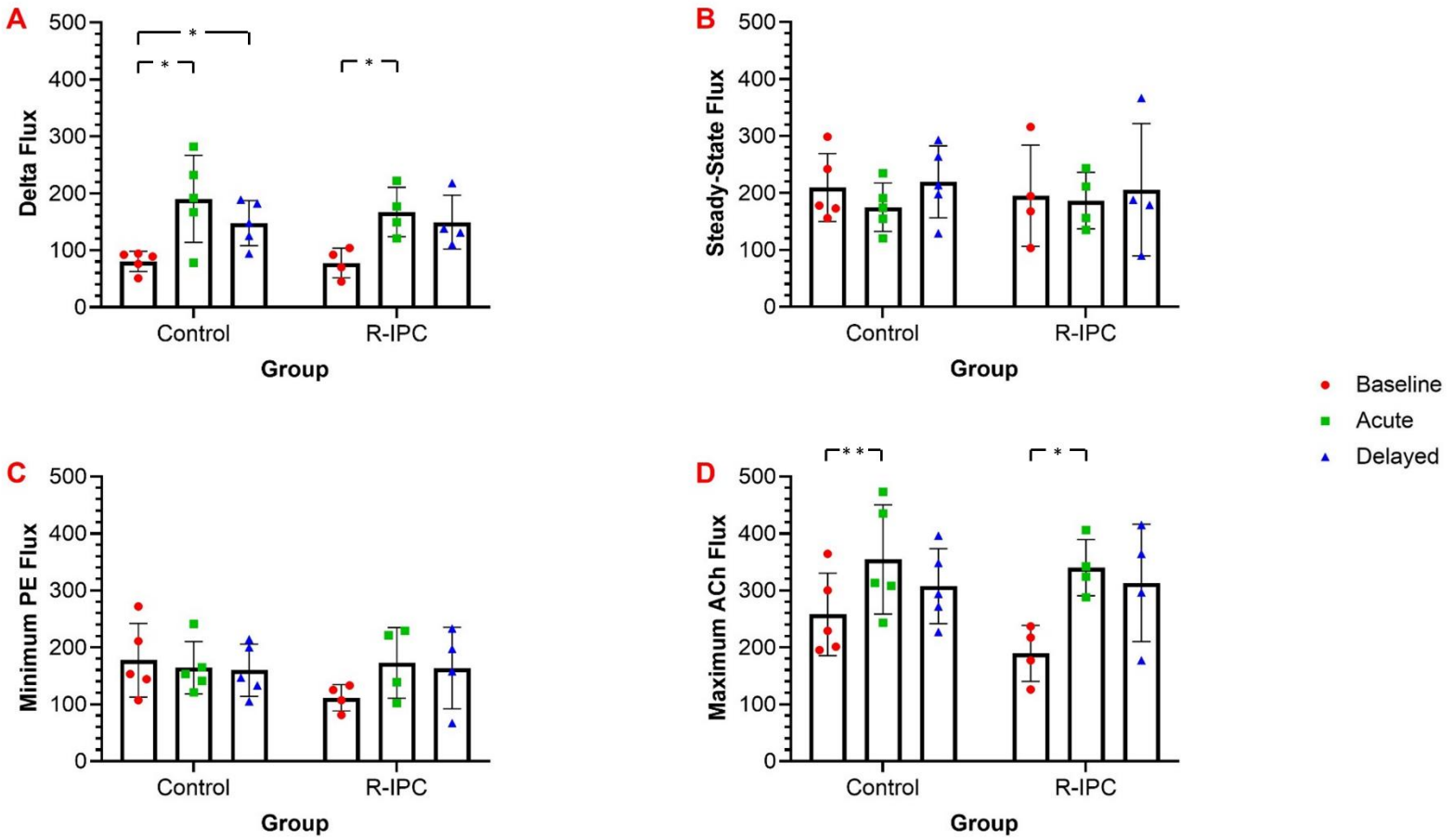

Fig. 3.3 Preliminary *in vivo* study LDI with PE/ACh iontophoresis. Mice had an LDI scan with PE/ACh iontophoresis immediately before (baseline), after (acute) and 72 hours post (delayed) R-IPC or control treatment. Delta flux (A) was found by subtracting the minimum flux due to PE induced vasoconstriction (C) from the maximum due to ACh induced vasodilation (D). Steady-state (B) refers to the flux prior to applying the current. Mean with SD and individual data points are plotted. Significant differences are indicated (* = $p<0.05$, ** = $p<0.01$).

3.2.3 R-IPC and Control Treatment Had No Significant Effects on Plasma KC/GRO, TNFα and IL-10 Concentrations

To determine whether R-IPC affected the inflammatory state of the animals, a cytokine array was performed using a small number of plasma samples obtained blood taken from the tail vein of mice immediately after the 3 scanning timepoints. Plasma samples were only used from animals that were not removed from the study following completion and that did not experience any respiratory distress, as discussed further in section 3.2.4. Out of the 10 cytokines probed for, only KC/GRO, TNFα and IL-10 had levels which could be detected and whose concentration could be determined in all subjects (Fig. 3.4). The role of TNFα and IL-10 in R-IPC are discussed further in section 1.5.5, whilst KC/GRO is a cytokine known to activate PI3K, mitogen-activated protein kinase (MAPK) and extracellular signal regulated kinase pathway under inflammatory conditions. Statistical analysis was performed using Bonferroni's repeated measures multiple comparisons 2-way ANOVA. No significant differences were identified in the plasma concentrations of any of these 3 cytokines within each treatment group. Additionally, there were no significant differences in the expression of these 3 cytokines between the treatment groups at each respective sampling timepoint. This non-significance was likely due to the small sample sizes in each group but there are trends worth noting which may become significant if more samples were analysed. Expression levels of the 3 detectable cytokines were similar in each treatment group in plasma taken at the baseline scan. There appeared to be a large increase in TNFα expression between the baseline and acute scan of R-IPC treated animals which was not observed in the controls although this is non-significant, and more samples would be required to confirm this. Additionally, there was a marked decrease in KC/GRO expression in the control group, between the baseline and acute scan, which was not seen in the R-IPC subjects. Again, this finding was non-significant and firm conclusions could only be made if the sample size was increased. However, the mean concentrations of both cytokines were similar between groups after the delayed scan. Finally, there was little change in the expression of IL-10 between the baseline and acute scans although there was an increase in concentration at the delayed scan in both groups.

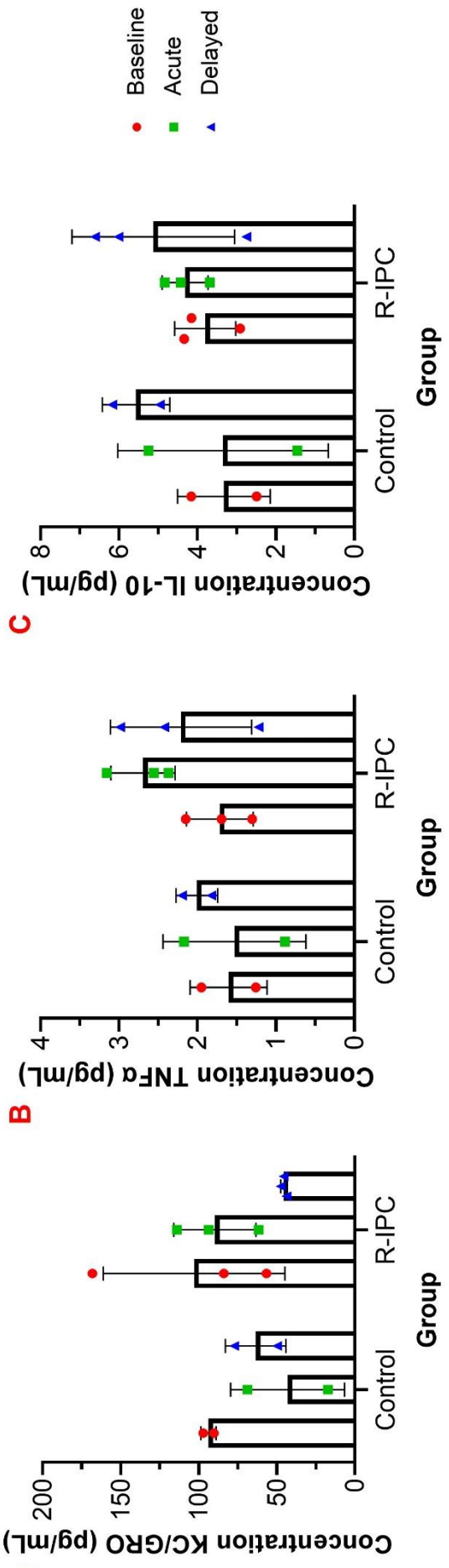

Fig. 3.4 Preliminary in vivo study plasma concentration of KC/GRO, TNFα and IL-10. Concentrations of KC/GRO (A), TNFα (B) and IL-10 in the plasma were determined using a cytokine array. Plasma was taken from mice immediately after the baseline, acute and delayed scans of the preliminary study. Mean with SD and individual data points are plotted.

3.2.4 Limitations and Improvements to the Preliminary Study

Significant issues arose whilst conducting this series of experiments. Of the 18 animals recruited onto the study, 9 had to be removed from analysis for the following reasons: identified as an outlier due to the Grubbs test which was conducted on the LDI with PE/ACh iontophoresis data (Fig 3.3) (1), did not complete the study due to poor health (4), found to have an uncertain genetic background after they had already completed the study (4). Individuals who did not complete the study experienced breathing difficulties whilst under anaesthetic on day 1 and did not recover full consciousness meaning they had to be euthanised. Many mice, who were able to complete the study, also experienced breathing abnormalities during this first day but were able to recover and continue to the subsequent scan 72 hours later. After consultation with a veterinarian, it was concluded that the reason for the prevalence of respiratory distress during day 1 was caused by the formation of lung dysfunction linked to i) duration of anaesthesia, at 90-120 minutes, ii) the need to reposition the mice several times to perform the different stages of the protocol, iii) oxygen flow rate, and iv) the percentage of oxygen within the gas used to carry the anaesthetic.

This preliminary study used 100% oxygen gas as a carrier for the isoflurane, although some studies suggest that a gas mixture containing just 21% oxygen would reduce the prevalence of respiratory issues. Wilding *et al*. (2017), found that mice exposed to isoflurane carried by 100% oxygen gas for 60 minutes exhibited an elevated alveolar-arterial gradient compared to what would be expected. This gradient is a marker of the efficiency of gas exchange between the lungs and circulation, with a higher value indicating impaired transfer. A raised gradient is associated with atelectasis, a form of lung collapse, which was more prominent in the animals receiving 100% oxygen. Atelectasis is dependent upon time meaning it is more likely to develop with prolonged anaesthesia periods (Wilding *et al*., 2017). In retrospect, atelectasis could have been confirmed by performing a haematoxylin and eosin stain on the lung tissue post-mortem but this was not conducted as initially the observed respiratory distress was believed to be due to the apparatus used to administer anaesthesia.

Additionally, the oxygen flow rate of 1L/min is higher than recommended for mice as it significantly exceeds their respiratory minute volume. Elevated flow

rates can be linked to increased risk of hypothermia, and the drying of the airways potentially causing inflammation and bronchospasm (Adelsperger *et al*., 2016). Severe bronchospasm has been associated with cases of negative pressure pulmonary oedema (NPPO), although it is speculated that the true incidence of this link is drastically underreported (Kordel *et al*., 2011). Whilst typically associated with blockage of the airways during intubation, NPPO is a form of pulmonary oedema which forms when obstruction of the airway leads to increased negative pressure. Following airway occlusion, inspiratory efforts continue causing a high-pressure gradient consequently resulting in elevated pulmonary capillary permeability. Fluid then moves from the capillaries into the alveolar and interstitial spaces thereby forming oedema and impairing alveoli function (Bhaskar and Fraser, 2011). Newer vaporisation systems will allow significantly lower flow rates to be used, but the more traditional apparatus utilised in the preliminary study had a minimum rate of 1L/min, hence its use. Previous studies conducted within the animal research facility, using LDI with iontophoresis, have not been affected by the anaesthesia apparatus used, but this is likely because normally the subjects would have been exposed to the anaesthetic for a significantly shorter time within an individual period of anaesthesia.

Moving the animal throughout the procedure could cause any areas without oedema, or lungs which have not collapsed, to become compressed by the surface upon which the mouse is lying. The already compromised respiratory system was then further aggravated by the weight of the iontophoresis ring adhered to the flank. The ideal solution to this would be to use a more appropriate anaesthetic administration apparatus enabling a more suitable oxygen concentration and flow rate for the size of the mice. However, as this was not possible, given the facilities available, it was suggested that subjects should be receiving anaesthesia, via the nose cone, for a minimal period per session of anaesthesia.

It is probable that the issues observed arose due to the duration of anaesthesia and the need to move the mice during the protocol on day 1. Past studies, conducted by investigators at other research institution using the same method of inducing R-IPC did not identify any issues relating to anaesthesia or report

elevated mortality rates. This is likely due to the apparatus utilised for the induction and maintenance of anaesthesia being more appropriate for use with small animals. Additionally, many use methods of assessing efficacy of their models which do not require moving the animal during a single prolonged anaesthesia exposure. The identification of these issues led to major alterations with the protocol. Firstly, by using the FLPI scan with reactive hyperaemia test, as opposed to LDI with PE/ACh iontophoresis, and removing an acute scan, the anaesthesia time for baseline and final scan timepoints was reduced by more than half. Secondly, the R-IPC and control treatments were to be given on separate days to the baseline and final scans, also to limit the period of anaesthesia exposure in a single session. Additionally, due to non-significant changes in the functional data and cytokine expression, there was concern that the 4 cycles of R-IPC were insufficient as a stimulus. Also, the ultimate aim would be to use the validated R-IPC treatment in animal models of diabetes. As mentioned in section 1.5.4, this population require a greater number of R-IPC cycles to achieve the threshold to invoke the protection conferred. Hence it was decided that the number of total R-IPC cycles received was increased from 4 to 9.

3.3 Primary Optimisation Study to Validate an *in vivo* R-IPC Model Using Reactive Hyperaemia as a Functional Test

The new model included 9 cycles of R-IPC given over a period of 3 days (Fig. 3.5). The cycle lengths remained at 5 minutes ischaemia/5 minutes reperfusion whilst the reactive hyperaemia test was used to perform functional analysis. On day 1, mice underwent the baseline reactive hyperaemia scan. To ensure the baseline reactive hyperaemia scan did not interfere with the R-IPC or control treatments, a 3-day gap was then allowed for animals to recover. Then, on days 5-7, mice either received R-IPC treatment, consisting of 3 cycles of 5 minutes ischaemia/5 minutes reperfusion per day, or control treatment, consisting of wearing a deflated pressure cuff for 30 minutes per day. A rest day was given on day 8 as this was when it was planned to introduce an additional hypoglycaemic stimulus upon successful validation of the R-IPC model. On day 9, mice then underwent a final reactive hyperaemia scan. Following completion of the experiment, mice were euthanised and tissue harvested. Protein expression of endothelial function markers in the aorta was determined using western blot. Due

to the promising results obtained from the cytokine array in the preliminary study, and its important role in mediating R-IPC, TNFα expression in the plasma was investigated using an ELISA. Dr Calum Forteath performed experiments on and harvested the tissues from 6 of the 12 mice used. All other protocols and all analyses were conducted by me. Statistical analysis of the data obtained from FLPI was performed using Bonferroni's multiple comparisons mixed effects model.

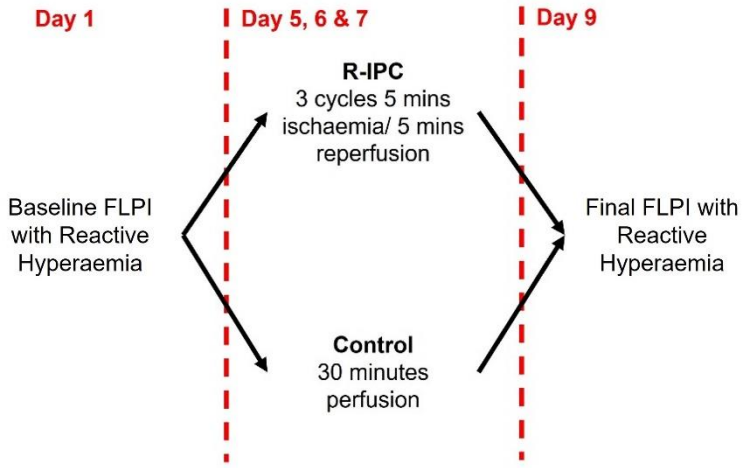

Fig. 3.5 Primary optimisation study protocol timeline. Schematic indicating the procedures C57BL/6J mice underwent in the primary optimisation study. Animals were anaesthetised with isoflurane for all procedures and randomly allocated into 1 of 2 groups depending on whether they received R-IPC or control treatment. All animals were euthanised and tissue harvested following completion of day 9.

3.3.1 R-IPC Appeared to Decrease Magnitude of Reactive Hyperaemia but not Total Excess Flux

For all mice, on days 1 and 9, to determine whether R-IPC improves endothelial function, both the magnitude of reactive hyperaemia and the total excess flux present during this period were calculated (Fig. 3.6). The method used to determine these factors is presented in section 2.4.4 (Fig. 2.4), but it additionally summarised here. The magnitude was determined by subtracting the post reactive hyperaemia steady-state flux (Fig. 8.1) from the peak flux reached during the reactive hyperaemic response (Fig. 8.1). Using this value, and the duration between the commencement and end of the reactive hyperaemic response (Fig. 8.1), the total excess flow was also calculated. In the R-IPC group, the magnitude was significantly decreased at the final scan (mean=38.71) compared to the

baseline scan (mean=69.21, p=0.0088). This would initially imply that the R-IPC treatment used causes a decrease in endothelial response. However, this finding was likely due to an abnormally elevated magnitude at the baseline scan in the R-IPC group. At the baseline scan in the R-IPC group, the magnitude and excess flux (mean=4503) were significantly higher (magnitude p=0.0342, excess flux p=0.0339) compared to the baseline scan in the control group (magnitude mean=26.03, excess flux mean=1126). The magnitude and total excess flux at the final scan in the R-IPC group appeared to be slightly, though non-significantly, higher than in the control group. However, baseline and final scans were conducted in the same animal and were therefore not independent. Hence, the apparent elevation in the magnitude of reactive hyperaemia and total excess flux in the R-IPC group at the final scan may not be associated with the R-IPC treatment but may instead be attributed to their elevation at the baseline scan.

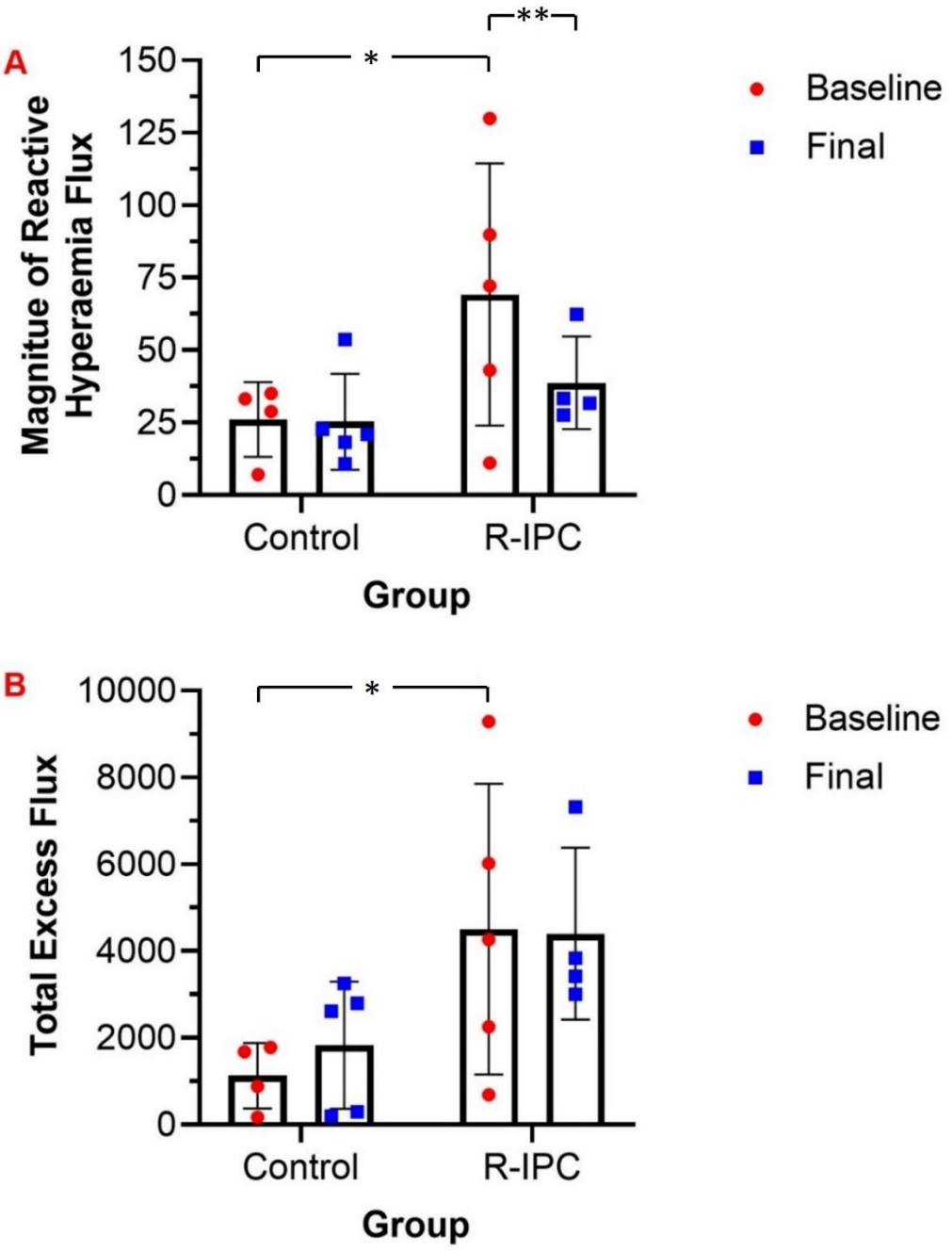

Fig. 3.6 Effects of R-IPC on reactive hyperaemia. Mice underwent baseline and final reactive hyperaemia scans on days 1 and 9 of the protocol described in figure 3.5. Magnitude of reactive hyperaemia (A) was determined by subtracting the peak flux, following ischaemia, from the post reactive hyperaemia steady-state. Total excess flux during reactive hyperaemia (B) was found using this magnitude value, and the duration of the response to calculate the area under the flux trace. Mean with SD and individual data points are plotted. Significant differences are indicated (* = $p<0.05$, ** = $p<0.001$).

3.3.2 Steady-states were not affected by reactive hyperaemia in either hindlimb in the primary optimisation model

To ascertain whether reactive hyperaemia affected the steady-state flux of both

hindlimbs during each baseline and final scan, statistical analysis was performed on these data sets. In doing this, the analysis also allowed the observation of whether R-IPC or control treatment influenced the effect of reactive hyperaemia on the steady-state fluxes. Due to the large variation between mice, to perform the analysis, fold change between the post reactive hyperaemia and pre reactive hyperaemia steady-state fluxes for each hindlimb during each of the scanning sessions was calculated. However, no significant differences in steady-state flux, of either hindlimb, before and after reactive hyperaemia was found in any of the baseline or final scans regardless of whether individuals received R-IPC or control treatment (Fig. 3.7). Whilst it would have been ideal to compare changes in the steady-state flux values between baseline and final scans, this was not practical as massive within subject variation between the scanning timepoints arose primarily due to issues identified with the technique which are discussed in depth in section 3.3.5.

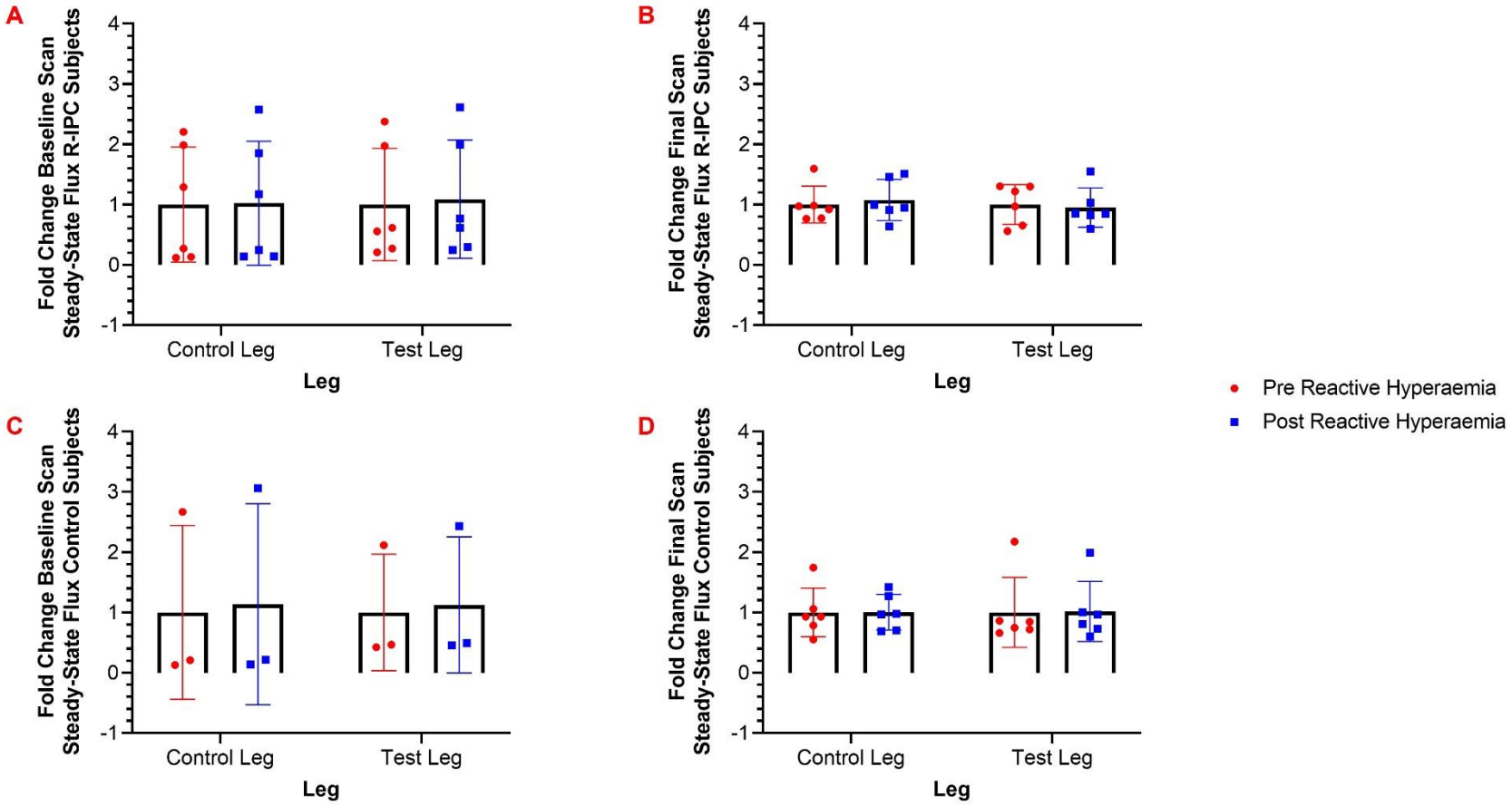

Fig. 3.7 Variation in steady-state flux during baseline and final scans in the primary optimisation study. Steady-state flux values for each hindlimb of the mice were recorded during the baseline (A and C) and final (B and D) scans for individuals in the R-IPC (A and B) and control (C and D) groups. Values were taken both before and after reactive hyperaemia. Data for each leg was separated depending on whether they underwent reactive hyperaemia (test leg) or not (control leg) during the baseline and final scans. For each leg, during each scanning session, fold change in the post reactive hyperaemia steady-state flux was calculated relative to the respective pre reactive hyperaemia steady-state flux. Mean with SD and individual data points are plotted

3.3.3 VCAM Expression, but not ICAM-1 or phospho-p38 MAPK (p-p38 MAPK), was Increased in the Aorta Following R-IPC in the Primary Optimisation Study

To validate the R-IPC model, biomarkers of endothelial function - VCAM, ICAM-1 and p-p38 MAPK - in the aortas were assessed (Fig. 3.8). Aortas were cleaned and lysed prior to having their total protein concentration determined with a Bradford protein quantification assay. As one had to be excluded due to insufficient yield, western blot samples were prepared for 11 of the 12 lysates collected. The expression of VCAM, ICAM-1, p-p38 MAPK and p38 MAPK was examined using the western blot procedure. These proteins of interest were normalised to the total protein content which was determined using the total protein stain. Additionally, the proportion of p-p38 MAPK was calculated by dividing the normalised value for the phosphorylated protein by that of p38 MAPK. The fold change in the R-IPC group was then calculated in comparison to the control group. Statistical analysis was performed using Welch's unpaired t tests to determine if the R-IPC treatment affected any of the markers of interest. In comparison to the control (mean=0.0065), VCAM expression was found to be significantly increased, 1.623-fold higher, in the R-IPC group (mean=0.0105, p=0.0110). However, no significant differences were found between the control and R-IPC groups in the expression of ICAM-1 or p-p38 MAPK. The expression of p-eNOS and eNOS (Fig. 8.2) could not be determined due to no visible bands appearing on the blot and having an insufficient amount of lysate to repeat the western blot protocol.

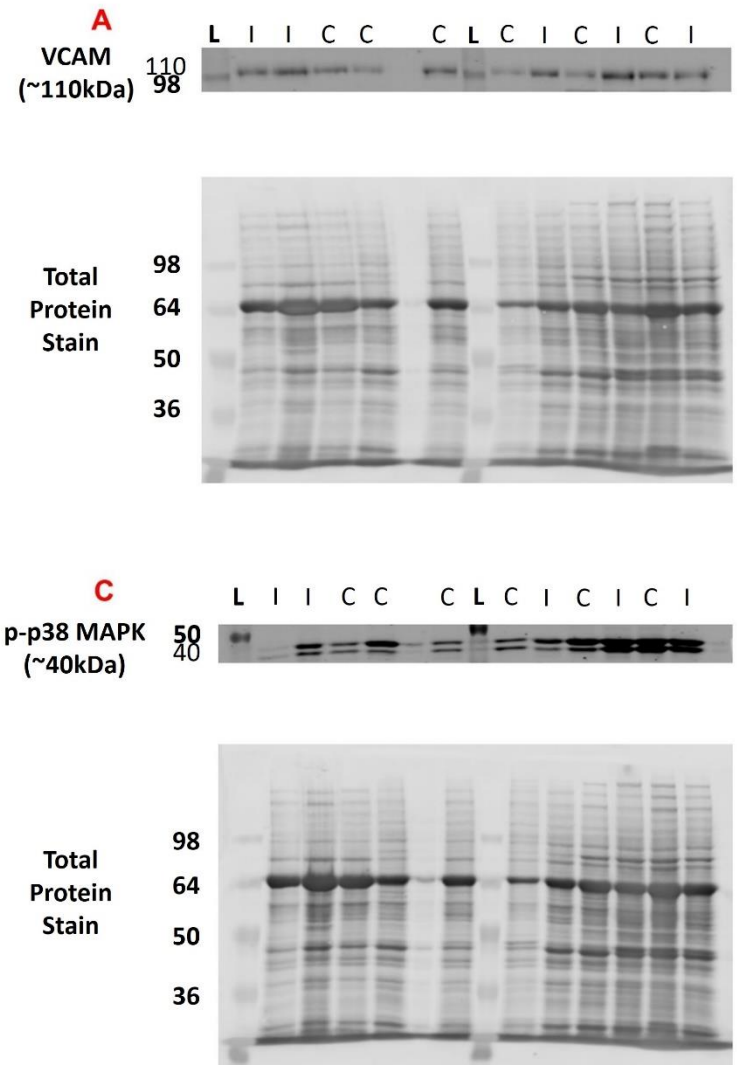
A
VCAM
(~110kDa)
L I I C C C L C I C I C I
110
98
Total
Protein
Stain
98
64
50
36
B
ICAM-1
(~110kDa)
L I I C C C L C I C I C I
110
98
Total
Protein
Stain
98
64
50
36
C
p-p38 MAPK
(~40kDa)
L I I C C C L C I C I C I
50
40
Total
Protein
Stain
98
64
50
36
D
p38 MAPK
(~40kDa)
L I I C C C L C I C I C I
50
40
Total
Protein
Stain
98
64
50
36

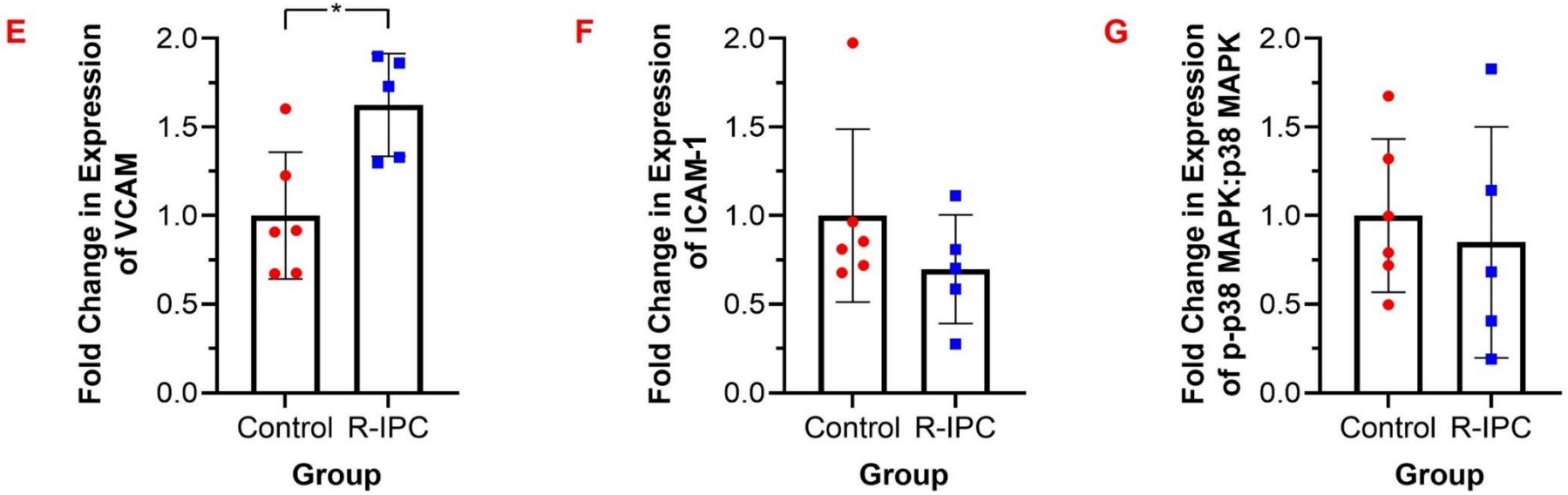

Fig. 3.8 Effects of R-IPC on aorta VCAM, ICAM-1 and p-p38 MAPK:p38 MAPK expression in the primary optimisation study. For each aorta, VCAM (A and E), ICAM-1 (B and F), and p-p38 MAPK and p38 MAPK (C, D and G) expression was quantified by conducting a western blot and normalising values to the total protein. To determine the proportion of p38 MAPK in its activated, phosphorylated f form, the normalised value for p-p38MAPK was divided by that of p38 MAPK. Fold change was then calculated for the expression of the proteins in the R-IPC group compared to the controls. Lysates from control group (C) and R-IPC (I) groups as well as two protein ladders (L) are annotated on the image of the membranes. Band sizes of the protein ladder (bold) and proteins of interest are indicated on respective blots (A-D). Mean with SD and individual data points are plotted. Significant differences in expression of the markers are indicated (* = $p<0.05$)

3.3.4 Plasma Concentration of TNFα at the End of the Study was Not Significantly Different Between the R-IPC and Control Groups

A TNFα ELISA was conducted on the plasma samples, obtained from trunk blood, after the final scan of each animal. Statistical analysis, using Welch's unpaired t test, revealed that there was no significant difference in the TNFα concentrations between the R-IPC and control groups at the end of the study (Fig. 3.9). Additionally, whilst there may appear to be an outlier within the R-IPC group, a Grubbs test determined that no anomalous results were present.

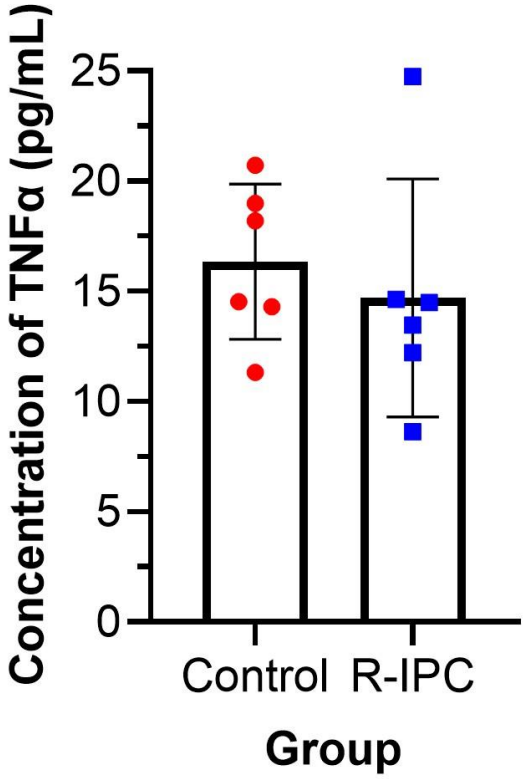

Fig. 3.9 Primary optimisation study plasma concentration of TNFα. Plasma samples were taken from mice immediately after completion of their final scan and TNFα concentration was determined using an ELISA. Mean with SD and individual data points are plotted

3.3.5 Limitations and Improvements to the Primary Optimisation Study

A major problem identified with this protocol was using the reactive hyperaemia test as the sole method of analysing endothelial function. Firstly, it can be inferred from the fold change in steady-state flux values that there was huge variation in the raw flux values between subjects regardless of treatment group (Fig. 3.7). There was also a large degree of variation in the magnitude flux and total excess

flux during the reactive hyperaemia periods, particularly at the baseline scan of the R-IPC group (Fig. 3.6), which has the consequence of masking any positive or negative effects of the R-IPC treatment. Whilst the FLPI laser was positioned the same distance from the hindlimbs when in use, it was exceedingly difficult to ensure the hindlimbs of all mice in each scanning session were in the same orientation in relation to the laser. The laser is extremely sensitive to any variation in the orientation of the feet. Therefore, given none of the animals appeared to be unwell, this is likely to be the reason for the variation observed which made comparisons between scanning sessions impractical and conclusions unreliable. This problem is further complicated by the other issues identified from this technique.

Secondly, the size of the cuff in relation to the hindlimb, and the square-like nature of the ROIs, meant that part of the cuff was often within the ROI when performing the analysis. This problem is virtually non-existent in clinical research as, in much larger subjects, the cuff can be placed far away from the part of the body being scanned. The motion that came from the inflation and deflation of the cuff around the hindlimb lead to a sudden rise in the flux value (Fig. 3.10). Therefore, in some circumstances, this made the identification of the reactive hyperaemic response impossible due to being disguised by significant interference caused by the cuff.

To counteract this, the cuff was placed as close to the torso as possible, and the leg extended. However, this did not prevent other issues from arising. Upon inflation of the cuff, the limb, occasionally, would contract to result in it being in a different location, relative to the FLPI laser, at the commencement of the scan (Fig. 3.11). This was less problematic when animals underwent R-IPC as the protocol began with the cuff being inflated. It did, however, become a concern during the baseline and final reactive hyperaemia response tests due to the initial 2 minutes of this procedure being conducted with the cuff deflated.

The fourth issue with this technique is that the analysis is highly subjective. The software will automatically allocate a mean flux value to each ROI for any given frame of the recording, but there is no defined threshold for the identification of the factors of interest. It is ultimately the analyst’s decision to determine at which points during the scan the baselines are achieved and the reactive hyperaemic

response occurs. This, alongside the inability for the investigator to be blinded for this study, could have contributed to a degree of subconscious bias which may have inadvertently affected the reported results.

Many data sets for the functional analysis were incomplete due to a combination of these problems. As this was down to technical complications, rather than direct issues with the animals, none were labelled as anomalous and removed. After much consideration, the conclusion was made that an alternative functional test should be used to support or disprove any conclusions deduced from the reactive hyperaemia data. LDI with PE/ACh iontophoresis does not present the same array of problems as FLPI with reactive hyperaemia, hence it was deemed to be a more suitable technique. Additionally, as there did appear to be some potentially promising data obtained after analysis of the aorta tissue (Fig. 3.8), it was decided to introduce a hypoglycaemic stimulus.

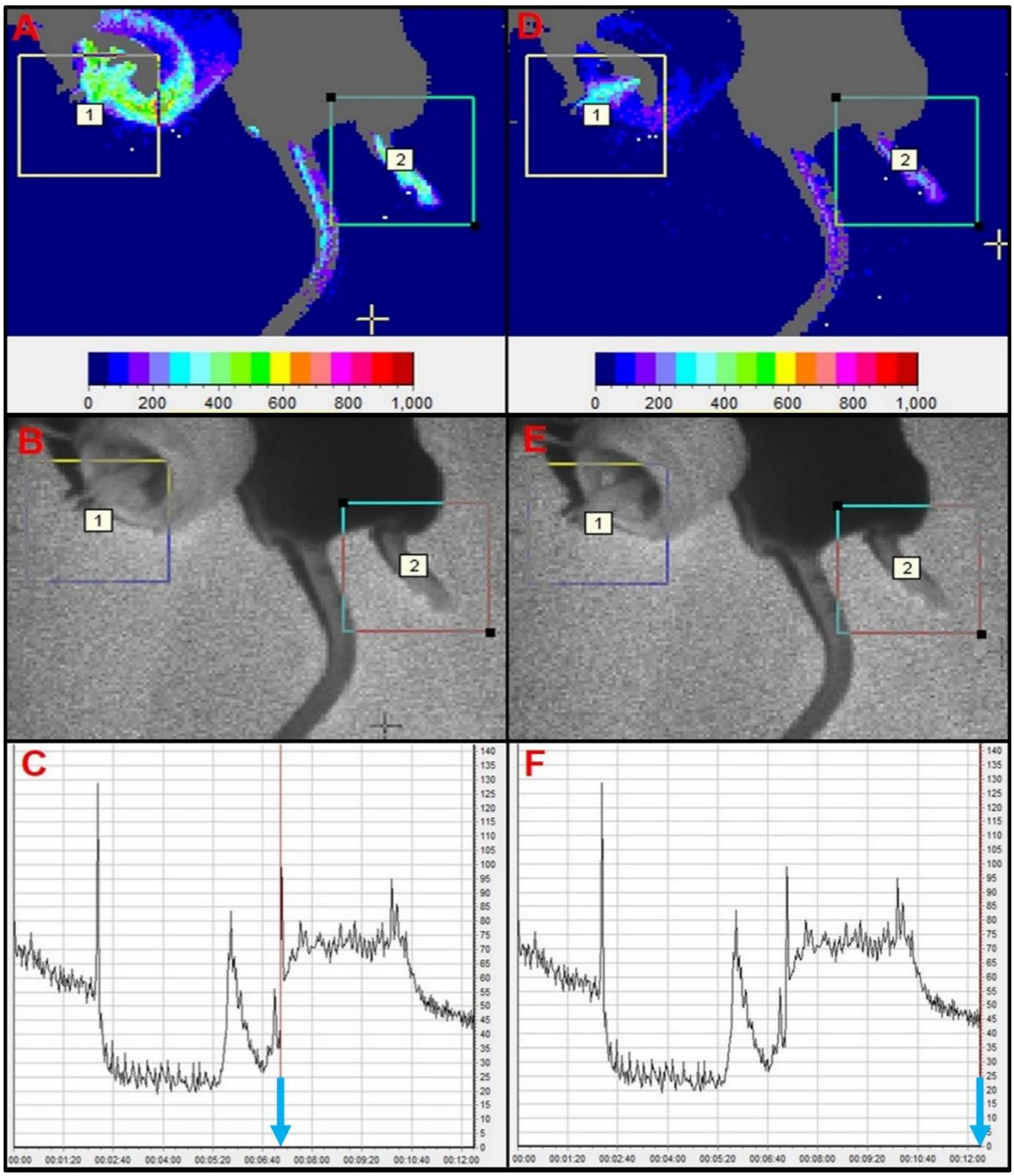

Fig. 3.10 Inflation and deflation of the blood pressure cuff caused an increase in flux. The panels exhibit the flux images (A and D), photo images (B and E) and flux traces (C and F) from hindlimbs of the same mouse undergoing reactive hyperaemia in a single scanning session. The timepoint to which the images relate to on the flux traces are indicated (blue arrow). The trace represents the flux from ROI 1. As the cuff was deflated (A-C), the air released leads to movement of the cuff causing a sudden increase in flux. When the cuff was not being inflated or deflated (D-F) the interference was no longer present.

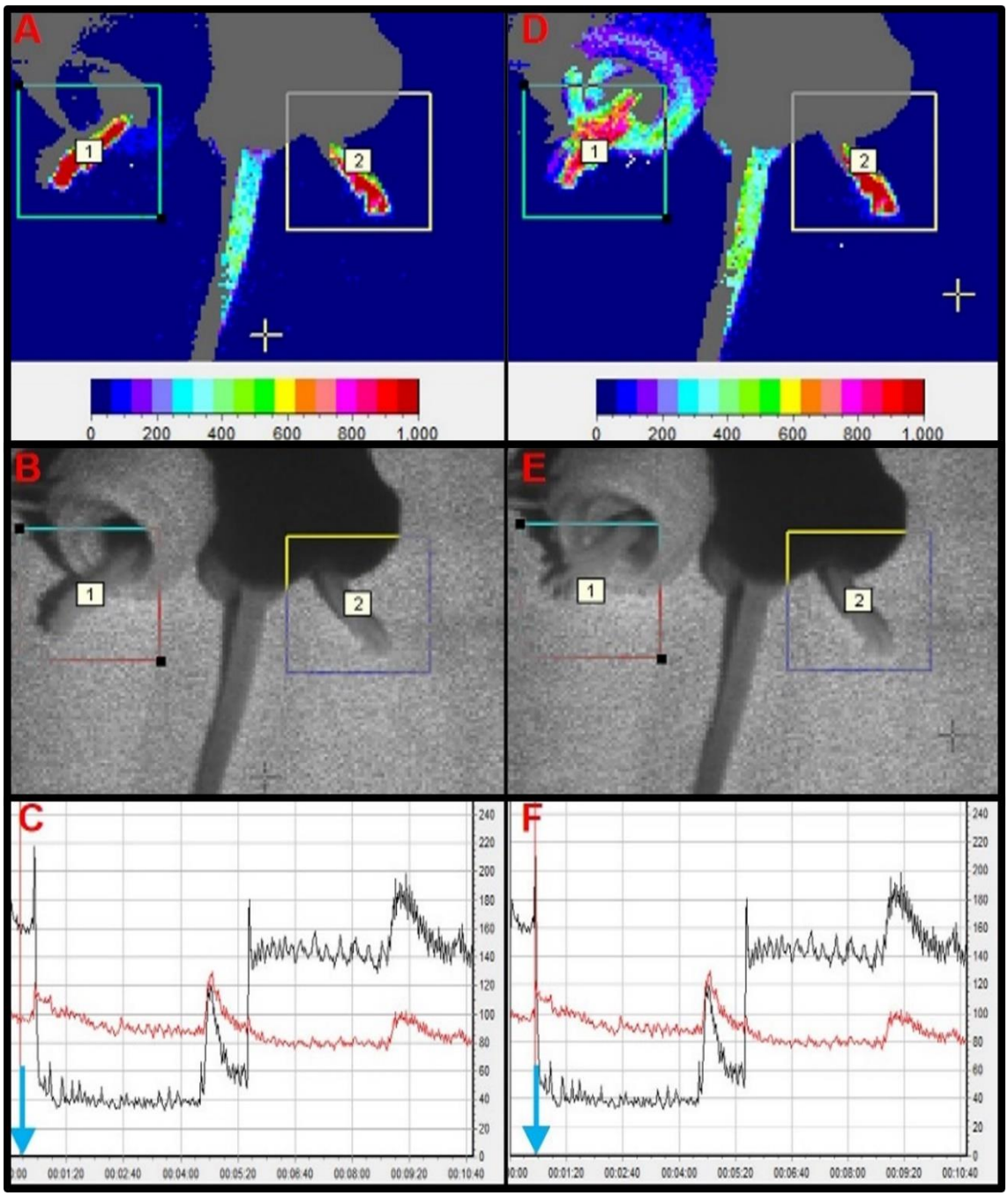

Fig. 3.11 Inflation of the blood pressure cuff caused contraction of the hindlimb. The panels exhibit the flux images (A and D), photo images (B and E) and flux traces (C and F) from hindlimbs of the same mouse undergoing reactive hyperaemia in a single scanning session. The timepoint to which the images relate to on the flux traces are indicated (blue arrow). The black flux trace represents ROI 1 whilst the red flux trace represents ROI 2. Prior to occlusion (A-C), the hindlimb, in ROI 1, was positioned to ensure the sole of the foot was within the scanning area of the FLPI laser and, to reduce interference, minimise its overlap with the cuff. The inflation of the cuff however caused the foot to withdraw (D-F) meaning it was no longer in the same position in relation to the laser.

3.4 Secondary Optimisation Study to Validate an *in vivo* R-IPC Model Using LDI with PE and ACh Iontophoresis as a Functional Test

Based on the recommendations made after the previous study, a secondary optimisation study was designed (Fig. 3.12). A total of 26 mice was used in the study and randomly assigned into 1 of 4 treatment groups: i) Control saline, ii) R-IPC saline, iii) Control hypoglycaemia, iv) R-IPC hypoglycaemia. On day 1 and 9, mice would undergo a baseline and final LDI with PE/ACh iontophoresis scan. They would be euthanised and have their tissue harvested immediately following completion of the final scan. Additionally, on each of days 5-7, mice would still receive either 3 cycles of R-IPC or 30 minutes of control treatment, consisting of wearing the deflated cuff for 30 minutes. On the eighth day, a single hypoglycaemic episode was induced, or a control treatment was given in lieu, in the form of a saline injection. Unless otherwise stated, all LDI with PE/ACh iontophoresis data was analysed using Bonferroni's repeated measures multiple comparisons 2-way ANOVA.

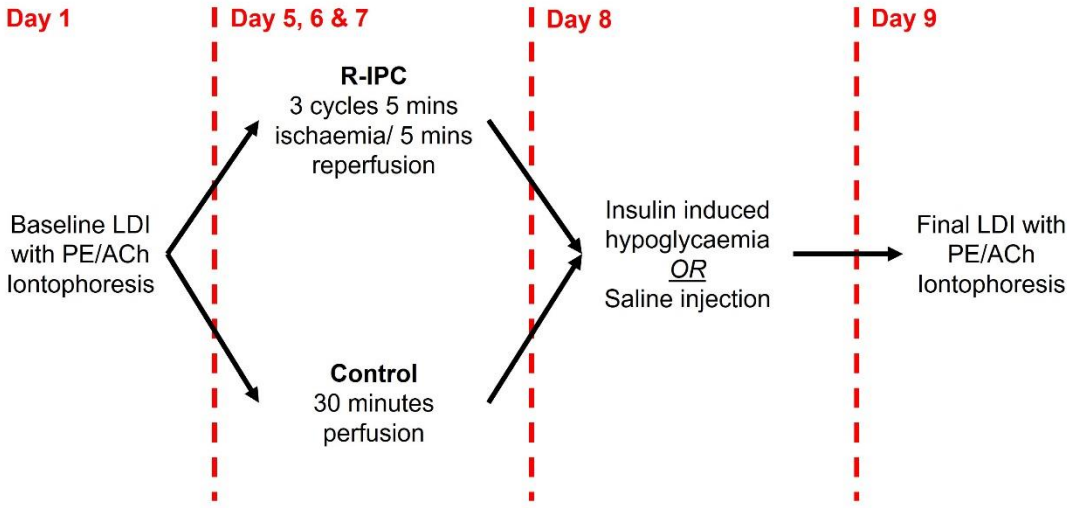

Fig. 3.12 Secondary optimisation study protocol timeline. Schematic indicating the procedures C57BL/6J mice underwent in the secondary *in vivo* study. Animals were anaesthetised with isoflurane for all procedures, except for those conducted on day 8, and randomly allocated into 1 of 4 groups depending on whether they received R-IPC or control treatment and were subjected to an insulin induced hypoglycaemic event or saline injection. All animals were euthanised and tissue harvested following completion of day 4.

3.4.1 A 1U/kg Insulin Injection Induced Hypoglycaemia Within 45 Minutes

To determine whether either of the saline and insulin treatments had a significant

impact on blood glucose levels, separate Wilcoxon matched pairs signed rank tests were conducted between the basal (saline mean=9.4mmol/L and insulin mean=9.1mmol/L) and +45 minutes (saline mean=8.4mmol/L and insulin mean=3.0mmol/L) timepoints (Fig. 3.13). There was a significant decrease in the blood glucose levels between the basal and +45 minutes readings in the insulin treated group (p=0.0005), thereby confirming hypoglycaemia was induced, but not it the saline treated.

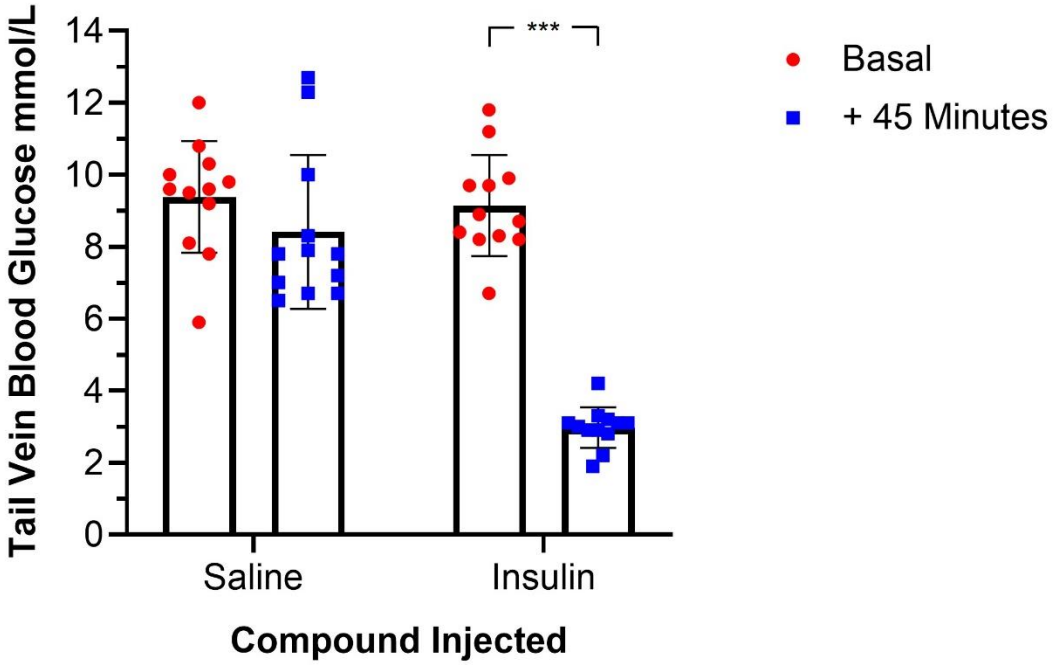

Fig. 3.13 Effects of 1U/kg insulin and saline on blood glucose levels. Mice were fasted for 5 hours. They had tail vein blood glucose levels taken prior to (Basal) and 45 minutes following (+45 Minutes) receiving either a saline or 1U/kg insulin injection. Significant differences between the blood glucose levels at the basal and +45 Minutes timepoints for both treatment groups are indicated (*** = p<0.001). Mean with SD and individual data points are plotted

3.4.2 The Timing of Hair Removal Did Not Affect the Degree of Vasodilation at Steady-State

There was a concern that the application of depilatory cream immediately prior to LDI with PE/ACh iontophoresis could cause an elevation in the degree of vasodilation at the baseline scans. Therefore, 14 of the mice enrolled onto the study had hair removed immediately prior to their baseline scan, whilst the remaining 10 had this done whilst conscious 48 hours before the baseline scan.

Welch's unpaired t test revealed there was no significant difference in the steady-state flux at the baseline scan dependent on the timing of hair removal (Fig. 3.14). This lack of difference allowed the combining of the LDI with PE/ACh Iontophoresis data regardless of the time at which hair was removed.

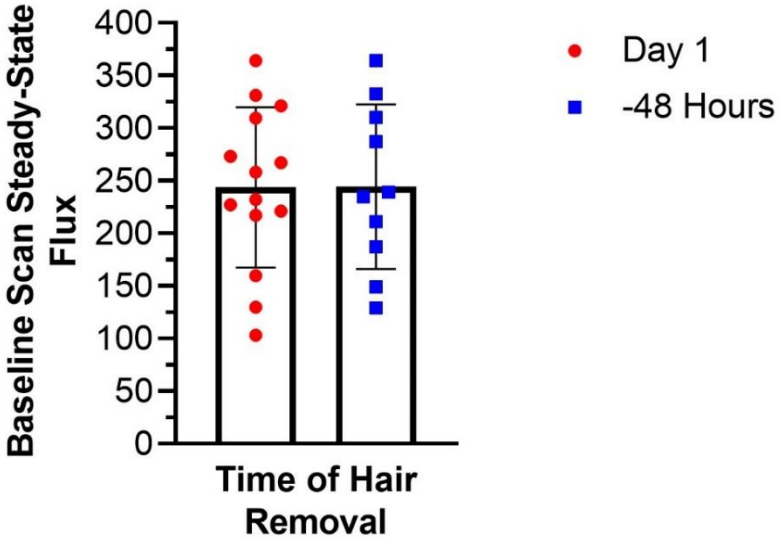

Fig. 3.14 Effect of the timing of hair removal on steady-state flux. Steady-state fluxes were recorded during baseline LDI with PE/ACh iontophoresis scans of the secondary optimisation study. Out of the 24 mice, 14 had hair removed on the day of the baseline scan (Day 1) whilst 10 had this done 48 hours prior (-48 Hours). For this analysis, animals are grouped based upon the timing of their hair removal and not their treatment group. Mean with SD and individual data points are plotted.

3.4.3 Neither R-IPC nor Control Treatment Affected the Endothelial Response to ACh or PE

To determine whether the R-IPC model was working, the change in the LDI with PE/ACh iontophoresis data obtained during baseline and final scans was calculated. There were no significant differences in the delta flux, steady-state flux, minimum PE flux or maximum ACh flux between the baseline and final scans in either the control saline or R-IPC saline groups (Fig. 3.15).

3.4.4 Hypoglycaemia Caused a Significant Decrease in Delta Flux in the Absence of R-IPC Treatment

To determine the effect of acute hypoglycaemia on endothelial function, as well as the effect of hypoglycaemia and R-IPC treatment combined, further statistical analysis was conducted on the LDI with PE/ACh iontophoresis data (Fig. 3.15). It confirmed that a single hypoglycaemic episode significantly ($p=0.0147$) reduces the delta flux between the baseline (mean=173) and final scans (mean=38.167).

However, when R-IPC was given beforehand, this effect was abolished as there was no significant difference in the delta flux between the baseline and final scans for individuals in the R-IPC hypoglycaemia group.

3.4.5 Steady-State Flux was Significantly Decreased by Induction of R-IPC when Preceding Hypoglycaemia

A significant decrease in the steady-state flux was observed between the baseline (mean=263.333) and final (mean=142.222) scans in the R-IPC hypoglycaemia group (p=0.0260). However, when only exposed to acute hypoglycaemia, without previous R-IPC treatment, this effect was no longer significant (Fig. 3.15)

3.4.6 Hypoglycaemia Reduced and Increased the Response to ACh and PE Respectively

Induction of hypoglycaemia correlated with a significant decrease, between the baseline and final scans, in the minimum PE flux both with (baseline mean=204.667, final mean=110.167, p=0.0224) and without (baseline mean=185.667, final mean=96.667, p=0.0337) R-IPC being given prior (Fig. 3.15). This indicates an increase in the vasoconstriction response to PE. Additionally, a similar reduction in the maximum ACh flux was also seen in the R-IPC hypoglycaemia (baseline mean=373.167, final mean=195.833, p=0.0202) and control hypoglycaemia (baseline mean=358.667, final mean=134.833, p=0.0030) groups (Fig. 3.15). This suggests that the vasodilatory response to ACh was suppressed.

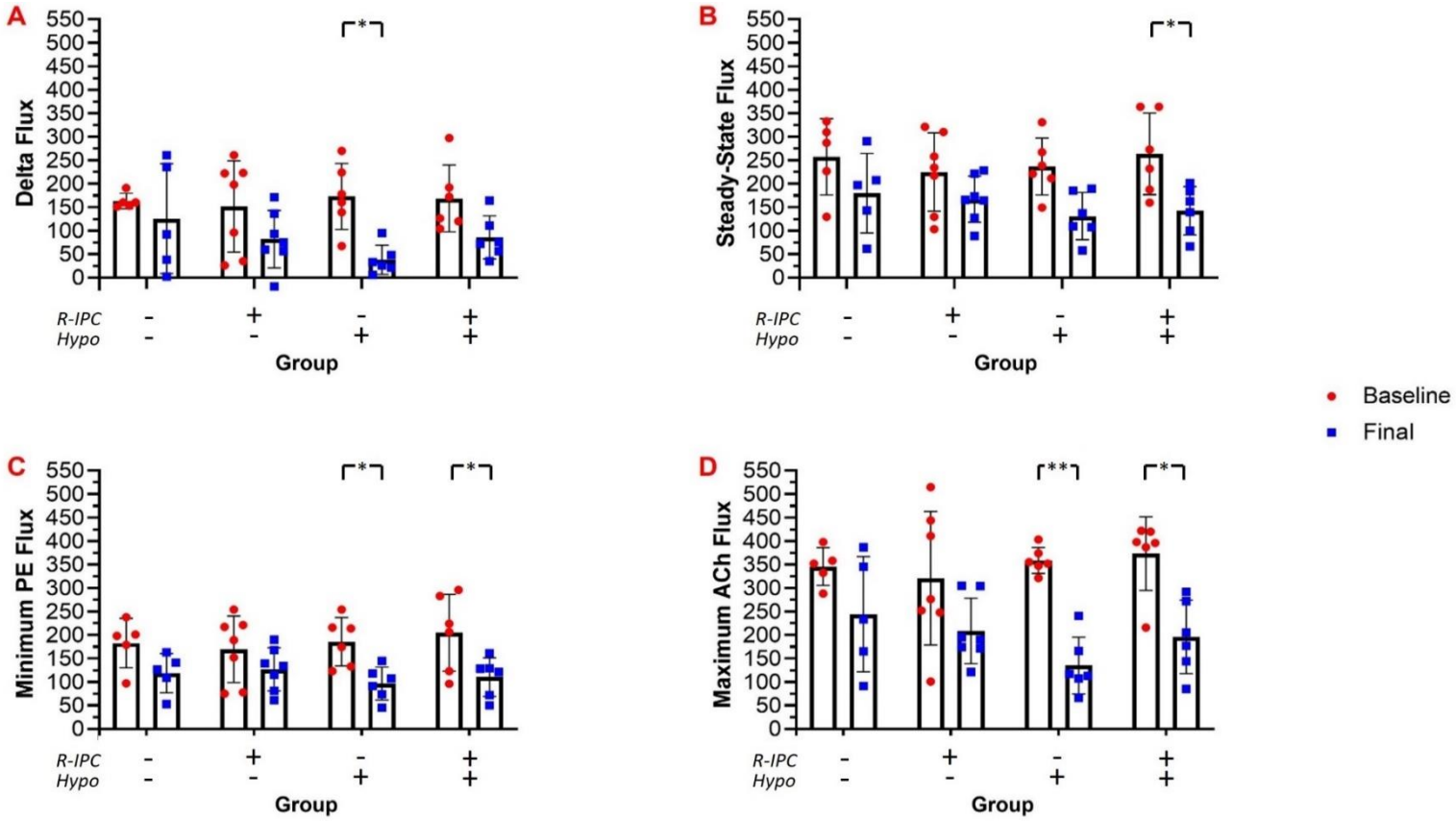

Fig. 3.15 Secondary optimisation *in vivo* study LDI with PE/ACh iontophoresis. Mice underwent an LDI scan with PE/ACh iontophoresis 4 days before (baseline) and 48 hours after (final) 3 days of R-IPCor control treatment and 1 day after an insulin induced hypoglycaemic episode or saline injection. Delta flux (A) was found by subtracting the minimum flux due to PE induced vasoconstriction (C) from the maximum due to ACh induced vasodilation (D). Steady-state (B) refers to the flux prior to applying the current. + and – indicates whether a group received an interventional treatment (R-IPC and/or hypoglycaemia) or the relevant control (preconditioning control and/or saline injection) respectively. Mean with SD and individual data points are plotted. Significant differences between final scans and their relative baselines within each group are indicated (* = p<0.05, ** = p<0.01).

3.4.7 Expression of VCAM, ICAM-1, p-p38 MAPK and p-eNOS in the Aorta were not Significantly Affected by R-IPC and Hypoglycaemia

To validate the R-IPC model, biomarkers of endothelial function - VCAM, ICAM-1, p-p38 MAPK and p-eNOS in the aortas were also quantified (Fig. 3.16). Aortas were cleaned and lysed prior to having their total protein concentration determined with a Bradford protein quantification assay. The expression of VCAM, ICAM-1, p-p38 MAPK and p38 MAPK, and p-eNOS and eNOS, were examined using the western blot procedure. These proteins of interest were normalised to actin. Additionally, the proportion of p-p38 MAPK was calculated by dividing the normalised value for the protein by that of p38 MAPK. The ratio of p-eNOS:eNOS was calculated similarly. Fold changes in expression of the proteins of interest between the control saline groups and the other 3 groups were calculated. Statistical analysis was performed, using Tukey's multiple comparisons ordinary one-way ANOVA, but no significant differences were found in the expression of any of the proteins between the 4 treatment groups.

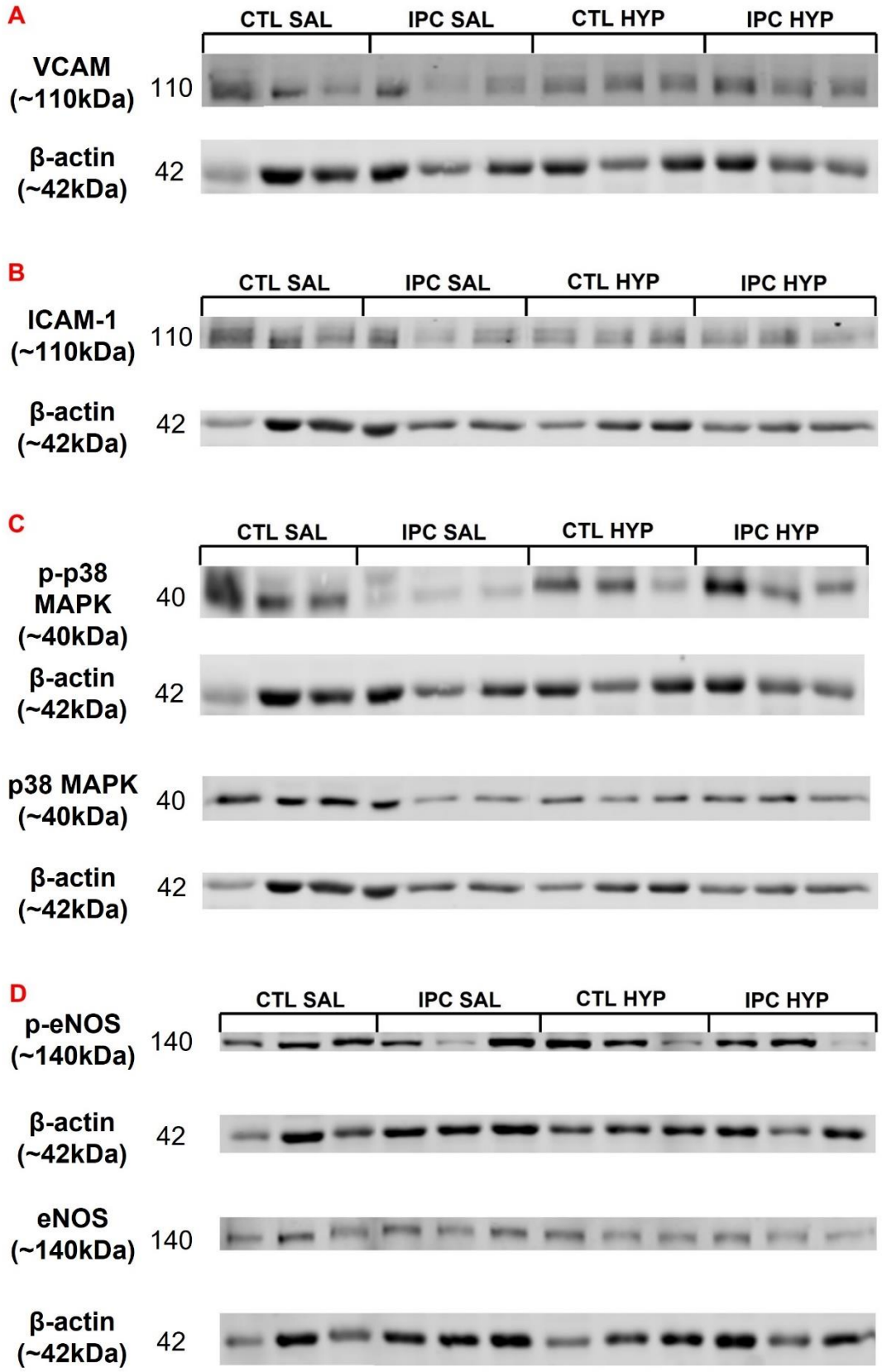
A
CTL SAL
IPC SAL
CTL HYP
IPC HYP
VCAM (~110kDa)
110
β-actin (~42kDa)
42
B
CTL SAL
IPC SAL
CTL HYP
IPC HYP
ICAM-1 (~110kDa)
110
β-actin (~42kDa)
42
C
CTL SAL
IPC SAL
CTL HYP
IPC HYP
p-p38 MAPK (~40kDa)
40
β-actin (~42kDa)
42
p38 MAPK (~40kDa)
40
β-actin (~42kDa)
42
D
CTL SAL
IPC SAL
CTL HYP
IPC HYP
p-eNOS (~140kDa)
140
β-actin (~42kDa)
42
eNOS (~140kDa)
140
β-actin (~42kDa)
42

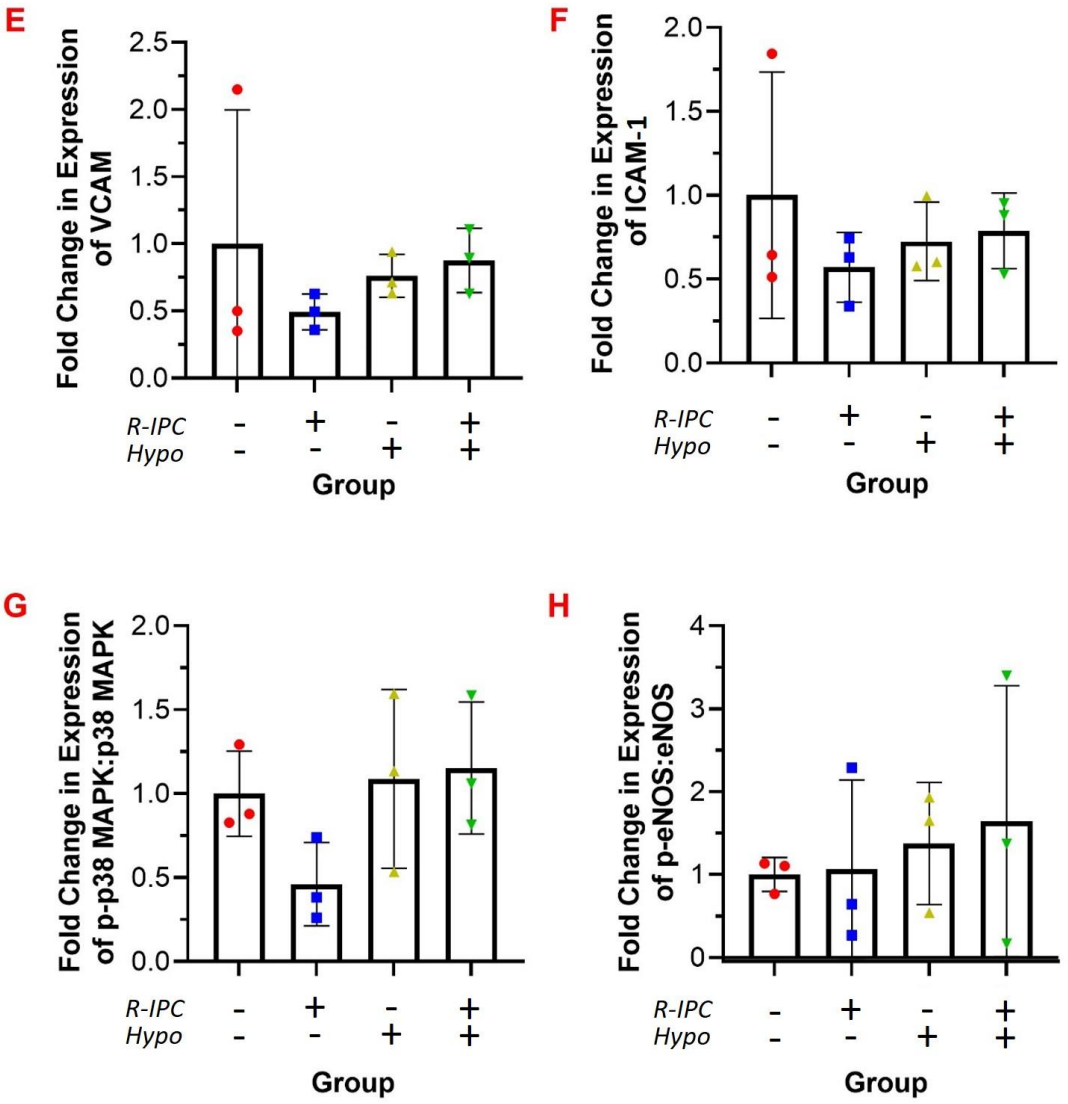

Fig. 3.16 Effects of R-IPC and hypoglycaemia on aortic VCAM, ICAM-1, p-p38 MAPK and p-eNOS expression in the secondary optimisation study. Mice underwent protocols, as described in figure 3.12, and aortas were harvested following completion of a final LDI with PE/ACh scan. For each aorta, VCAM (A and E), ICAM-1 (B and F), p-p38 MAPK and p38 MAPK (C and G), and p-eNOS and eNOS (D and H) expression was quantified by conducting a western blot and normalising values to β-actin. To determine the proportion of p38 MAPK in its activated, phosphorylated, form, the normalised value for p-p38MAPK was divided by that of p38 MAPK. This process was also conducted to determine the proportion of eNOS that existed as p-eNOS. Fold changes in expression were calculated between the groups using control saline as a reference. + and – indicates whether a group received an interventional treatment (R-IPC and/or hypoglycaemia) or the relevant control (preconditioning control and/or saline injection) respectively. Band sizes of the protein ladder (bold) and proteins of interest are indicated on respective blots (A-D). Mean with SD and individual data points are plotted.

3.5 Discussion

3.5.1 The Preliminary and Optimisation Study Protocols were Unable to Validate an in vivo R-IPC Model

The principal aim of this chapter was to validate an in vivo model of R-IPC. Unfortunately, this aim was not achieved in any of the 3 studies conducted here.

Altering the R-IPC protocol from 4 cycles over 1 day to 9 cycles over 3 days improved the study completion rate for the subjects and abolished breathing issues of any severity. No animals experienced respiratory distress in the primary optimisation study and only 1 was removed from the secondary optimisation study due to breathing issues whilst anaesthetised. This is likely due to a combination of reducing the time of each anaesthesia session and performing the baseline scan on a separate day from the R-IPC or control treatment, meaning there was negligible movement of the animal whilst anaesthetised. Therefore, it was concluded that the risk of an individual developing atelectasis or oedema was decreased.

Although great consideration was put into designing the *in vivo* model of R-IPC, the lack of improvement in endothelial function indicates that no model could be validated. It has already been demonstrated, throughout section 1.5, that with a working model, detectable improvements in endothelial function, at both the molecular and functional levels, would be expected following R-IPC treatment. However, no significant improvements were identified in the reactive hyperaemic response or steady-state flux in mice treated with R-IPC in the primary optimisation study (Fig. 3.6-3.7), although this may have largely been down to previously discussed problems with the technique in section 3.3.5. Additionally, in the secondary optimisation model, there were no significant increases in the delta flux or maximum ACh flux values between baseline and final scans for R-IPC saline mice (Fig. 3.15). There was, however, a slight unexpected decrease in these variables between the 2 scanning timepoints in both the control saline and R-IPC saline groups. There were no significant changes in any of the molecular markers in either the preliminary or optimisation models (Fig. 3.4, 3.8-3.9 and 3.16). The only exception to this was the increased VCAM expression in the aorta of R-IPC treated animals in the primary optimisation study (Fig. 3.8). However, no such effect was observed in the secondary optimisation study (Fig.

3.16) although this may be related to the sample size being much smaller and the variation within the actin used as a housekeeping protein.

3.5.2 Hypoglycaemia Significantly Decreased Endothelial Function

A single injection of 1U of insulin significantly decreased blood glucose levels to within the defined hypoglycaemic range. Using the LDI with PE/ACh data from the secondary optimisation study (Fig. 3.15), it was therefore possible to understand how hypoglycaemia affects endothelial function. The significantly reduced delta flux at the final scan in the control hypoglycaemia group indicates that a single hypoglycaemic episode appears to reduce endothelial function. This tallies with the literature, discussed in section 1.4.4 which states that acute hypoglycaemia induces endothelial dysfunction.

Interestingly, in comparison to these subjects, those previously treated with R-IPC experienced a smaller, and non-significant, decrease in the delta flux at the same timepoint. This therefore implies that rather than worsening the R-IPC as initially hypothesised, R-IPC could offer a degree of protection against hypoglycaemia induced CV dysfunction. As a major component of ischaemia is glucose deprivation, it could be suggested that IPC is a combination of HPC and hypoglycaemic preconditioning, rather than a separate form of preconditioning in its own right. Hence, it would not be surprising that prior exposure to ischaemia would be able to prime and protect the body from a further severe hypoglycaemic episode. This would be an example of cross tolerance which is a phenomenon in which exposure to drug or stimulus ‘A’ can induce tolerance to drug or stimulus ‘B’. However, a closer look at the data indicates that there was no protective effect of R-IPC against hypoglycaemia induced endothelial dysfunction as the vasodilatory response to ACh was significantly reduced in both the control hypoglycaemia and R-IPC hypoglycaemia groups at the final scan. This instead simply reinforces the theory that hypoglycaemia induces microvascular dysfunction. Conversely, there was a reduction in the proportion by which the maximum ACh flux decreases in the R-IPC hypoglycaemia cohort compared to the control hypoglycaemia group. Thus, whilst endothelial dysfunction was induced by acute hypoglycaemia, the extent of the damage caused may be inhibited slightly by pre-treatment with R-IPC (Fig. 3.15). Data obtained from Zhao

et al. (2015) implies that this conclusion could be correct. In their study, bEnd.3 cells were exposed to hypoglycaemia or normoglycaemia for 24 hours using 0.5mM and 5.5mM glucose respectively. Hypoglycaemia treated cells exhibited an increased Na-F permeability coefficient, compared to those exposed to normoglycaemia, indicating they suffered from structural disruption linked to the low glucose environment. By culturing the cells with 100ng/mL VEGF, during the hypoglycaemic and normoglycaemic periods, the Na-F permeability coefficient was significantly reduced back to near normal levels in cells treated with 0.5mM glucose (Zhao *et al*., 2015). This therefore highlights that VEGF offers a degree of protection to endothelial cells when challenged with hypoglycaemia. Ueno *et al*. (2016) found that C57BL/6 mouse plasma VEGF levels were elevated 24 hours after R-IPC treatment, although they had reduced back to normal 24 hours later (Ueno *et al*., 2016). In the secondary optimisation study, the hypoglycaemic episode was induced 24 hours after the final day of R-IPC treatment. Hence, the absence of a significant decrease in delta flux between the baseline and final scans of the R-IPC hypoglycaemia group may be explained by raised VEGF levels.

The lower minimum PE flux at the final scan indicates that there was greater PE induced vasoconstriction of the vessels in all mice treated with hypoglycaemia. Most research appears to focus on the effect of hypoglycaemia on the vasodilatory response. However, in a Masters dissertation from the University of Lisbon by Neves (2016), data was obtained to suggest that hypoglycaemia affects the vascular response to both vasodilatory and vasoconstrictive compounds. In this dissertation, reactivity of murine aortic rings was determined following a 30-minute incubation period in a euglycaemic, 5.5mM, or hypoglycaemic, 2.2mM, medium. Both ACh and PE were tested as vasoactive stimuli, and the degree of vasodilation and vasoconstriction were decreased and increased, respectively, in the rings exposed to hypoglycaemia compared to those incubated in normoglycaemia (Neves, 2016). This supports the LDI with PE/ACh data obtained in the secondary optimisation study as there was a decrease in the vasodilatory response, and an increase in the vasoconstrictive one. ACh induces vasodilation by binding to muscarinic ACh receptors on the endothelium and invoking the production of NO which then acts directly on the smooth muscle. As discussed in section 1.4.4, Joy *et al*. (2016) found that there

was a significant reduction in endogenous NO induced vasodilation during a hyperinsulinaemic-hypoglycaemic clamp in human subjects (Joy *et al*., 2016). Interestingly, Dieguez *et al*. (1997) concluded that insulin induced hypoglycaemia induces cerebellar nitric oxide release. However, this was associated with a decrease in the ability of the vasculature to release NO following treatment with ACh. This therefore indicates an impairment in either the pathways leading to its synthesis or translocation in response to ACh (Dieguez *et al*., 1997). Therefore, whilst the reduced response to ACh can almost certainly be attributed to the increased endothelial dysfunction associated with hypoglycaemia, perhaps due to a lack of interest in this area, the mechanisms underlying the increased response to PE are not well understood. It is unclear from the available abstract, by Neves, what duration of time was allowed between the exposure to hypoglycaemia and administration of PE to the aortic rings (Neves, 2016). Therefore, further investigations would be required to determine whether the hypoglycaemia induced effect on the vasoconstrictive response is a direct or indirect result of exposure to glucose deprivation.

Finally, there was a significant reduction in the steady-state flux of individuals in the R-IPC hypoglycaemia group, but not in the saline hypoglycaemia group. However, the difference between the steady-state flux during the final scans of these 2 groups were extremely similar. Additionally, there was a slightly elevated steady-state flux in the baseline scan of the R-IPC hypoglycaemia group compared to that of the control hypoglycaemia group. This is possibly the cause for the statistically significant change in steady-state flux in the former group, but not the latter, rather than variations in endothelial function between the cohorts. Reasons for the marginally higher baseline steady-state flux in the R-IPC hypoglycaemia group include many factors including room temperature, humidity and stress caused by an external stimulus.

Whilst statistical analysis alone implied that a single episode of hypoglycaemia significantly reduces endothelial function, the delta flux values were similarly decreased, albeit non-significantly, at the final LDI with PE/ACh iontophoresis scan in the other 3 experimental groups. Additionally, all treatment groups exhibit an apparent or significant decrease in steady-state flux and endothelial response to ACh. These common trends imply that endothelial function was decreased

regardless of R-IPC/control or hypoglycaemia/saline treatment. This indicates that a separate element of the protocol was inducing this effect meaning it cannot truly be concluded that hypoglycaemia was associated with decreased endothelial function within this study. The lack of a successful R-IPC model limits the validity of any conclusions made regarding how the hypoglycaemia and R-IPC treatments affect each other. In order to investigate this, it was essential that a R-IPC model could be validated. To continue with model development, it was, therefore important to identify the cause of the negative results obtained.

3.5.3 Techniques for Functional Analysis

Neither of the functional techniques used to analyse endothelial function were able to validate a R-IPC model. Therefore, it could be debated that these methods were not the most appropriate for this particular purpose.

Theoretically, an array of techniques could be utilised (Table 3.1) as there is evidence of their use to assess CV function in mice. However, many experimental designs must consider the cost, accessibility and safety of a technique when deciding which tests to employ. Due to the large expenses involved, analysis using positron emission tomography (PET) could be instantly discounted. Additionally, whilst MicroCT is becoming an increasingly popular method, the use of radiation in this, as well as in performing X-ray angiograms, meant these techniques were excluded due to safety concerns for the investigators and animals. Cardiac catheterisation also was not considered as the desired method needed to be non-invasive.

Echocardiograms would have been an excellent way to observe changes in the cardiac structure and function using ultrasound technology. However, an inability in accessing the necessary equipment meant that this technique could not have been used. Also, the technique may not be able to detect subtle vascular changes, which can occur with R-IPC, and cannot be used to observe the coronary arteries due to its poor resolution in comparison to other techniques. Assessment of arterial stiffness was another method which could have been utilised, although research into the effects of R-IPC on arterial stiffness in healthy humans is extremely limited. Muller *et al*. (2019) found that, in healthy humans, there is no short-term effect of R-IPC on arterial stiffness, although this was

assessed immediately after R-IPC treatment which may have been too early (Muller *et al*., 2019). Additionally, in individuals due to undergo vascular surgery, Kepler *et al*. (2019) could not confirm that their R-IPC protocols improved arterial stiffness (Kepler *et al*., 2019). This data, combined with a distinct lack of literature regarding the effect of R-IPC on arterial stiffness in healthy humans during the delayed phase of protection, resulted in this technique being excluded from consideration. Out of the remaining methods, namely LDI, iontophoresis, FLPI, reactive hyperaemia and ECG, it was decided that the latter would not be suitable. This was largely due to the difficulties involved in interpreting an ECG trace and it needing to be used in addition to a second functional test. Any alterations in heart rhythm and sympatho-vagal balance can be observed through direct analysis of the heart rate. Additionally, by focussing on the waves and QRS complex of the trace within each heartbeat, the effect of a treatment on the coordination of the relaxation and contraction of the atria and ventricles can be defined. The resulting conclusions made from an ECG are largely relating to the function of the heart itself. Therefore, techniques allowing assessment of cardiac or macrovascular function, rather than that of the microvasculature, such as the echocardiogram, may be a more suitable choice to use in conjunction with the ECG.

Both LDI and FLPI can be used, alongside iontophoresis and reactive hyperaemia respectively, to evaluate microvascular function. LDI with iontophoresis was a well-established technique used regularly by other investigators within the laboratory. Although its use is well established in humans, within the MSRU, FLPI with reactive hyperaemia in mice was a novel idea and there was no indication of any limitations when designing the study protocols, as the issues which arose regarding this technique only did so following its use in the primary optimisation study. LDI is only able to provide a snapshot of what is occurring within the microvasculature, whereas FLPI gives real-time images, albeit with reduced penetrative power of the laser. Therefore, given these circumstances, it was concluded that the best approach was to use both of these imaging techniques, alongside iontophoresis and reactive hyperaemia respectively, to produce a clearer image of the state of microvascular function.

Technique	Variable Measured	Limitations
LDI	Snapshot vasodilation and vasoconstriction of cutaneous microvasculature	Unable to provide real time images and unsuitable for pigmented skin
Iontophoresis	Vasoactive drugs applied via the skin using a electric current often used alongside LDI	Causes skin irritation or pain from the electrical current or drugs
FLPI	Real time vasodilation and vasoconstriction of cutaneous microvasculature	Reduced penetrative power compared to LDI and unsuitable for pigmented skin
Reactive Hyperaemia	Used alongside FLPI to assess the magnitude of flux reached during reperfusion following a period of	Data analysis is subjective, and the use of a blood pressure cuff can interfere with the flux readout
Echocardiogram	High frequency sound waves are used to show real time structural changes in the heart or vasculature	Resonance does not allow observation of coronary arteries and blockages
Arterial Stiffness Ultrasound	High frequency sound waves are used to measure pulse wave velocity to evaluate arterial stiffness	Only suitable for larger vessels
ECG	Electrodes placed on the skin to measure electrical activity of the heart	Multiple interpretations available for one ECG trace hence other diagnostic tools must be used in conjunction

PET	Detection of gamma rays by positron emitting isotopes reveal sites of metabolic activity	Expensive, and, particularly in older animals, there may be signal interference from cancerous tissues
X-ray Angiograms	Imaging of blood vessels using a contrast medium to identify blockages or narrowing	Viscous contrasts may not sufficiently fill the vessels for imaging and X-ray exposure could cause tissue damage
Micro-CT	Uses radio dense contrast and opaque agents to visualise the microvasculature	Radiation exposure limits long term use

Table 3.1 Techniques used to assess CV function. A list of the techniques employed to assess various aspects of CV function in rodents plus the variable measured, and the limitations of its use.

3.5.4 Biomarker Selection

The molecular mechanisms responsible for R-IPC mediated protection are extremely complex with multiple pathways being involved. However, the biphasic nature of the period of protection is largely due to the timing at which certain proteins will exhibit increased or decreased expression. Therefore, the suitability of the targets of interest selected to validate the R-IPC model, and their expression at the time at which the tissue was harvested in relation to the final R-IPC treatment, must be considered.

A review by Hausenloy and Yellon identifies 3 categories of R-IPC mediators: triggers, early mediators, and distal mediators (Hausenloy and Yellon, 2010). The early phase of preconditioning is mediated by the triggers, whilst the delayed phase is by the distal mediators, with the early mediators acting as an intermediary between the two. The triggers are released immediately following ischaemia/reperfusion and generally return to their normal expression levels at the end of the early phase of preconditioning. Most R-IPC related cytokines, including TNFα, act as triggers. Therefore, this may be why the slight, if non-significant, increase in TNFα at the acute scan of the preliminary model was no longer present at the delayed scan (Fig. 3.4). Additionally, this would explain why no differences were seen in its expression, between the R-IPC and control groups, in the plasma taken after the final scan in the primary optimisation study (Fig. 3.9). These triggers can act directly to invoke protection but also recruit early mediators. Stimulation of these early mediators, such as the PI3-K pathway, ultimately leads to the activation of transcription factors causing the production of the distal mediators. These processes of transcription and protein synthesis can take 12-24 hours which explains the temporary disappearance of R-IPC induced protection following completion of the early phase (Hausenloy and Yellon, 2010). Barnes and Karin explain changes in VCAM and ICAM-1 expression are, at least partially, regulated by the transcription factor NF-κB thereby indicating these are distal mediators (Barnes and Karin, 1997).

Unusually for a cytokine, IL-10 appears to exert its effects in the delayed phase of R-IPC. Cai *et al*. (2012) treated C57BL/6 mice with 3 cycles of 5 minutes ischaemia/5 minutes reperfusion via temporary ligation and release of the femoral artery. 24 hours after R-IPC treatment, western blot analysis of cardiac tissue

detected levels of IL-10 were significantly elevated, signifying its role in the delayed phase (Cai *et al*., 2012)

eNOS can act as a trigger and is largely responsible for the early increase in NO during R-IPC (Hausenloy and Yellon, 2010). He *et al*. (2012) however, reported that eNOS also acts as a distal mediator. Sprague-Dawley rats were either given R-IPC by performing 3 cycles of 5-minutes ischaemia/5-minutes reperfusion or a sham surgery control. 24 hours later, the mesenteric artery was occluded for 30 minutes and reperfused for an additional 60 minutes. Western blot analysis revealed a significant increase in p-eNOS in R-IPC treated individuals thereby indicating the role of eNOS as a distal mediator (He *et al*., 2012).

Similarly, p38 MAPK is also defined as both an early and distal mediator of R-IPC (Hausenloy and Yellon, 2010). In a study by Sun *et al*. (2006), Wistar rats were either treated with R-IPC, by 3 cycles of 10 minutes occlusion/10 minutes reperfusion of the femoral artery or, allocated to a sham group. Rats were euthanised and the CA1 and CA3/DG regions of the hippocampus dissected at 6 hours, 12 hours, 1 day, 3 day and 5 days following sham or R-IPC treatment. Western blot analysis found that p-p38 MAPK expression was significantly increased in the CA1 region at the 6-hour timepoint and peaked after 12 hours. However, it had dropped back to baseline levels within 1 day. This therefore indicates p38 MAPK is an early mediator and that it’s increase in activity is likely linked to activation of the p38 MAPK pathway by triggers. However, in the CA3/DG region, p-p38 MAPK levels were not significantly elevated until the 1-day timepoint. They continued to rise until 3 days had passed and had not returned to normal levels until the fifth day (Sun *et al*., 2006). Hence, p38 MAPK is also associated with the delayed phase of R-IPC, although the time at which it undergoes changes in expression appears to be tissue dependent. Therefore, it is possible that in the aorta, p38 MAPK acts solely as an early mediator meaning variations in its phosphorylation are not detected 48 hours after R-IPC treatment.

Therefore, as the aorta were collected within 48 hours of the final R-IPC and control treatments in the optimisation studies, which is within the delayed phase of preconditioning, changes in VCAM, ICAM-1, IL-10 p-eNOS, and possibly p-p38 MAPK, expression, should still be visible. Hence, it is unlikely that the

selection of biomarkers, except for TNFα, was a significant reason for the lack of molecular data to support the validation of the R-IPC model. On the contrary, particularly with reference to the cytokine array performed in the preliminary study (Fig. 3.4) and western blot analysis conducted in the secondary optimisation study (Fig. 3.16), the absence of changes in biomarker expression may simply be due to the small sample sizes and large variation in the values obtained.

3.5.5 Improving Healthy Physiology

As these studies were conducted in WT mice, it is a fair question as to whether it is possible to invoke the benefits of R-IPC in a physiological system that is already healthy. Most previous clinical studies have investigated the efficacy of R-IPC in a population either due to undergo surgery with a prominent risk of CV complications, or an illness that places the individual at a significantly increased probability of developing CV dysfunction.

Jones *et al*. (2014) however, confirmed that 7 days of R-IPC improved microvascular function as determined using FMD and cutaneous vascular conductance (CVC) in healthy male humans. On each day, 4 cycles of 5-minutes ischaemia/5-minutes reperfusion were given on the upper arm. Prior to the first R-IPC session, as well as 1 and 8 days after the final one, FMD of the brachial artery and CVC of the forearm were assessed in both arms. In each arm, brachial artery FMD increased between assessments and was significantly raised by the third assessment 8 days after R-IPC. CVC followed a similar trend and was also significantly elevated at the final assessment in both arms. Also, during the assessment the day after R-IPC, CVC was increased in only the arm to which the ischaemia/reperfusion cycles were not applied (Jones *et al*., 2014). This could imply that the improvements in microvascular function following repeated R-IPC arise over a longer period and cannot be detected using Doppler flowmetry techniques in the first few day's post-treatment. It would have been more ideal if the investigators in this study had performed daily FMD and CVC assessments after R-IPC to ascertain whether any changes occurred within the second window of protection of 24-72 hours. However, as previously discussed, changes in protein expression associated with endothelial function should still be detected during the second window of protection regardless of whether the FLPI with

reactive hyperaemia and LDI with PE/ACh iontophoresis were able to do so at this time.

Perhaps the issue is that this improved vascular function in healthy individuals can only be detected following multiple sessions of R-IPC. However, Rytter *et al*. (2020) have shown that this is not the case, and that a single session is sufficient to promote better endothelial function. 12 healthy human subjects underwent R-IPC treatment consisting of 4 cycles of 5 minutes ischaemia/5 minutes reperfusion induced using a blood pressure cuff inflated to 220mmHg on a forearm. The vasodilatory response to ACh in the leg was significantly increased at 5 and 90 minutes after R-IPC treatment. However, no such changes were found in the preconditioned arm. Therefore, this data can be used to confirm that improvements in microvascular function should be observable, by measuring the vasodilatory response to ACh, in a location remote from the region at which the ischaemia/reperfusion treatment was directly applied, after a single session of R-IPC. This data supports the increase in delta flux and maximum ACh flux at the acute scan in the R-IPC group of the preliminary *in vivo* study (Fig. 3.3). However, as there was no additional evaluation of vascular function 24-72 hours following treatment, it could be possible that the observed improvements only lasted for the acute phase of preconditioning when just a single session is given (Rytter *et al*., 2020). Nevertheless, if this is indeed the case, due to the naturally biphasic nature of R-IPC conferred protection, and the knowledge that a selection of the biomarkers of interest quantified during the optimisation studies exhibit protein expression variations in the delayed phase, molecular changes should again still be present with the 3-day preconditioning protocol.

Even though it is improbable, it could be that the improvements in CV function in healthy subjects are only observed in humans. A significant proportion of the accessible published literature regarding R-IPC in mice involves the induction of a myocardial infarction to validate the models used (Table 1.1). It would, however, be preferable to use a less severe validation technique which provides data quickly, such as LDI with PE/ACh iontophoresis. Unfortunately, no studies could be identified using this method in murine models of R-IPC. Therefore, whilst results may have been enhanced by using animals with diabetes, or by testing whether the R-IPC was successful by inducing a myocardial infarction, the

literature regarding clinical trials indicates that effective R-IPC should probably be perceptible in healthy individuals, using the analytical methods selected in the optimisation studies, using the selected R-IPC treatment regimen. Consequently, this indicates that the issues with the data resulting in the inability to validate the 3-day R-IPC model did not arise due to the analytical methods or the subjects themselves, but instead must have originated elsewhere.

3.5.6 Effect of Isoflurane on CV Function and R-IPC

The predominant flaw identified with all *in vivo* studies was the use of isoflurane as an anaesthetic agent. Isoflurane is one of the most common compounds used for rodent anaesthesia due to producing very few side effects and a fast recovery. Unfortunately, whilst there are multiple hypotheses, like most anaesthetic agents, the mechanism of action of isoflurane is still somewhat uncertain, meaning its use can have unexpected physiological consequences.

One general issue with using an inhalational anaesthetic was that, due to the apparatus available, the flow rate exceeded what was ideal for the mice. A consequence of using a high flow rate is hypothermia which can trigger vasoconstriction. This would result in a reduction in blood flow and may explain why the delta flux was decreased, although not always significantly, in all groups at the final scan in the secondary optimisation model (Fig. 3.15). However, this theory is cast into doubt as the exposure time during the baseline and final scans was identical, therefore, one would expect to see a similar degree of vasoconstriction in each. Besides, even if a more suitable flow rate was used, this would be unlikely to produce improved results due to the anaesthetic agent used, isoflurane.

In the preliminary study (Fig. 3.3), it was speculated that it was likely that the observed increases in delta flux and response to ACh, particularly in the control group, were linked to the prolonged exposure to isoflurane. In a study by Marano *et al*. (1996), New Zealand white rabbits were anaesthetised with either 0.9%, 1.8% or 2.7% isoflurane for 30 minutes, after which haemodynamic measurements were taken. Rabbits were then administered one of the remaining isoflurane concentrations for 30 minutes, then additional recordings were made.

Anaesthesia with 1.8% and 2.7% isoflurane resulted in a significant decrease in SAP, DAP and MAP when compared to non-anaesthetised animals, thereby indicating that isoflurane is a potent vasodilator which exerts a visible effect after just a 30-minute period of exposure (Marano *et al*., 1996).

One study by Lucchinetti *et al*. (2012) states that isoflurane completely abolishes the protection conferred by R-IPC in patients undergoing on-pump coronary artery bypass graft (CABG) surgery. Patients had anaesthesia induced using propofol, opioids and rocuronium. This was maintained using 0.5-2 minimum alveolar concentration (MAC) of isoflurane. Prior to the CABG, R-IPC was given to approximately half of the subjects, using a blood pressure cuff, whilst the remaining individuals received a control treatment. The primary outcome was the level of high sensitivity cardiac troponin T released. Additionally, due to the risk of emboli caused by the surgery, levels of S100, a marker of cerebral damage, were also measured. Other secondary outcomes were the release of NT-proBNP, a marker of contractile dysfunction, and high sensitivity C-reactive protein, an inflammatory response marker. Biomarkers were measured: pre anaesthesia, post-R-IPC, post-CABG, 1-hour post-release of the aortic cross-clamp, and then 1-, 2- and 3- days following surgery. None of the 4 biomarkers showed any significant differences in their expression levels between the groups indicating a lack of protection conferred by the R-IPC. On day 3, the number of patients with new perioperative myocardial infarctions and atrial fibrillation was also recorded. 3 and 1 new myocardial infarctions, and 10 and 5 novel cases of atrial fibrillation had occurred in the R-IPC and control-treated individuals respectively. This elevated prevalence of perioperative CV complications suggests that R-IPC could in fact be exacerbating the CV dysfunction caused by the surgery. However, data revealed that there was no difference in the long-term CV outcomes, over a period of 6 months, between the groups (Lucchinetti *et al*., 2012).

Kottenberg *et al*. (2012) found contradictory data to this, however, when comparing the effects of 2 anaesthetic agents on the efficacy of R-IPC in CABG patients. All patients received 1µg/kg sufentanil, 0.3mg/kg etomidate and 0.6mg/kg rocuronium for the induction of anaesthesia which was then maintained by either 0.7-0.8% isoflurane or 0.7-0.15mg/kg/minute propofol infusion. For each of the 2 anaesthesia types, individuals received either R-IPC, using a blood

pressure cuff, or control treatment. All patients then underwent CABG surgery. cTnI, a marker of myocardial injury, was measured prior to anaesthesia and for 72 hours following the surgery. The isoflurane anaesthetised persons who received R-IPC exhibited significantly lower cTnI levels, from 1 to 72 hours post-surgery, in comparison to those treated with the control. There was, however, no difference in the cTnI levels between the propofol anaesthetised individuals treated with R-IPC when compared to those who were not. Therefore, it was concluded that propofol anaesthesia prevented R-IPC from being effective whilst isoflurane did not. Additionally, there were no significant differences in the cTnI levels between the isoflurane and propofol groups who were given the control treatment indicating the isoflurane itself was not offering a degree of protection (Kottenberg *et al*., 2012).

Reasons for the discrepancy in the findings of these studies could be rooted in the use of propofol as an induction agent by Lucchinetti *et al*. (2012). As proven by Kottenberg *et al*. (2012), propofol was linked to the inhibition of R-IPC induced cardioprotection. This was later supported by a study comparing the effect of different anaesthesia regimens on the efficacy of R-IPC. Male Wistar rats had anaesthesia maintained with either: 40mg/kg pentobarbital, 1 MAC sevoflurane with 0.5µg/kg/min remifentanil or 12mg/kg/h propofol with 0.5µg/kg/min remifentanil. 6 rats were treated with R-IPC whilst the remaining 6 acted as a control. Myocardial infarction was induced via ligation of the LAD coronary artery for 25 minutes. The infarct size was found to be significantly reduced in rats receiving R-IPC with anaesthesia maintained by pentobarbital and sevoflurane. This effect had been abolished in the R-IPC treated rats who were under the influence of propofol indicating this agent can interfere with the R-IPC process (Behmenburg *et al*., 2018).

Alternatively, both the Lucchinetti *et al*. (2012) and Kottenberg *et al*. (2012) studies appear to have overlooked the potential impact of isoflurane on blood glucose levels, which may explain how its exposure could inhibit R-IPC. In a prior study, male C57BL/6 mice anaesthetised with 1.5% or 2% isoflurane for 90 minutes exhibited significantly elevated peak mean blood glucose levels, at 239.0mg/dL and 204.6mg/dL respectively, compared to levels of 195.7mg/dL exhibited by mice inhaling 1% isoflurane (Constantinides *et al*., 2012). By

referring to previously discussed studies, in section 1.5.4, one can recall that hyperglycaemia can abolish any protective effects mediated by R-IPC. In the Kottenberg *et al*. (2012) and Lucchinetti *et al*. (2012) studies, subjects received 3 and 4 cycles of R-IPC respectively. Therefore, the extended anaesthesia exposure time in the Lucchinetti *et al*. (2012) study may have tipped the fragile glycaemic balance rendering R-IPC ineffective. Consequently, the conclusions made by Lucchinetti *et al*. could be discounted due to the poor methods used as it appears that a single exposure of isoflurane does not necessarily inhibit R-IPC.

An additional complication associated with isoflurane exposure, which goes some way to explaining the slightly elevated steady-state baseline scans in the secondary optimisation study (Fig. 3.15), is isoflurane preconditioning. This is a phenomenon in which previous isoflurane exposure leads to the development of tolerance and confers cardioprotection against a further infarction. Upon reflection, early evidence of this was the need to marginally increase the isoflurane concentration required to maintain anaesthesia with each session.

One of the earliest examples of isoflurane preconditioning in the literature comes from Cope *et al*. (1997). New Zealand white rabbits were anaesthetised with either injectable agents or 1 of 3 inhalational anaesthetics including 1.7% isoflurane. A myocardial infarct was induced by ligation of the coronary branch for 30 minutes. The injectable anaesthetic agents, pentobarbital, propofol and a ketamine/xylazine mix, were associated with infarct sizes of 39.4%, 39.6% and 45.0% respectively. Conversely, isoflurane anaesthesia led to a significantly reduced infarct size, in comparison to any of these injectable agents, at just 17%, demonstrating the cardioprotective potential of this anaesthetic agent (Cope *et al*., 1997).

Albrecht *et al*. (2014) also demonstrated that changes in haemodynamics are affected by short periods of isoflurane when given repeatedly in male Wistar rats. Rats were assigned to receive 1 of 3 anaesthetic agents: i) 2-3% isoflurane for 40 minutes, ii) 100mg/kg ketamine with 5mg/kg xylazine, iii) 0.15mg/kg medetomidine, 2mg/kg midazolam and 0.005mg/kg fentanyl antagonised with 0.75mg/kg atipamezole, 0.2mg/kg flumazenil and 0.12mg/kg naloxone after 40 minutes. Rats were anaesthetised, as described, twice a week for 3 weeks. MAP,

SAP, and DAP were all significantly decreased during the surgical tolerance period of the fifth and sixth session of isoflurane exposure when compared to the first. The vasodilatory properties of isoflurane were also apparent as MAP, SAP and DAP decreased between the baseline and surgical tolerance periods within each session. The heart rate was significantly lower in the surgical tolerance period during days 3 to 6 in comparison to day 1. The same trend was also seen during the non-surgical tolerance and waking up periods of days 2 to 6. This indicates that the heart's ability to respond appropriately to an increase in blood pressure is diminished with repeated isoflurane exposure (Albrecht *et al*., 2014).

It could be suggested that to overcome the isoflurane preconditioning effect, simply using a greater R-IPC stimulus, such as an increase in the frequency and number of ischaemia/reperfusion cycles in a single session, would be sufficient. However, numerous studies have found that there are several similarities in the molecular mechanisms by which isoflurane preconditioning and R-IPC exert their effects. Indeed, the majority of the targets of interest identified in this chapter can be influenced by isoflurane, most likely via the PI3-K pathway.

As mentioned in section 1.5.5, the PI3-K pathway is pivotal in eliciting the protective effects of R-IPC. A study by Pi *et al*. (2018) also demonstrated that isoflurane mediates its protective effects via upregulation of this pathway. Male C57BL/6 mice were anaesthetised with either 0.5% isoflurane or 35mg/kg sodium pentobarbital as a control. All subjects underwent myocardial ischaemia by ligation of the LAD artery for 1 hour and the cardioprotective effects of isoflurane assessed 3 days later. In those anaesthetised with isoflurane, pain scores were significantly reduced, and isolated cardiomyocytes exhibited increased cell viability, proliferative activity, and decreased apoptosis, compared to the controls, therefore confirming the protective effects of isoflurane. Molecular analysis determined that PI3-K and Akt expression were increased in myocardial cells from isoflurane anaesthetised mice, but not in the controls. Furthermore, the proportion of total Akt that had been phosphorylated was also elevated, indicating an increase in the activity of the PI3-K pathway. To ascertain whether the PI3-K pathway was a crucial mediator of the invoked protection, investigators treated myocardial cells with 1mg/mL of the PI3-K inhibitor LY293002. The anti-apoptotic effects and increased cell survival previously observed in those exposed to

isoflurane was abolished when LY293002 was also given highlighting the role of the PI3-K pathway in eliciting isoflurane mediated cardioprotection (Pi *et al*., 2018).

Chiari *et al*. (2005), hypothesised that the delayed phase of isoflurane preconditioning is dependent on increased NOS activity. The investigators were also able to determine which, if any, of the 3 NOS enzymes, namely iNOS, neuronal nitric oxide synthase (nNOS) and eNOS, were the most important in eliciting isoflurane induced cardioprotection. Male New Zealand white rabbits were allocated into 1 of 4 groups: i) control, ii) isoflurane, iii) inhibitors and antagonists preceding isoflurane, iv) inhibitors and antagonists preceding occlusion. Rabbits in groups ii to iv were anaesthetised with isoflurane for 2 hours. The following day, all animals, from all groups, underwent surgery to ligate a branch of the LAD coronary artery for 30 minutes. The size of the infarct was significantly reduced in animals in group ii who had received the isoflurane preconditioning treatment in comparison to those who did not. The NOS enzymes were implicated as treatment with NOS inhibitor L-NAME in groups 3 and 4 appeared to abolish the protective effects of isoflurane against a larger infarct size. Interestingly, iNOS antagonist AG and 1400W dihydrochloride, and nNOS inhibitor 7-NI did not affect the isoflurane-induced reduction in infarct size. Further tissue analysis also revealed that eNOS protein and gene expression were increased in the left ventricle of rabbits exposed to isoflurane, both immediately and 24 hours after anaesthesia, when compared to the controls. This, therefore, suggests that eNOS is the principal NOS mediating isoflurane preconditioning throughout the duration in which cardioprotection is conferred (Chiari *et al*., 2005). As eNOS activation can be induced by an array of stimuli, such as shear stress, oestrogen and angiopoietin, Liu *et al.* (2019) determined whether the PI3-K pathway could be mediating the isoflurane related increase in p-eNOS. As part of this *in vitro* study, human coronary artery endothelial cells and neonatal rat cardiomyocytes were cocultured and divided into groups: i) normoxia, ii) hypoxia, iii) isoflurane. Cells in group iii were exposed to 1.4% isoflurane for 60 minutes. After an additional 15 minutes, cells in groups ii and iii were injured by exposing them to 2 hours of hypoxia, at 0.1% oxygen, followed by 2 hours of reoxygenation. Lactate dehydrogenase activity was employed as a biomarker for hypoxia/reoxygenation induced cellular damage. In group ii, there was an

increase in lactate dehydrogenase activity following hypoxia/reoxygenation confirming sufficient severity of the insulting stimulus. Pre-treating cells with isoflurane abolished this effect indicating there was a marked decrease in cellular damage and that the isoflurane preconditioning treatment was given with success. There was a significant increase in p-eNOS expression and NO production in cells exposed to isoflurane. This elevation in NO would likely cause an increase in vasodilation and therefore a decrease in blood pressure associated with exposure to this anaesthetic. Wortmannin, an Akt inhibitor, eliminated the isoflurane-induced rise in NO production. This suggests that Akt is responsible for this NO elevation which is likely generated by the increased p-eNOS activity. Akt activation is a significant step within the PI3-K pathway, of which VEGF is an activator, therefore implying that the increase in isoflurane-induced expression of p-eNOS is associated with activation of the PI3-K pathway (Liu Y *et al*., 2019).

As previously discussed, in section 1.5.5, TNFα expression is also increased by activity of the PI3-K pathway (Qiu *et al*., 2008). There is evidence to suggest that the TNFα stimulation processes are affected by isoflurane exposure. WT mice were anaesthetised with 1.4% isoflurane, brains were harvested 6-, 12- and 24-hours post exposure and were stained for TNFα. Expression was significantly elevated in the brains at all timepoints, in comparison to time matched controls which were not given any isoflurane. Furthermore, it was confirmed that TNFα mRNA expression had also increased suggesting that isoflurane affects its generation as opposed to its degradation (Wu *et al*., 2012). These findings are in line with the predicted outcome whereby isoflurane increases both PI3-K and TNFα stimulation potentially linking these effects together by a common pathway. Additionally, not only is stimulated TNFα expression itself affected by isoflurane exposure, *in vitro* experiments have shown that isoflurane interferes with TNFα signalling and its ability to induce expression of VCAM and ICAM-1. HUVECs were divided into 1 of 4 groups: i) control, ii) isoflurane, iii) 10ng/mL TNFα, iv) isoflurane and 10ngmL TNFα. Groups ii and iv underwent isoflurane preconditioning which consisted of 3 cycles of 5-minutes 0.43 MAC isoflurane/5-minutes anaesthesia free washout, except for the final cycle which consisted of a 10-minute washout. A nonradioactive infrared electrophoretic mobility shift assay revealed that isoflurane exposure prevented the increased transcriptional

activity of NF-κB normally associated with elevated TNFα levels. NF-κB is a transcription factor which induces expression of cellular adhesion molecules, meaning, it was predicted that isoflurane resulted in a reduced presence of ICAM-1 and VCAM when stimulated by TNFα (Barnes and Karin, 1997). This was indeed the case as, in a study by Weber *et al*. (2008), TNFα induced protein expression of both ICAM-1 and VCAM-1 was found to be significantly decreased in HUVECs which had been exposed to isoflurane compared to those that had not. Additionally, isoflurane reduced the mean TNFα induced mRNA expression of ICAM-1, from 2.1 to 0.8 average light intensity, and VCAM, which fell to 3.3 from 9.6 average light intensity. Interestingly, the proportion by which the mRNA levels decreased was greater for ICAM-1 than VCAM (Weber *et al*., 2008). This indicates that either TNFα plays a more significant role in the expression of ICAM-1 than that of VCAM, or, there is an alternative stimulus or pathway, not affected by isoflurane, which mediates VCAM expression during R-IPC, but not ICAM-1. This may explain why in the VCAM western blot from the primary optimisation study (Fig. 3.8), a significant increase in its expression was observed following R-IPC that was not seen in the control group.

As previously mentioned, in section 1.5.5, p38 MAPK and TNFα can regulate each other's expression and activity. An increase in TNFα activates p38 MAPK which in turn stimulates the translation of more TNFα (Sabio and Davis, 2014). Zheng and Zuo (2003) showed that a single exposure to isoflurane, prior to permanent middle cerebral artery occlusion (MCAO), can offer a significant degree of neuroprotection mediated via p38 MAPK activation. Adult, male Sprague Dawley rats were allocated into 1 of 3 groups: i) isoflurane preconditioning plus MCAO, ii) MCAO only, iii) no preconditioning or MCAO. The isoflurane preconditioning procedure consisted of being anaesthetised for 30 minutes with a concentration of 2% isoflurane. 24 hours later, groups i and ii had MCAO surgery, under isoflurane anaesthesia. Rats in group i were found to have significantly reduced infarct sizes and a greater number of morphologically intact neurons compared to those in group ii. Through western blot analysis of parietal neocortex tissue, it was found that p-p38 MAPK expression remained elevated for at least 24 hours following the isoflurane preconditioning. To confirm the role of p38 MAPK in exerting the protection conferred by isoflurane preconditioning, a p38 MAPK inhibitor, SB203580, or p38 MAPK activator, anisomycin, were

administered to rats assigned to groups i and ii either 30 minutes before the isoflurane preconditioning or 24 hours prior to MCAO. SB203580 abolishes the benefit of the preconditioning on infarct size and reduces the expression of p-p38 MAPK previously observed following isoflurane preconditioning. Conversely, anisomycin increases p-p38 MAPK expression and significantly reduces the percentage of infarct tissue in rats from group ii, who had not been preconditioned, whilst also appearing to further enhance the protection conferred by isoflurane preconditioning in rats from group i (Zheng and Zuo, 2003).

From this data, it is evident that in addition to its involvement in R-IPC, the PI3-K pathway is essential for mediating isoflurane mediated cardioprotection. The discussed effects of isoflurane are not only limited to the heart but also can influence pathways within the brain and vasculature as a whole. This means that even if there was evidence to suggest that the 3-day R-IPC model was working, it would not be possible to completely exclude any effects of the isoflurane due to its influence on the PI3-K pathway.

3.6 Chapter Summary

Through these *in vivo* studies, it was not possible to validate a R-IPC model using the functional, and most of the molecular, tests. Following extensive analysis of the techniques employed, it was theorised that that isoflurane, and its preconditioning effect, was the most likely reason for the results obtained. However, there were 2 pieces of data, obtained from the optimisation studies, which indicated the treatment has the potential to be successful. Firstly, there was increased VCAM expression in the aorta of R-IPC treated animals. Secondly, there appeared to be a minor protective effect of the R-IPC protocol on hypoglycaemia induced endothelial dysfunction. As it is not possible to perform *in vivo* R-IPC without anaesthesia, it was therefore concluded that to optimise the proposed model, mice should be anaesthetised with an alternative anaesthetic agent using the same 9 cycle regimen.

Chapter 4

Anaesthesia Optimisation for Inducing an *in vivo* Model of R-IPC

4.1 Introduction

It was speculated, in chapter 3, that the use of isoflurane was profoundly affecting endothelial function meaning a R-IPC model could not be validated. Therefore, the aim of this chapter was to optimise the use of anaesthesia subsequently allowing the development of an *in vivo* model of R-IPC. Improvements in endothelial function, assessed using LDI with PE/ACh iontophoresis, following receipt of preconditioning treatment would indicate a valid R-IPC model. There were however indications that the 3-day R-IPC model would improve endothelial function should a more appropriate anaesthetic agent be used. It is understood that most, if not all, anaesthetic agents would have at least some effects on CV function. Therefore, a selection of alternatives were identified, and the literature was analysed to determine which option would have the fewest side effects on the CVS. Midazolam and Alfaxan were selected as the most appropriate anaesthetic agents, and an attempt was made to validate a 9 cycle 3-day *in vivo* R-IPC model.

4.1.1 Choosing an Appropriate Anaesthetic Agent

The first option available would be to continue using an inhalational agent to induce anaesthesia. Whilst isoflurane is perhaps the most common anaesthetic to be administered in this manner, others are also utilised. Their main benefits are that they allow rapid induction of anaesthesia and recovery of the animal. However, as stated in a review by Swyers *et al*. (2013) other commonly used volatile anaesthetics, such as sevoflurane and desflurane, act as potent vasodilators and can induce preconditioning (Swyers *et al*., 2013). Therefore, only injectable agents had the potential to be used when developing an *in vivo* 3-day R-IPC model.

Initially, publications in which R-IPC was induced in mice, employing either internal or external methods of invoking vessel occlusion/reperfusion, were used to compare different injectable anaesthetic agents used (Table 1.1). From this, 3 options were identified: sodium pentobarbital (Cai *et al*., 2012), ketamine with xylazine (Konstantinov *et al*., 2005), and tribromoethanol (Abdul Ghani *et al*., 2017).

Whilst pentobarbital appears to be the injectable anaesthetic of choice in R-IPC studies, the drug induces significant respiratory and CV depression with its effects appearing to be cumulative with each administration making it unsuitable for the proposed studies (Murphy *et al*., 2012).

Xu *et al*. (2007) reported that using ketamine and xylazine in conjunction is the most common method of inducing anaesthesia for echocardiography in mice. A study conducted by Xu *et al*. (2007) determined the optimum doses of the 2 drugs required to achieve sedation and immobility without having a profound effect on CV parameters such as heart rate. Based on the data obtained, 100mg/kg ketamine with 0.1mg/kg xylazine could be used to reduce the effects on CV function. This would only allow the animals to become lightly anaesthetised meaning they may still exhibit a reflex response when the blood pressure cuff is inflated around the hindlimb. Additionally, the period of anaesthesia may be limited to 20 minutes before the subjects begin to regain consciousness, which is shorter than the 30 minutes of R-IPC or control treatment (Xu *et al*., 2007). Whilst ketamine is normally used alongside xylazine, it can be administered in conjunction with another agent to combat the issues identified with xylazine use. However, Han *et al*. (2002) found that ketamine abolishes IPC in rabbit hearts making this anaesthetic highly unsuitable for a study aiming to validate a model of R-IPC (Han *et al*., 2002).

Tribromoethanol causes suppression of the respiratory and CV systems but allows rapid induction and recovery from anaesthesia. However, peritonitis and serositis are side effects found when this agent is administered to mice. Additionally, whilst the mortality rate for a single injection is low, this increases significantly with additional administrations therefore would not be recommended for the proposed study (Lee *et al*., 2018).

As none of these anaesthetic agents were deemed suitable, it was decided that alternative drugs should be investigated. Alfaxalone came highly recommended by Professor Thorbjorn Akerstrom of the University of Copenhagen due to experiencing negligible effects of the agent on CV function. In the literature, in a study using cats, alfaxalone is reported as reducing DAP and MAP, and increasing heart rate in a dose-dependent manner (Muir *et al*., 2009). However,

there appear to be no reports of alfaxalone eliciting a preconditioning effect or causing unwanted harm upon repeated administration. Additionally, Cremer and Ricco (2017) suggested that the cardiorespiratory effects of alfaxalone take longer to become apparent in comparison to those associated with ketamine (Cremer and Ricco, 2017). Therefore, alfaxalone, branded as Alfaxan, was selected as the anaesthetic agent for the purposes of this study. For the purposes of this preliminary study, Alfaxan was to be injected via the intramuscular route. As Alfaxan does not possess analgesic properties, and intramuscular injection can cause discomfort to the recipient, midazolam was injected intraperitoneally prior to sedate the subjects and reduce pain.

All procedures conducted, and data collected, within this chapter were performed by Dr Calum Forteath whilst images were generated, and statistics performed by myself.

4.2 Injectable Anaesthesia Study

A study protocol was designed to investigate whether the proposed R-IPC model could be validated when anaesthesia was induced using injectable agents midazolam and Alfaxan. This pilot study consisted of 2 experimental groups, dependent on whether R-IPC or control were given, with 3 subjects per group. The protocol timeline employed was similar to that used in the secondary optimisation study, as in section 3.4, with the exclusion of the insulin-induced hypoglycaemic episode or administration of a saline injection on day 8. Baseline and final LDI with PE/ACh iontophoresis scans were still conducted on days 1 and 9 respectively, and R-IPC and control treatments were given on days 5, 6 and 7. In addition, FLPI with reactive hyperaemia scans were performed immediately after the baseline and final LDI with PE/ACh iontophoresis scans (Fig. 4.1). To overcome the issues raised with the FLPI with reactive hyperaemia technique, highlighted in section 3.3.5, it was theorised that by taking precautions to limit the movement of the blood pressure cuff or hindlimb, and by attempting to improve the consistency of foot placement in relation to the FLPI laser, it may be possible to obtain meaningful results from this method. Additionally, the new anaesthetic regimen negates the need to use a nose cone allowing the investigator to have more control over the positioning of the mouse whilst

anaesthetised. Tissue was harvested and plasma collected immediately following completion of the final FLPI with reactive hyperaemia scan. Tail vein blood glucose levels were also measured after the baseline and final FLPI with reactive hyperaemia scans were conducted. Bonferroni's repeated measures multiple comparisons 2-way ANOVA was utilised to analyse all LDI with PE/ACh iontophoresis data. Due to there being no effects on the response to PE, this is not reported in depth here. As this was a pilot study, sample sizes were small meaning it would not be unexpected if non-significant data arose. However, the results can be used to perform power calculations to determine what group sizes would be required to achieve significance. Therefore, it was considered important to interpret any clear trends within the data as well as differences exhibiting statistical significance.

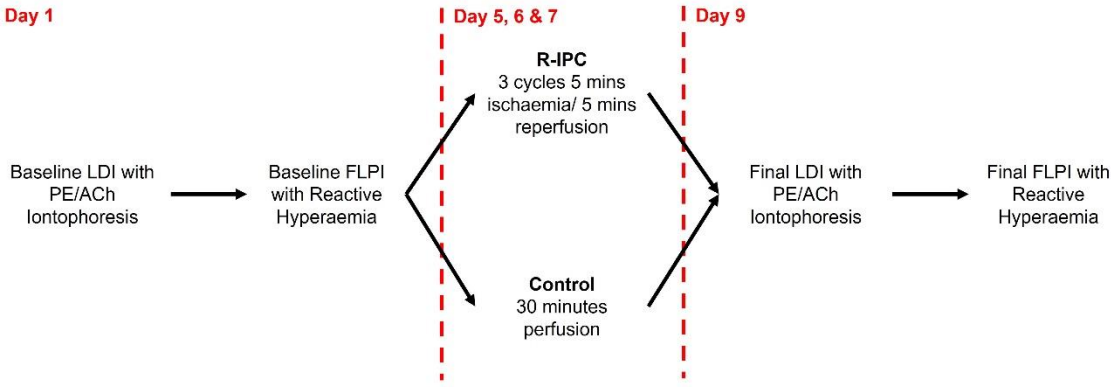

Fig. 4.1 Injectable anaesthesia study protocol timeline. Schematic indicating the procedures wild-type (WT) C57BL/6J mice underwent in the R-IPC model validation study in which anaesthesia was induced and maintained using the injectable agents midazolam and Alfaxan. Animals were randomly allocated into 1 of 2 groups depending on whether they received R-IPC or control treatment. Tail vein blood glucose levels were measured immediately following completion of the baseline and final FLPI with reactive hyperaemia scans. All animals were euthanised and tissue harvested following completion of day 9.

4.2.1 R-IPC and Control Treatments were Associated with a Non-Significant Increase in Delta Flux and Steady-State Flux

In the R-IPC group, there was an apparent, yet non-significant, increase in the mean delta flux values between the baseline (mean ± standard deviation (SD)=211.3 ± 21.1) and final (mean ± SD=347.0 ± 84.2) scans (Fig. 4.2). In the control group, there was an apparent increase in the mean delta flux values

between the baseline (mean ± SD=196.7 ± 25.1) and final (mean ± SD=257.3 ± 69.1) scans (Fig. 4.2).

In the R-IPC group, there was an apparent, yet non-significant, increase in the mean steady-state flux values between the baseline (mean ± SD=182.3 ± 38.8) and final (mean ± SD=239.9 ± 14.6) scans (Fig. 4.2). In the control group, there was an apparent, yet non-significant, increase in the mean steady-state flux values between the baseline (mean ± SD=163.8 ± 93.9) and final (mean ± SD=240.2 ± 115.8) scans (Fig. 4.2).

No significant differences were found in the steady-state flux and delta flux values between treatment groups at the same scanning timepoint.

4.2.2 R-IPC and Control Treatments Significantly Increased Endothelial Response to ACh

In the R-IPC group, there was a significant increase in the maximum flux achieved due to ACh induced vasodilation between the baseline (mean=374.0) and final (mean=517.0, p=0.0335) scans (Fig. 4.2). In the control group, there was a significant increase in the maximum flux achieved due to ACh induced vasodilation between the baseline (mean=300.0) and final (mean=426.7, p=0.0497) scans (Fig. 4.2).

No significant differences were found in the maximal flux achieved due to ACh induced vasodilation between treatment groups at the same scanning timepoint.

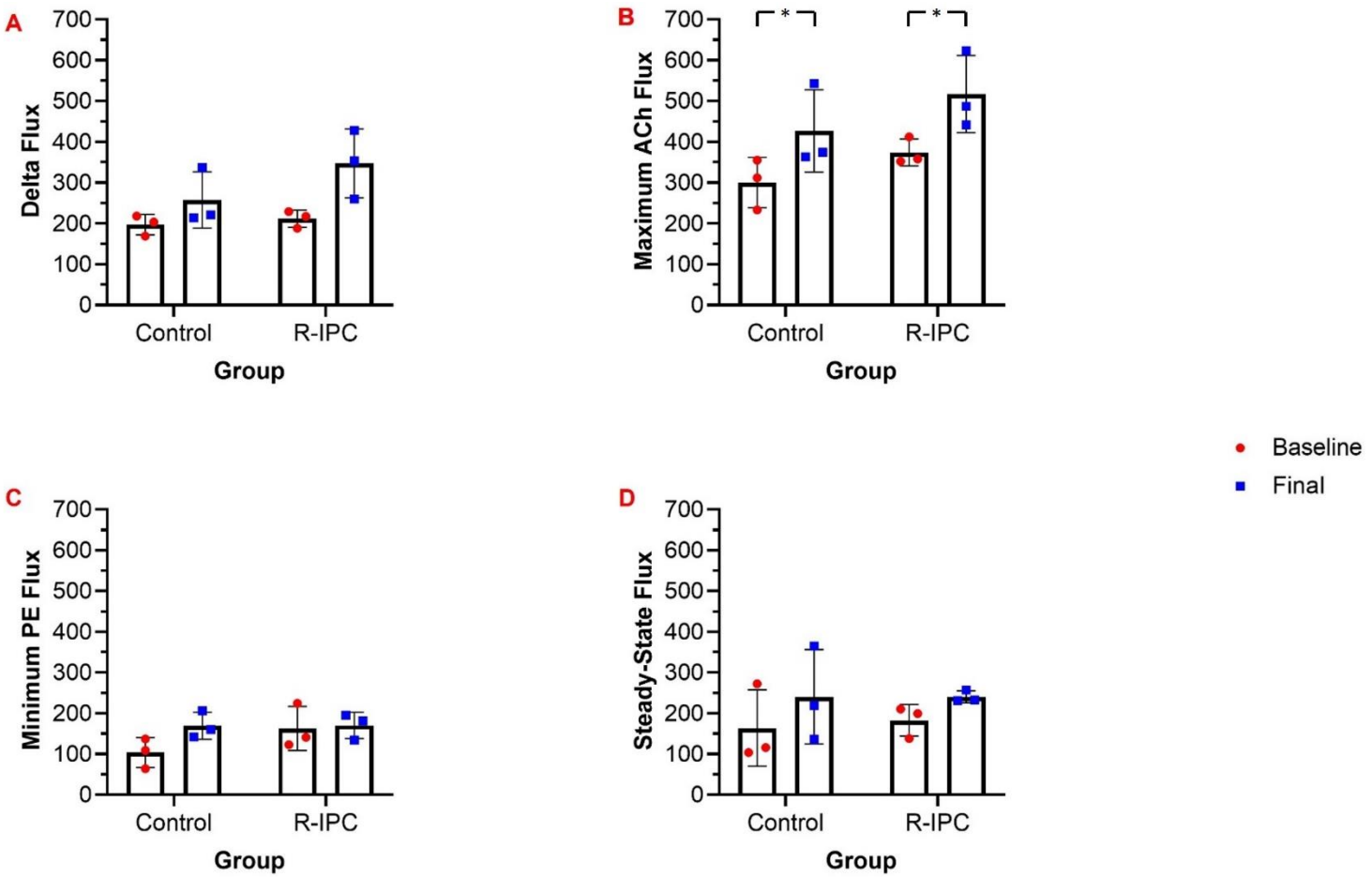

Fig. 4.2 Injectable anaesthesia study LDI with PE/ACh iontophoresis. Mice underwent an LDI scan with PE/ACh iontophoresis 4 days before (baseline) and 48 hours after (final) 3 days of R-IPC or control treatment. Delta flux (A) was found by subtracting the minimum flux due to PE induced vasoconstriction (C) from the maximum due to ACh induced vasodilation (D). Steady-state (B) refers to the flux prior to applying the current. Mean with SD and individual data points are plotted. Significant differences between final scans and baselines within each group are indicated (* = $p<0.05$).

4.2.3 Blood Glucose Levels Appeared to Increase Between Day 1 and Day 9 of the Protocol

Blood glucose levels were compared between experimental groups and timepoints using Bonferroni's repeated measures multiple comparisons 2-way ANOVA (Fig. 4.3). In the R-IPC group, there was a significant increase in the blood glucose levels measure after the final FLPI with reactive hyperaemia scan on day 9 (mean=10.4) in comparison to those taken after the baseline FLPI with reactive hyperaemia scan on day 1 (mean=7.5, p=0.0347). In the control group, there was a similar apparent, yet non-significant, increase in tail vein blood glucose levels between day 1 (mean ± SD=5.8 ± 2.4) and day 9 (mean ± SD=8.1 ± 1.5) of the protocol. After the baseline FLPI with reactive hyperaemia scans, blood glucose levels appear slightly higher in the R-IPC group in comparison to the controls. Whilst non-significant (p=0.0561), the blood glucose levels after the final FLPI with reactive hyperaemia scan in the R-IPC group appeared higher than those in the control group at the same timepoint.

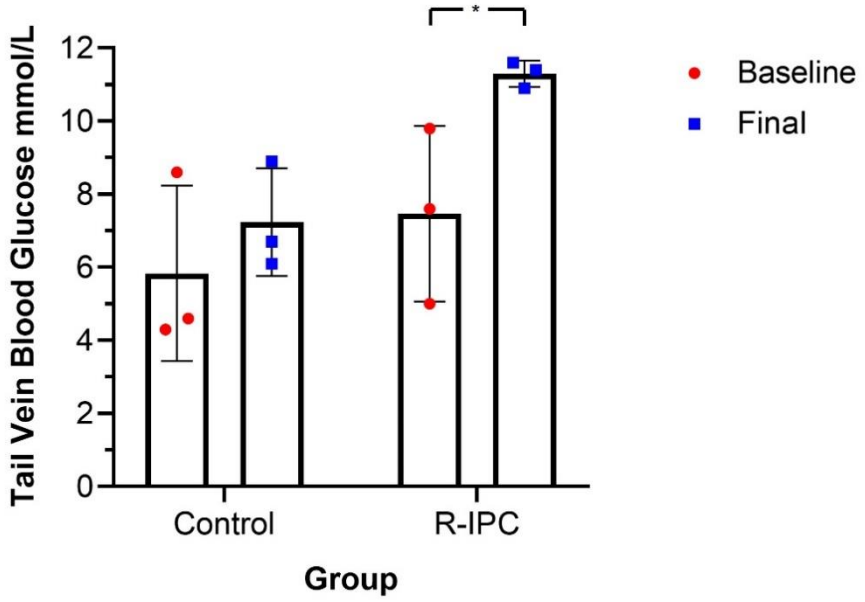

Fig. 4.3 Changes in blood glucose between scanning sessions. Tail vein blood glucose levels were measured immediately following completion of the baseline and final FLPI with reactive hyperaemia scans. Mean with SD and individual data points are plotted. Significant differences in the blood glucose levels between the baseline and final scans within treatment groups are indicated (* = p<0.05).

4.3 Discussion

4.3.1 Preliminary Data Indicated a R-IPC Model Could be Validated Using Injectable Anaesthesia if Group Sizes were Increased

The aim of this study was to optimise and develop an *in vivo* model of R-IPC using an alternative anaesthesia regimen to that used in chapter 3. Preliminary data indicates that, with an increased sample size, the selected R-IPC model may be valid.

In both the control and R-IPC treated groups there was an apparent increase in delta flux between the baseline and final scans. Although non-significant, this increase appears to be greater in the R-IPC group potentially indicating success of the treatment. However, further work to increase sample sizes is required to confirm this. In both groups, this elevation appears to be attributed to a significant increase in response to ACh, implied by the elevated flux value achieved due to ACh induced vasodilation at the final scan. This suggests an improvement in endothelial function, which was predicted in the R-IPC group but unexpected in the control group and therefore could potentially be a result of repeated Alfaxan anaesthesia. Despite this possible issue, the slight increase in delta flux indicates that the injectable anaesthetic regimen does not elicit a preconditioning effect and is unlikely to inhibit R-IPC.

Ideally, at baseline, the 4 factors should be similar between the 2 experimental groups. However, this does not appear to be the case, particularly regarding the maximum ACh flux and minimum PE flux. Whilst this is concerning, it could be potentially explained by normal mouse to mouse variation, given the small sample sizes used in this study. Alternatively, environmental factors, such as temperature, could have affected the degree of vasodilation, and vasoconstriction, of an individual mouse.

Therefore, despite the potential concerns highlighted, the preliminary data obtained in this study remain promising and further investigation is warranted to increase sample sizes.

4.3.2 Limitations

The principal limitation with this study, and any *in vivo* R-IPC study, was the requirement to anaesthetise animals during the treatment procedure. As briefly mentioned in section 4.1.1, whilst it is possible to identify anaesthetic agents which have a limited effect on CV function, none could be identified as having no influence. Therefore, as humans undergoing R-IPC treatment do not need to be anaesthetised, *in vivo* models of R-IPC will always be limited by necessity to use anaesthesia. However, *in vivo* studies can rapidly provide one with an insight into molecular mechanisms which cannot be achieved through clinical trials making them useful for the progression of medical research.

One problem with using anaesthesia is that there may be an undesired effect on blood glucose levels. Whilst this would not be a major issue regarding this study, it should be taken into consideration when investigating the effects of glycaemic variability on the validated R-IPC model in future studies, as discussed in section 6.2. An observation made in this study was that there was a slight increase in blood glucose levels between day 1 and day 9 in all individuals, although all measurements were within a euglycaemic range (Fig. 4.3). In the R-IPC group, this increase was statistically significant which may initially indicate that the R-IPC treatment is associated with a rise in blood glucose levels. Ji *et al*. (2013) exhibited that, following myocardial infarction injury, there is a marked increase in the glucose uptake into the heart in rats who also received IPC in comparison to those who did not. This in turn was associated with increased GLUT4 translocation to the cell membranes induced by the PI3-K pathway (Ji *et al*., 2013). Therefore, whilst it appears that IPC induces cardioprotection by modulation of glucose homeostasis, the effects of R-IPC alone, in the absence of subsequent ischaemia-reperfusion injury, on glucose metabolism and availability are unclear. Other anaesthetic agents, including isoflurane, have been associated with transient changes in blood glucose levels (Schwarzkopf *et al*., 2013), but there is no evidence in the literature to suggest that midazolam and Alfaxan would have a such an effect. The animals were not fasted prior to any of the procedures performed, hence it was possible that the animals had not eaten immediately before undergoing the baseline scans but had on the day of the final scans. Alternatively, prior to the final scans, the subjects may have inadvertently been stressed by an environmental stimulus, which are known to cause increases

in blood glucose levels. However, as this increased trend was observed in all animals, despite being performed in multiple batches, it is conceivable that something within the protocol itself was causing the slight elevation in glucose levels. To determine whether the anaesthetic regimen alone is influencing glucose levels, the injectable agents could be tested on a small cohort of fasted animals ensuring the removal of external stressful stimuli unrelated to the protocol.

An additional problem reported with this protocol, from a practical aspect, was that recovery from anaesthesia was exceptionally slow in comparison to isoflurane. It is necessary to monitor animals until they regain consciousness and they have recovered satisfactorily. Therefore, if there is only one investigator, just 2 or 3 animals can go through the 9-day protocol at a time. Hence, by using injectable anaesthesia, this pilot study took 2-3 times longer to complete compared to if isoflurane was used in lieu. Subsequently, any future studies, utilising the R-IPC protocol validated using injectable anaesthesia, would also take far longer to conduct than if isoflurane was administered. However, whilst the overall length of the study would be significantly prolonged, the current data implies that the injectable anaesthesia regimen did not induce a preconditioning effect, although further work to increase sample sizes is required to confirm this. Therefore, it could be concluded that this limitation of utilising midazolam and Alfaxan are negated.

A final potential issue identified was that the reactive hyperaemia test could technically be counted as a single R-IPC cycle. To control for this, it was always performed immediately after the LDI with PE/ACh iontophoresis scans. As the protective effects of R-IPC are generally considered to only last up to 96 hours (Bolli, 2000), it was assumed that by day 9, any residual effects of the baseline FLPI with reactive hyperaemia scan would have no effect on the final LDI with PE/ACh iontophoresis scan. As discussed in section 3.5.5, Jones *et al*. (2014) found that, in humans, improvements in microvascular function, assessed using FMD of the brachial artery and CVC of the forearm, were still observed 8 days following completion of R-IPC treatment (Jones *et al*., 2014). However, in this clinical trial, R-IPC was given daily, for 7 days, and consisted of 4 cycles of 5 minutes ischaemia/5 minutes reperfusion per day, whereas the reactive

hyperaemia used in our study would constitute just a single cycle given 9 days prior to the final LDI with PE/ACh iontophoresis scan. Therefore, whilst it was acknowledged that it could be possible for the baseline FLPI with reactive hyperaemia scan to influence endothelial function 9 days later, it was concluded that this was highly improbable, and any effect would be negligible in comparison to the effect of the R-IPC treatment given on days 5-7. It is important to consider that the final FLPI with reactive hyperaemia scan may influence changes in the expression of cytokines within the plasma in both the control and R-IPC groups. However, expression of proteins mediating the delayed phase of R-IPC induced protection, such as VCAM and ICAM-1, should not be affected by this final FLPI with reactive hyperaemia scan as the tissue was harvested immediately following its completion.

4.3.3 Future Directions

Whilst the LDI with PE/ACh iontophoresis data was promising, due to small sample sizes, the statistical significance desired to allow validation of the R-IPC model has not yet been achieved. Power calculations were performed utilising the mean delta flux values and standard deviations obtained from the baseline and final LDI with PE/ACh iontophoresis scans in the R-IPC group. Assuming an alpha level of $p<0.05$ and power of 95%, it was determined that a minimum of 5 animals per group would be required to observe a significant increase in the delta flux between the baseline and final scans of R-IPC treated individuals. Model validation can also be conducted by analysing the FLPI with reactive hyperaemia data and changes in biomarker expression associated with R-IPC as described in chapter 3. Briefly, this would consist of quantifying protein expression of endothelial function markers within the aorta and performing a cytokine array on the plasma collected from mice following completion of the final scanning session. It is best that this process is delayed until all subjects have completed the study as samples are only truly comparable when analysis is performed using the same plates or gels. Following validation, it would be possible to investigate the effects of glycaemic variability on the R-IPC treatment as is discussed in more detail in section 6.2.

4.4 Chapter Summary

The preliminary LDI with PE/ACh iontophoresis data obtained from this study indicates that both the 3-day R-IPC and control protocols were associated with improvements in endothelial function. However, in the R-IPC group, the degree of improvement appears to be slightly larger therefore potentially indicating a successful model was produced. Additionally, whilst there may be some effects of the injectable anaesthetic agents used on CV function, a suitable anaesthesia regimen which does not induce preconditioning seems to have been identified. Therefore, by utilising midazolam and Alflaxan, it would be possible to continue with validating the R-IPC model and investigating the effects of glycaemic variability on its efficacy.

Chapter 5

Effects of Glycaemic Variability on HPC and IPC in HUVECs

5.1 Introduction

The main aim of this final results chapter was to validate *in vitro* models of HPC, IPC and R-IPC. Models would be validated if cell viability was increased, and apoptosis was decreased following a severe hypoxic or ischaemic event in cells that received the preconditioning treatment. Subsequently, a secondary aim was to investigate the effect of an acute hypoglycaemic and hyperglycaemic event on the ability for these models to improve cell viability following a hypoxic or ischaemic insult. In this, either IPC or HPC treatment would be given to the cells followed by a 24-hour period of recovery, and either a severe ischaemic or hypoxic insult respectively. Hypoglycaemia and hyperglycaemia could then be introduced at different timepoints within the protocol to ascertain whether they influenced the preconditioning treatments. The initial step in performing this investigation was to validate the relevant models. Both IPC and HPC involve oxygen deprivation, and 2 principal methods of inducing hypoxia *in vitro* were identified with the aim of comparing them both: gas and chemical mediated.

5.1.1 Hypoxic Incubator Induced Hypoxia

Gas induced hypoxia is conducted using a hypoxic incubator. This apparatus is akin to a standard cell incubator but contains an oxygen sensor and has an input for nitrogen gas enabling the oxygen levels to drop to 1%. When an oxygen target is set, nitrogen gas is pumped into the incubator and displaces the oxygen within causing a hypoxic environment.

The principal advantage of this technique, over the chemical method, is that nitrogen gas is physiologically inert meaning there are no undesired interactions within cells. Additionally, as the hypoxic incubator creates a low oxygen environment, and hypoxia is generally defined by a lack of oxygen available, this technique could be considered more aetiologically relevant regarding the onset of hypoxia in humans.

To mimic the IPC and HPC protocols more commonly used *in vivo*, investigators have induced HPC in HUVECs by using multiple cycles of hypoxia reperfusion, including 2 cycles of 30 minutes hypoxia/30 minutes reoxygenation (Rath *et al*., 2012) and 3 cycles of 15 minutes hypoxia/15 minutes reoxygenation

(Hummitzsch *et al*., 2014). It was hypothesised that the greater the number of cycles results in a stronger preconditioning response, and that the slower the frequency of the cycles prolongs the preconditioning response (Rankin *et al*., 2009). Hence, a combination of these protocols was used for the gas mediated *in vitro* preconditioning models discussed in this chapter. Therefore, 3 cycles of 30 minutes ischaemia/30 minutes reperfusion or 30 minutes hypoxia/30 minutes reoxygenation would be utilised to induce IPC and HPC respectively. The ischaemic and hypoxic insult duration used to treat endothelial cells varies across different studies with 30 minutes (Zeng *et al*., 2016), 40 minutes (Nernpermpisooth *et al*., 2017), or 2 hours (Chen *et al*., 2020) being employed. At the time of experimental design, it was noted that Liu *et al*. (2010) had exposed their endothelial cells to ischaemia for 4 hours although the relevant article in which this was published has now been retracted (Liu *et al*., 2010).

Due to the relatively short period – 30 minutes – that cells would be spending in the hypoxic media and ischaemic buffer during preconditioning cycles, these solutions required deoxygenating prior to use. The best way to achieve this is to directly bubble nitrogen gas through the media or buffer to cause displacement of the oxygen. Newby *et al.* (2005) found that when this was conducted on M199 media, oxygen levels dropped to 0% after just 30 minutes (Newby *et al*., 2005) This facility was not available to conduct the desired experiments, but it is possible to deoxygenate media using a hypoxic incubator. When M199 media was exposed to 2% oxygen in a hypoxic incubator, it takes approximately 16 hours for the oxygen concentration within the media to drop to 3%, and an additional 8 hours for it to reach 2%. Therefore, to deoxygenate the basal media and ischaemic buffer, they were placed in the hypoxic incubator, set to 1%, for at least 24 hours (Newby *et al*., 2005).

5.1.2 $CoCl_2$ Induced Hypoxia

The second method of inducing hypoxia *in vitro* is to use the chemical $CoCl_2$ which mimics hypoxia by stabilising HIF1α.

A major concern with using a chemical mediator of hypoxia, is that there is a risk of the drug affecting pathways which are not normally influenced during hypoxia.

Additionally, $CoCl_2$ could not be used to treat humans with HPC or IPC due to it being highly toxic. A significant advantage of this method, however, is that it is possible to perform multiple experiments simultaneously which is not practical when using the hypoxic incubator available.

As there was no data found to indicate how $CoCl_2$ can be used as a HPC stimulus in HUVECs, the protocol for the HPC model was loosely based upon one by Yu *et al*. (2013) Whilst these investigators utilised bone marrow mesenchymal stem cells for their experiments, the dose-response curves which they generated provided the basis for preliminary experiments. They tested the effect of 8 $CoCl_2$ concentrations, between 0 and 600µM, administered for 6 different timescales, ranging from 0 to 72 hours, on cell growth inhibition and apoptosis (Yu *et al*., 2013). To determine the optimal $CoCl_2$ dose to induce HPC in HUVECs, a similar dose-response experiment was conducted, using a 24-hour timescale. Interestingly, only single hypoxia-reoxygenation cycles appear to be performed when $CoCl_2$ is used to invoke HPC rather than the multiple cycles associated with gas mediated induction and *in vivo* models.

Whilst there is a significant quantity of published research using $CoCl_2$ as an HPC stimulus *in vitro*, none was found to indicate how it may be used to induce IPC. Typically, OGD is used to induce ischaemia *in vitro*. Therefore, it was hypothesised that it would be possible to mimic ischaemic conditions by dissolving the $CoCl_2$ in an ischaemic buffer containing no glucose. Hence, a protocol for this was based upon the, later confirmed, hypothesis that 3 hours of glucose deprivation induced a hypoglycaemic response akin to what may be expected during a cycle of IPC. To validate both the IPC and HPC models using $CoCl_2$, it was decided to use 2 doses of $CoCl_2$ as the hypoxic and ischaemic insults to determine if their severity affects the efficacy of the preconditioning treatments. Additionally, as the purpose of the preconditioning treatments is to protect against a more severe stimulus, each of the hypoxic and ischaemic insults would be performed by exposing cells to a higher $CoCl_2$ concentration than was used for the HPC and IPC stimulus, respectively.

5.1.3 Methods of Validating in vitro HPC and IPC

To validate the preconditioning following the insult periods, markers of cell viability, proliferation, and apoptosis were utilised. Analysis of the literature reveals that these are the 3 most significant markers used for this purpose and that more in-depth molecular analysis is commonly performed once the models have been confirmed as working.

5.1.3.1 Cell Proliferation and Viability

The trypan blue assay was initially considered as a method of determining cell viability. However, initial tests revealed issues regarding the practicality of using this technique on a large number of samples simultaneously. Therefore, to assess cell viability and proliferation, MTS assays were used. The MTS assay is technically a metabolic assay although it is commonly utilised as a marker of cell viability within a sample. The yellow MTS reagent added to the cells contains MTS tetrazolium which is reduced to orange formazan. The degree of colour change generally relates to the number of mitochondria present in each well, which itself correlates to the number of living cells. The darker the orange colour after incubation, the more viable cells there are in the well. Therefore, when absorbance is determined, differences between the values obtained for various experimental groups can be analysed and interpreted as changes in cell viability, with higher absorbance indicating greater cell viability. Additionally, if at least 2 MTS assays are performed at separate timepoints, ideally the length of a complete cell cycle, differences in proliferative state between groups can be inferred. The main benefit of this assay is that multiple samples can be analysed together within a short time frame.

5.1.3.2 Apoptosis

There are numerous techniques which may be utilised to analyse apoptosis, each of which have their own benefits and are used to target separate aspects of the apoptotic process. Many of these techniques are unable to differentiate between apoptotic and necrotic cells. Therefore, it is common for more than one assay to be used. Whilst several techniques were considered, it was decided that the caspase 3/7 activity assay and TUNEL assay were deemed the most

appropriate and selected to analyse the early and late phases of apoptosis respectively.

There are at least 11 caspases known to be involved in the early phase of apoptosis, with some of these, namely caspases 1, 4, 5, 8 and 11, also playing a role in necrosis, meaning this selection should not be used in an apoptosis assay (Yuan *et al*., 2016). Caspase cleavage, and activation, is traditionally monitored using western blot analysis, a time-consuming process. However, recent technological advances mean caspase 3/7 activity can be quickly determined using an IncuCyte® imaging device.

A TUNEL assay identifies DNA fragmentation, which occurs in the latter stages of apoptosis and can be detected using flow cytometry or fluorescence microscopy. Whilst it is possible to accidentally label necrotic cells, modern TUNEL assays more reliably label cells in the late stage of apoptosis making it a popular choice of assay.

5.2. Optimising Growth Conditions for HUVECs

Primary cells are extremely precious due to the limited number of replications they can undergo before being unusable. Therefore, optimising their growth conditions is imperative to achieve the maximum yield particularly whilst passaging them. Other research groups within the University of Dundee have successfully cultured HUVECs using EGM, whilst groups elsewhere were able to do this using DMEM (Zhang *et al*., 2019). Therefore, experiments were conducted to assess whether these cells required EGM to promote their survival or if the DMEM would work equally as well.

5.2.1 EGM, but not DMEM, Supported HUVEC Culture

A single biological repeat (N=1) of P5 HUVECs was plated and cultured in either EGM or DMEM prior to undergoing the cell proliferation assay, cell adhesion assay, and cell viability assay. The proportion of adhered cells, percentage increase in cell number, and proportion of viable cells were higher for HUVECs incubated in EGM than those in DMEM (Fig. 8.3). Hence, it was concluded that EGM, and not DMEM, should be used to culture the HUVECs for all subsequent

experiments. Such substantial differences were likely due to the components of the media used. Although Zhang *et al*. (2019) found success when using DMEM, their failure to specify precisely which DMEM they had utilised resulted in the assumption that standard DMEM would be sufficient. However, it is possible that these investigators used a GlutaMAX supplement, in lieu of the L-Glut used to supplement our DMEM, which is associated with increased cell viability. Additionally, as DMEM contains no growth factors, lipids or proteins, the endothelial growth supplement, used to make EGM, possibly contains nutrients required for the growth and survival of HUVECs which were not present in the correct quantities within DMEM supplemented only with HI FBS.

5.3 Validating Hypoxic Incubator Induced HPC and IPC

5.3.1 Induction of a Sufficient Hypoxic and Ischaemic Insult was Unsuccessful Using a Hypoxic Incubator

A critical part of validating the *in vitro* HPC and IPC models was to induce a severe hypoxic or ischaemic stimulus to test whether protection had been successfully conferred. Therefore, the initial stage in model development, using the hypoxic incubator technique, was to determine how long HUVECs needed to be exposed to hypoxia or ischaemia to induce a severe insult. HUVECs were exposed to 1% oxygen hypoxia or ischaemia for 30 minutes, 1 hour, 2 hours and 4 hours in a hypoxic incubator. MTS assays were conducted both immediately (0 hour) and 18 hours after treatment to determine at what point the duration of exposure becomes detrimental to cell survival. Dunnett's repeated measures multiple comparisons 2-way ANOVA analysis was performed by comparing MTS assay data from the hypoxia and ischaemia treated cells to their relative controls (Fig. 5.1).

At the 18 hour MTS assay timepoint, cells treated with 4 hours of ischaemia (mean=1.355) exhibited significantly higher absorbance values compared to the controls (mean=0.9352, p=0.0155). Additionally, at the 18 hour MTS assay timepoint, cells treated with 4 hours of hypoxia (mean=1.549) exhibited significantly higher absorbance values compared to the controls (mean=1.047, p=0.0026). This indicates that 4 hours of ischaemia and hypoxia treatment causes an increase in the number of viable cells 18 hours following exposure.

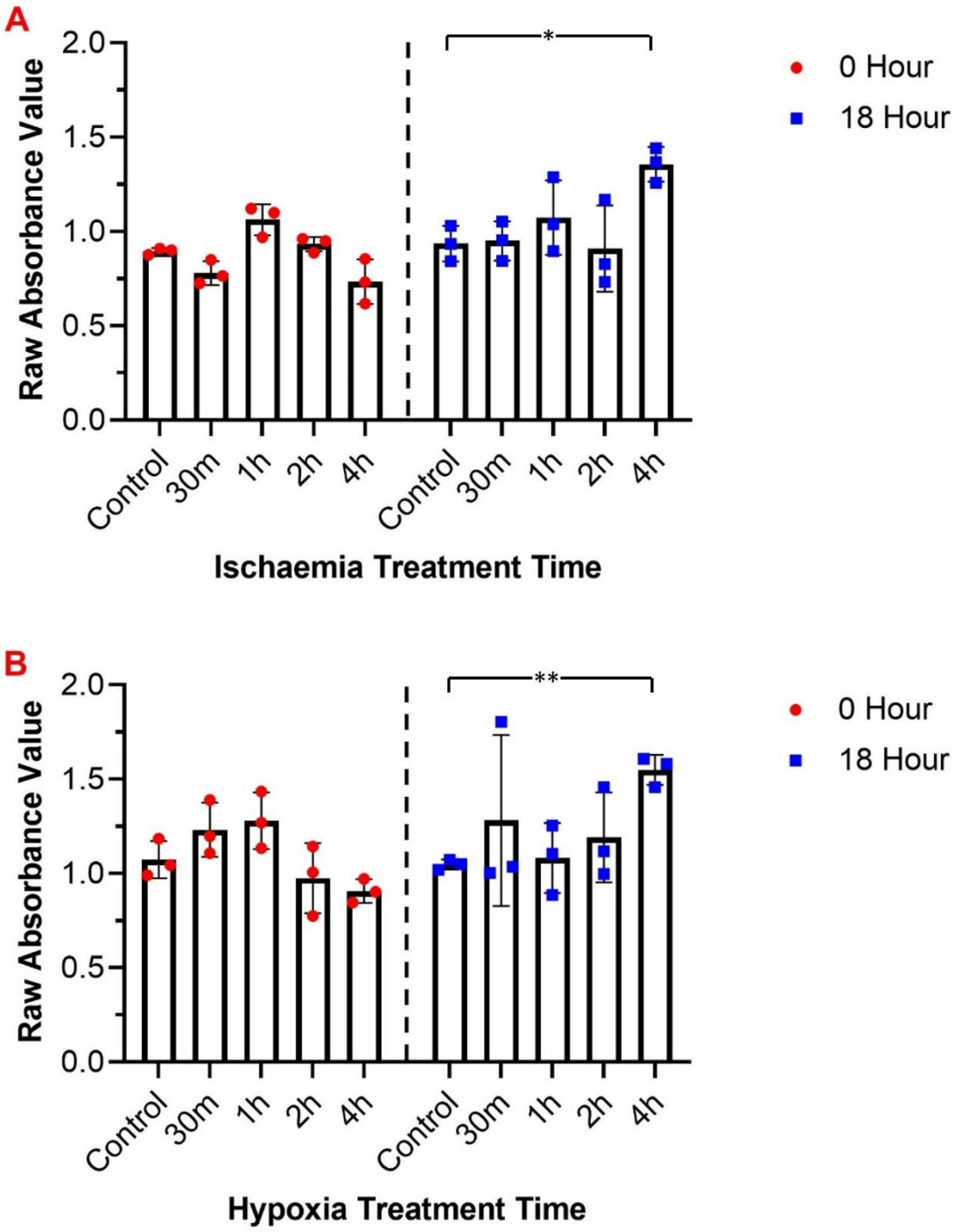

Fig. 5.1 Hypoxia and ischaemia timelapse. HUVECs were treated with ischaemia (A) or hypoxia (B) in a 1% oxygen hypoxic incubator for 5 timescales, where control indicates no treatment was given. MTS assays were completed 0- and 18-hours following exposure. Mean, individual data points and SD for raw absorbance values are shown. Significant differences between the controls and the ischaemia or hypoxia treatment groups are indicated (* = $p<0.05$, ** = $p<0.01$).

5.3.2 Limitations of Using a Hypoxic Incubator to Induce Ischaemia and Hypoxia in HUVECs

A successful severe hypoxic or ischaemic insult would be indicated by a significant decrease in cell viability at the 18-hour MTS assay timepoint when compared to the control. The 18-hour MTS assay timepoint revealed that exposure to hypoxia or ischaemia, with 1% oxygen, for up to 4 hours does not induce a reduction in the number of viable cells in HUVECs as predicted. Additionally, the lack of a significant decrease in the absorbance, and therefore number of viable cells, at the 0-hour MTS assay timepoint implies there was not even an acute deleterious effect of the hypoxia or ischaemia treatments. This therefore suggests that the proposed preconditioning and insult protocols would not be suitable. However, even with 1% oxygen, most cells would experience pathological hypoxia and a decrease in cell survival after these durations of hypoxia or ischaemia (McKeown, 2014).

5.3.2.1 Endothelial Cell Metabolism

The reason for the lack of reduction in cell viability may be linked to the metabolic preferences of HUVECs. Most endothelial cells are extremely glycolytic, with one study indicating that 99% of glucose in rat cardiac microvascular endothelial cells is metabolised into lactate via this process (Krutzfeldt *et al*., 1990). Glycolysis is a metabolic process, which occurs in the cytoplasm, and converts glucose to pyruvate through a series of enzyme mediated reactions. Under aerobic conditions, pyruvate can be used in the citric acid cycle to maintain mitochondrial oxidative phosphorylation whilst it is converted into lactate when the environment is anaerobic (Melkonian and Schury, 2019). In endothelial cells, which have substantially fewer mitochondria, a vast quantity of the pyruvate will be metabolised into lactate regardless of the amount of oxygen available. Relying so heavily on glycolysis is an exceedingly inefficient way of generating ATP (Eelen *et al*., 2018) implying that HUVECs do not prioritise energy production.

As well as providing a barrier between the lumen of blood vessels and the surrounding tissues, endothelial cells are important for mediating angiogenesis. Angiogenesis often occurs under hypoxic conditions as vessel construction is intended to return oxygen to the hypoxic cells. As mentioned in section 1.2.1,

hypoxia triggers the transcription of pro-angiogenic genes via the HIF1α pathway. Activation of this proliferative pathway could explain why, with 4 hours of 1% oxygen exposure, HUVECs exhibited elevated cell viability at the 18-hour MTS assay timepoint (Fig. 5.1). There are therefore at least two benefits offered by increased glycolysis allowing the cells to perform this particular job. Firstly, glycolysis does not depend on the presence of oxygen meaning the small amounts of ATP required by the cells can be produced under the hypoxic conditions which they often find themselves during angiogenesis. Secondly, lactate is a proangiogenic molecule, hence, as the increased glycolysis causes more lactate production, angiogenesis can be continuously promoted in the absence of other activators (Eelen *et al*., 2018). Therefore, by prioritising glycolysis over other forms of glucose metabolism, endothelial cells are well suited for growth in a low oxygen environment and can survive and function under hypoxic conditions which would lead to the death of other cell types.

5.3.2.2 Insufficient Duration of Ischaemic or Hypoxic Insult

As the environment was not anoxic, a longer duration of insult may have been required to induce a significant degree of ischaemic or hypoxic damage. Jiang *et al*. (2018) used 6 hours of 1% oxygen exposure to induce hypoxia/reoxygenation injury in HUVECs (Jiang *et al*., 2018). Even stronger stimuli have also been used with hypoxic periods of 12 hours at 1% oxygen (Sheikh *et al*., 2022), and 24 hours with 0-1% oxygen (Sierra Parraga *et al*., 2020). Conversely, Rath *et al*. (2012) utilised a 4-hour hypoxic insult at 1% oxygen with success in HUVECs (Rath *et al*., 2012). It is, therefore, unclear why there was no reduction in cell viability after 4 hours of hypoxia or ischaemia treatment and suggests other factors must be responsible for these differing findings.

5.3.2.3 Practical Limitations of Using a Hypoxic Incubator

A potential cause of the discrepancy between this data and that of Rath *et al*. relates to the practical limitations of using this technique to induce hypoxia or ischaemia in this manner. To change the cells from their regular EGM or basal media to hypoxic media or ischaemic buffer, the deoxygenated solutions had to be removed from the incubator and transferred to a biological tissue culture cabinet. Whilst, only exposed to room air for 1 minute, this could have allowed

the media and buffer to reoxygenate as the oxygen and nitrogen gases diffuse in and out of them. A second problem akin to this, was that each time the incubator door had to be opened to remove the media and buffer, or to place the cells inside, room air would enter causing the oxygen levels to rise to above 5%. It could take up to 10 minutes for this to drop back down to 1%. This would increase the time that cells containing hypoxic media or ischaemic buffer were incubated in a gas mixture with more oxygen than desired, thereby causing them to reoxygenate further. Therefore, it is possible that the HUVECs were exposed to O_2 levels above 1% putting them within the range of physiological hypoxia, instead of pathological hypoxia. This is unlikely to cause a significant degree of cell death, without a much longer exposure time, as the situation can be handled by activation of the HIF1α pathway without the initiation of necrosis (McKeown, 2014).

The ideal solution to these problems would be to use an anoxic chamber. These chambers can produce detectable oxygen levels of 0%. Additionally, all tissue culture work can be conducted within the chamber meaning buffers, media and cells do not have to be exposed to oxygen and so hypoxia and ischaemia can be maintained as desired. However, as this was not possible due to the lack of resources available, the decision was made to use $CoCl_2$ as an IPC and HPC stimulus.

5.4 Validating $CoCl_2$ Induced IPC

5.4.1 Dose-Response Curves Identified Treatment with 400-800μM $CoCl_2$ for 3 Hours Would Potentially Induce IPC

A dose-response experiment was conducted to ascertain the optimal concentration of $CoCl_2$ in ischaemic buffer to use to induce IPC. HUVECs were starved for 21 hours and then treated with either control buffer or $CoCl_2$, at 400μM, 800μM, 1200μM, 1600μM, in ischaemic buffer for 3 hours. MTS assays were conducted immediately (0 hour) and 24 hours after treatment (Fig. 5.2). Dunnett's repeated measures multiple comparisons 2-way ANOVA was used to compare the absorbance values between the controls and ischaemia exposed cells at the same MTS assay timepoint (Fig. 5.3).

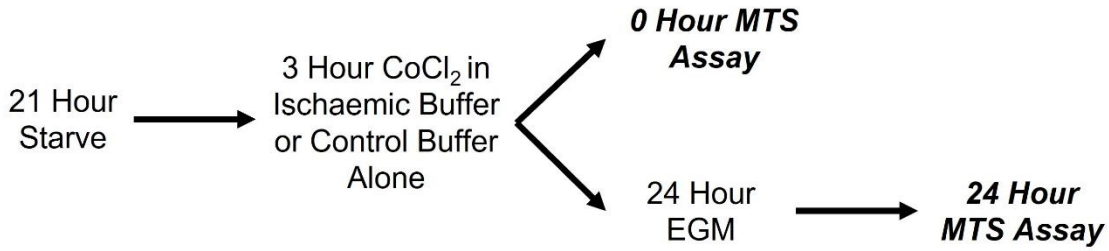

Fig. 5.2 Protocol timeline for $CoCl_2$ induced IPC dose-response curves. Timeline displaying the dose-response curve experiment used to determine the optimal dose for an IPC stimulus in HUVECs using $CoCl_2$ in an ischaemic buffer. MTS assays were conducted 0- and 24-hours following exposure to the 3-hour ischaemic or control stimulus. EGM indicates HUVECs were recovering in standard EGM.

At the 0-hour timepoint, there was a significant reduction in the absorbance values in the 800µM (mean=0.4237, p=0.0062), 1200µM (mean=0.2683, p=0.0.0001) and 1600µM (mean=0.2402, p=<0.0001) $CoCl_2$ groups in comparison to those treated with the control buffer (mean=0.6033) indicating a reduction in the number of viable cells.

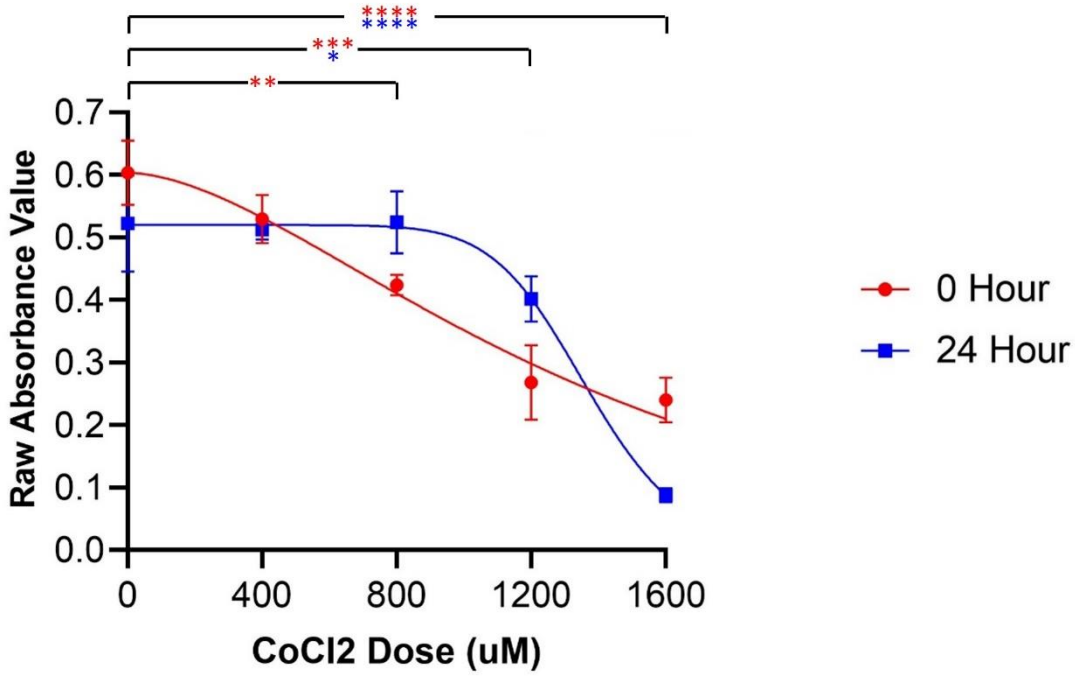

Fig. 5.3 $CoCl_2$ induced IPC dose-response curves. HUVECs were exposed to a control buffer or 4 different concentrations of $CoCl_2$ in ischaemic buffer for 3 hours. MTS assays were conducted 0- and 24-hours following exposure to ischaemia. Mean raw absorbance values and SD are shown. Significances between $CoCl_2$ treated cells and those treated with a control buffer at the corresponding MTS assay timepoints are indicated (* = p<0.05, ** = p<0.01, *** = p<0.001, **** = p<0.0001).

At the 24-hour timepoint, only the 1200µM (mean=0.4013, p=0.0482) and

1600µM $CoCl_2$ treated cells (mean=0.08792, p=<0.0001) exhibited a significant reduction in absorbance values compared to the control group (mean=0.5221) suggesting the reduced number of viable cells was only sustained when the 2 highest concentrations of $CoCl_2$ were used whereas the number of viable cells had recovered when treated with 800µM $CoCl_2$.

The optimum $CoCl_2$ concentration to induce IPC would invoke an initial, but not sustained, decrease in cell viability compared to untreated cells. Therefore, statistical analysis identified a dose of $CoCl_2$ around 800µM as a potential IPC stimulus. However, observations of the trends of both curves indicate that anywhere between 400µM and 800µM $CoCl_2$ may be suitable. This conclusion was inferred as cells exposed to 400µM $CoCl_2$ do show a decrease, albeit non-significant, in absorbance value, and therefore number of viable cells, at the 0-hour timepoint compared to those treated with control buffer, a difference not seen at the 24-hour timepoint. Hence, it was recommended that the initial IPC validation study should be performed using the more modest concentration of 600µM $CoCl_2$.

5.4.2 Treatment with 600µM $CoCl_2$ for 3 hours was too Harsh to Induce IPC

To validate an *in vitro* IPC model using $CoCl_2$, HUVECs were allocated into 4 groups, represented by their abbreviations from this point onwards: i) IPC control plus insult control (CIP CTL), ii) IPC plus insult control (IPC CTL), iii) IPC control plus ischaemic insult (CIP ISC), iv) IPC plus ischaemic insult (IPC ISC). All cells were starved for 21 hours and subsequently treated for 3 hours with either a control buffer, groups i and iii, or 600µM $CoCl_2$ in ischaemic buffer, groups ii and iv. A 24-hour recovery period in EGM was allowed after which cells were exposed to either control buffer, groups i and ii, or 900µM or 1000µM $CoCl_2$ ischaemic insult, groups iii and iv, for 3 hours. An MTS assay was completed immediately (0 hour) and 18 hours after this (Fig. 5.4).

Statistical analysis was completed using Bonferroni's repeated measures multiple comparisons 2-way ANOVA (Fig. 5.5). Cells in both the CIP ISC and IPC ISC groups exhibited a significant decrease in absorbance value, and therefore number of viable cells, at both the 0- and 18-hour MTS assay timepoints compared to those in the CIP CTL group regardless of the $CoCl_2$ dosage used to

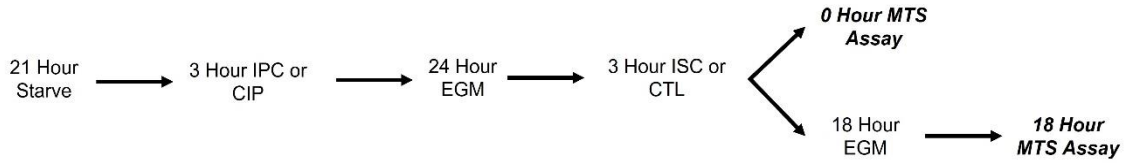

Fig. 5.4 Protocol timeline for 600µM $CoCl_2$ induced IPC validation. HUVECs were allocated into 1 of 4 groups: i) IPC control plus insult control (CIP CTL), ii) IPC plus insult control (IPC CTL), iii) IPC control plus ischaemic insult (CIP ISC), iv) IPC plus ischaemic insult (IPC ISC). MTS assays were conducted 0- and 18-hours following ISC and CTL treatment. EGM indicates HUVECs were recovering in standard EGM.

induce the ischaemic insult (Table 5.1). There was no significant difference in the absorbance values between the CIP ISC and IPC ISC groups at either assay timepoint regardless of the severity of the ischaemic insult employed. This indicates that whilst the ischaemic insults were of the desired severity, the IPC stimulus was unsuccessful in conferring any protection to the cells.

It was possible to deduce whether a chosen IPC stimulus was too harsh by comparing the absorbance values between the CIP CTL and IPC CTL treated cells. At the 0-hour MTS assay timepoint, in panel A of Fig. 5.5, the absorbance value for the IPC CTL group (mean=0.8204) was significantly lower compared to the CIP CTL group (mean=1.024, p=0.0037) whilst an apparent decrease was also observed in panel B of Fig. 5.5. This indicates the number of viable cells was reduced in the IPC CTL group at the 0-hour MTS assay timepoint in comparison to the CIP CTL group. It was desired that at the 0-hour MTS assay timepoint, the number of viable cells would have recovered. As this does not seem to be the case when 600µM $CoCl_2$ was used as an IPC stimulus, it was concluded that a milder concentration should be used in lieu.

Panel	MTS Timepoint	CIP CTL Mean	CIP ISC		IPC ISC	
			Mean	p Value	Mean	p Value
A	0 Hour	1.024	0.6117	<0.0001	0.5122	<0.0001
	18 Hour	1.331	0.9898	0.0002	0.9756	0.0002
B	0 Hour	0.9452	0.5171	0.0051	0.4899	0.0037
	18 Hour	1.267	0.8136	0.0038	0.8111	0.0036

Table 5.1 Summary of significances between the CIP CTL and ischaemic insult groups displayed in Fig. 5.5. Numerical summary of the mean raw absorbance values and statistical analyses for a selection of the data exhibited in Fig. 5.5, where panel A and B indicate the graph within the figure as annotated. p values between the CIP CTL means and both the CIP ISC and IPC ISC means at corresponding MTS assay timepoints were determined using Bonferroni's 2-way ANOVA.

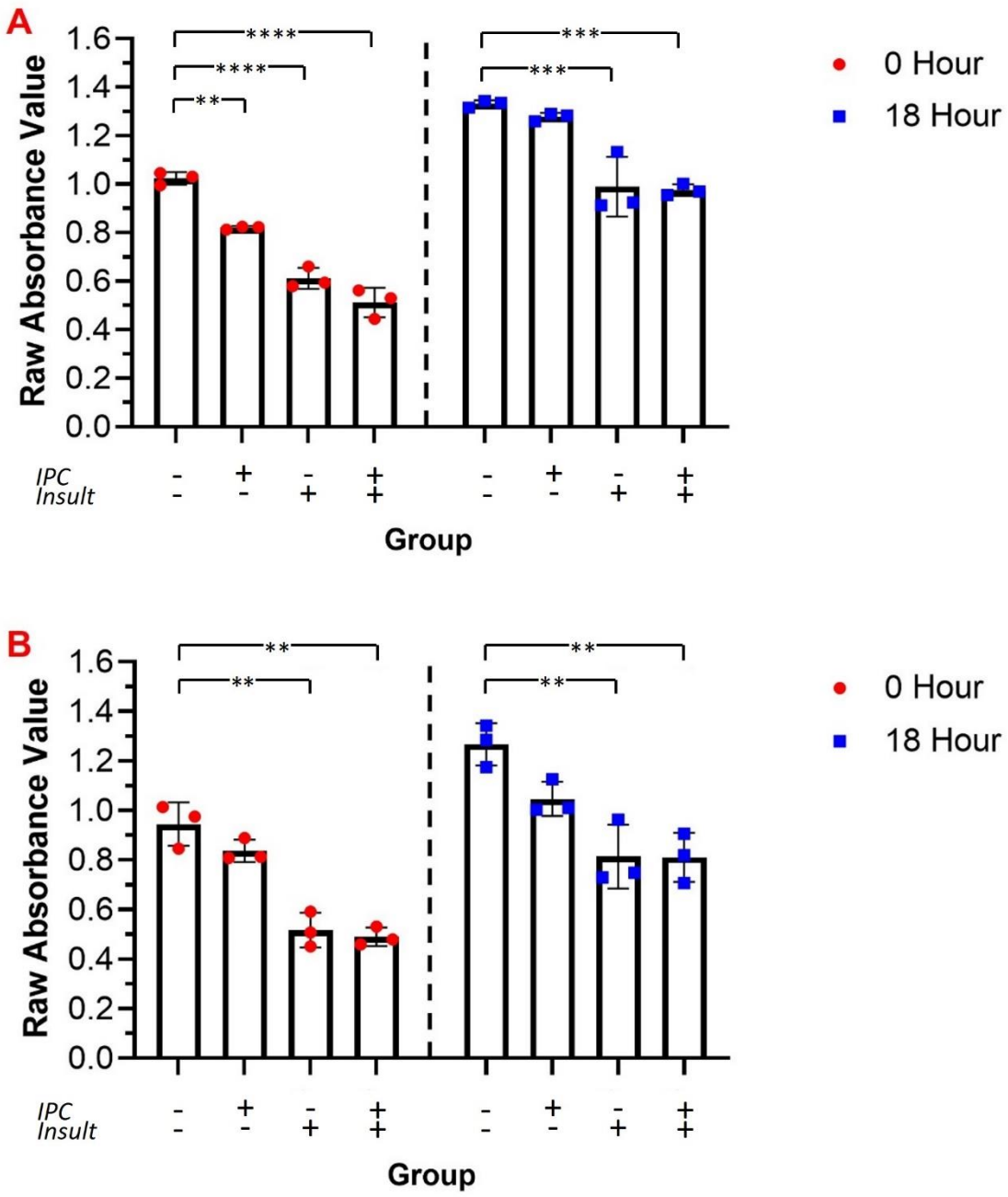

Fig. 5.5 600µM $CoCl_2$ induced IPC MTS assay. HUVECs were exposed to a control buffer or 600µM $CoCl_2$ in ischaemic buffer for 3 hours. After a 24-hour recovery in EGM, either a 900µM (A) or 1000µM (B) $CoCl_2$ ischaemic insult or control buffer treatment were given for 3 hours. MTS assays were conducted 0- and 18-hours following the insult period. Mean, individual data points and SD for raw absorbance values are shown. + and – indicates whether a group received an interventional treatment (IPC and/or ischaemic insult) or the relevant control (preconditioning control and/or insult control) respectively. Significant differences are indicated (** = $p<0.01$, *** = $p<0.001$, **** = $p<0.0001$).

5.4.3 Repeated Treatment with 400µM $CoCl_2$, for 3 Hours per Cycle, was too Mild to Induce IPC

As 600µM $CoCl_2$ proved to be too strong a stimulus, it was decided that 400µM $CoCl_2$ should be attempted. Additionally, it was predicted that increasing the number of exposures to the stimulus would be more likely to induce the IPC. Hence, a protocol was designed in which cells, divided into the same experimental groups listed in the prior 600µM $CoCl_2$ IPC protocol in section 5.4.2, were exposed to 1, 2, 3 or 4 IPC cycles over a 2-day period (Fig. 5.6). A 3-hour recovery period in EGM separated cycles 1 and 2, and 3 and 4, whilst one 15-hour recovery period was allowed between cycles 2 and 3. 400µM $CoCl_2$ was utilised as the IPC stimulus whilst both 900µM (Fig. 5.7) and 1000µM (Fig. 5.8) $CoCl_2$ were given as the ischaemic insult. MTS assays were performed immediately (0 hour) and 18 hours after the ISC and CTL treatment period. Bonferroni's repeated measures multiple comparisons 2-way ANOVA was utilised to analyse the data obtained from the MTS assays

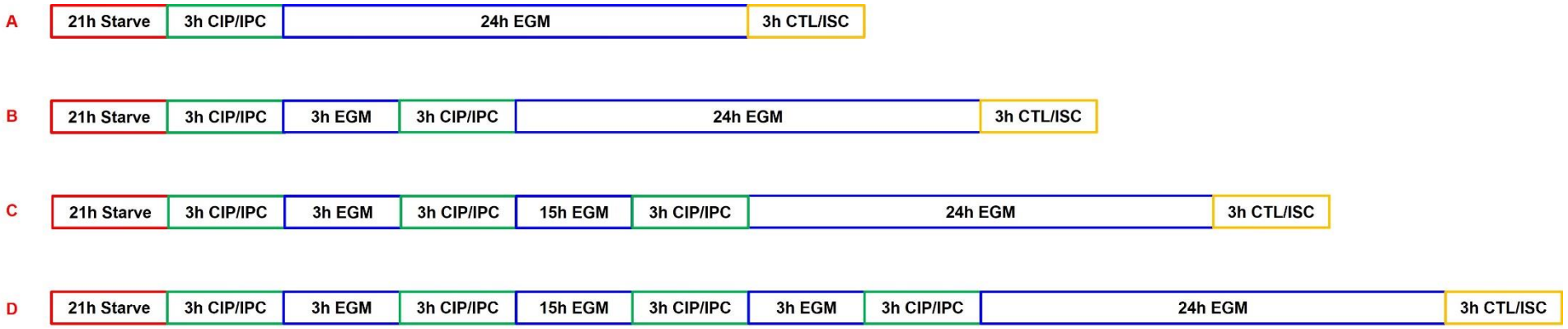

Fig. 5.6 Protocol timeline for validation of CoCl2 induced IPC with repeated IPC cycles. HUVECs were allocated into 1 of 4 groups: i) IPC control plus insult control (CIP CTL), ii) IPC plus insult control (IPC CTL), iii) IPC control plus ischaemic insult (CIP ISC), iv) IPC plus ischaemic insult (IPC ISC). These groups were subdivided further depending on whether they received 1 (A), 2 (B), 3 (C) or 4 (D) cycles of IPC and CIP treatment. MTS assays were conducted 0- and 18-hours following ISC and CTL treatment. EGM indicates HUVECs were recovering in standard EGM.

At both the 0- and 18-hour MTS assay timepoints, there was a significant reduction in the absorbance values, and therefore the number of viable cells, in the CIP ISC and IPC ISC groups in comparison to the CIP CTL groups, when cells were treated with 2 cycles of CIP and IPC (Table 5.2). At both the 0- and 18-hour MTS assay timepoint, there was no significant difference between the absorbance values, and therefore the number of viable cells, in the CIP CTL group and both the CIP ISC and IPC ISC groups in which 1 and 4 cycles of CIP and IPC were given. This indicates that the ischaemic insult was unsuccessful in these groups. At the 18-hour MTS assay timepoint, there was a significant increase in the absorbance values, and therefore the number of viable cells, in the CIP ISC group (mean=1.536, p=0.0445) compared to the CIP CTL group (mean=1.095) when 3 cycles of CIP and IPC were given. This indicates that not only was the ischaemic insult unsuccessful, but it appears to have promoted proliferation in this group of cells.

Regardless of the number of IPC and CIP cycles given, and the MTS assay timepoint, there were no significant differences in absorbance values, and therefore the number of viable cells, between the CIP ISC and IPC ISC groups further indicating that 400µM was an insufficient IPC stimulus. However, as the 900µM $CoCl_2$ ischaemic insult did not consistently result in a significant reduction in absorbance value, and therefore number of viable cells, in the CIP ISC treatment group, it was concluded that this concentration of $CoCl_2$ was not reliable as an ischaemic insult and that the protocol should be repeated using 1000µM instead.

Cycles	MTS Timepoint	CIP CTL Mean	CIP ISC		IPC ISC	
			Mean	p Value	Mean	p Value
2	0	1.044	0.6569	0.0017	0.7038	0.0034
	18	1.534	0.9322	0.0001	0.7723	<0.0001

Table 5.2 Summary of significances between the CIP CTL and both the CIP ISC and IPC ISC treatment groups displayed in Fig. 5.7. Numerical summary of the mean raw absorbance values and statistical analyses for a selection of the data exhibited in Fig. 5.7, where cycles indicate the number of CIP or IPC cycles given as described in Fig. 5.6. p values between the CIP CTL means and both the CIP ISC and IPC ISC means at corresponding MTS assay timepoints were determined using Bonferroni's 2-way ANOVA.

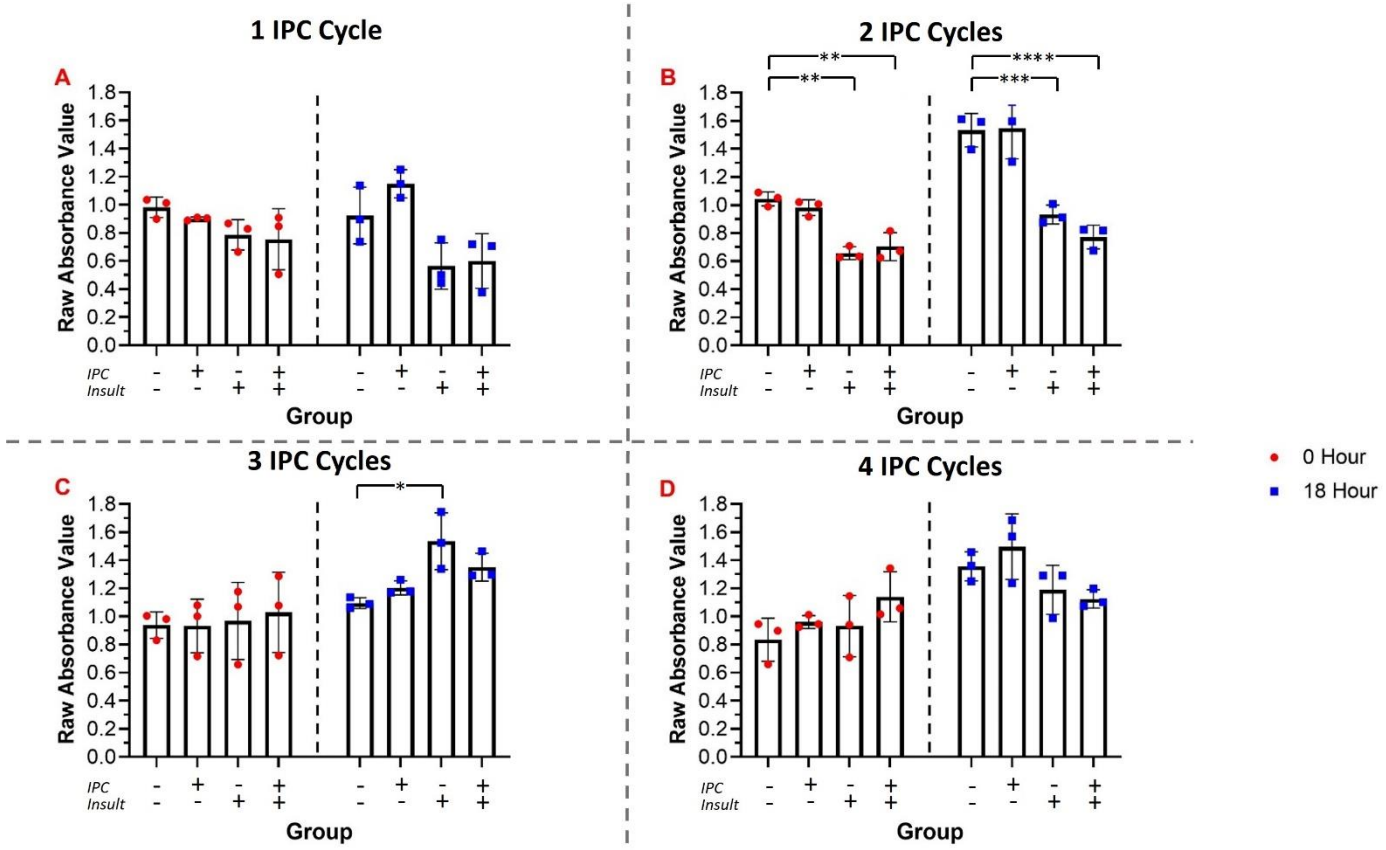

Fig. 5.7 MTS assay results obtained from attempting to induce IPC with 1-4 cycles of 400µM $CoCl_2$ where 900µM $CoCl_2$ was used as an ischaemic insult. HUVECs were exposed to 1 (A), 2 (B), 3 (C) or 4 (D) 3-hour cycles of control buffer or 400µM $CoCl_2$ in ischaemic buffer IPC treatment. for 3 hours. Following completion of the appropriate number of cycles, there was a 24-hour recovery in EGM and either a 900µM $CoCl_2$ ischaemic insult or control buffer treatment were given for 3 hours. MTS assays were conducted 0- and 18-hours following the insult period. Mean, individual data points and SD for raw absorbance values are shown. + and – indicates whether a group received an interventional treatment (IPC and/or ischaemic insult) or the relevant control (preconditioning control and/or insult control) respectively. Significant differences are indicated (* = $p<0.05$, ** = $p<0.01$, *** = $p<0.001$, **** = $p<0.0001$)

To continue the investigation as to whether 400µM $CoCl_2$ in ischaemic buffer would make a suitable IPC stimulus, the variable IPC cycle study protocol was repeated (Fig. 5.6) with 1000µM $CoCl_2$ in ischaemic buffer being used as the ischaemic insult. Again, Bonferroni's repeated measures multiple comparisons 2-way ANOVA was utilised to analyse the data obtained from the MTS assays (Fig. 5.8). Regardless of both the number of IPC or CIP cycles given and the MTS assay timepoint, the absorbance values, and therefore the number of viable cells, were significantly reduced in both the CIP ISC and IPC ISC groups when compared to the CIP CTL group (Table 5.3). This consistent reduction, particularly within the CIP ISC group at the 18-hour MTS assay timepoint, suggests that an ischaemic insult of 1000µM $CoCl_2$ reliably reduces the number of viable cells as desired.

Cycles	MTS Timepoint	CIP CTL Mean	CIP ISC		IPC ISC	
			Mean	p Value	Mean	p Value
1	0	0.9136	0.4735	0.0071	0.4933	0.0090
	18	1.107	0.3027	0.0003	0.2429	0.0002
2	0	0.9730	0.3078	0.0001	0.4118	0.0003
	18	1.043	0.3461	<0.0001	0.3262	<0.0001
3	0	1.132	0.5612	0.0004	0.4164	0.0001
	18	1.167	0.4411	0.0001	0.3252	<0.0001
4	0	1.055	0.5743	0.0060	0.5708	0.0058
	18	0.9989	0.6248	0.0213	0.3937	0.0166

Table 5.3 Summary of significances between the CIP CTL and both the CIP ISC and IPC ISC treatment groups displayed in Fig. 5.8. Numerical summary of the mean raw absorbance values and statistical analyses for a selection of the data exhibited in Fig. 5.8, where cycles 1-4 indicate the number of CIP or IPC cycles given as described in Fig. 5.6. p values between the CIP CTL means and both the CIP ISC and IPC ISC means at corresponding MTS assay timepoints were determined using Bonferroni's 2-way ANOVA.

Regardless of both the number of IPC or CIP cycles given and the MTS assay timepoint, there was no significant difference in the absorbance values, and therefore the number of viable cells, between the CIP ISC and IPC ISC groups. This therefore implies protection against a severe insult was not conferred when using 400µM $CoCl_2$ as an IPC stimulus. The data within Fig. 5.7 and 5.8

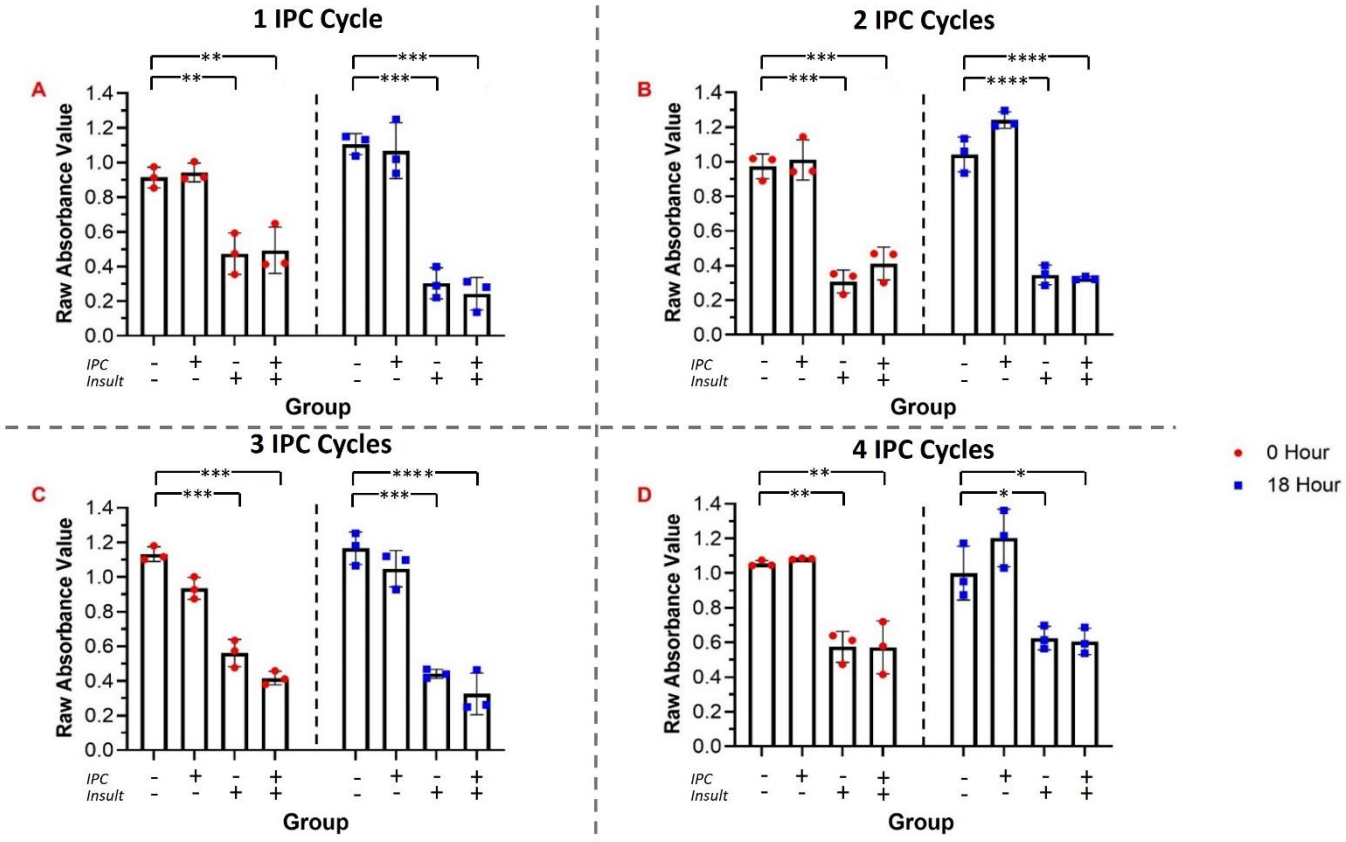

Fig. 5.8 MTS assay results obtained from attempting to induce IPC with 1-4 cycles of 400µM $CoCl_2$ where 1000µM $CoCl_2$ was used as an ischaemic insult. HUVECs were exposed to 1 (A), 2 (B), 3 (C) or 4 (D) 3-hour cycles of control buffer or 400µM $CoCl_2$ in ischaemic buffer IPC treatment. for 3 hours. Following completion of the appropriate number of cycles, there was a 24-hour recovery in EGM and either a 1000µM $CoCl_2$ ischaemic insult or control buffer treatment were given for 3 hours. MTS assays were conducted 0- and 18-hours following the insult period. Mean, individual data points and SD for raw absorbance values are shown. + and – indicates whether a group received an interventional treatment (IPC and/or ischaemic insult) or the relevant control (preconditioning control and/or insult control) respectively. Significant differences are indicated (* = $p<0.05$, ** = $p<0.01$, *** = $p<0.001$, **** = $p<0.0001$)

indicate, again regardless of both the number of IPC or CIP cycles given and the MTS assay timepoint, there was no significant difference in the absorbance values, and therefore the number of viable cells, between the CIP CTL and IPC CTL groups. This suggests that 400µM $CoCl_2$ was not having a prolonged deleterious effect on cell viability as was observed when 600µM was used (Fig. 5.5). Therefore, it was predicted that using a concentration of $CoCl_2$ in between these, 500µM, would be the most likely way to invoke IPC.

5.4.4 Repeated Treatment with 500µM $CoCl_2$, for 3 Hours per Cycle, did not Induce IPC

To determine whether it was simply necessary to use a stronger stimulus than 400µM $CoCl_2$ to induce IPC, the multi-cycle protocol was repeated using 500µM $CoCl_2$ with the same 4 experimental groups and numbers of cycles tested. As 900µM $CoCl_2$ had proven to be an insufficient ischaemic insult, only 1000µM $CoCl_2$ in ischaemic buffer was utilised as the ischaemic insult to assess the efficacy of the 500µM $CoCl_2$ IPC treatments. Bonferroni's repeated measures multiple comparisons 2-way ANOVA was used to analyse the resulting MTS assay data (Fig. 5.9).

Regardless of both the number of IPC cycles given and the MTS assay timepoint, the absorbance values, and therefore the number of viable cells, were significantly reduced in the IPC ISC groups when compared to the CIP CTL group. The significant decreases were similarly observed in the CIP ISC groups except for absorbance values obtained at the 0-hour MTS assay timepoint for cells exposed to 1 cycle of CIP treatment (Table 5.4). This consistent reduction, particularly within the CIP ISC group at the 18-hour MTS assay timepoint, suggests that an ischaemic insult of 1000µM $CoCl_2$ reliably reduces the number of viable cells as desired.

Additionally, at the 0-hour MTS assay timepoint, the absorbance values, and therefore number of viable cells, was significantly decreased in the 3-cycle IPC CTL group (mean=0.7793) in comparison to the respective CIP CTL group (mean=1.214, p=0.0007). This, as discussed in section 5.4.2, could indicate that the selected IPC stimulus was too harsh although this significant decrease was

not observed when 1, 2 or 4 cycles of IPC were given using 500µM $CoCl_2$ in ischaemic buffer.

Regardless of both the number of IPC or CIP cycles given and the MTS assay timepoint, there was no significant difference in the absorbance values, and therefore the number of viable cells, between the CIP ISC and IPC ISC groups. This therefore implies protection against a severe insult was not conferred when using 500µM $CoCl_2$ as an IPC stimulus.

Cycles	MTS Timepoint	CIP CTL Mean	CIP ISC		IPC ISC	
			Mean	p Value	Mean	p Value
1	0	1.206	0.9267	NSD	0.8001	0.0177
	18	1.507	0.7701	0.0005	0.7553	0.0004
2	0	1.022	0.3663	0.0002	0.4169	0.0003
	18	1.121	0.3470	<0.0001	0.3222	<0.0001
3	0	1.214	0.6081	<0.0001	0.4252	<0.0001
	18	1.165	0.3251	<0.0001	0.2836	<0.0001
4	0	1.079	0.5940	0.0002	0.5357	<0.0001
	18	1.296	0.7167	<0.0001	0.7520	<0.0001

Table 5.4 Summary of significances between the CIP CTL and ischaemic insult groups displayed in Fig. 5.9. Numerical summary of the mean raw absorbance values and statistical analyses for a selection of the data exhibited in Fig. 5.9, where cycles 1-4 indicate the number of CIP or IPC cycles given as described in Fig. 5.6. p values between the CIP CTL means and both the CIP ISC and IPC ISC means at corresponding MTS assay timepoints were determined using Bonferroni's 2-way ANOVA. NSD indicates no significant difference for a particular comparison.

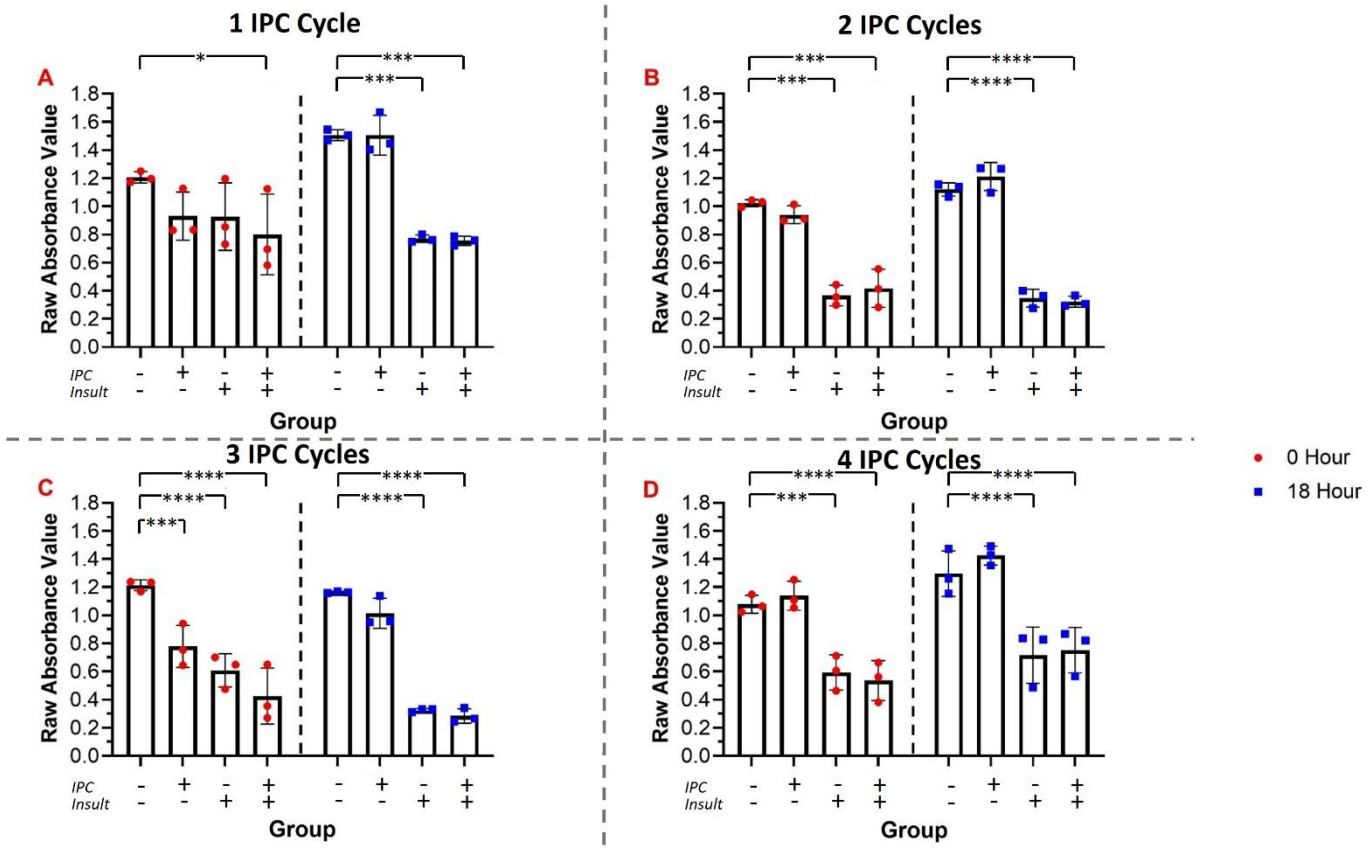

Fig. 5.9 MTS assay results obtained from attempting to induce IPC with 1-4 cycles of 500µM $CoCl_2$ where 1000µM $CoCl_2$ was used as an ischaemic insult. HUVECs were exposed to 1 (A), 2 (B), 3 (C) or 4 (D) 3-hour cycles of control buffer or 500µM $CoCl_2$ in ischaemic buffer IPC treatment. for 3 hours. Following completion of the appropriate number of cycles, there was a 24-hour recovery in EGM and either a 1000µM $CoCl_2$ ischaemic insult or control buffer treatment were given for 3 hours. MTS assays were conducted 0- and 18-hours following the insult period. Mean, individual data points and SD for raw absorbance values are shown. + and – indicates whether a group received an interventional treatment (IPC and/or ischaemic insult) or the relevant control (preconditioning control and/or insult control) respectively. Significant differences are indicated (* = $p<0.05$, *** = $p<0.001$, **** = $p<0.0001$)

5.4.5 Limitations of Using $CoCl_2$ to Induce IPC

Two ways of interpreting the statistics from the MTS absorbance assays were identified to confirm whether IPC was successfully induced. Firstly, the absorbance values from the MTS assay, and therefore the number of viable cells, would be significantly lower at the 18-hour timepoint in the CIP ISC group, compared to the CIP CTL group, but not in the IPC ISC group. Alternatively, at the 18-hour timepoint, the IPC ISC group would have significantly elevated MTS absorbance values, and therefore number of viable cells, in comparison to the CIP ISC group. Based upon these criteria for validation, it was deduced, using the MTS absorbance data (Fig. 5.5 and 5.7-5.9), that the attempts to invoke IPC using 1 3-hour cycle of 600µM $CoCl_2$ in ischaemic buffer, or 1-4 3-hour cycles of both 400µM and 500µM $CoCl_2$ in ischaemic buffer, were unsuccessful.

As previously indicated, there was no evidence in the literature that $CoCl_2$ can be used alongside an ischaemic buffer to induce IPC *in vitro*. It was uncertain as to whether this was because no one had employed this approach, or other research groups have found this technique to be unsuccessful causing the data to remain unpublished.

There was clearly a level of sustained cellular damage being induced by the 1000µM $CoCl_2$ ischaemic insults. However, this may be due to the toxic nature of $CoCl_2$ which at higher doses may become destructive to the cells regardless of whether there was any interaction with the HIF1α pathway. The cellular uptake mechanisms of the Co^{2+} ions may explain why 3 hours was not sufficiently long enough to allow enough to enter the cells and exert their effects on the HIF1α pathway. As an ion, Co^{2+} cannot simply diffuse across the membrane alone using the concentration gradient. Instead, it will require, as a minimum, a transporter or channel to facilitate its diffusion. Prior studies have indicated that the Co^{2+} competes with Ca^{2+} ions and is brought into the cell via a Ca^{2+} transporter. Ca^{2+} signalling is exceptionally important for maintaining cellular function. Therefore, it is believed that the competition brought on by the presence of the Co^{2+} ions is partly why the drug is so cytotoxic as Ca^{2+} becomes inhibited from entering cells and binding to intracellular proteins when required. Simonsen *et al*. (2011) concluded that that Ca^{2+} and Co^{2+} may share transport carriers to travel into the RBCs although not necessarily with the same affinity. This study, by Simonsen

et al. (2011), used human RBCs, but it could be hypothesised that this is how Co^{2+} would also enter other cell types, including endothelial cells. Whilst Ca^{2+} ions can be removed from the cells again via the Ca^{2+} pump, the Co^{2+} ions are unable to do this thereby causing its accumulation within the cytosol (Simonsen *et al*., 2011). This, therefore, implies that there is a concentration threshold for Co^{2+} within the cell that must be reached to enable the chemical to affect the stability of the HIF1α protein. This threshold may not be achieved within 3 hours leading to the failure of validating an IPC model using this method.

5.5 Validating $CoCl_2$ Induced HPC

5.5.1 Dose-Response Curves Identified Treatment with 200-400μM $CoCl_2$ for 24 Hours Would Potentially Induce HPC

A dose-response curve was conducted to ascertain the optimal potential concentration of $CoCl_2$ in basal media to use to induce HPC (Fig. 5.10). HUVECs were treated with either basal media or one of the following concentrations of $CoCl_2$ in basal media for a period of 24 hours: 200μM, 400μM, 600μM, 800μM or 1000μM. MTS assays were conducted immediately (0 hour) and 24 hours after treatment. Dunnett's repeated measures multiple comparisons 2-way ANOVA was used to compare the absorbance values between the controls and hypoxia exposed cells at the same MTS assay timepoint (Fig. 5.11).

At the 0-hour MTS assay timepoint, there was a significant reduction in the

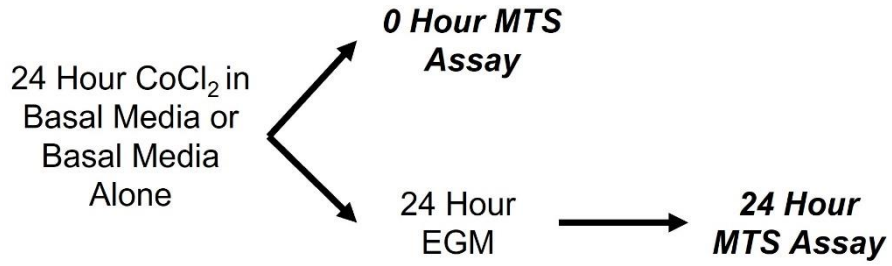

Fig. 5.10 Protocol timeline for $CoCl_2$ induced HPC dose-response curves. Timeline displaying the dose-response curve experiment used to determine the optimal dose for an HPC stimulus in HUVECs using $CoCl_2$ in basal media. MTS assays were conducted 0- and 24-hours following exposure to the 3-hour ischaemic or control stimulus. EGM indicates HUVECs were recovering in standard EGM.

absorbance values, and therefore number of viable cells, in 200μM (mean=0.6903, p=0.0002), 400μM (mean=0.7123, p=0.0003), 600μM (mean=,

p=0.0040), 800µM (mean=0.7062, p=0.0002) and 1000µM (mean=0.6979, p=0.0002) $CoCl_2$ treated cells compared to those kept in basal media (mean=0.9958).

At the 24-hour timepoint, the absorbance values, and therefore number of viable cells, in the basal media group (mean=1.197) were significantly higher than those in the 600µM (mean=1.062, p=0.0394), 800µM (mean=0.9883, p=0.0027) and 1000µM (mean=0.5662, p=<0.0001) $CoCl_2$ groups.

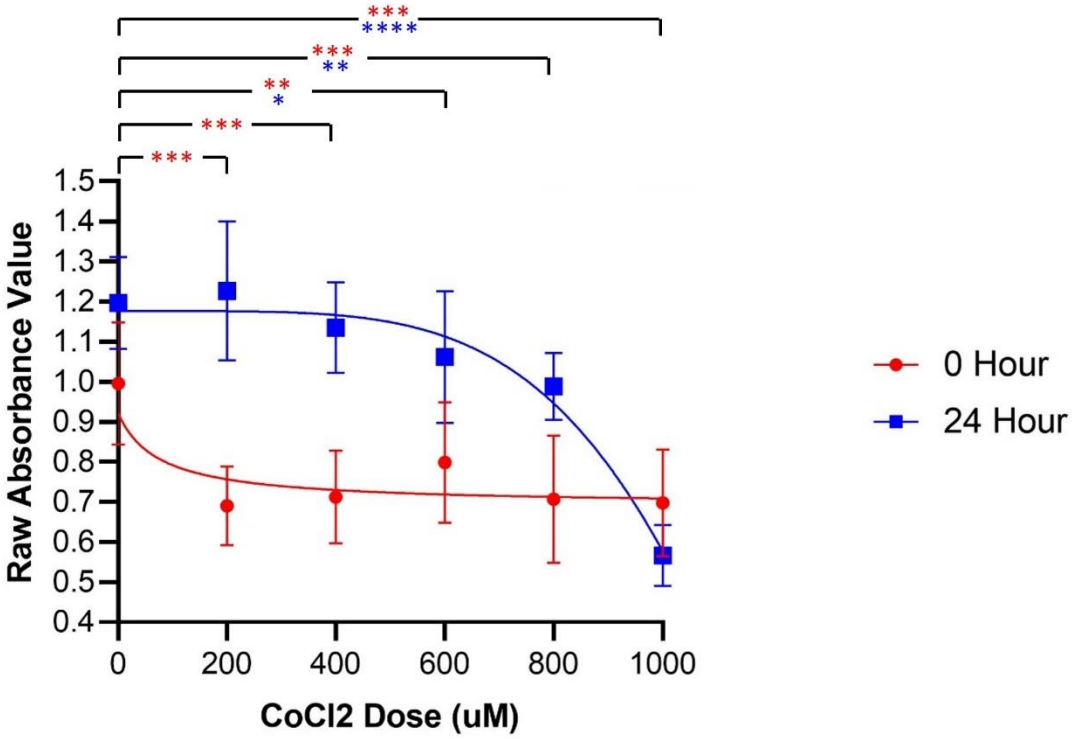

Fig. 5.11 $CoCl_2$ induced HPC dose-response curves. HUVECs were exposed to a basal medium or 5 different concentrations of $CoCl_2$ in basal media for 24 hours. MTS assays were conducted 0- and 24-hours following exposure to hypoxia. Mean raw absorbance values and SD are shown. Significances between $CoCl_2$ treated cells and those treated with a control buffer at the corresponding MTS assay timepoints are indicated (* = p<0.05, ** = p<0.01, *** = p<0.001, **** = p<0.0001).

This suggests that whilst all tested $CoCl_2$ concentrations caused an initial decrease in the number of viable cells, those exposed to 200µM and 400µM $CoCl_2$ were able to recover within 24 hours of the removal of the hypoxic stimulus. Using the same criteria when conducting the IPC $CoCl_2$ dose-response experiment, mentioned in section 5.4.1, it was determined that a $CoCl_2$ concentration between 200µM and 400µM would be suitable as a HPC stimulus.

As the stronger tested stimulus had been too harsh when attempting to validate $CoCl_2$ induced IPC in section 5.4.2 (Fig. 5.5), it was decided to begin the HPC validation process with the lower concentration of 200µM.

5.5.2 Treatment with 200µM $CoCl_2$ for 24 Hours Induced HPC and Protected Against a Severe Hypoxic Insult

To validate an *in vitro* HPC model using $CoCl_2$, HUVECs were allocated into 4 groups, represented by their abbreviations from this point onwards: i) HPC control plus insult control (CHP NMX), ii) HPC plus insult control (HPC NMX), iii) HPC control plus hypoxic insult (CHP HPX), iv) HPC plus hypoxic insult (HPC HPX). Cells underwent either 200µM $CoCl_2$ induced HPC or a basal media control treatment. After a 24-hour recovery period, cells were either exposed to a severe 600µM or 700µM $CoCl_2$ induced hypoxic insult or a basal media control (Fig. 5.12).

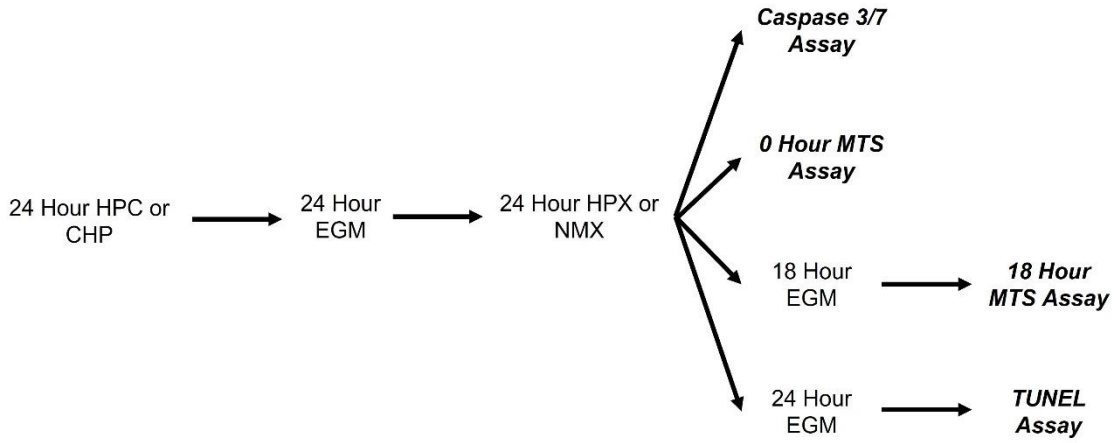

Fig. 5.12 Protocol timeline for 200µM CoCl2 induced HPC validation. HUVECs were allocated into 1 of 4 groups: i) HPC control plus insult control (CHP NMX), ii) HPC plus insult control (HPC NMX), iii) HPC control plus hypoxic insult (CHP HPX), iv) HPC plus hypoxic insult (HPC HPX). A caspase 3/7 activity assay was conducted immediately after completion of HPX and NMX treatment. MTS assays were conducted 0- and 18-hours following HPX and NMX treatment. HUVECs were fixed and a TUNEL apoptosis assay conducted 24 hours following HPX and NMX treatment. EGM indicates HUVECs were recovering in standard EGM.

An MTS assay was performed immediately (0 hour) and 18 hours after conclusion of the insult period. The resulting data was analysed using Bonferroni's repeated measures multiple comparisons 2-way ANOVA (Fig. 5.13). At the 0-hour MTS assay timepoint, the absorbance values, and therefore number of viable cells,

were significantly decreased in the CHP HPX (mean=0.7078, p=0.0115) and HPC HPX (mean=0.7579, p=0.0300) groups in comparison to the CHP NMX group (mean=0.9881) when 700µM $CoCl_2$ was utilised as the hypoxic insult.

Similarly, when 700µM $CoCl_2$ was used as the hypoxic insult, at the 18-hour MTS assay timepoint, the absorbance values, and therefore number of viable cells, was significantly decreased in the CHP HPX (mean=0.3512, p=0.0003) and HPC HPX (mean=0.5852, p=0.0066) groups in comparison to the CHP NMX group (mean=0.8975). The same trend at the 18-hour MTS assay timepoint was also observed regarding the CHP HPX (mean=0.3834, p=<0.0001), HPC HPX (mean=0.6249, p=0.0003) and CHP NMX (mean=1.590) groups when 600µM $CoCl_2$ was employed as a hypoxic insult. These data, particularly the decreased absorbance values, and therefore number of viable cells, at the 18-hour MTS assay timepoint obtained for the CHP HPX groups, indicate that the $CoCl_2$ concentrations of both 600µM and 700µM were sufficient to induce a hypoxic insult.

Also, at the 18-hour MTS assay timepoint, the absorbance values, and therefore number of viable cells, were significantly decreased in the CHP HPX group in comparison to the HPC HPX group (p=0.0278) when 700µM $CoCl_2$ was used as the hypoxic insult. Although non-significant, a similar difference was also seen between the absorbance values, and therefore number of viable cells, between the CHP HPX and HPC HPX groups. This difference suggests that by treating HUVECs, using 200µM $CoCl_2$, protection against a more severe hypoxic insult was conferred and that the HPC model could be deemed a success.

Further validation was performed by conducting a caspase 3/7 assay for 18 hours immediately following the hypoxic insult, or insult control, period using 200µM $CoCl_2$ as the HPC stimulus (Fig. 5.14). As the MTS assays had indicated that 600µM $CoCl_2$ had successfully induced a hypoxic insult (Fig. 5.13), this concentration was selected for the caspase 3/7 assay. Bonferroni's repeated measures multiple comparisons 2-way ANOVA was performed to analyse changes in the ratio of cells exhibiting caspase 3/7 activity for each hour of the assay. Whilst non-significant, the data presented demonstrates that there was an apparent increase in the proportion of caspase 3/7 positive cells in the CHP HPX

group compared to all other treatment groups at each timepoint of the assay. The large standard deviations in the CHP HPX group at hours 0-16 were likely responsible for the lack of significance. as at both the 17 and 18 hour timepoints, when the standard deviations decrease, the ratio of caspase 3/7 positive cells:total cells becomes statically significantly greater in the CHP HPX group (17 hours: mean=0.2378, p=0.0454; 18 hours: mean=0.2385, p=0.0368) compared to the CHP NMX group (17 hours: mean=0.0066; 18 hours: mean=0.0091). The elevation in the proportion of caspase 3/7 positive cells indicates increased apoptosis in the CHP HPX group. This data not only signifies that the 600µM $CoCl_2$ hypoxic insult was administered successfully, but that a degree of protection was conferred to the preconditioned cells against the hypoxic insult.

To conclude validation of the HPC model using 200µM $CoCl_2$, cells were fixed and stained using the TUNEL apoptosis assay 24 hours after the insult, or insult control, period (Fig. 5.15). For this assay, only the 600µM $CoCl_2$ insult was used, and not the 700µM, following confirmation from the prior MTS and caspase 3/7 assays that this was sufficient to induce a hypoxic insult (Fig. 5.13 and 5.14). Tukey's repeated measures multiple comparisons one way ANOVA was utilised to analyse changes in the percentage of TUNEL positive cells between treatment groups. Whilst non-significant, there was an apparent increase in the percentage of TUNEL positive cells, and therefore the proportion of cells undergoing apoptosis, in the CHP HPX group (mean ± SD=48.28% ± 12.76) compared to the CHP NMX (mean ± SD=4.27% ± 2.07), HPC NMX (mean ± SD=2.43% ± 2.44) and HPC HPX (mean ± SD=16.94% ± 5.98) groups. Additionally, as can be observed in the images obtained from the fluorescent microscope (Fig. 5.15), there was an apparent decrease in the number of intact nuclei in the CHP HPX group, in comparison to all other groups. This apparent elevation in the number of TUNEL positive cells, and apparent decrease in DAPI staining, suggests that the 600µM $CoCl_2$ hypoxic insult was administered successfully, and that a degree of protection was conferred to the preconditioned cells against the hypoxic insult.

In summary, the number of viable cells appeared elevated, and the number of caspase 3/7 and TUNEL positive cells appeared decreased in the HPC HPX group compared to the CHP HPX group. This suggests that a degree of protection

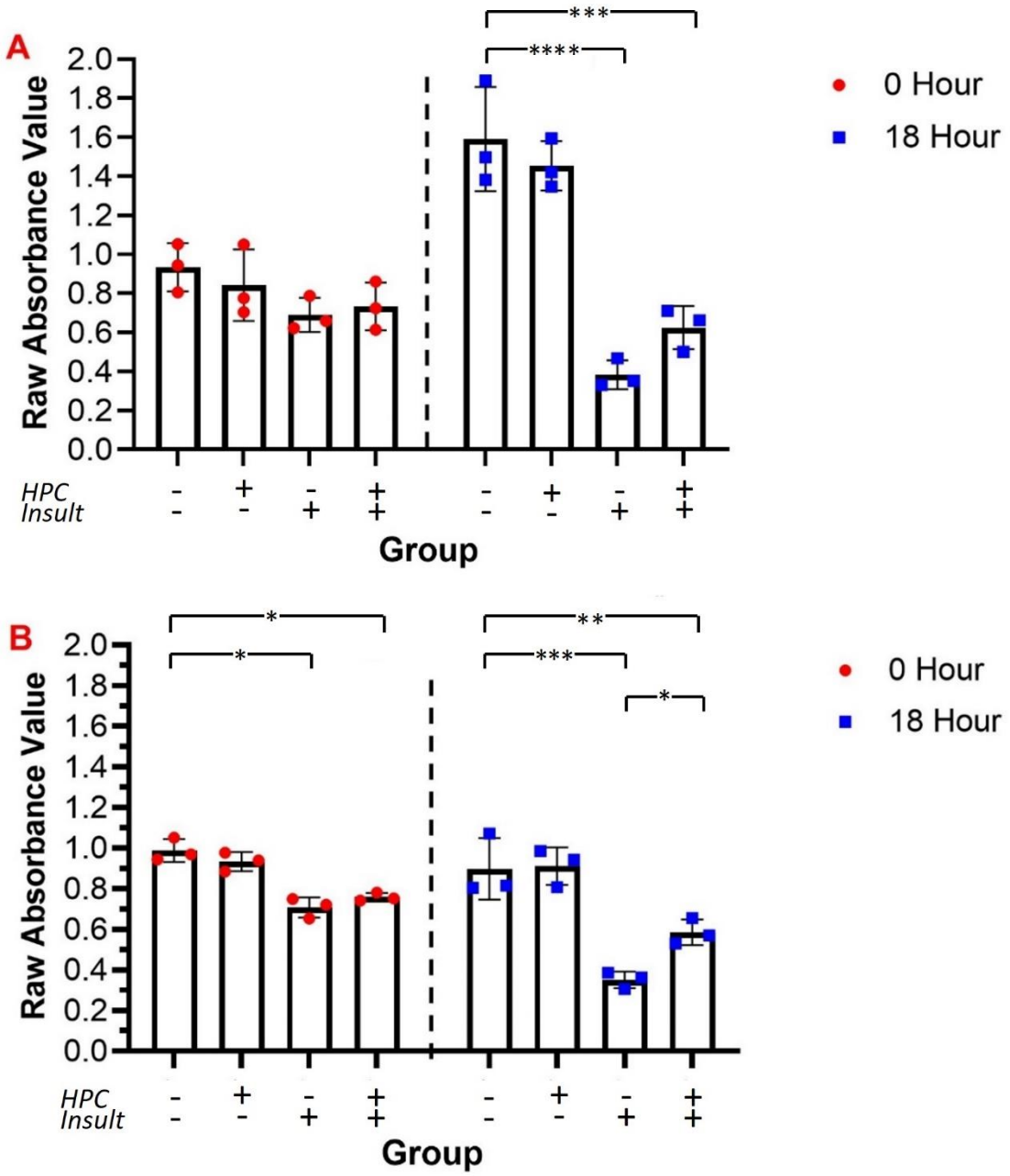

Fig. 5.13 200µM CoCl2 induced HPC MTS assay. HUVECs were exposed to basal media or underwent HPC with 200µM $CoCl_2$ in basal media for 24 hours. After a 24-hour recovery in EGM, either a 600µM (A) or 700µM (B) $CoCl_2$ hypoxic insult or basal media treatment were given for 24 hours. MTS assays were conducted 0- and 18-hours following the insult period. Mean, individual data points and SD for raw absorbance values are shown. + and – indicates whether a group received an interventional treatment (HPC and/or hypoxic insult) or the relevant control (preconditioning control and/or insult control) respectively. Significant differences are indicated (* = p<0.05, ** = p<0.01, *** = p<0.001, ****=p<0.0001).

against a severe $CoCl_2$ induced hypoxic insult has been conferred to the preconditioned HUVECs. It is important to note that, in the absence of statistical significance, to be certain of these conclusions, sample sizes would require

increasing. However, it was concluded that treatment of 200µM $CoCl_2$ in basal media induces HPC confirming the validity of this model.

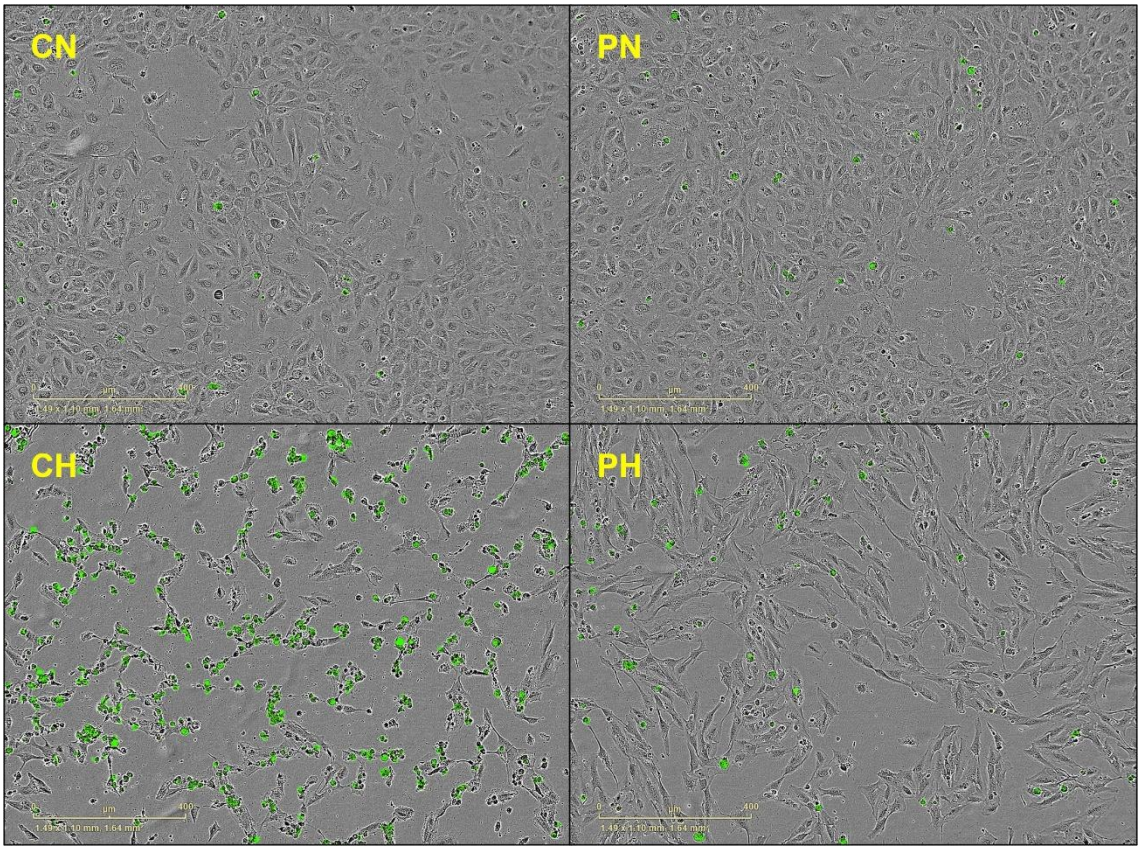

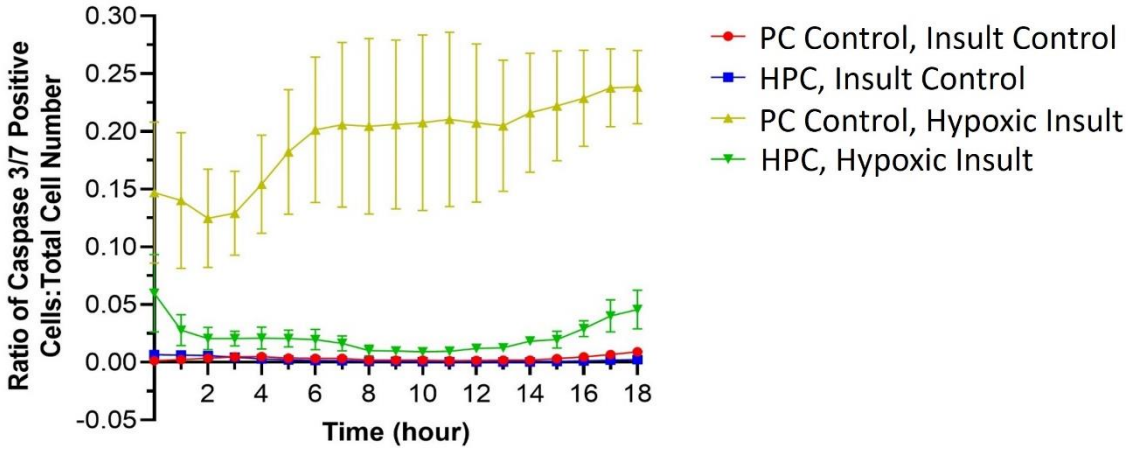

Fig. 5.14 Caspase 3/7 assay for HPC validation. HUVECs underwent a preconditioning-insult protocol in which cells were preconditioned with 200µM (P), treated with basal media (C), received a 600µM hypoxic insult (H), or an insult control (N) as described in the protocol in figure 5.12. Cells underwent the caspase 3/7 assay for 18 hours immediately following completion of the insult period. Caspase 3/7 positive cells are indicated by the green staining on the cell images obtained from the IncuCyte®. Mean data points, calculated from 3 biological samples, of the ratio of caspase 3/7 positive cells:total cells and SD are shown.

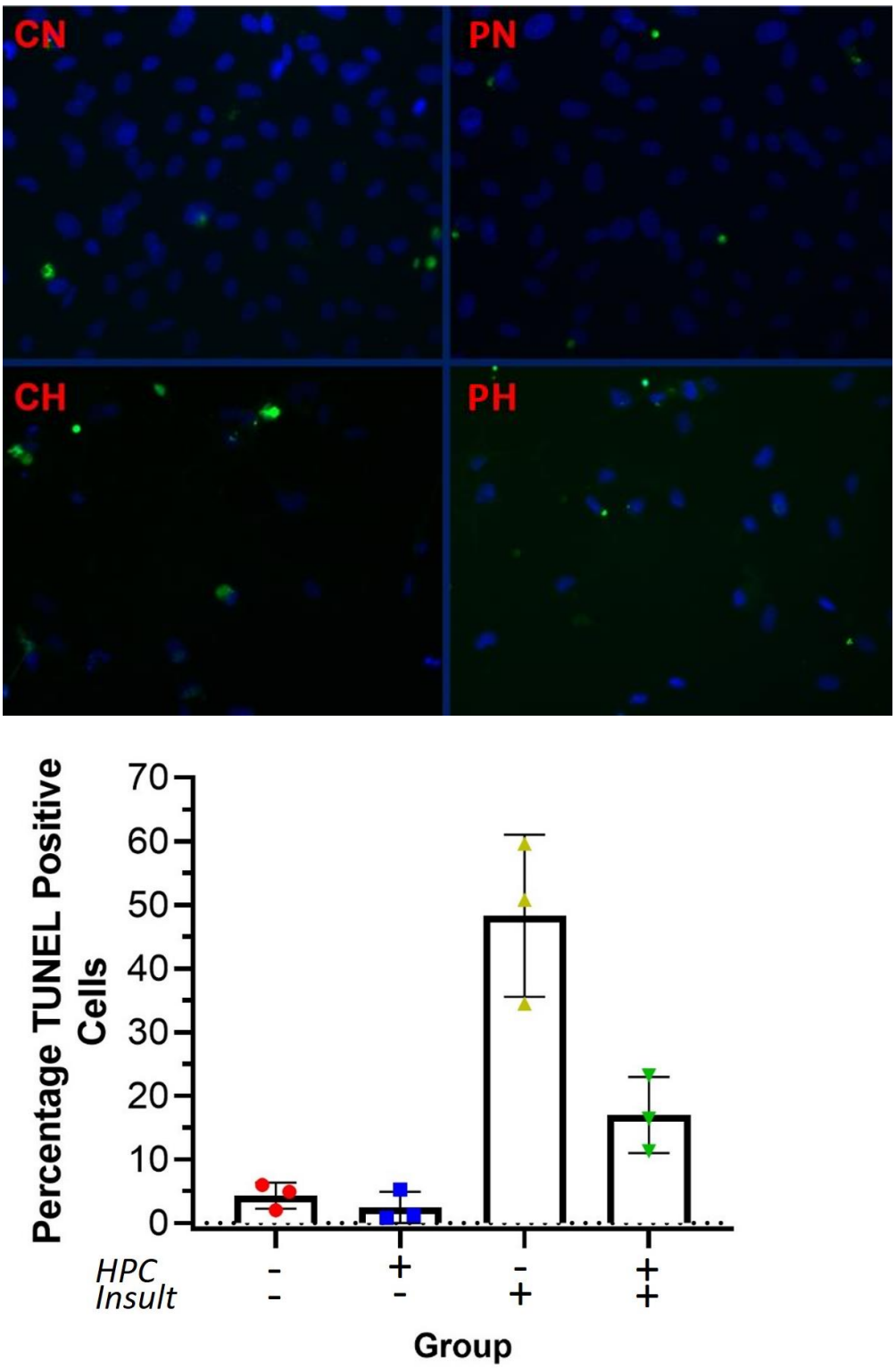

Fig. 5.15 TUNEL apoptosis assay for HPC validation. HUVECs underwent a preconditioning-insult protocol in which cells were preconditioned with 200µM (P), treated with basal media (C), received a 600µM hypoxic insult (H), or an insult control (N) as described in the protocol in figure 5.12. + and – indicates whether a group received an interventional treatment (HPC and/or hypoxic insult) or the relevant control (preconditioning control and/or insult control) respectively. Cells underwent the TUNEL apoptosis assay 24 hours after completion of the insult period and imaged. Nuclei were stained with DAPI (blue) and the cells with TUNEL (green).

5.5.3 $CoCl_2$ Mimicked Hypoxia by Stabilising HIF1α

To test whether $CoCl_2$ induces stabilisation of HIF1α, HUVECs were allocated into 4 groups: i) HPC control only, ii) HPC only, iii) HPC control plus hypoxic insult, iv) HPC control plus normoxia. Cells in groups i) and ii) were treated with basal media or 200µM $CoCl_2$ for 24 hours. They were then immediately lysed using the specialised protocol, as described in section 2.10.1.2, which was recommended due to the difficulties other research labs within the University of Dundee experienced when attempting to detect HIF1α expression. Cells in groups iii) and iv) were treated with basal media for 24 hours, allowed to recover in EGM for an additional 24 hours, then treated with 600µM or basal media for another 24 hours. Cells were again lysed using the specialised protocol. A Bradford protein concentration assay was conducted on the lysates and HIF1α, and α-tubulin, quantified using western blot. There was no detectable protein band for HIF1α in the CHP and NMX groups. Whilst very faint, there were slight bands visible for the protein in the 200µM $CoCl_2$ HPC treated cells. This band was found to be much stronger in the HPX group of cells exposed to 600µM $CoCl_2$ (Fig. 5.16). There was also an increase in expression with the higher concentration of $CoCl_2$ in comparison with the lower.

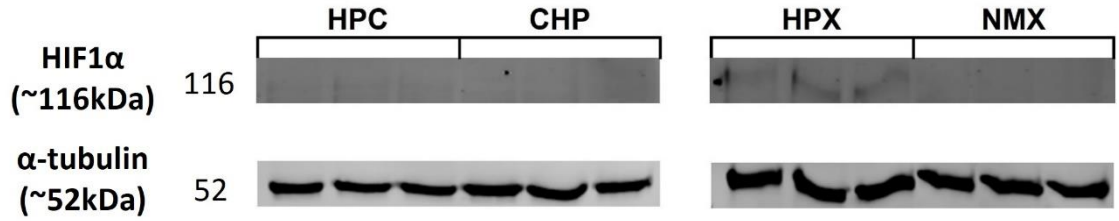

Fig. 5.16 HIF1α expression in $CoCl_2$ treated HUVECs. HUVECs were exposed to either basal media (CHP) or 200µM $CoCl_2$, in basal media (HPC), for 24 hours. After 24 hours of recovery in EGM, half of the CHP cells were given either a 600µM $CoCl_2$ hypoxic insult (HPX) or control insult (NMX). Cells were lysed and HIF1α and α-tubulin expression were determined using western blot. Nitrocellulose membranes show the absence of a HIF1α band in the CHP and NMX groups, faint bands in the HPC group, and stronger bands in the HPX group. Band sizes of the proteins of interest are indicated on respective blots.

5.6 Effects of Acute Hypoglycaemia and Hyperglycaemia on HPC

As discussed in section 1.6, an aim was devised to investigate whether hypoglycaemia and hyperglycaemia have an effect on HPC and IPC. Following establishment of the *in vitro* HPC model, a series of experiments was designed to investigate whether a single 3 hour hypoglycaemic or hyperglycaemic episode

disrupt HPC in HUVECs. As controls, cells were exposed to 3-hour episodes of euglycaemia in saline solution at matching timepoints. The 200µM $CoCl_2$ HPC with 600µM $CoCl_2$ hypoxic insult protocol was conducted, as validated in section 5.5.2, with an episode of hypoglycaemia, euglycaemia or hyperglycaemia being induced at 1 of 6 timepoints through this procedure, leading to 18 experimental groups per treatment type (Fig. 5.17). When referring to this series of experiments, the term experimental group refers to the timepoint at which hypoglycaemia, euglycaemia and hyperglycaemia were introduced whilst treatment group indicates which combination of preconditioning and insult treatments HUVECs received. As the appropriate $CoCl_2$ dose for the HPC stimulus and hypoxic insult were previously validated (Fig. 5.13-5.15), it was decided that MTS assays were only to be conducted 18 hours after completion of the hypoxic insult. To induce hypoglycaemia, euglycaemia and hyperglycaemia, 0mM, 5.5mM and 30mM glucose saline solutions were used respectively. MTS assay data from each of the experimental groups was analysed by comparing the absorbance values between each of the 4 treatment groups using Tukey's repeated measures multiple comparisons 1-way ANOVA. All key statistical significances regarding the effects of hypoglycaemia and hyperglycaemia on the efficacy of HPC are indicated in the results described below in section 5.6.2 and 5.6.3.

The data regarding the euglycaemic controls are not presented in depth here but graphs are displayed in the appendix indicating points of statistical significance (Fig. 8.4). Additionally, within the discussion in section 5.8, when intervention with hyperglycaemia or hypoglycaemia has been initially indicated as interfering with the HPC or hypoxic insult, the relevant euglycaemic control data was used to confirm whether the protocol or the glycaemic event was the probable cause for this observed result.

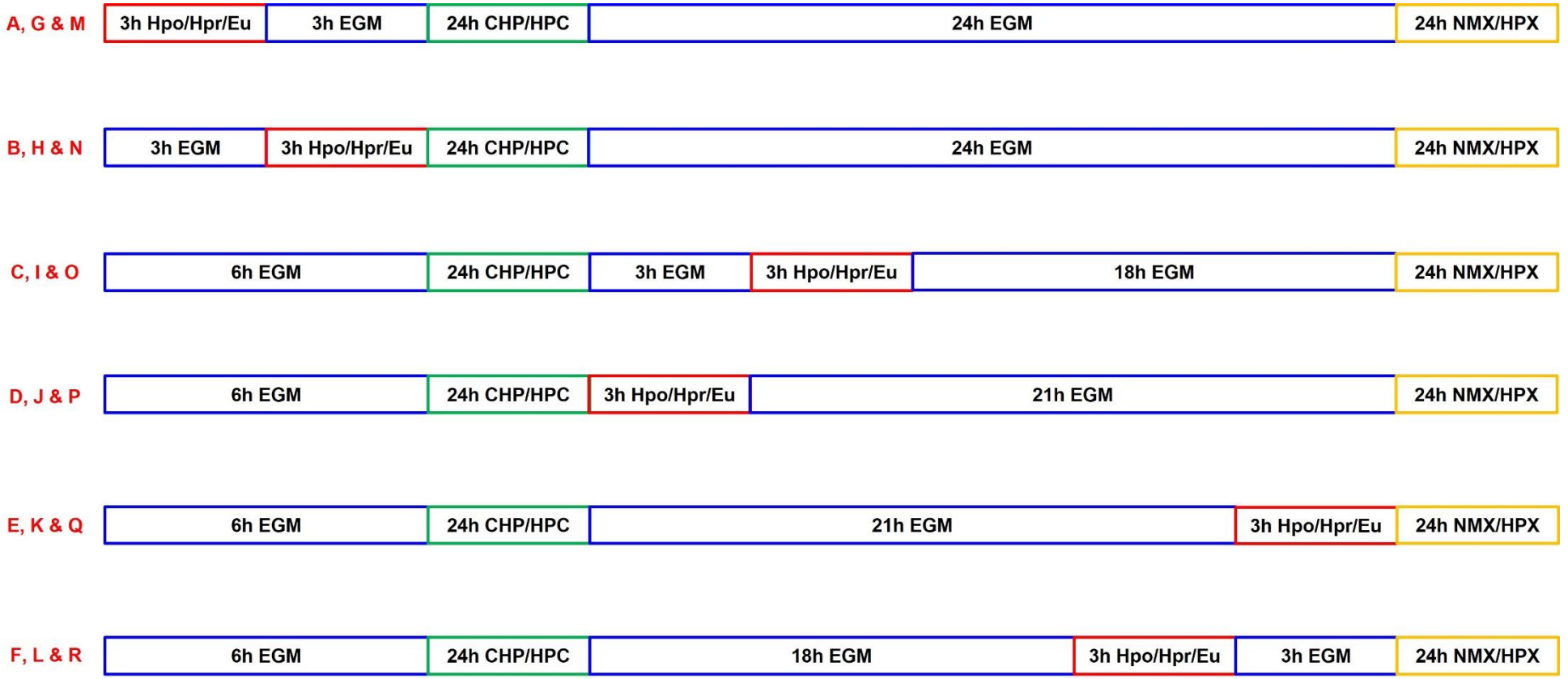

Fig. 5.17 Protocol timeline investigating the effect of acute hypoglycaemia and hyperglycaemia on $CoCl_2$ induced HPC. HUVECs were allocated into 1 of 4 groups: i) HPC control plus insult control (CHP NMX), ii) HPC plus insult control (HPC NMX), iii) HPC control plus hypoxia insult (CHP HPX), iv) HPC plus hypoxic insult (HPC HPX). These groups were subdivided further depending on when they received acute hypoglycaemia (Hpo) (A-F) or hyperglycaemia (Hpr) (G-L) or euglycaemia (Eu) (M-R) within the preconditioning-insult protocol. An MTS assay was conducted 18-hours following HPX and NMX treatment. EGM indicates HUVECs were recovering in standard EGM. For the purposes of the HPC and hypoxic insult, $CoCl_2$ concentrations of 200μM and 600μM were used respectively. The hypoglycaemic, euglycaemic and hyperglycaemic events were conducted at 0mM, 5.5mM and 30mM glucose respectively.

5.6.1 Treating HUVECS for 3 Hours with a 0mM Glucose Saline Solution Induced a Hypoglycaemic State

To confirm the induction of a hypoglycaemic state after 3 hours, HUVECs were treated with either a 0mmol/L, low glucose, or 5.5mmol/L, normal glucose, saline solution for this time, and phospho-AMPK (p-AMPK) expression determined.

Adenosine monophosphate activated kinase (AMPK) phosphorylation can be used as a marker for adenosine diphosphate (ADP)/ATP and adenosine monophosphate (AMP)/ATP ratios. AMPK is a protein made up of 3 subunits, namely α, β and γ. ATP, ADP and AMP all compete to bind to the γ subunit, but it is only when ATP is bound that the threonine 172 residue on the α subunit, which becomes phosphorylated by kinases, can be dephosphorylated, whilst both ADP and AMP block access to the site for phosphatases. Therefore, when glucose levels are higher, enabling an increased production in ATP, there is reduced p-AMPK expression (Jeon, 2016). Under hypoglycaemic conditions, however, causing depletion of ATP, both AMP and ADP will be more likely to block the residue meaning it remains phosphorylated hence increasing p-AMPK expression.

Following completion of the hypoglycaemic and normoglycaemic episodes, cells were immediately lysed, and a Bradford protein concentration conducted on the lysates. Using a western blot, β-actin, AMPK, and p-AMPK expression were determined and the values of AMPK and p-AMPK normalised to those for β-actin on their respective membranes. To calculate the ratio of AMPK which had been phosphorylated, the normalised p-AMPK value was divided by that of AMPK. Fold change in the proportion of AMPK in its phosphorylated form was calculated between the 5.5mmol/L and 0mmol/L glucose treatments (Fig. 5.18).

A paired t test confirmed that there was a significant 3.345-fold increase ($p=0.0197$) in expression of p-AMPK in the 0mM glucose (mean=0.5234) treated cells compared to those exposed to 5.5mM glucose (mean=0.1565) indicating this period of hypoglycaemia was sufficient.

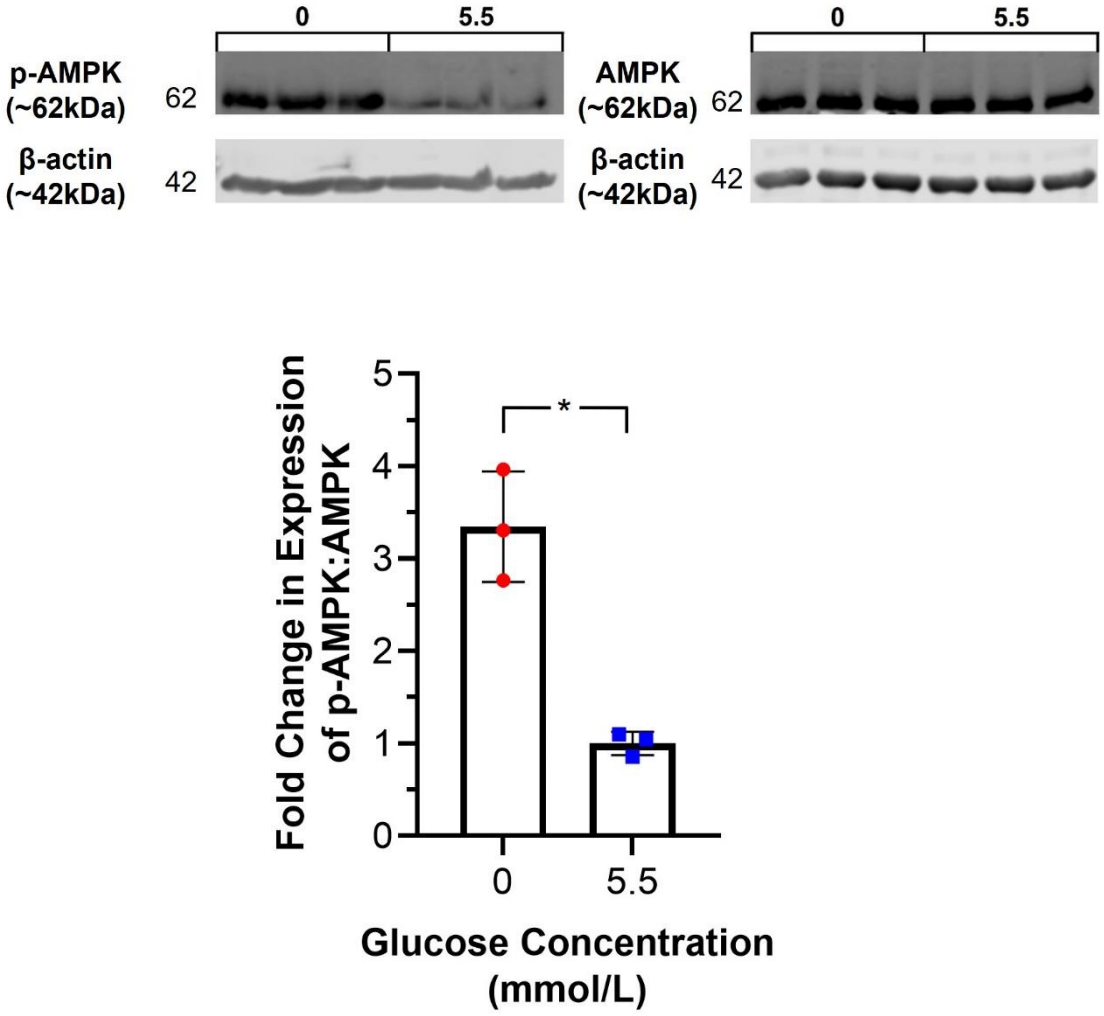

Fig. 5.18 p-AMPK expression in hypoglycaemic HUVECs. HUVECs were treated for 3 hours with either no glucose or a 5.5mmol/L glucose saline solution. Cells were lysed and p-AMPK, AMPK and β-actin expression were determined using western blot with the nitrocellulose membranes presented here. p-AMPK and AMPK expression was normalised to their respective β-actins. The ratio of AMPK which had been phosphorylated was determined by dividing the normalised p-AMPK value by that of AMPK. Fold change in the expression of p-AMPK between the 5.5mmol/L and 0mmol/L treated cells was calculated and plotted. Band sizes of the proteins of interest are indicated on respective blots. Mean, individual data points and SD for fold change in p-AMPK:AMPK expression are shown. Significance in fold change in expression is indicated (* = $p<0.05$).

5.6.2 Acute Hypoglycaemia Appeared to Render HPC Ineffective when Given Immediately After HPC Treatment

All MTS assay data referred to here was obtained from experimental groups A-F in which acute hypoglycaemia was used as a potential disruptive stimulus (Fig. 5.19) as described (Fig. 5.17).

In experimental group A, when hypoglycaemia was given in the 3-6 hours preceding HPC or CHP treatment, there was no significant difference in the absorbance values, and therefore number of viable cells, between the CHP NMX and CHP HPX groups. However, absorbance values, and therefore number of viable cells, in the HPC HPX group were significantly higher (mean=1.099) than those in both the CHP NMX (mean=0.9872, p=0.0006) and CHP HPX (mean=0.9857, p=0.0075) groups.

In experimental group B, when hypoglycaemia was given immediately preceding HPC or CHP treatment, the absorbance values, and therefore number of viable cells, were significantly decreased in both the CHP HPX (mean=0.2022, p=0.0027) and HPC HPX groups (mean=0.4701, p=0.0062) compared to the CHP NMX group (mean=0.8144). Compared to the CHP NMX group the absorbance values, and therefore number of viable cells, in the HPC NMX group (mean=0.9319, p=0.0493) were significantly elevated. Finally, the values, and therefore the number of viable cells, in the HPC HPX group were significantly elevated (p=0.0395) in comparison to the CHP HPX group.

In experimental group C, when hypoglycaemia was given 3-6 hours following HPC or CHP treatment, absorbance values, and therefore the number of viable cells, were significantly decreased in both the CHP HPX (mean=0.2579, p=0.0251) and HPC HPX groups (mean=0.5432, p=0.0473) in comparison to the CHP NMX group (mean=0.7138). treated cells. Whilst non-significant, the absorbance values, and therefore number of viable cells, appeared to be higher in the HPC HPX group compared to the CHP HPX group.

In experimental group D, when hypoglycaemia was given immediately after HPC or CHP treatment, no significant differences were found between treatment groups. However, by observing the trends within this data, it was possible to see there was an apparent decrease in the absorbance values, and therefore the number of viable cells, in the CHP HPX and HPC HPX groups in comparison to the CHP NMX group. It appears that this apparent decrease was slightly larger in the HPC HPX group, when compared to the CHP HPX group.

In experimental group E, when hypoglycaemia was given 21-24 hours following

HPC or CHP treatment, the absorbance values, and therefore number of viable cells, were significantly decreased in both the CHP HPX (mean=0.4471, p=0.0342) and HPC HPX groups (mean=0.7521, p=0.0220) compared to the CHP NMX group (mean=0.8609). Compared to the CHP NMX group the absorbance values, and therefore number of viable cells, in the HPC NMX group (mean=1.128, p=0.0436) were significantly elevated. Finally, the values, and therefore the number of viable cells, in the HPC HPX group were significantly elevated (p=0.0490) in comparison to the CHP HPX group.

In experimental group F, when hypoglycaemia was given 18-21 hours following HPC or CHP treatment, there were no significant differences between any of the treatment groups. However, by observing the trends within this data, it was possible to see there was an apparent decrease in the absorbance values, and therefore the number of viable cells, in the CHP HPX and HPC HPX groups in comparison to the CHP NMX group. This apparent decrease was slightly reduced in the HPC HPX group, when compared to the CHP HPX group, although this difference seems negligible.

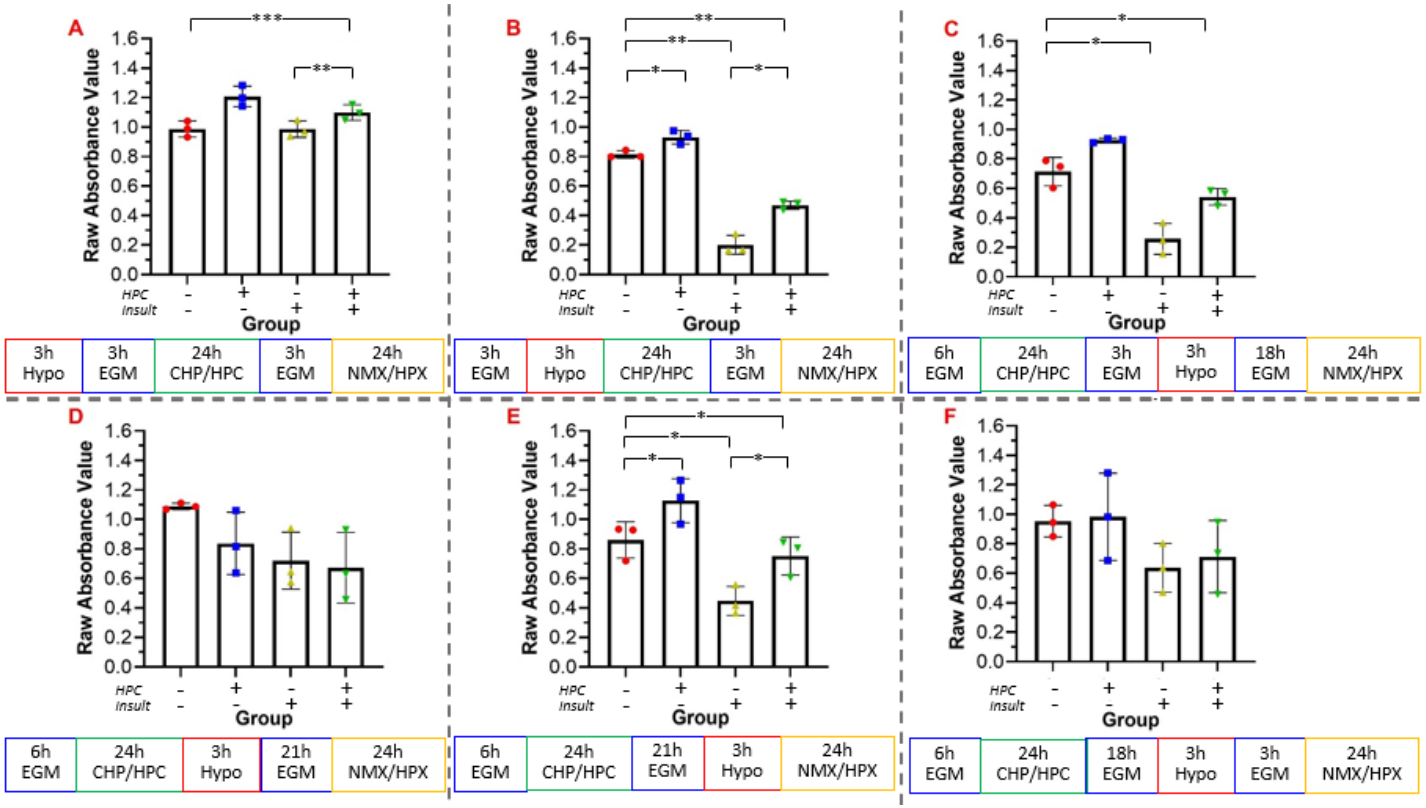

Fig. 5.19 Effect of acute hypoglycaemia on $CoCl_2$ induced HPC. HUVECs were exposed to basal media (CHP) or underwent HPC with 200µM $CoCl_2$ in basal media (HPC) for 24 hours. After a 24-hour recovery in EGM, a 600µM $CoCl_2$ hypoxic insult (HPX) or basal media treatment (NMX) were given for 24 hours. MTS assays were conducted 18-hours following the insult period. Cells were allocated into experimental groups to receiving a 3-hour hypoglycaemic episode at 1 of 6 timepoints, where A-F correspond to the experimental groups indicated in Fig. 5.17. Protocol timelines for each experimental group are located beneath their respective graphs. + and – indicates whether a group received an interventional treatment (HPC and/or hypoxic insult) or the relevant control (preconditioning control and/or insult control) respectively. Mean, individual data points and SD for raw absorbance values are shown. Significant differences are indicated (* = $p<0.05$, ** = $p<0.01$, *** = $p<0.001$).

5.6.3 Acute Hyperglycaemia Appeared to Render HPC Ineffective when Given Immediately After HPC Treatment

All MTS assay data referred to here was obtained from experimental groups G-J in which acute hyperglycaemia was used as a potential disruptive stimulus (Fig. 5.20) as described (Fig. 5.17).

In experimental group G, when hyperglycaemia was given in the 3-6 hours preceding HPC or CHP treatment, there was no significant difference in the absorbance values, and therefore number of viable cells, between the CHP NMX and CHP HPX groups. However, there was an apparent decrease in the absorbance values, and therefore the number of viable cells, in the CHP HPX group, but not in the HPC HPX group, when compared to the CHP NMX group.

In experimental group H, when hyperglycaemia was given immediately preceding HPC or CHP treatment, the absorbance values, and therefore the number of viable cells, were significantly decreased in the CHP HPX (mean=0.1781, p=0.0064) and HPC HPX (mean=0.4446, p=0.0234) groups in comparison to the CHP NMX group (mean=0.8458). Although non-significant, the absorbance values, and therefore number of viable cells, appeared elevated in the HPC HPX group in comparison to the CHP HPX group.

In experimental group I, when hyperglycaemia was given 3-6 hours following HPC or CHP treatment, the absorbance values, and therefore the number of viable cells, were significantly decreased in the CHP HPX (mean=0.2887, p=0.0094) and HPC HPX (mean=0.5632, p=0.0475) groups in comparison to the CHP NMX group (mean=0.9363). Also, absorbance values, and therefore the number of viable cells, obtained from the CHP HPX group were also significantly lower (p=0.0061) than those in the HPC HPX treated cells.

In experimental group J, when hyperglycaemia was given immediately after HPC or CHP treatment, no significant differences were found between treatment groups. However, by observing the trends within this data, it was possible to see there was an apparent decrease in the absorbance values, and therefore the number of viable cells, in the CHP HPX and HPC HPX groups in comparison to

the CHP NMX group. This apparent decrease was slightly larger in the HPC HPX group, when compared to the CHP HPX group.

In experimental group K, when hyperglycaemia was given 21-24 hours following HPC or CHP treatment, absorbance values, and therefore the number of viable cells, were significantly decreased in both the CHP HPX (mean=0.3003, p=0.0254) and HPC HPX (mean=0.5836, p=<0.0001) groups in comparison to the CHP NMX group (mean=0.9333). Although non-significant, the absorbance values, and therefore number of viable cells, appeared elevated in the HPC HPX group in comparison to the CHP HPX group.

In experimental group L, when hyperglycaemia was given 18-21 hours following HPC or CHP treatment, there were no significant differences between any of the treatment groups. However, by observing the trends within this data, it was possible to see there was an apparent decrease in the absorbance values, and therefore the number of viable cells, in the CHP HPX and HPC HPX groups in comparison to the CHP NMX group. It appears that this apparent decrease was slightly reduced in the HPC HPX group, when compared to the CHP HPX group.

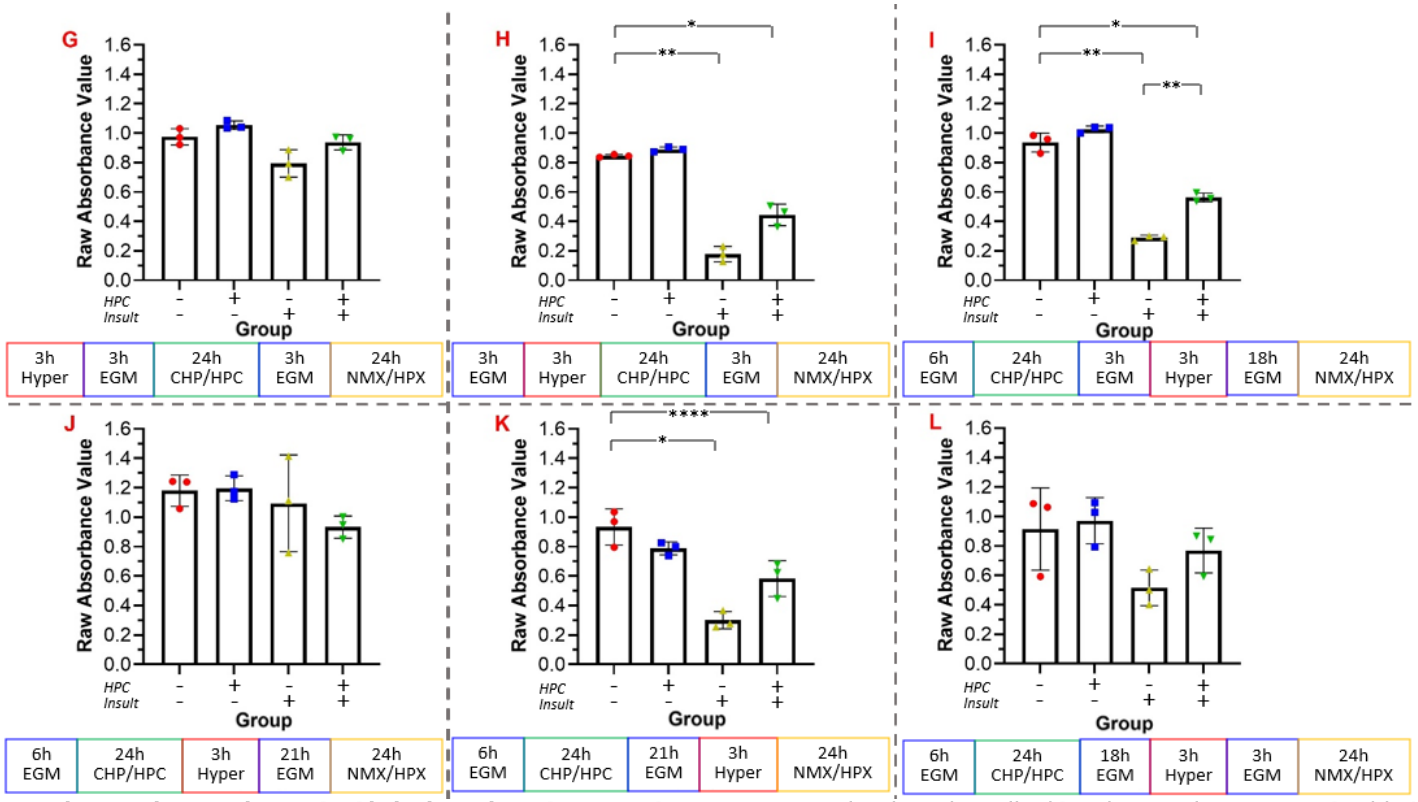

Fig. 5.20 Effect of acute hyperglycaemia on $CoCl_2$ induced HPC. HUVECs were exposed to basal media (CHP) or underwent HPC with 200µM $CoCl_2$ in basal media (HPC) for 24 hours. After a 24-hour recovery in EGM, a 600µM $CoCl_2$ hypoxic insult (HPX) or basal media treatment (NMX) were given for 24 hours. MTS assays were conducted 18-hours following the insult period. Cells were allocated into experimental groups to receiving a 3-hour hypoglycaemic episode at 1 of 6 timepoints, where G-L correspond to the experimental groups indicated in Fig. 5.17. Protocol timelines for each experimental group are located beneath their respective graphs. + and – indicates whether a group received an interventional treatment (HPC and/or hypoxic insult) or the relevant control (preconditioning control and/or insult control) respectively. Mean, individual data points and SD for raw absorbance values are shown. Significant differences are indicated (* = p<0.05, ** = p<0.01, **** = p<0.0001).

5.7 HPC Conferred Protection Against Severe Hypoxia in Chronically Hyperglycaemic Cells

To determine the effect of the chronic hyperglycaemia associated with diabetes on HPC, the preconditioning-insult protocol, validated in section 5.5.2, was repeated in HUVECs exposed to chronic hyperglycaemia. From being plated at P5 until completion of the experiment, cells were incubated with media containing 30mM glucose. An MTS assay was conducted 18 hours after completion of the hypoxic insult. Statistical analysis was performed using Tukey's repeated measures multiple comparisons 1-way ANOVA (Fig. 5.21). Absorbance values, and therefore the number of viable cells, were significantly decreased in the CHP HPX group (mean=0.5010) in comparison to those in the CHP NMX cohort (mean=0.7193, p=0.0213).

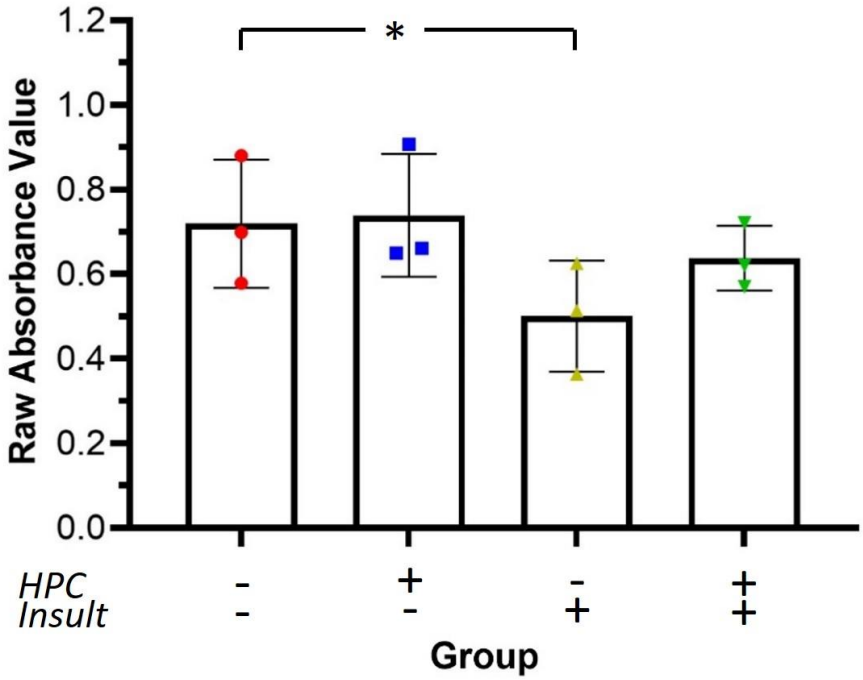

Fig. 5.21 Effect of chronic hyperglycaemia on HPC. HUVECs were cultured and experimented upon in continuous hyperglycaemia using 30mM glucose. Cells were exposed to basal media or underwent HPC with 200μM $CoCl_2$ in basal media for 24 hours. After a 24-hour recovery in EGM, a 600μM $CoCl_2$ hypoxic insult or basal media treatment were given for 24 hours. An MTS assay was conducted 18-hours following the insult period. + and – indicates whether a group received an interventional treatment (HPC and/or hypoxic insult) or the relevant control (preconditioning control and/or insult control) respectively. Mean, individual data points and SD for raw absorbance values are shown. Significant differences in raw absorbance values are indicated (* = $p<0.05$).

5.8 Discussion

The aim of this chapter was to develop *in vitro* models of HPC, IPC and R-IPC. Whilst models of IPC and R-IPC could not be validated, a model of HPC using $CoCl_2$ was validated. A secondary aim was to investigate the effects of acute hypoglycaemia or hyperglycaemia on any of the validated models. A preliminary screening study has indicated that acute glycaemic events may disrupt HPC in a time dependent manner although further research is required to increase sample sizes to confirm this hypothesis.

5.8.1 Acute Hypoglycaemia and Hyperglycaemia May Affect the Efficacy of HPC Depending on the Timing of the Glycaemic Event

Using the same criteria as utilised when validating the initial HPC model, it was concluded that the effect of acute hypoglycaemia (Fig. 5.19) and hyperglycaemia (Fig. 5.20) on the efficacy of HPC may depend on the timing of the abnormal glucose exposure within the preconditioning-insult protocol. However, it is important to highlight that this was a preliminary study and that further experiments are required to increase sample sizes as much of the data remained non-significant. In the absence of statistical significance, trends were reported when visual inspection of means appeared to show a difference between groups. Interpretation of the data from so many experimental groups was somewhat complex and a detailed description is provided below. However, to summarise, when a 3-hour hypoglycaemic or hyperglycaemic event was experienced immediately after HPC treatment, the protective effect appeared to have been abolished. Additionally, disruption of the protective effect was also observed when a 3-hour hypoglycaemic event was experienced 18-21 hours following HPC treatment. In all other treatment groups, the protective effect of HPC appears to have been preserved.

In experimental groups B, C, E, H, I and K, the significantly decreased absorbance values in the CHP HPX group in comparison to the CHP NMX group indicate that the number of viable cells has reduced in response to the hypoxic insult thereby confirming its efficacy. However, in experimental groups A, D, F, G, J and L, there was no statistical evidence to indicate that the hypoxic insult causes any change in absorbance values, and therefore the number of viable cells, even in the CHP HPX group, as would be predicted. However, the non-

significant trends, observed by focussing solely on the means, would suggest that, in experimental groups D, F, G, and L, an effect of the hypoxic insult would potentially become apparent if the sample sizes were increased.

In experimental group A, however, the absorbance values, and therefore the number of viable cells, were exceedingly similar between the CHP NMX and CHP HPX treatment groups, and it is likely that an unrealistically large increase in sample size would be required to observe a detrimental effect of the hypoxic insult. Technical error was unlikely to underpin the effect since experimental groups A and G shared the same working solution of 600µM $CoCl_2$ and, as previously discussed, the successful elicitation of the hypoxic insult was confirmed in the latter. The data may instead imply that exposing the cells to acute hypoglycaemia, in the 3-6 hours prior to HPC treatment, offers some protective effect against an imminent hypoxic insult warranting further analysis using experimental group A. A similar trend was also observed in experimental group J, paired with experimental group D, with the hypoxic insult appearing to affect the CHP HPX group in only the latter. Whilst it could be that the hyperglycaemic event, given 21-24 hours before the hypoxic insult, has protected the cells slightly against severe hypoxia, it was also possible that the large variation in absorbance values with no obvious anomalous data point, obtained from the CHP HPX group in experimental group J, were responsible for this ambiguity.

In experimental groups B, E and I, the elevated absorbance values in the HPC HPX group, in comparison to the CHP HPX group, indicate a higher number of viable cells and, therefore, that HPC was still effective and unaffected by acute hypoglycaemia or hyperglycaemia under these circumstances. As previously mentioned, in experimental group A, the data would suggest that there was no effect of the hypoxic insult on the cells. However, an elevation in the absorbance values, and therefore the number of viable cells, seen in the HPC HPX group compared to the CHP NMX group, indicates that even without the hypoxic insult, there was an increase in HPC induced proliferation suggesting the HPC treatment was not affected by the hypoglycaemia when given in the 3-6 hours preceding HPC.

There was no statistical evidence to suggest that HPC was successful in experimental groups C, G, H, K, L. However, observation of the trends within these data sets shows that the absorbance values, and therefore the number of viable cells, were increased in the HPC HPX groups compared to the CHP HPX groups. This implies that HPC was still able to offer a degree of protection against severe hypoxia.

Within each pair of experimental groups involving glycaemic events (Fig. 5.17) – such as A and G, B and H etc. – the trends were similar regardless of whether HUVECs were treated with hypoglycaemia or hyperglycaemia. However, in experimental group F, which is paired with experimental group L, the absorbance values, and therefore the number of viable cells, in the CHP HPX and HPC HPX group were similar. Hence, it could be predicted that whilst in experimental group L, HPC efficacy was preserved, as previously discussed, in experimental group F it was not. This would imply that hypoglycaemia, but not hyperglycaemia given 18-21 hours following completion of the HPC treatment abolishes the protection normally conferred. To confirm whether this effect was likely due to the protocol or the glycaemic events themselves, these findings can be compared to the data from the time matched euglycaemic control in experimental group R (Fig. 8.4). In experimental group R, the absorbance values, and therefore number of viable cells, were significantly lower in the HPC HPX group compared to the CHP NMX group. Therefore, by relying solely upon the statistical analysis of experimental group R, it would appear that the HPC treatment has not afforded any protection against a hypoxic insult. However, by observing the non-significant trends of the means, the absorbance values, and therefore the number of viable cells, in the CHP HPX group appear lower than those in both the CHP NMX and HPC HPX groups. This would therefore indicate that, contrary to the statistical findings, in experimental group R the hypoxic insult has caused a reduction in the number of viable cells and a degree of protection was conferred against the hypoxic insult by HPC. Hence, the conclusions made regarding the effect of hypoglycaemia and hyperglycaemia on HPC in experimental groups F and L respectively were likely due to the glycaemic event themselves and not the protocol.

Previous studies, discussed in section 1.5.4, have displayed how

hyperglycaemia prior to IPC renders the preconditioning treatment ineffective. However, the data in experimental groups B and H indicates that exposure to acute hypoglycaemia and hyperglycaemia does not affect the efficacy of HPC. It may be that acute glycaemic events experienced immediately prior to preconditioning treatment have a negligible effect on HPC whilst profoundly disrupting IPC. This could potentially make HPC a more viable option for individuals prone to experiencing acute glycaemic events in lieu of IPC. Therefore, further analysis, using the regimen in experimental groups B and H, would be warranted to determine whether this theory is supported.

Perhaps the most intriguing data obtained in this series of experiments was obtained from experimental groups D and J, in which cells were treated with acute hypoglycaemia and hyperglycaemia immediately after HPC or CHP treatment. In both cases, there was an apparent, non-significant, reduction in the mean absorbance, and therefore the number of viable cells, in the HPC HPX cohort than that in the other 3 treatment groups. If this finding is proven to be correct by increasing sample sizes, it not only implies that HPC was unable to confer protection to the cells against a severe hypoxic insult, but that the glycaemic events potentially cause the HPC treatment to have a detrimental effect on cell viability. Therefore, it could be suggested that future studies should primarily focus on experimental groups D and J with the aim of obtaining more evidence to test this hypothesis. However, when the data was observed for the euglycaemic control for this timepoint, in experimental group P (Fig. 8.4), there was an apparent, although non-significant, reduction in the absorbance values, and therefore number of viable cells, in the HPC HPX treatment group indicating HPC had not been successfully administered. Unsuccessful induction of HPC could have arisen because of the timepoints at which the media had to be changed in these experimental groups, as discussed in section 5.8.3. However, in the HPC NMX group of experimental group P, there was an apparent increase in the absorbance values, and therefore the number of viable cells. Such a result was not observed in either of experimental groups D and J. This could suggest that in experimental group P, but not experimental groups D and J, whilst HPC was unable to offer protection against a hypoxic insult, it did successfully induce proliferative pathways indicating partial success of the HPC treatment in the euglycaemic controls. Therefore, in an *in vivo* study, in which the issue of media

change becomes irrelevant, it is still possible that HPC would be interrupted when immediately proceeded by a glycaemic event as in experimental groups D and J.

As discussed throughout sections 1.2-1.4, hyperglycaemia is associated with poor CV outcomes. Despite aggressive glycaemic control, there is little change in the macrovascular outcomes primarily due to the occurrence of hypoglycaemia. The findings of this series of *in vitro* studies indicate acute glycaemic events, including hypoglycaemia, may potentially interrupt HPC and abolish its protective effects against a severe hypoxic insult. Hence, this could indicate that HPC is not suitable for those with diabetes if they are at risk of such glycaemic events, although further work is required to confirm this.

5.8.2 Chronic Hyperglycaemia Alone Does Not Affect the Efficacy of HPC

Contrary to the predictions made, based upon the literature discussed in section 1.5.4, the MTS assay data implies that HPC confers protection against a severe hypoxic insult against chronically hyperglycaemic HUVECs (Fig. 5.21). However, it is known that the evidence regarding the efficacy of IPC in those with diabetes is somewhat contradictory. There is a distinct lack of research investigating the effects of HPC in those with diabetes. It may be that whilst IPC is less effective in these individuals, HPC is still able to exert its protective effects. This is perhaps due to HPC only relying upon oxygen deprivation rather than the OGD involved in IPC. This could mean that HPC is possibly a more viable treatment option for those with diabetes in lieu of IPC. Therefore, it would be advised to conduct further research to gain evidence to test this hypothesis.

5.8.3 Limitations

Many of the limitations identified with this series of studies stem from the research being conducted *in vitro*. Discrepancies between *in vitro* and *in vivo* data are not always unsurprising, often highlighting the importance of using both methods prior to translation into clinical trials. A potential issue with the acute glycaemic event studies, in section 5.6, is that media was changed after the preconditioning stimulus in experimental groups C-F, I-L and M-R to alter the glycaemic state within the wells. This could potentially result in the loss of mediators secreted immediately following HPC treatment thereby rendering the

preconditioning ineffective. This could be particularly problematic in groups C, D, I, J, O and P where there was a media change within 3 hours following the completion of the HPC treatment. This was within the early phase of protection when most secreted cytokines exhibit increased expression and any loss of these could be detrimental to the success of HPC mediated protection. This may be why in experimental group P, the euglycaemic control for experimental groups D and J, the data indicates that HPC has been unsuccessful in eliciting protection against severe hypoxia. It was considered that this problem could be resolved by replacing the post glycaemic insult media with preconditioned media. However, it was important for the media to be changed and for cells to be washed with PBS after completion of the HPC treatment to remove any residual $CoCl_2$, a process which was possibly removing the early mediators of HPC. Additionally, regarding experimental groups D, J and P, as the cells were incubated with the saline solutions throughout the period during which the early mediators are expected to be released, it would not be possible to apply the preconditioned EGM generated by these cells in the 21-hour recovery period following the glycaemic insult and prior to the hypoxic insult, or insult control. Therefore, it was decided that this approach would not solve the limitation highlighted.

The aetiologies of the acute hypoglycaemia and both the acute and chronic hyperglycaemia were different to that used *in vivo* or indeed in individuals with diabetes. This may be particularly relevant as hypoglycaemia in those with diabetes is most likely to arise due to insulin therapy. The counterregulatory response is mediated by hormones which could potentially interfere with the HPC. These hormones, including insulin, would not be present when completing the studies in this chapter meaning the effects observed may not truly reflect those that would be seen in animals or humans. If desired, in the future, a separate project could be designed to investigate whether introducing these hormones to the media would affect the efficacy of HPC. A similar problem to this also arises from the use of a chemical hypoxia mimetic, $CoCl_2$, to induce HPC and the hypoxic insult as the Co^{2+} ions may exert effects on pathways not normally affected by hypoxia.

There could also be limitations of using the MTS assay as a technique for

analysing the efficacy of preconditioning following interventional treatments. The MTS assay is essentially a metabolic assay, and absorbance values are proportional to the number of mitochondria and their metabolic rate. Therefore, changes in glucose availability may lead to alterations in the metabolic rate which could result in absorbance values which are not directly correlational with the number of viable cells.

5.8.4 Future Directions

The MTS assay results suggest that glycaemic variability could potentially affect the efficacy of HPC depending upon when the glycaemic event occurs in relation to the HPC treatment. However, the series of studies discussed in section 5.6 was essentially conducted as a screening exercise to identify protocol combinations of interest. Therefore, this data was only preliminary, and more work would be required to confirm these findings. It would be recommended to increase the sample sizes to clarify whether HPC is effective where there appears to be a conflict between the statistical conclusions and those made based upon visual inspection of the mean absorbance values. Further caspase 3/7 and TUNEL assays could also be performed to support or disprove the conclusions made after receiving the MTS assay data. Additionally, it would be advisable to conduct these apoptosis assays to continue the investigation of the effects of chronic hyperglycaemia on HPC and to assess whether the MTS assay data, in section 5.7, can be supported. It could also be advisable to repeat the acute hypoglycaemia studies with the addition of insulin to mimic the hyperinsulinaemia experienced by persons with diabetes whose hypoglycaemia is caused by their insulin therapy.

Whilst HPC can be used for the management of CV dysfunction in humans, R-IPC would be an infinitely more practical technique to employ. HPC requires specialist equipment and would be less convenient for high-risk individuals to administer themselves at home. Hypoxic gas cylinders would require regular replacement and supply shortages may become a significant issue if this technique is widely used. Hence, it could be advised that HPC treatment should only be given in emergency settings, such as during a suspected myocardial infarction, or before surgery with a significant risk of inducing CV dysfunction.

Blood pressure cuffs, however, are accessible and affordable pieces of equipment available from many medical device retailers. They are significantly smaller and lighter than a hypoxic gas cylinder, and delivery system, and therefore are easier to store and transport. Many individuals already test their own blood pressure at home indicating that teaching people how to use the blood pressure cuff to perform the R-IPC procedure should be relatively simple. Modern advances in blood pressure technology have resulted in the development of automated blood pressure cuffs, which, with appropriate programming of the internal computer system, would allow the preconditioning protocol to run with little input required from the administrator. Therefore, it would be optimal to investigate the effects of glycaemic variability in an *in vitro* model of R-IPC.

The first step of this process would be to develop the *in vitro* IPC model. Due to the unsuccessful attempts at validation using $CoCl_2$ and the hypoxic incubator available, it is proposed that an anoxic chamber should be employed to develop one. The protocol used would be that described in the introduction to this chapter, using 3x 30-minute cycles of ischaemia/reperfusion, but with the complete absence of oxygen during the ischaemic periods. The techniques of MTS assays, caspase 3/7 assays and TUNEL assays would still be utilised to validate the model based upon cell viability, proliferation, and apoptosis.

Upon the establishment of a working IPC model, the next aim would be to validate a R-IPC model. The idea for this would be to precondition HUVECs, using ischaemia, and transfer the media onto cardiomyocytes. Cardiomyocytes would then be subjected to a severe ischaemic insult to mimic a myocardial infarction. In theory, protection should be conferred to the cardiomyocytes via the mediators secreted within the preconditioned media. In preparation for this future experiment, optimisation of a protocol to isolate neonatal rat cardiomyocytes was conducted with success (Fig. 8.5). Whilst beating cardiomyocytes were identified, it was unlikely that the resulting population will be 100% pure and will also include endothelial cells and fibroblasts. However, this is unlikely to be a significant issue as a mixed population more accurately represents the physiology of an *in vivo* heart, and the fibroblasts and endothelial cells may be important in mediating the HPC induced cardioprotection. Therefore, although not crucial, it would be advisable to perform immunocytochemistry on the isolated cells to determine the

proportion of each cell type within. The validation of the R-IPC model could again be done using
the same techniques as done in the development of HPC and IPC models discussed throughout this chapter.

5.9 Chapter Summary

To summarise the findings within this chapter, a hypoxic chamber with 1% oxygen was unsuitable for the validation of either a HPC or IPC protocol of HUVECs. It is likely that this was due to the issues with maintaining a truly hypoxic environment and the ability for the cells to thrive in low oxygen environments. However, these models could be developed if there was availability of an anoxic chamber. Additionally, it was not possible to validate an IPC model using $CoCl_2$ diluted in an ischaemic buffer, regardless of the number of IPC cycles given. This was perhaps due to slow uptake of the Co^{2+} ions into the cells, leading to an insufficient intracellular concentration within the 3-hour period of exposure. Conversely, it was possible to confirm that HPC could be induced using 200µM $CoCl_2$ in basal media for 24 hours. Using this model, initial evidence obtained using MTS assays suggests that acute hypoglycaemia and acute hyperglycaemia may affect the efficacy of HPC. However, further work is needed, and sample sizes require increasing, to support these findings.

Chapter 6

Concluding Remarks

6.1 Key Findings

At the commencement of this project, it was hypothesised that glycaemic variability would affect HPC and IPC. To investigate this hypothesis, 4 aims were devised: i) develop an *in vitro* model of HPC and IPC, ii) develop and *in vitro* model of R-IPC, iii) develop an *in vivo* model of R-IPC, iv) investigate the effects of glycaemic variability on the validated HPC, IPC and R-IPC models. With regards to aim i), an *in vitro* model of HPC, but not IPC, was validated. Development of an *in vitro* R-IPC model, as in aim ii) was unsuccessful, and only recent preliminary data indicates a valid *in vivo* R-IPC model, as in aim iii), was developed, although further research to increase sample sizes is required to confirm this. Finally, aim iv) was partially completed as a preliminary screening study was conducted to investigate the effect of acute hypoglycaemia and hyperglycaemia on the validated *in vitro* HPC model. Here, the key findings of this project are summarised and discussed.

As discussed in chapter 3, a preliminary study attempting to validate an *in vivo* model of R-IPC, by performing 4 cycles of 5 minutes ischaemia/5 minutes reperfusion on a murine hindlimb with a blood pressure cuff, proved unsuccessful largely as a consequence of respiratory difficulties that developed with prolonged anaesthesia use. Therefore, following redesign of the protocol, it was decided to focus on attempting to validate a R-IPC model in which 9 cycles of 5 minutes of ischaemia/5 minutes reperfusion were given over a 3-day period. The *in vivo* studies conducted and described in chapter 3 indicate that there was no improvement in endothelial function with R-IPC treatment. Indeed, inspection of the LDI with PE/ACh iontophoresis suggest that endothelial function decreases. This failure to validate a model of R-IPC meant it was not possible to draw firm conclusions regarding the effect of hypoglycaemia on endothelial function, and whether it might interfere with R-IPC treatment. After an extensive literature review, it was concluded that, isoflurane is not only a potent vasodilator but can in itself elicit a preconditioning effect. Isoflurane additionally is a modulator of the PI3-K pathway which itself is vital for mediating R-IPC meaning the former can mask the positive effects of the latter. Thus, the commonly used rodent anaesthetic isoflurane should not be used in studies of this nature.

The selected R-IPC model was subsequently tested using injectable

anaesthesia, midazolam and Alfaxan, in lieu of isoflurane, as discussed in chapter 4. Preliminary data suggests that this new anaesthesia regimen does not inhibit R-IPC treatment. While there was an apparent increase in endothelial function in both the control and R-IPC treatment groups, this increase appeared to be greater following R-IPC indicating this approach was more valid than the use of inhaled anaesthesia. However, these apparent changes were non-significant and should not be overstated. Hence it would be necessary to increase sample sizes, based upon power calculations, to confirm this.

Regarding the *in vitro* studies, conducted and discussed in chapter 5, attempts to validate a model of IPC and HPC in HUVECs using a hypoxic incubator were unfortunately unsuccessful due to the practical limitations of the apparatus available. Additionally, it was not possible to induce IPC using $CoCl_2$ presumably due to insufficient uptake of Co^{2+} ions into the cells. However, HPC was invoked by treating cells with 200µM $CoCl_2$ for 24 hours. This was confirmed as following a hypoxic insult, preconditioned cells exhibited increased cell viability and reduced apoptosis in comparison to those which were not preconditioned prior to insult.

Using the validated *in vitro* HPC model, a screening study was performed investigating whether a single 3-hour episode of hypoglycaemia or hyperglycaemia would disrupt the preconditioning effect. These glycaemic events were introduced at 6 different timepoints relative to the timing of HPC treatment. Preliminary cell viability data indicates that either acute hypoglycaemia or hyperglycaemia may disrupt the process of HPC mediated protection against a severe hypoxic insult. However, any apparent effects of the glycaemic event on HPC were non-significant and should not be overstated. Hence it would be necessary to increase sample sizes, based upon power calculations, to confirm this.

To summarise, preliminary data suggests a valid *in vivo* R-IPC model can be developed using the proposed protocol, and an *in vitro* model of HPC was validated using $CoCl_2$. Whilst further work is required to validate the *in vivo* R-IPC model, data was obtained from a screening study implying that acute hypoglycaemia or hyperglycaemia may affect the efficacy of HPC in a manner

dependent upon when the glycaemic event occurs in reference to the preconditioning treatment.

It is worth highlighting at this point the significant impact of the COVID-19 pandemic on this project. The laboratory was closed for a total of 5 months with an additional month of research being lost due to relocating laboratories and, upon returning to the laboratory, re-establishing cell lines. Additionally, obtaining reagents and basic supplies, such as gloves and pipette tips, became difficult due to a worldwide shortage and the need to prioritise facilities involved in patient care. Finally, the servicing of equipment was delayed during the pandemic resulting in the breakdown of many appliances necessary to complete the research.

6.2 Potential Future Projects

Recommendations have been made for projects to be conducted in the near future within the relevant sections of chapters 3-5. Briefly, these include increasing sample sizes to validate an *in vivo* R-IPC model using injectable anaesthetic agents and performing further functional and molecular analysis to confirm conclusions regarding the results of the *in vitro* screening study. However, it is important to consider what the next steps could be following completion of these studies.

Following confirmation of a successful R-IPC model *in vivo*, the next stage would be to assess the effect of glycaemic variability on its efficacy. It is predicted that confirmation of the results obtained from the *in vitro* screening study will identify timepoints of interest at which a glycaemic event will interfere with the efficacy of HPC. Therefore, as done with the *in vitro* HPC model, a glycaemic event could be introduced at these identified timepoints of interest in reference to the R-IPC treatment *in vivo* and assess endothelial function to ascertain if there is any interference with the R-IPC. Whilst experiments thus far have focussed on acute glycaemic events, it is possible to also determine whether recurrent hypoglycaemia exerts similar effects. Experiments could then be repeated using *in vivo* models of T1D and T2D to determine whether the diabetic status of the mice affects the effect of glycaemic events on the efficacy of R-IPC.

A final idea could also be to develop an *in vivo* myocardial infarct model. Up until now, assessment of endothelial function has been used as the principal method of validating a model of R-IPC and determining the effects of glycaemic variability on its efficacy. However, whilst microvascular and endothelial function is a good indicator of cardiac health and the cardioprotective effect of R-IPC, induction of a myocardial infarct will allow the assessment of the true impact of R-IPC, and potential effects of glycaemic variability, on cardiac function. Data achieved from an *in vitro* screening study suggested that glycaemic events can potentially interfere with HPC induced protection against hypoxia. The ability for hypoglycaemia to disrupt HPC could explain why CV outcomes are so poor in those with diabetes. However, an improvement in microvascular outcomes, but not macrovascular outcomes, as highlighted by clinical trials discussed in section 1.3, suggests that aggressive glycaemic control, which leads to an increase in the occurrence of hypoglycaemia, does not necessarily affect microvascular and macrovascular function in the same manner. Therefore, introduction of a myocardial infarct model would allow the assessment of whether potential interference of glycaemic events on efficacy of protective preconditioning treatments affects the various components of the CVS similarly or in a tissue specific manner.

References

Abdul Ghani S, Angelini DF, Suleiman MS (2014) Microcirculatory Blood Flow in Hindlimbs During Remote Ischaemic Preconditioning, *Heart*, vol 100, supplement 1

Abdul Ghani S, Fleishman AN, Khaliulin I, Meloni M, Angelini GD, Suleiman MS (2017) Remote ischemic preconditioning triggers changes in autonomic nervous system activity: implications for cardioprotection, *Physiological Reports*, vol 5(3), e13085

Aberer F, Pferschy PN, Tripolt NJ, Sourji C, Obermayer AM, Pruller F, Novak E, Reitbauer P, Kojzar H, Prietl B, Kofler S, Brunner M, Svehlikova E, Stojakovic T, Scharnagl H, Oulhaj A, Aziz F, Riedl R, Sourij H (2019) Hypoglycaemia leads to a delayed increase in platelet and coagulation activation markers in people with type 2 diabetes treated with metformin only: results from a stepwise hypoglycaemic clamp study, *Diabetes Obesity and Metabolism*, vol 22(2), pg 212-221

ACCORD Study Group (2007) Action to Control Cardiovascular Risk in Diabetes (ACCORD) Trial: Design and Methods, *The American Journal of Cardiology*, vol99(12A), pg 21i-331

Adelsperger AR, Bigiarelli-Nogas KJ, Toore I, Goergen CJ (2016) Use of a Low-flow Digital Anesthesia System for Mice and Rats, *Journal of Visualized Experiments*, vol 115, 5436

Abete P, Testa G, Cacciatore F, Della Morte D, Galizia G, Langellotto A, Rengo F (2011) Ischemic Preconditioning in the Younger and Aged Heart, *Aging and Disease*, vol 2(2), pg 138-148

Abu Amara M, Yang SY, Quaglia A, Rowley P, Fuller B, Seifalian A, Davidson B (2011) Role of endothelial nitric oxide synthase in remote ischemic preconditioning of the mouse liver, *Liver Transplantation*, vol 17(5), pg 610-619

Ahmed N (2005) Advanced glycation endproducts – role in pathology of diabetic complications, *Diabetic Research and Clinical Practice*, vol 67(1), pg 3-21

Akbar N (2014) *Systemic Cytokine Expression and Endothelial Dysfunction: Insights from Innate Immune Models of Protein Phosphorylation*, Doctor of Philosophy Dissertation, University of Dundee

Akella NM, Ciraku L, Reginato MJ (2019) Fueling the fire: emerging role of the hexosamine biosynthetic pathway in cancer, *BMC Biology*, vol 17, article 52

Al Mamun A, Hayashi H, Yamamura A, Nayeem MJ, Sato M (2020) Hypoxia induces the translocation of glucose transporter 1 to the plasma membrane in vascular endothelial cells, *The Journal of Physiological Sciences*, vol 70, article 44

Albrecht M, Henke J, Tacke S, Markert M, Guth B (2014) Influence of repeated anaesthesia on physiological parameters in male Wistar rats: a telemetric study about isoflurane, ketamine-xylazine and a combination of medetomidine, midazolam and fentanyl, *BMC Veterinary Research*, vol 10, article 310

Amore A, Cirina P, Mitola S, Peruzzi L, Gianoglio B, Rabbone I, Sacchetti C, Cerutti F, Grillo C, Coppo R (1997) Nonenzymatically glycated albumin (Amadori adducts) enhances nitric oxide synthase activity and gene expression in endothelial cells, *Kidney International*, vol 51(1), pg 27-35

Antovic J, Blomback M (2013) Essential Guide to Blood Coagulation (2nd Edition), Chichester: John Wiley & Sons Ltd.

Barnes PJ, Karin M (1997) Nuclear Factor-κB – A Pivotal Transcription Factor in Chronic Inflammatory Diseases, *The New England Journal of Medicine*, vol 336(15), pg 1066-1071

Beckman JA, Goldfine AB, Gordon MB, Garrett LA, Creager MA (2002) Inhibition of Protein Kinase Cβ Prevents Impaired Endothelium-Dependent Vasodilation Caused by Hyperglycemia in Humans, *Circulation Research*, vol 90(1), pg 107-111

Behmenburg F, Van Caster P, Bunte S, Brandenburger T, Heinen A, Hallmann MW, Huhn R (2018) Impact of Anesthetic Regimen on Remote Ischemic Preconditioning in the Rat Heart In Vivo, *Anesthesia and Analgesia*, vol 126(4), pg 1377-1380

Bento CF, Fernandes R, Ramalho J, Marques C, Shang F. Taylor A. Pereira P (2010) The Chaperone-Dependent Ubiquitin Ligase CHIP Targets HIF-1α for Degradation in the Presence of Methylglyoxal, *PLoS ONE*, vol 5(11), e15062

Bento CF, Pereira P (2011) Regulation of hypoxia-inducible factor 1 and the loss of the cellular response to hypoxia in diabetes, *Diabetologia*, vol 54(8), pg 1946-1956

Berendji Grun D, Kolb Bachofen V, Kroncke KD (2001) Nitric Oxide Inhibits Endothelial IL-1β-induced ICAM-1 Gene Expression at the Transcriptional Level Decreasing Sp1 and AP-1 Activity, *Molecular Medicine*, vol 7, pg 748-754

Berridge MJ, Bootman MD, Roderick HL (2003) Calcium signalling: dynamics, homeostasis and remodelling, *Nature Reviews Molecular Cell Biology*, vol 4(7), pg 517-529

Bhaskar B, Fraser JF (2011) Negative pressure pulmonary edema revisited: Pathophysiology and review of management, *Saudi Journal of Anaesthesia*, vol 5(3), pg 308-313

Bolli R (2000) The Late Phase of Preconditioning, *Circulation Research*, vol 87, pg 972-983

Botusan IR, Sunkari VG, Savu O, Catrina AI, Grunler J, Lindberg S, Pereira T, Yla-Herttuala S, Poellinger L, Brismar K, Catrina SB (2008) Stabilization of HIF-1α is critical to improve wound healing in diabetic mice, *PNAS*, vol 105(49), pg 19426-19431

Bradford MM (1976) A Rapid and Sensitive Method for the Quantitation of Microgram Quantities of protein Utilizing the Principle of Protein-Dye Binding, *Analytical Biochemistry*, vol 72(1-2), pg 248-254

Brager AJ, Yang T, Ehlen JC, Simon RP, Meller R, Paul KN (2016) Sleep is Critical for Remote Preconditioning-Induced Neuroprotection, *Sleep*, vol 39(11), pg 2033-2040

Brownlee M (2004) The pathobiology of diabetic complications: A unifying mechanism, *Diabetes*, vol 54(6), pg 1615-1625

Cai Z, Luo W, Zhan H, Semenza GL (2013) Hypoxia-inducible factor 1 is required for remote ischemic preconditioning of the heart, *PNAS*, vol 110(43), pg 17462-17467

Cai ZP, Parajuli N, Zheng X, Becker L (2012) Remote ischemic preconditioning confers late protection against myocardial ischemia-reperfusion injury in mice by upregulating interleukin-10, *Basic Research in Cardiology*, vol 107, article 277

Ceradini DJ, Yao D, Grogan RH, Callaghan MJ, Edelstein D, Brownlee M, Gurtner GC (2008) Decreasing Intracellular Superoxide Corrects Defective Ischemia-induced New Vessel Formation in Diabetic Mice, *The Journal of Biological Chemistry*, vol 283(16), pg 10930-10938

Chatham JC, Young ME, Zhang J (2021) Role of O-linked N-acetylglucosamine (O-GlcNAc) modification of proteins in diabetic cardiovascular complications, *Current Opinion in Pharmacology,* vol 57(April 2021), pg 1-12

Chatterjee S, Khunti K, Davies MJ (2017) Type 2 diabetes, *The Lancet*, vol 389(10085), pg 2239-2251

Chen L, Luo W, Zhang W, Chu H, Wang J, Dai X, Cheng Y, Zhu T, Chao J (2020) circDLPAG4/HECTD1 mediates ischaemia/reperfusion injury in endothelial cells via ER stress, *RNA biology*, vol 17(2), pg 240-253

Cheung MMH, Kharbanda RK, Konstantinov IE, Shimizu M, Frndova H, Li J, Holtby HM, Cox PN, Smallhorn JF, Van Arsdell GS, Redington AN (2006) Randomized Controlled Trial of the Effects of Remote Ischemic Preconditioning on Children Undergoing Cardiac Surgery, *Journal of the American College of Cardiology*, vol 47(11), pg 2277-2282

Chiari PC, Bienengraeber MW, Weihrauch D, Krolikowski JG, Kersten JR, Warltier DC, Pagel PS (2005) Role of endothelial nitric oxide synthase as a trigger and mediator of isoflurane-induced delayed preconditioning in rabbit myocardium, *Anesthesiology*, vol 103(1), pg 74-83

Chibber R, Molinatti PA, Rosatto N, Lambourne B, Kohner EM (1997) Toxic action of advanced glycation end products on cultured retinal capillary pericytes and endothelial cells: relevance to diabetic retinopathy, *Diabetologia*, vol 40, pg 156-164

Cho K, Min SI, Ahn S, Min SK, Ahn C, Yu KS, Jang IJ, Cho JW, Ha J (2017) Integrative Analysis of Renal Ischemia/Reperfusion Injury and Remote Ischemic Preconditioning in Mice, *Journal of Proteome Research*, vol 16(8), pg 2877-2886

Constantinides C, Mean R, Janssen B (2012) Effects of Isoflurane Anesthesia on the Cardiovascular Function of the C57BL/6 Mouse, *Institute for Laboratory Animal Research (ILAR) Journal*, vol 52(3), pg e21-e31

Cope DK, Impastato WK, Cohen MV, Downey JM (1997) Volatile Anesthetics Protect the Ischemic Rabbit Myocardium from Infarction, *Anesthesiology*, vol 86(3), pg 699-709

Cremer J, Ricco CH (2017) Cardiovascular, respiratory and sedative effects of intramuscular alfaxalone, butorphanol and dexmedetomidine compared with ketamine, butorphanol and dexmedetomidine in healthy cats, *Journal of Feline Medicine and Surgery*, vol 20(10), pg 973-979

Dalsgaard Nielsen J, Madsbad S, Hilsted J (1982) Changes in Platelet Function, Blood Coagulation and Fibrinolysis During Insulin-Induced Hypoglycaemia in Juvenile Diabetics and Normal Subjects, *Journal of Thrombosis and Haemostasis*, vol 47(3), pg 254-258

Dave KR, Tamariz J, Desai KM, Brand FJ, Liu A, Saul I, Bhattacharya SK, Pileggi A (2011) Recurrent hypoglycemia exacerbates cerebral ischemic damage in streptozotocin induced diabetic rats, *Stroke*, vol 42(5), pg 1404-1411

DCCT/EDIC Study Research Group (2000) Retinopathy and Nephropathy in Patients with Type 1 Diabetes Four Years After a Trial of Intensive Therapy, *The New England Journal of Medicine*, vol 342(6), pg 381-389

DCCT/EDIC Study Research Group (2005) Intensive Diabetes Treatment and Cardiovascular Disease in Patients with Type 1 Diabetes, *The New England Journal of Medicine*, vol 353(25), pg 2643-2653

Dieguez G, Fernandez N, Garcia JL, Garcia-Villalon AL, Monge L, Gomez B (1997) Role of nitric oxide in the effects of hypoglycemia on the cerebral circulation in awake goats, *European Journal of Pharmacology*, vol 30(2-3), pg 185-193

Dimitrov S, Lange T, Born J (2010) Selective Mobilization of Cytotoxic Leukocytes by Epinephrine, vol 184(1), pg 503-511

Dunn AK (2012) Laser Speckle Contrast Imaging of Cerebral Blood Flow, *Annals of Biomedical Engineering*, vol 40(2), pg 367-377

Eelen G, De Zeeuw P, Treps L, Harjes U, Wong BW, Carmeliet P (2018) Endothelial Cell Metabolism, *Physiological Reviews*, vol 98(1), pg 3-58

Fisher B, Gillen G, Dargie HJ, Inglis GC, Frier BM (1987) The effects of insulin induced hypoglycaemia on cardiovascular function in normal man: studies using radionuclide ventriculography, *Diabetologia*, vol 30(11), pg 841-845

Fisher BM, Quin JD, Rumley A, Lennie SE, Small M, MacCuish AC, Lowe GD (1991) Effects of acute insulin-induced hypoglycaemia on haemostasis, fibrinolysis and haemorheology in insulin dependent diabetic patients and control subject, *Clinical Science*, vol 80, pg 525-531

Forbes JM, Thallas V, Thomas MC, Founds HW, Burns WC, Jerums G, Cooper ME (2003) The breakdown of pre-existing advanced glycation end products is associated with reduced renal fibrosis in experimental diabetes, *Federation of American Societies for Experimental Biology*, vol 17(12), pg 1762-1764

Forouhi NG, Wareham NJ (2014) Epidemiology of diabetes, *Medicine (Abingdon)*, vol 42(12), pg 698-702

Genuth S, Ismail-Beigi F (2012) Clinical Implication of the ACCORD Trial, *The Journal of Clinical Endocrinology and Metabolism*, vol 97(1), pg 41-48
Gillespie KM (2006) Type 1 diabetes: pathogenesis and prevention, *Canadian Medical Association Journal*, vol 175(2), pg 165-170

Gimenez M, Gilabert R, Monteagudo J, Alonso A, Casamitjana R, Pare C, Conget I (2010) Repeated Episodes of Hypoglycemia as a Potential Aggravating Factor for Preclinical Atherosclerosis in Subjects With Type 1 Diabetes, *Diabetes Care,* vol 34(1), pg 198-203

Han J, Kim N, Joo H, Kim E (2002) Ketamine abolishes ischemic preconditioning through inhibition of K(ATP) channels in rabbit hearts, *American Journal of Physiology Heart and Circulatory Physiology*, vol 283(1), pgH13-H21

Hausenloy DJ, Yellon DM (2010) The Second Window of Preconditioning (SWOP) Where Are We Now?, *Cardiovascular Drugs and Therapy*, vol 24, pg 235-254

He X, Zhao M, Bi XY, Yu XJ, Zang WJ (2013) Delayed preconditioning prevents ischemia/reperfusion-induced endothelial injury in rats: role of ROS and eNOS, *Laboratory Investigation*, vol 93, pg 168-180

Hegab Z, Gibbons S, Neyses L, Mamas MA (2012) Role of advanced glycation end products in cardiovascular disease, *World Journal of Cardiology*, vol 4(4), pg 90-102

Heller SR (2009) A Summary of the ADVANCE Trial, Diabetes Care, vol 32 (supplement 2), pg 5357-5361

Hex N, Bartlett C, Wright D, Taylor M, Varley D (2012) Estimating the current and future costs of Type 1 and Type 2 diabetes in the UK, including direct health costs and indirect societal and productivity costs, *Diabetic Medicine*, vol 29(7), pg 855-862

Holman RR, Paul SK, Bethel MA, Matthews DR, Neil HAW (2008) 10-Year Follow-up of Intensive Glucose Control in Type 2 Diabetes, *The New England Journal of Medicine*, vol 359(15), pg 1577-1589

Howangyin KY, Silvestre JS (2014) Diabetes mellitus and Ischemic Diseases: Molecular Mechanisms of Vascular Repair Dysfunction, *Arteriosclerosis, Thrombosis and Vascular Biology*, vol 34, pg 1126-1135

Hummitzsch L, Zitta K, Bein B, Steinfath M, Albrecht M (2014) Culture media from hypoxia conditioned endothelial cells protect human intestinal cells from hypoxia/reoxygenation injury, *Experimental Cell Research*, vol 322(1), pg 62-70

Jaffe EA, Nachman RL, Becker CG, Minick CR (1973) Culture of Human Endothelial Cells Derived from Umbilical Veins. IDENTIFICATION BY MORPHOLOGIC AND IMMUNOLOGIC CRITERIA, *The Journal of Clinical Investigation*, vol 52(11), pg 2745-2756

Jeon SM (2016) Regulation and function of AMPK in physiology and disease, *Experimental & Molecular Medicine*, vol 48, e245

Ji YY, Wang ZD, Wang SF, Wang BT, Yang ZA, Zhou XR, Lei NN, Yue WN (2015) Ischemic preconditioning ameliorates intestinal injury induced by ischemia-reperfusion in rats, *World Journal of Gastoenterology*, vol 21(26), pg 8081-8088

Ji L, Zhang X, Liu W, Huang Q, Yang W, Fu F, Ma H, Su H, Wang H, Wang J, Zhang H, Gao F (2013) AMPK-Regulated and Akt-Dependent Enhancement of Glucose Uptake is Essential in Ischemic Preconditioning Alleviated Reperfusion Injury, *PLoS ONE*, vol 8(7), e69910

Jiang Y, Xie H, Tu W, Fang H, Ji C, Yan T, Huang H, Yu C, Hu Q, Gao Z, Lv S (2018) Exosomes secreted by HUVECs attenuate hypoxia/reoxygenation-induced apoptosis in neural cell by suppressing miR-21-3p, *American Journal of Translational Research*, vol 10(11), pg 3529-3541

Jones H, Hopkins N, Bailey T, Green DJ, Cable NT, Thijssen DHJ (2014) Seven-Day Remote Ischemic Preconditioning Improves Local and Systemic Endothelial Function and Microcirculation in Healthy Humans, *American Journal of Hypertension*, vol 27(7), pg 918-925

Joshi MS, Williams D, Horlock D, Samarasinghe T, Andrews KL, Jefferis AM, Berger PJ, Chin Dusting JP, Kaye DM (2015) Role of mitochondrial dysfunction in hyperglycaemia-induced coronary microvascular dysfunction: Protective role of resveratrol, *Diabetes and Vascular Disease Research*, vol 12(3), pg 208-216

Joy NG, Hedrington MS, Briscoe VJ, Tate DB, Ertl AC, Davis SN (2010) Effects of Acute Hypoglycemia on Inflammatory and Pro-atherothrombotic Biomarkers in Individuals With Type 1 Diabetes and Healthy Individuals, *Diabetes Care*, vol 33(7), pg 1529-1535

Joy NG, Perkins JM, Mikeladze M, Younk L, Tate DB, Davis SN (2016) Comparative effects of acute hypoglycemia and hyperglycemia on pro-atherothrombotic biomarkers and endothelial function in non-diabetic humans, *Journal of Diabetes and its Complications*, vol 30(7), pg 1275-1281

Joy NG, Tate DB, Younk LM, Davis SN (2015) effects of acute and antecedent hypoglycemia on endothelial function and markers of atherothrombotic balance in healthy humans, *Diabetes*, vol 64(7), pg 2571-2580

Kalakech H, Tamareille S, Pons S, Godin-Ribuot D, Carmeliet P, Furber A, Martin V, Berdeaux A, Ghaleh B, Prunier F (2013) Role of hypoxia inducible factor-1α in remote limb ischemic preconditioning, *Journal of Molecular and Cellular Cardiology*, vol 65, pg 98-104

Kepler T, Kuusik K, Lener U, Starkopf J, ZIlmer M, Eha J, Lieberg J, Vahi M, Kals J (2019) The Effect of Remote Ischaemic Preconditioning on Arterial Stiffness in Patients Undergoing Vascular Surgery: A Randomised Clinical Trial, *European Journal of Vascular and Endovascular Surgery*, vol 57(6), pg 868-875

Kerr D, MacDonald IA, Heller SR, Tattersall RB (1990) β-adrenoceptor blockade and hypoglycaemia. A randomised double-blind, placebo controlled comparison of metoprolol CR, atenolol and propranolol LA in normal subjects, *British Journal of Clinical Pharmacology*, vol 29(6), pg 685-693

Kersten JR, Schmeling TJ, Orth KG, Pagel PS, Warltier DC (1998) Acute hyperglycemia abolishes ischemic preconditioning in vivo, *The Americacn Journal of Physiology*, vol 275(2), pg H721-H725

Kersten JR, Toller WG, Gross ER, Pagel PS, Warltier DC (2000) Diabetes abolishes ischemic preconditioning: role of glucose, insulin, and osmolality, *American Journal of Physiology: Heart and Circulatory Physiology*, vol 278(4), pg H1218-H1224

Kilkpatrick ES, Rigby AS, Atkin SI (2008) A1C Variability and the Risk of Microvascular Complications in Type 1 Diabetes: Data from the Diabetes Control and Complications Trial, *Diabetes Care*, vol 31(11) pg 2198-2202

Kleinsinger F (2018) The Unmet Challenge of Medication Nonadherence, *The Permanente Journal*, vol 22, 18-033

Koivikko ML, Karsikas M, Salmela PI, Tapanainen JS, Ruokonen A, Seppanen T, Huikuri HV, Perkiomaki JS (2008) Effects of controlled hypoglycaemia on cardiac repolarisation in patients with type 1 diabetes, *Diabetologia*, vol 51(3), pg 426-435

Koivikko ML, Salmela PI, Juhani Airaksinen KE, Tapanainen JS, Ruokonen A, Makikallio TH, Huikuri HV (2005) Effects of Sustained Insulin Induced Hypoglycemia on Cardiovascular Autonomic Regulation in Type 1 Diabetes, *Diabetes*, vol 54(3), pg 744-750

Konstantinov IE, Arab S, Li J, Coles JG, Boscarino C, Mori A, CUkerman E, Dawood F, Cheung MMH, Shimizu M, Liu PP, Redington AN (2005) The remote ischemic preconditioning stimulus modifies gene expression in mouse myocardium, *The Journal of Thoracic and Cardiovascular Surgery*, vol 130(5), pg 1326-1332

Kordel DJ, Bittner EA, Abdulnour REE, Brown RH, Eikermann M (2011) Negative Pressure Pulmonary Edema Following Bronchospasm, *CHEST*, vol 140(5), pg 1351-1354

Kottenberg E, Thielmann M, Bergmann L, Heine T, Jakob H, Heusch G, Peters J (2012) Protection by remote ischemic preconditioning during coronary artery bypass graft surgery with isoflurane but not propofol – a clinical trial, *Acta Anaesthesiologica Scandinavica*, vol 56(1), pg 30-38

Krutzfeldt A, Spahr R, Mertens S, Siegmund B, Piper HM (1990) Metabolism of exogenous substrates by coronary endothelial cells in culture, *Journal of Molecular and Cellular Cardiology*, vol 22(12), pg 1393-1404

Larsen A, Hojlund K, Poulsen MK, Madsen RE, Juhl CB (2013) Hypoglycemia-Associated Electroencephalogram and Electrocardiogram Changes Appear Simultaneously, *Journal of Diabetes Science and Technology*, vol 7(1), pg 93-99

Lee AY, Chung SS (1999) Contributions of polyol pathway to oxidative stress in diabetic cataract, *The FASEB*, Journal, vol 13(1), pg 23-30

Lee MR, Suh HR, Kim MW, Cho JY, Song HK, Jung YS, Hwang DY, Kim KS (2018) Comparison of the anesthetic effects of 2,2,2-tribromoethanol on ICR mice derived from three different sources, *Laboratory Animal Research*, vol 34(4), pg 270-278

Li DY, Shi XJ, Li W, Sun XD, Wang GY (2016) Ischemic preconditioning and remote ischemic preconditioning provide combined protective effect against ischemia reperfusion injury, *Life Science*, vol 150, pg 76-80

Liu C, Liang B, Wang Q, Wu J, Zou MH (2010) Activation of AMP-activated Protein Kinase α1 Alleviated Endothelial Cell Apoptosis by Increasing the Expression of Anti-apoptotic Proteins Bcl-2 and Survivin, *Journal of Biological Chemistry*, vol 285(20), pg 15346-15355

Liu C, Yang J, Zhang C, Geng X, Zhao H (2020) Remote ischemic conditioning reduced cerebral ischemic injury by modulating inflammatory responses and ERK activity in type 2 diabetic mice, *Neurochemistry International*, vol 135, article 104690

Liu C, Zhang C, Du H, Geng X, Zhao H (2019) Remote ischemic preconditioning protects against ischemic stroke in streptozotocin-induced diabetic mice via anti-inflammatory response and anti-apoptosis, *Brain Research*, vol 1724, article 146429

Liu Y, Paterson M, Baumgardt SL, Irwin M, Xia Z, Bosnjak ZJ, Ge ZD (2019) Vascular endothelial growth factor regulation of endothelial nitric oxide synthase phosphorylation is involved in isoflurane cardiac preconditioning, *Cardiovascular Research*, vol 115(1), pg 168-178

Liu Y, Thornton JD, Cohen MV, Downey JM, Schaffer SW (1993) Streptozotocin-Induced Non-Insulin-Dependent Diabetes Protects the Heart From Infarction, *Circulation*, vol 88, pg 1273-1278

Lu N, Li X, Tan R, An J, Cai Z, Hu X, Wang F, Wang H, Lu C, Lu H (2018) HIF-1α/Beclin1-Mediated Autophagy Is Involved in Neuroprotection Induced by Hypoxic Preconditioning, *Journal of Molecular Neuroscience*, vol 66(2), pg 238-250

Lucchinetti E, Bestmann L, Feng J, Freidank H, Clanachan AS, Finegan BA, Zaugg M (2012) Remote Ischemic Preconditioning Applied during Isoflurane Inhalation Provides No Benefit to the Myocardium of Patients Undergoing ON-pump Coronary Artery Bypass Graft Surgery, *Anesthesiology*, vol 166(2), pg 296-310

Marano G, Grigioni M, Tiburzi F, Vergari A, Zanghi F (1996) Effects of Isoflurane on Cardiovascular System and Sympathovagal Balance in New Zealand White Rabbits, *Journal of Cardiovascular Pharmacology*, vol 28(4), pg 513-518

Masoud GN, Li W (2015) HIF-1α pathway: role, regulation and intervention for cancer therapy, *Acta Pharmaceutica Sinica B*, vol 5(5), pg 378-389

Mattson DL (2001) Comparison of arterial blood pressure in different strains of mice, *American Journal of Hypertension*, vol 14(5), pg 405-408

Maxwell J, Carter H, Hellsten Y, Miller GD, Sprung V, Cuthbertson D, Thijssen D, Jones H (2019) Seven-day remote ischaemic preconditioning improves endothelial function in patients with type 2 diabetes mellitus: a randomised pilot study, *European Journal of Endocrinology*, vol 191(6), pg 659-669

McGowan JE, Chen L, Gao D, Trush M, Wei C (2006) Increased mitochondrial reactive oxygen species production in newborn brain during hypoglycemia, *Neuroscience Letters*, vol 399(1-2), pg 111-114

McKeown SR (2014) Defining normoxia, physoxia and hypoxia in tumours – implications for treatment response, *The British Journal of Radiology*, vol 87(1035), 20130676

Melkonian EA, Schury MP (2021) Biochemistry, Anaerobic Glycolysis, Florida: StatPearls Publishing

Mocanu MM, Baxter GF, Yue Y, Critz SD, Yellon DM (2000) The p38 MAPK inhibitor, SB203580, abrogates ischaemic preconditioning in rat heart but timing of administration is critical, *Basic Research in Cardiology*, vol 95(6), pg 472-478

Muir W, Lerche P, Wiese A, Nelson L, Pasloske K, Whittem T (2009) The cardiorespiratory and anesthetic effects of clinical and supraclinical doses of alfaxalone in cats, *Veterinary Anaesthesia and Analgesia*, vol 36(1), pg 42-54

Muller J, Taebling M, Oberhoffer RM (2019) Remote Ischemic Preconditioning Has No Short Term Effect on Blood Pressure, Heart Rate, and Arterial Stiffness in Healthy Young Adults, *Frontiers in Physiology*, vol 10, 1094

Murata T, Ishibashi T, Khalil A, Hata Y, Yoshikawa H, Inomata H (1995) Vascular Endothelial Growth Factor Plays a Role in Hyperpermeability of Diabetic Retinal Vessels, *Ophthalmic Research*, vol 27(1), pg 48-52

Murphy KL, Baxter MG, Flecknell PA (2012) Chapter 17 – Anesthesia and Analgesia in Nonhuman Primates, In C Abee, K Mansfield, S Tardif & T Morris (Eds.), *Nonhuman Primates in Biomedical Research (2nd Edition)*, p403-435

Murray AK, Herrick AL, King TA (2004) Laser Doppler imaging: a developing technique for application in the rheumatic diseases, Rheumatology, vol 43(10), pg 1210-1218

Murry CE, Jennings RB, Reimer KA (1986) Preconditioning with ischemia: a delay of lethal cell injury in ischemic myocardium, *Circulation*, vol 74(5), pg 1124-1136

Nernpermpisooth N, Prompunt E, Kumphune S (2017) An in vitro endothelial cell protective effect of secretory leukocyte protease inhibitor against simulated ischaemic/reperfusion injury, *Experimental and Therapeutic Medicine,* vol 14(6), pg 5793-5800

Neves MV (2016) Effects of hypoglycaemia on vascular reactivity, Master's Degree Dissertation, University of Lisbon

Newby D, Marks L, Lyall F (2005) Dissolved oxygen concentration in culture medium: assumptions and pitfalls, *Placenta*, vol 26(4), pg 353-357

Nong Z, Hoylaerts M, Van Pelt N, Collen D, Janssens S (1997) Nitric Oxide Inhalation Inhibits Platelet Aggregation and Platelet-Mediated Pulmonary Thrombosis in Rats, *Circulation Research*, vol 81, pg 865-869

Oberkofler CE, Limani P, Jang JH, Rickenbacher A, Lehmann K, Raptis DA, Ungethuem U, Tian Y, Grabliauskaite K, Humar R, Graf R, Humar B, Clavien PA (2014) Systemic protection through remote ischemic preconditioning is spread by platelet-dependent signaling in mice, *Hepatology*, vol 60(4), pg 1409-1417

Oxman T, Arad M, Klein R, Avazov N, Rabinowitz B (1997) Limb ischemia preconditions the heart against reperfusion tachyarrhythmia, *American Journal of Physiology – Heart and Circulatory Physiology,* vol 273(4), pg H1707-1712

Paelestik KB, Jespersen NR, Jensen RV, Johnsen J, Botker HE, Kristiansen ST (2017) Effects of hypoglycemia on myocardial susceptibility to ischemia-reperfusion injury and preconditioning in hearts from rats with and without type 2 diabetes, *Cardiovascular Diabetology*, vol 16(10), 148

Pan T, Jia P, Chen N, Fang Y, Liang Y, Guo M, Ding X (2019) Delayed Remote Ischemic Preconditioning Confers Renoprotections against Septic Acute Kidney Injury via Exosomal miR-21, *Theranostics*, vol 9(2), pg 405-423

Pi Z, Lin H, Yang J (2018) Isoflurane reduces pain and inhibits apoptosis of myocardial cells through the phosphoinsitide 3-kinase/protein kinase B signaling pathway in mice during cardiac surgery, *Molecular Medicine Reports*, vol 17(5), pg 6497-6505

Pivovarova NB, Andrews SB (2010) Calcium dependent mitochondrial function and dysfunction in neurons, *FEBS Journal*, vol 277(18), pg 3622-3636

Przyklenk K, Bauer B, Ovize M, Kloner RA, Whittaker P (1993) Regional ischemic 'preconditioning' protects remote virgin myocardium from subsequent sustained coronary occlusion, *Circulation*, vol 87(3), pg 893-899

Qiu L, Zhang L, Zhu L, Yang D, Li Z, Qin K, Mi X (2008) PI3K/Akt mediates expression of TNF-α mRNA and activation of NF-κB in calyculin A-treated primary osteoblasts, *Oral Diseases*, vol 14(8), pg 727-733

Quagliaro L, Piconi L, Assaloni R, Da Ros R, Maier A, Zuodar G, Ceriello A (2005) Intermittent high glucose enhances ICAM-1, VCAM-1 and E-selectin expression in human umbilical vein endothelial cells in culture: The distinct role of protein kinase C and mitochondrial superoxide production, *Atherosclerosis*, vol 183(2), pg 259-267

Qureshi MH, Cook Mills J, Doherty DE, Garvy BA (2003) TNF-α Dependent ICAM-1- and VCAM-1-Mediated Inflammatory Responses Are Delayed In Neonatal Mice Infected with Pneumocystis carinii, *The Journal of Immunology*, vol 171(9), pg 4700-4707

Rankin CH, Abrams T, Barry RJ, Bhatnagar S, Clayton DF Colombo J, Coppola G, Geyer MA, Glanzman DL, Marsland S, McSweeney FK, Wilson DA, Wu CF, Thompson RF (2009) Habituation Revisited: An Updated and Revised Description of the Behavioral Characteristics of Habituation, *Neurobiology of Learning and Memory*, vol 92(2), pg 135-138

Rao Kondapally Seshasai S, Kaptoge S, Thompson A, Di Angelantonio E, Gao P, Sarwar N, Whincup PH, Mukamal KJ, Gillum RF, Holme I, Njolstad I, Fletcher A, Nilsson P, Lewington S, COllincs R, Gudnason V, Thompson SF, Sattar N, Selvin E, Hu FB, Danesh J, Emerging Risk Factors Collaboration (2011) Diabetes mellitus, fasting glucose, and risk of cause-specific death, *The New England Journal of Medicine*, vol 364(9), pg829-841

Rath G, Saliez J, Behets G, Romero-Perez M, Leon-Gomez E, Bouzin C, Vriens J, Nilius B, Feron O, Dessy C (2012) Vascular Hypoxic Preconditioning Relies on TRPV4-Dependent Calcium Influx and Proper Intercellular Gap Junctions Communication, *Arteriosclerosis, Thrombosis and Vascular Biology*, vol 32(9), pg 2241-2249

Rassaf R, Totzeck M, Hendgen Cotta UB, Shiva S, Heusch G, Kelm M (2014) Circulating Nitrite Contributes to Cardioprotection by Remote Ischemic Preconditioning, *Circulation Research*, vol 114, pg 1601-1610

Ratter JM, Rooijackers HMM, Tack CJ, Hijmans AGM, Netea MG, de Galan BE, Stienstra R (2017) Pro-inflammatory effects of hypoglycemia in humans with or without diabetes, *Diabetes*, vol 66(4), pg 1052-1061

Rehni AK, Nautiyal N, Perez Pinzon MA, Dave KR (2015) Hyperglycemia/hypoglycemia-induced mitochondrial dysfunction and cerebral ischemic damage in diabetics, *Metabolic Brain Disease*, vol 30(2), pg 437-447

Rolo AP, Palmeira CM (2006) Diabetes and mitochondrial function: Role of hyperglycemia and oxidative stress, *Toxicology and Applied Pharmacology*, vol 212(2), pg 167-178

Rossello X, Riquelme JA, Davidson SM, Yellon DM (2018) Role of PI3K in myocardial ischaemic preconditioning: mapping pro-survival cascades at the trigger phase and at reperfusion, *Journal of Cellular and Molecular Medicine*, vol 22(2), pg 926-935

Russell JS, Griffith TA, Helman T, Du Toit EF, Peart JN, Headrick JP (2019) Chronic type 2 but not type 1 diabetes impairs myocardial ischaemic tolerance and preconditioning in C57BL/6 mice, *Experimental Physiology*, vol 104, pg 1868-1880

Rytter N, Carter H, Piil P, Sorensen H, Ehlers T, Holmegaard F, Tuxen C, Jones H, Thijssen D, Gliemann L, Hellsten Y (2020) Ischemic Preconditioning Improves Microvascular Endothelial Function in Remote Vasculature by Enhanced Prostacyclin Production, *Journal of the American Heart Association*, vol 9, e016017

Sabio G, Davis RJ (2014) TNF and MAP kinase signalling pathways, *Seminars in Immunology*, vol 26(3), pg 237-245

Schenning KJ, Anderson S, Alkayed NJ, Hutchens MP (2015) Hyperglycemia abolishes the protective effect of ischemic preconditioning in glomerular endothelial cells in vitro, *Physiological Reports*, vol 3(3), e12346

Schwarzkopf TM, Horn T, Lang D, Klein J (2013) Blood gases and energy metabolites in mouse blood before and after cerebral ischemia: the effects of anesthetics, *Experimental Biology and Medicine*, vol 238(1), pg 84-89

Scott ES, Januszewski AS, O'Connell R, Fulcher G, Scott R, Kesaniemi A, Wu L, Colagiuri S, Keech A, Jenkins AJ (2020) Long-Term Glycemic Variability and Vascular Complications in Type 2 Diabetes: Post Hoc Analysis of the FIELD Study, *The Journal of Clinical Endocrinology and Metabolism*, vol 105(10), pg e3638-e3649

Serafin A, Rosello-Catafau J, Prats N, Gelpi E, Rodes J, Peralta C (2004) Ischemic preconditioning affects interleukin release in fatty livers of rats undergoing ischemia/reperfusion, *Liver Biology and Pathobiology*, vol 39(3), pg 688-698

Shao B, Bayraktutan U (2014) Hyperglycaemia promotes human brain microvascular endothelial cell apoptosis via induction of protein kinase C-β_1 and prooxidant enzyme NADPH oxidase, *Redox Biology*, vol 2, pg 694-701

Sharma S, Yang B, Xi XP, Grotta JC, Aronowski J, Savitz SI (2011) IL-10 directly protects cortical neurons by activating PI-3 kinase and STAT-3 pathways, *Brain Research*, vol 1373, pg 189-194

Sheikh MSA, Almaeen A, Alduraywish A, Alomair BM, Salma U, Fei L, Yang TL (2022) Overexpression of miR-126 Protects Hypoxic-Reoxygenation-Exposed HUVEC Cellular Injury through Regulating LRP6 Expression, *Oxidative Medicine and Cellular Longevity*, vol 17, 3647744

Shizukuda Y, Mallet RT, Lee SC, Downey HF (1992) Hypoxic preconditioning of ischaemic canine myocardium, *Cardiovascular Research*, vol 26(5), pg 534-542

Sierra Parraga JM, Merino A, Eijken M, Leuvenink H, Ploeg R, Moller BK, Jespersen B, Baan CC, Hoogdujin MJ (2020) Reparative effect of mesenchymal stromal cells on endothelial cells after hypoxic and inflammatory injury, *Stem Cell Research and Therapy*, vol 11, 352

Simonsen LO, Harbak H, Bennekou P (2011) Passive transport pathways for Ca^{2+} and Co^{2+} in human red blood cells. $^{57}Co^{2+}$ as a tracer for Ca^{2+} influx, *Blood Cells, Molecules, and Disease*, vol 47(4), pg 214-225

Singh RM, Cummings E, Pantos C, Singh J (2017) Protein kinase C and cardiac dysfunction: a review, *Heart Failure Reviews*, vol 22(6), pg 843-859

Snell-Bergeon JK, Wadwa RP (2012) Hypoglycemia, Diabetes and Cardiovascular Disease, *Diabetes Technology and Therapeutics*, vol 14(Suppl 1), pg S51-S58

Sprague JE, Arbelaez AM (2011) Glucose Counterregulatory Responses to Hypoglycemia, *Pediatric Endocrinology Reviews*, vol 9(1), pg 463-475

Srivastava K, Bayraktutan U (2017) Suppression of Protein Kinase C-α Ameliorates Hyperglycaemia-Evoked In Vitro Cerebral Barrier Dysfunction, *Stroke Research & Therapy*, vol 2(1)

Stitt AW (2003) The role of advanced glycation in the pathogenesis of diabetic retinopathy, *Experimental and Molecular Pathology*, vol 75(1), pg 95-108

Sun XC, Li WB, Li QJ, Zhang M, Xian XH, Qi J, Jin RL, Li SQ (2006) Limb ischemic preconditioning induces brain ischemic tolerance via p38 MAPK, *Brain Research*, vol 1084(1), pg 165-174

Swyers T, Redford D, Larson DF (2013) Volatile anesthetic-induced preconditioning, *Perfusion*, vol 29(1), pg 10-15

Swystun LL, Liaw PC (2016) The role of leukocytes in thrombosis, *Blood*, vol 128(6), pg 753-762

Takahashi K, Ghatei MA, Lam HC, O'Halloran DJ, Bloom SR (1990) Elevated Plasma Endothelin in Patients With Diabetes Mellitus, *Diabetologia*, vol 33(5), pg 306-310

Talukder MAH, Yang F, Shimokawa H, Zweier JL (2010) eNOS is required for acute in vivo ischemic preconditioning of the heart: effects of ischemic duration and sex, *American Journal of Physiology – Heart and Circulatory Physiology*, vol 299(2), pg H437-H445

Tatsumi T, Matoba S, Kobara M, Keira N, Kawahara A, Tsuruyama K, Tanaka T, Katamura M, Nakagawa C, Ohta B, Yamahara Y, Asayama J, Nakagawa M (1998) Energy Metabolism After Ischemic Preconditioning in Streptozotocin-Induced Diabetic Rat Hearts, *Journal of the American College of Cardiology*, vol 31(3), pg 707-715

Thangarajan H, Yao D, Chang EI, Shi Y, Jazayeri L, Vial IN, Galiano RD, Du XL, Grogan R, Galcez MG, Januszyk M, Brownlee M, Gurtner GC (2009) The molecular basis for impaired hypoxia-induced VEGF expression in diabetic tissues, *PNAS*, vol 106(32), pg 13505-13510

Tsang A, Hausenloy DJ, Mocanu MM, Carr RD, Yellon DM (2005) Preconditioning the Diabetic Heart – The Importance of Akt Phosphorylation, *Diabetes*, vol 54(8), pg 2360-2364

Tuncali B, Karci A, Tuncali BE, Mavioglu O, Ozkan M, Bacakoglu AK, Baydur H, Ekin A, Elar Z (2006) A New Method for Estimating Arterial Occlusion Pressure in Optimizing Pneumatic Tourniquet Inflation Pressure, *Anesthesia & Analgesia*, vol 102(6), pg 1752-1757

Turner RC (1998) The U.K. Prospective Diabetes Study, *Diabetes Care*, vol 21(S3), pgC35-C38

Ueno K, Samura M, Nakamura T, Tanaka Y, Takeuchi Y, Kawamura D, Takahashi M, Hosoyama T, Morikage N, Hamano K (2016) Increased plasma VEGF levels following ischemic preconditioning are associated with downregulation of miRNA-762 and miR-3072-5p, *Scientific Reports*, vol 6, 36758

Van der Reest J, Lilla S, Zheng L, Zanivan S, Gottlieb R (2018) Proteome-wide analysis of cysteine oxidation reveals metabolic sensitivity to redox stress, *Nature Communications*, vol 9, article 1581

Wada R, Yagihashi S (2005) Role of Advanced Glycation End Products and Their Receptors in the Development of Diabetic Neuropathy, *Annals of the New York Academy of Sciences*, vol 1043(1), pg 598-604

Weber NC, Kandler J, Schlack W, Grueber Y, Fradorf J, Preckel B (2008) Intermitted Pharmacologic Pretreatment by Xenon, Isoflurane, Nitrous Oxide, and the Opioid Morpjine Prevents Tumor Necrosis Factor α-induced Adhesion Molecule Expression in Human Umbilical Vein Endothelial Cells, *Anesthesiology*, vol 108(2), pg 199-207

Weinbrenner C, Nelles M, Herzog N, Sarvary L, Strasser RH (2002) Remote preconditioning by infrarenal occlusion of the aorta protects the heart from infarction: a newly identified non-neuronal but PKC-dependent pathway, *Cardiovascular Research*, vol 55(3), pg 590-601

Wilding LA, Hampel JA, Khoury BM, Kang S, Machado Aranda D, Raghavendran K, Nemzek JA (2017) Benefits of 21% Oxygen Compared with 100% Oxygen for Delivery of Isoflurane to Mice (Mus musculus) and Rats (Rattus norvegicus), *Journal of the American Association for Laboratory Animal Science*, vol 56(2), pg 148-154

Wright RJ, Macleod KM, Perros P, Johnston N, Webb DJ, Frier BM (2007) Plasma endothelin response to acute hypoglycaemia in adults with Type 1 diabetes, *Diabetic Medicine*, vol 24(9), pg 1039-1042

Wright RJ, Newby DE, Stirling D, Ludlam CA, Macdonald IA, Frier BM (2010) Effects of Acute Insulin Induced Hypoglycemia on Indices of Inflammation: putative mechanism for aggravating vascular disease in diabetes, *Diabetes Care*, vol 33(7), pg 1591-1597

Wu X, Lu Y, Dong Y, Zhang G, Zhang Y, Xu Z, Culley DJ, Crosby G, Marcantonio ER, Tanzi R, Xie Z (2012) The inhalation anesthetic isoflurane increases levels of proinflammatory TNFα, IL-6, and IL-1β, *Neurobiology of Aging*, vol 33(7), pg 1364-1378

Xu Q, Ming Z, Dart AM, Du XJ (2007) Optimizing dosage of ketamine and xylazine in murine echocardiography, *Clinical and Experimental Pharmacology and Physiology*, vol 34(5-6), pg 499-507

Yamagishi S, Amano S, Inagaki Y, Okamoto, Sasaki N, Yamamoto H, Takeuchi M, Makita (2002) Advanced Glycation End Products-Induced Apoptosis and Overexpression of Vascular Endothelial Growth Factor in Bovine Retinal Pericytes, *Biochemical and Biophysical Research Communications*, vol 290(3), pg 973-978

Yang C, Talukder MAH, Varadharaj S, Velayutham M, Zweier JL (2013) Early ischaemic preconditioning requires Akt-and PKA-mediated activation of eNOS via serine1176 phosphorylation, *Cardiovascular Research*, vol 97(1), pg 33-43

Yang Z, Tian Y, Liu Y, Hennessy S, Kron IL, French BA (2013) Acute Hyperglycemia Abolishes Ischemic Preconditioning by Inhibiting Akt Phosphorylation: Normalizing Blood Glucose before Ischemia Restores Ischemic Preconditioning, *Oxidative Medicine and Cellular Longevity*, vol 2013, article 329183

Yellon DM, He Z, Khambata R, Ahluwalia A, Davidson SM (2018) The GTN patch: a simple and effective new approach to cardioprotection?, *Basic Research in Cardiology*, vol 113(3), article 20

Yu X, Lu C, Liu H, Rao S, Cai J, Liu S, Kriegel AJ, Greene AS, Liang M, Ding X (2013) Hypoxic Preconditioning with Cobalt of Bone Marrow Mesenchymal Stem Cells Improves Cell Migration and Enhances Therapy for Treatment of Ischemic Acute Kidney Injury, *PLoS ONE*, vol 8(5), e62703

Yuan J, Najafov A, Py BF (2016) Roles of Caspases in Necrotic Cell Death, *Cell*, vol 167(7), pg 1693-1794

Zeng M, Wei X, Wu Z, Li W, Zheng Y, Li B, Meng X, Fu X, Fei Y (2016) Simulated ischemia/reperfusion-induced p65-Beclin 1-dependent autophagic cell death in human umbilical vein endothelial cells, *Scientific Reports,* vol 6, article 37488

Zhang J, Guo Y, Ge W, Zhou X, Pan M (2019) High glucose induces apoptosis of HUVECs in a mitochondria-dependent manner by suppressing hexokinase 2 expression, *Experimental and Therapeutic Medicine*, vol 18(1), pg 621-679

Zhang Y, Han H, Wang J, Wang H, Yang B, Wang Z (2003) Impairment of Human Ether-à-Go-Go-related Gene (HERG) K^+ Channel Function by Hypoglycemia and Hyperglycmeia SIMILAR PHENOTYPES BUT DIFFERENT MECHANISMS, *Membrane Transport Structure Function and Biogenesis*, vol 278(12) pg 10417-10426

Zhao F, Deng J, Yu X, Li D, Shi H, Zhao Y (2015) Protective effects of vascular endothelial growth factor in cultured brain endothelial cells against hypoglycaemia, *Metabolic Brain Disease*, vol 30(4), pg 999-1007

Zheng S, Zuo Z (2003) Isoflurane Preconditioning Induces Neuroprotection against Ischemia via Activation of p38 Mitogen-Activated Protein Kinases, *Molecular Pharmacology*, vol 65(5), pg 1172-1180

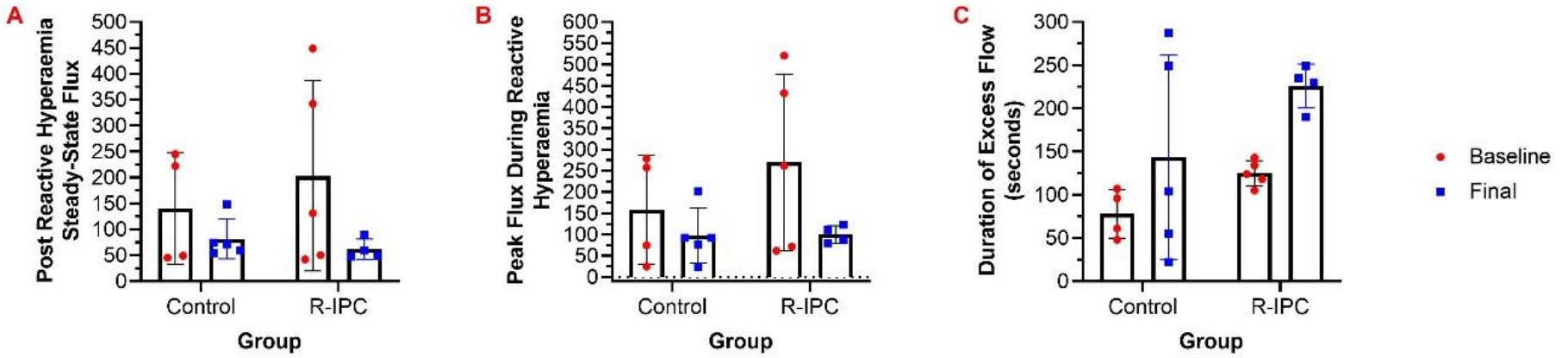

Fig. 8.1 Variables used to calculate magnitude of reactive hyperaemia and the excess flow of blood during this period in the primary optimisation model. Post reactive hyperaemia steady-state flux (A) is the flux in the hindlimb once a steady-state had been reached following the reactive hyperaemia period. Peak flux (B) is the maximum flux reached during the reactive hyperaemic response. The duration of the excess flow (C) is the period of time between restoration of blood flow following ischaemia and the post reactive hyperaemia steady-state being achieved.

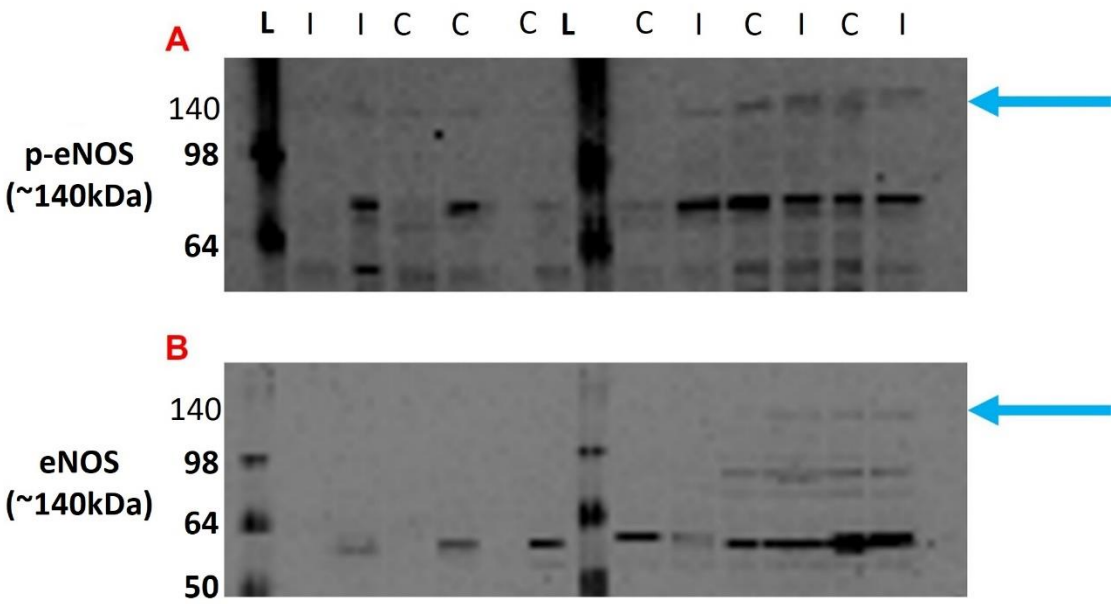

Fig. 8.2 Primary optimisation study eNOS and p-eNOS western blot membranes. Aortas from the primary optimisation study were lysed and p-eNOS (A) and eNOS (B) expression observed using western blots. Lysates from control group (C) and R-IPC (I) groups as well as two protein ladders (L) are annotated on the image of the membranes. Blue arrows indicate where the bands should be present but proteins were not successfully transferred onto the membrane for all samples. Band sizes of the protein ladder (bold) and proteins of interest are indicated on respective blots.

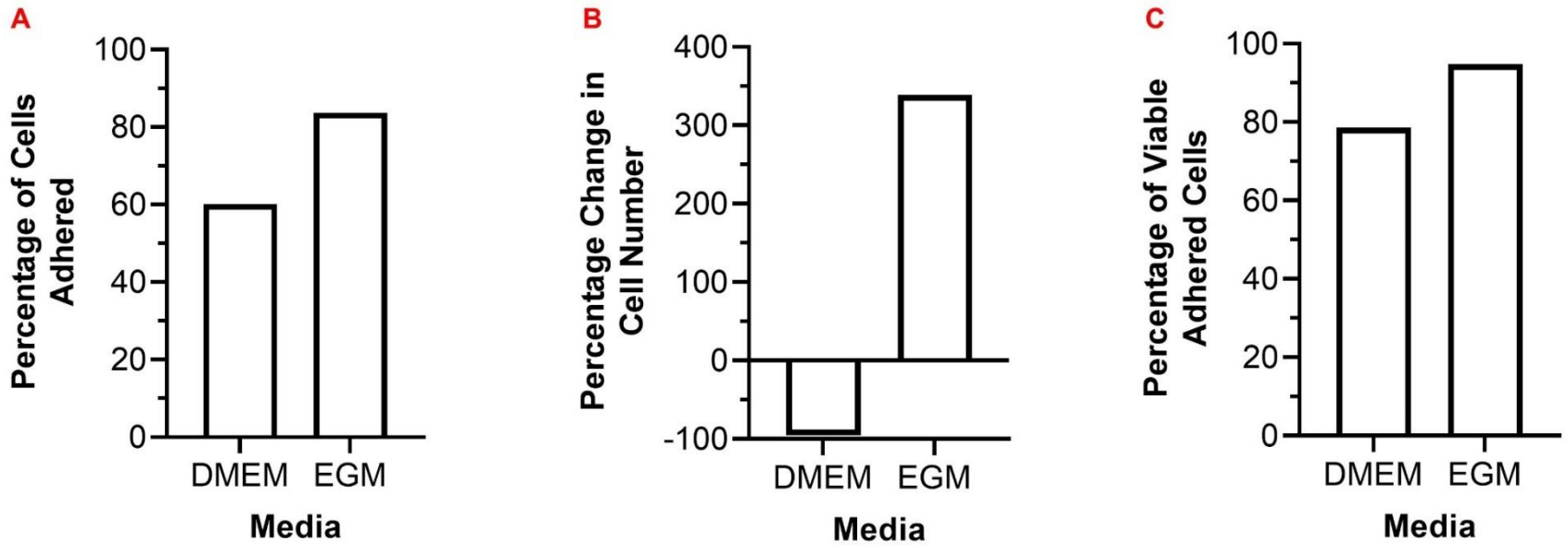

Fig. 8.3 Comparing the Effects of EGM and DMEM on HUVEC Culture. HUVECs were cultured in DMEM or EGM. They underwent a cell adhesion assay (A), cell proliferation assay (B), and cell viability assay (C). 24 hours after plating, for cell adhesion, the total number of cells, both floating and adhered, were counted. To calculate the percentage change in cell number, cells were counted prior to seeding and 72 hours after plating. Cell viability was calculated, 72 hours after plating, by counting the total number of adhered cells and the number that had not been stained with trypan blue. All bars are formed from a single biological repeat (N=1)

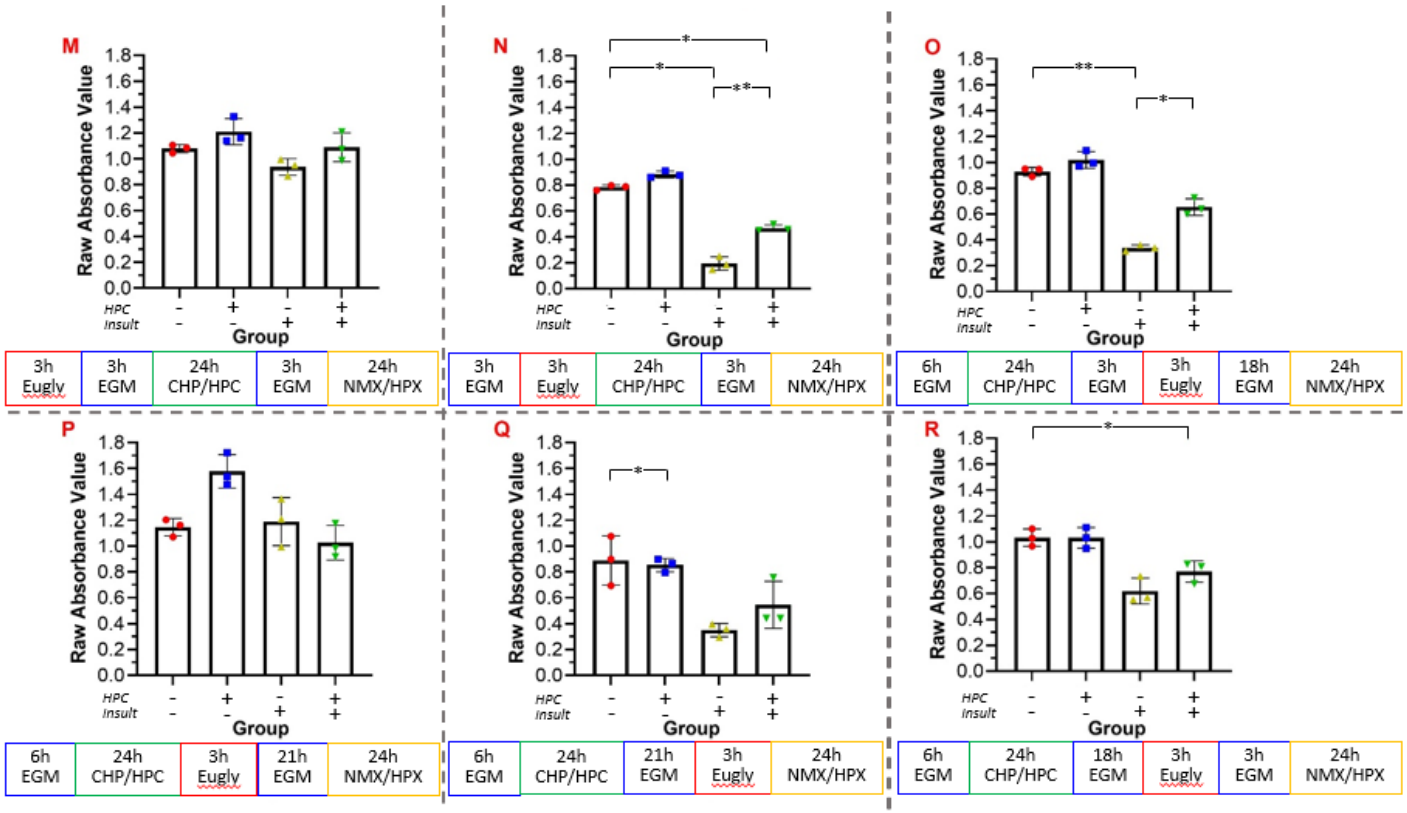

Fig. 8.4 Effect of acute euglycaemia on $CoCl_2$ induced HPC. HUVECs were exposed to basal media (CHP) or underwent HPC with 200µM $CoCl_2$ in basal media (HPC) for 24 hours. After a 24-hour recovery in EGM, a 600µM $CoCl_2$ hypoxic insult (HPX) or basal media treatment (NMX) were given for 24 hours. MTS assays were conducted 18-hours following the insult period. Cells were allocated into experimental groups to receiving a 3-hour euglycaemic episode in saline at 1 of 6 timepoints, where M-R correspond to the experimental groups indicated in Fig. 5.17. Protocol timelines for each experimental group are located beneath their respective graphs. + and – indicates whether a group received an interventional treatment (HPC and/or hypoxic insult) or the relevant control (preconditioning control and/or insult control) respectively. Mean, individual data points and SD for raw absorbance values are shown. Significance differences are indicated (* = $p<0.05$, ** = $p<0.01$)

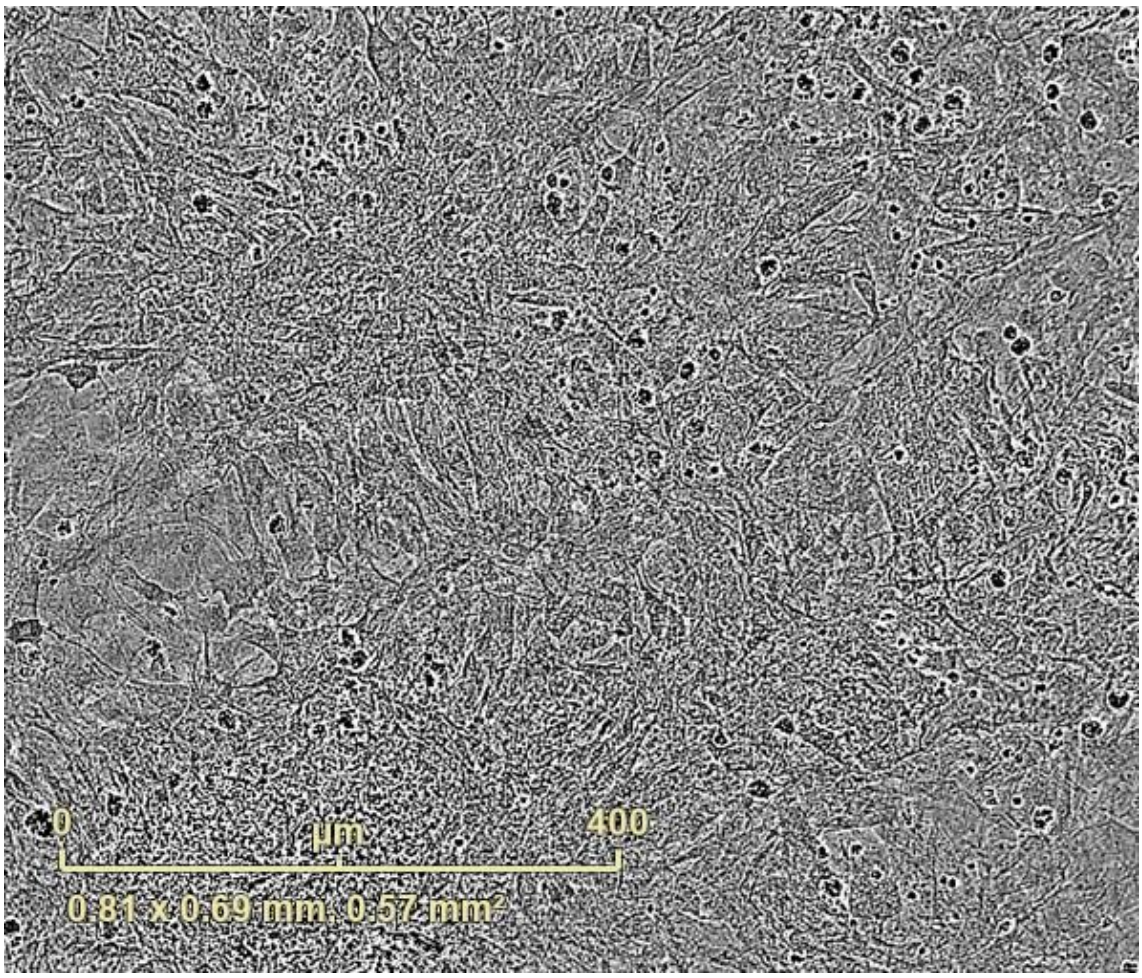

Fig. 8.5 Primary neonatal rat cardiomyocytes. Neonatal rat cardiomyocytes were cultured from rats aged 4 days old. Cells were found to be beating within 1 week and were imaged using the IncuCyte®.

Ingredient	Volume (mL)
Base Media [PromoCell®, C-22210]	500
Endothelial Growth Supplement [PromoCell®, C-39215]	1X Tube
HI FBS	40
Penicillin/Streptomycin (Pen/Strep) [Thermo Fisher Scientific, 10500064]	5

Table 8.1 EGM. Growth media for HUVECs. Filtered before using and warmed to 37^{o}C before applying to cells.

Ingredient	Volume (mL)
No Glucose DMEM	500
1M Glucose Solution	2.5
L-Glutamine	8
HI FBS	50
Pen/Strep	10

Table 8.2 DMEM. DMEM for HUVECs. Filtered before using and warmed to 37^{o}C before applying to cells.

Ingredient	Volume (mL)
Base Media	500
HI FBS	2.5
Pen/Strep	5

Table 8.3 Basal media. Starving and experimental media for HUVECs. Filtered before using and warmed to 37^{o}C before applying to cells.

Ingredient	Final Concentration (mM)	Mass (g)
Sodium Phosphate Monobasic	1	0.120
Sodium Bicarbonate	24	2.016
Calcium Chloride Dihydrate	2.5	0.368
Sodium Lactate	20	2.241
Sodium EDTA	0.5	0.186
Sodium Chloride	118	6.896
Potassium Chloride	16	1.193

Table 8.4 Ischaemic buffer. Ischaemic buffer used to induce ischaemia in HUVECs as in section 2.8. Filtered and warmed to 37^{o}C before applying to cells. Stored long term at 4^{o}C.

Ingredient	Final Concentration (mM)	Mass (g)
Sodium Phosphate Monobasic	0.9	0.108
Sodium Bicarbonate	20	1.680
Calcium Chloride Dihydrate	1	0.145
Magnesium Sulphate Heptahydrate	1.2	0.296
HEPES	20	4.766
Sodium Chloride	129.5	7.568
Potassium Chloride	5	0.373
Glucose	5.5	0.991

Table 8.5 Control buffer. Control buffer used as a control for the ischaemic buffer, in table 8.4, used as in section 2.8. Filtered and warmed to 37^{o}C before applying to cells. Stored long term at 4^{o}C.

Ingredient	Final Concentration (mM)	Mass (g)
Sodium Chloride	135	7.889
Potassium Chloride	5	0.373
Magnesium Chloride Hexahydrate	1	0.203
Calcium Chloride Dihydrate	1	0.147
HEPES	10	2.383

Table 8.6 Saline. Saline used alongside the relevant volume of 0.5M glucose solution to induce acute hypoglycaemia, euglycaemia and hyperglycaemia in HUVECs as in section 2.8.3. Filtered and warmed to 37^{o}C before applying to cells. Stored long term at 4^{o}C.

Ingredient	Final Concentration	Volume (mL)
dH_2O	N/A	416.5
1M Tris pH 7.4	50mM	25
0.5M EDTA	1mM	1
0.2M EGTA	1mM	2.5
Glycerol	10%	50
TritonX100	1%	5

Table 8.7 Extraction buffer. Extraction buffer used to prepare standard lysis buffer as in Table 8.8. Stored long term at 4ºC.

Ingredient	Final Concentration	Volume (mL)
Extraction Buffer	N/A	8.933
0.1M DTT	1mM	0.1
0.1M PMSF	1mM	0.1
100X HALT Protease Inhibitor	1X	0.1
0.75M Sodium Fluoride	50mM	0.667
0.5M NaPp	5mM	0.1

Table 8.8 Standard lysis buffer. Standard lysis buffer to lyse cells and tissue as in section 2.10.1.1. NaPp required warming to 80ºC prior to addition to re-dissolve the precipitated crystals. Prepared no more than 30 minutes before use and could not be stored short or long term.

Ingredient	Final Concentration	Volume (mL)
8M Urea Solution	5.4M	6.7
Glycerol	10%	1
1M Tris pH 6.8	10mM	0.1
10% SDS	1%	1
0.1M DTT	1mM	0.1
0.1M PMSF	1mM	0.1
100X HALT Protease Inhibitor	1X	0.1
dH_2O	N/A	0.9

Table 8.9 Specialised lysis buffer. Lysis buffer to lyse cells for the purpose of analysing HIF1α expression as in section 2.10.1.2.

Ingredient	Volume (µL)
Loading Dye Base	950
β-mercaptoethanol (2-BME)	50

Table 8.10 Loading dye base. Loading dye base used to make the complete loading dye as in table 8.11.

Ingredient	Quantity
dH_2O	100mL
1M Tris pH 7.0	5mL
20% SDS	25mL
Glycerol	20mL
Bromophenol Blue	2mg

Table 8.11 Complete loading dye. Loading dye base used to make western blot samples as in section 2.10.2.1.

Ingredient	Volume (µL)
4X LDS Sample Buffer [Thermo Fisher Scientific, NP0007]	950
2-BME	50

Table 8.12 LDS Sample Buffer. Loading dye solution used to make western blot samples as in section 2.10.2.1.

Ingredient	Volume (mL)
dH_2O	4.15
Lower Buffer	3.15
30% Acrylamide	3.75
10% SDS	0.11
Tetramethylethylenediamine (TEMED)	0.011
20% Ammonium Persulfate (APS)	0.05535

Table 8.13 Lower gel 10%. One lower gel for SDS-PAGE, as in section 2.10.2.2. Recipe for the lower buffer is located within Table 8.15.

Ingredient	Volume (mL)
dH_2O	2.8
Upper Buffer	1.25
30% Acrylamide	0.85
10% SDS	0.05
TEMED	0.00535
20% APS	0.05

Table 8.14 Upper gel 4%. One upper gel for SDS-PAGE, as in section 2.10.2.2. Recipe for upper buffer is located within Table 8.16.

Ingredient	Quantity
dH_2O	800-1000mL
Tris	181.65g

Table 8.15 Lower buffer. Lower buffer for making the lower gel as in Table 8.13. Tris was dissolved in 800mL dH_2O. pH was set to 8.8 using HCl. This was topped up with dH_2O to a total volume of 1000mL. Kept at RT for long term storage.

Ingredient	Quantity
dH_2O	700-1000mL
Tris	181.65g

Table 8.16 Upper buffer. Upper buffer for making the upper gel as in Table 8.14. Tris was dissolved in 700mL dH_2O. pH was set to 6.8 using HCl. This was topped up with dH_2O to a total volume of 1000mL. Kept at RT for long term storage.

Ingredient	Quantity
dH_2O	950mL
Tris	30.3g
Glycine	144g
20% SDS	50mL

Table 8.17 10X running buffer. 10X stock of running buffer used to make the 1X solution for SDS-PAGE as in section 2.10.2.2. Kept at RT for long term storage.

Ingredient	Quantity
dH_2O	1L
Tris	30.3g
Glycine	144g

Table 8.18 10X transfer buffer. 10X stock of transfer buffer used to make the 1X solution for wet transfer as in section 2.10.2.3. Kept at RT for long term storage.

Ingredient	Quantity
dH_2O	800-1000
Tris	48.4g
Sodium Chloride	160g

Table 8.19 20X Tris Buffered Saline (TBS). 20X TBS stock used to make TBS-T as in table 8.20. Tris and sodium chloride were dissolved in 800mL dH_2O. pH was set to 7.6 with HCl. This was topped up with dH_2O to a total volume of 1000mL. Kept at RT for long term

Ingredient	Volume (mL)
dH_2O	1900
20X TBS	100
Tween-20	1

Table 8.20 1X TBS-T. 1X working solution of TBS-T. Kept at RT for long term storage.

Ingredient	Volume (mL)
DMEM GlutaMAX [Thermo Fisher Scientific, 10566016]	67
M199 GlutaMAX [Thermo Fisher Scientific, 41150020]	17
Horse Serum [Sigma Aldrich, H1270-500ML]	10
HI FBS	5
Pen/Strep	1

Table 8.21 M1 Media. M1 media for cardiomyocyte culture, as in section 2.7.5. Filtered before using and warmed to 37^{o}C before applying to cells.

Ingredient	Volume (mL)
DMEM GlutaMAX	76
M199 GlutaMAX	17.5
Horse Serum	5
HI FBS	0.5
Pen/Strep	1

Table 8.22 M2 Media. M2 media for cardiomyocyte culture, as in section 2.7.5. Filtered before using and warmed to 37°C before applying to cells.

Target	Dilution	Supplier	Cat No.
AMPK	1:1000	Cell Signalling Technology	2795S
p-AMPK	1:1000	Cell Signalling Technology	2531S
p38 MAPK	1:1000	Cell Signaling Technology	9212S
p-p38 MAPK	1:1000	Cell Signaling Technology	4511S
VCAM	1:2000	Abcam	ab134047
ICAM-1	1:1600	Cell Signaling Technology	Unspecified
eNOS	1:1000	Cell Signaling Technology®	9572S
p-eNOS	1:1000	Cell Signaling Technology®	9571S
HIF1α	1:2000	Thermo Fisher Scientific	MA1-516
β-Actin	1:1000	Sigma Aldrich	A2066
α-Tubulin	1:1000	Cell Signaling Technology®	3873S

Table 8.23 Primary antibodies for western blot. Primary antibodies used for western blot analysis and their dilutions. Supplier and catalogue number (Cat No.) are also detailed.

Target	Dilution	Supplier	Cat No.
Goat Anti-Mouse 2°	1:10,000	Thermo Fisher Scientific	A-21057
Anti-Rabbit 2°	1:10,000	Li-Cor	926-32211

Table 8.24 Secondary antibodies for western blot. Secondary antibodies used for western blot analysis and their dilutions. Supplier and catalogue number (Cat No.) are also detailed.